Non-canonical activation of PI3Kγ by Ca^{2+}/PKCβ in mast cells

Inauguraldissertation

zur

Erlangung der Würde eines Doktors der Philosophie

vorgelegt der

Philosophisch-Naturwissenschaftlichen Fakultät

der Universität Basel

von

Romy Walser

aus Herisau, AR

Basel, 2014

Genehmigt von der Philosophisch-Naturwissenschaftlichen Fakultät auf Antrag von

Prof. Dr. Matthias P. Wymann (Universität Basel)

Prof. Dr. Dr. Bernd Nürnberg (Universität Tübingen)

Basel, den 13.12.2011

Prof. Dr. Martin Spiess
Dekan

Namensnennung-Keine kommerzielle Nutzung-Keine Bearbeitung 3.0 Schweiz
(CC BY-NC-ND 3.0 CH)

Sie dürfen: **Teilen** — den Inhalt kopieren, verbreiten und zugänglich machen

Unter den folgenden Bedingungen:

Namensnennung — Sie müssen den Namen des Autors/Rechteinhabers in der von ihm festgelegten Weise nennen.

Keine kommerzielle Nutzung — Sie dürfen diesen Inhalt nicht für kommerzielle Zwecke nutzen.

Keine Bearbeitung erlaubt — Sie dürfen diesen Inhalt nicht bearbeiten, abwandeln oder in anderer Weise verändern.

Wobei gilt:

- **Verzichtserklärung —** Jede der vorgenannten Bedingungen kann **aufgehoben** werden, sofern Sie die ausdrückliche Einwilligung des Rechteinhabers dazu erhalten.
- **Public Domain (gemeinfreie oder nicht-schützbare Inhalte) —** Soweit das Werk, der Inhalt oder irgendein Teil davon zur Public Domain der jeweiligen Rechtsordnung gehört, wird dieser Status von der Lizenz in keiner Weise berührt.
- **Sonstige Rechte —** Die Lizenz hat keinerlei Einfluss auf die folgenden Rechte:
    - Die Rechte, die jedermann wegen der Schranken des Urheberrechts oder aufgrund gesetzlicher Erlaubnisse zustehen (in einigen Ländern als grundsätzliche Doktrin des **fair use** bekannt);
    - Die **Persönlichkeitsrechte** des Urhebers;
    - Rechte anderer Personen, entweder am Lizenzgegenstand selber oder bezüglich seiner Verwendung, zum Beispiel für **Werbung** oder Privatsphärenschutz.
- **Hinweis —** Bei jeder Nutzung oder Verbreitung müssen Sie anderen alle Lizenzbedingungen mitteilen, die für diesen Inhalt gelten. Am einfachsten ist es, an entsprechender Stelle einen Link auf diese Seite einzubinden.

Quelle: http://creativecommons.org/licenses/by-nc-nd/3.0/ch/ Datum: 12.11.2013

Index

1. Summary

Mast cells are key effector cells in allergic disease triggering inflammation through mediator release. Allergens activate mast cells through the high-affinity receptor for IgE (FcεRI), which initiates signalling pathways that regulate the release of inflammatory mediators from secretory granules and the production of lipid mediators and cytokines. Receptor aggregation is coupled to the activation of protein tyrosine kinases (PTK) that coordinate Ca^{2+} mobilisation and protein kinase C (PKC) activation. Also essential is the activation of phosphoinositide 3-kinase (PI3K), as mast cell degranulation is blocked by pan PI3K inhibition in cells or genetic inactivation of class IB PI3Kγ in mice. Analysis of bone marrow-derived mast cells (BMMCs) showed that PI3Kγ regulates mast cell hyperactivaton by boosting PIP_3 production via autocrine-paracrine adenosine/G protein-coupled receptor (GPCR) signalling.

Here we demonstrate a direct pathway from the FcεRI to PI3Kγ. Degranulation triggered by IgE/antigen or stimulators of Ca^{2+} mobilisation such as Thapsigargin is blocked in PI3Kγ$^{-/-}$ BMMCs. FcεRI- and Thapsigargin-induced PI3Kγ activation depends on a high threshold concentration of intracellular Ca^{2+} and subsequent PKCβ activation. Thapsigargin to PI3Kγ signalling occurs completely in an adenosine- and GPCR-independent manner. Active PKCβ interacts with and phosphorylates PI3Kγ in vitro and in vivo on Ser582. This residue sits at the beginning of the helical domain, a region that has attracted attention in PI3Kα as mutation hot-spot in cancer. Analyses of phosphorylation-mimicking mutants indicate that Ser582 functions as switch-site for PI3Kγ activation. Furthermore, we show that PKCβ-regulated PI3Kγ operates free of the adaptor protein p84. By biochemical and structural approaches we mapped the p84 binding interphase on PI3Kγ to the region around S582 and demonstrate that PI3Kγ-bound p84 blocks S582 phosphorylation.

This study is the first to unravel a pathway and mechanism by which a protein tyrosine kinase (PTK)-coupled receptor engages PI3Kγ. Contemporaneously we defined the role of PKC in mast cell degranulation. The results of this work change our view on PI3-kinase regulation, opening fascinating new insights into mechanisms of isoform-specific PI3K activation.

2. Introduction

2.1 Phosphoinositide 3-kinases (PI3Ks)

Phosphoinositide 3-kinases are lipid kinases that phosphorylate the inositol head group of phosphoinositides (PIs) (Vanhaesebroeck B, Annu Rev Biochem, 2001). The inositol ring of PIs is linked via a phosphate group to a diacylglycerol tail that anchors the lipid to membranes. PI3Ks catalyse the transfere of the γ-phosphate of adenosine 5'-triphosphate (ATP) to the hydroxyl group at the 3' position of the inositol moiety. PIs include phosphatidylinositol (PtdIns) and its phosphorylated derivatives, of which PI3Ks phosphorylate PtdIns, PtdIns(4)*P*, and PtdIns(4,5)P_2. Class I isoenzymes for example modulate intracellular signalling through the generation of PtdIns(3,4,5)P_3 from PtdIns(4,5)P_2 (Fig. a).

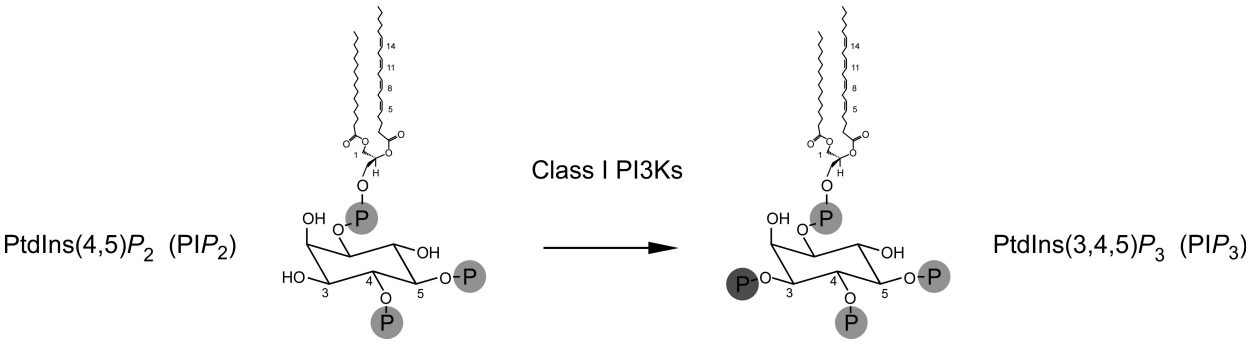

Fig. a: PI3Ks phosphorylate the 3'-OH-group of phosphoinositides

The 3-phosphorylated PIs function as docking sites for proteins containing a phosphoinositide binding domain leading to their recruitment to a specific membrane compartment. Examples of PI-binding domains are the pleckstrin homology (PH) domain which preferentially binds PI(3,4,5)P_3 or the FYVE and Phox homology (PX) domains which prefer PI(3)*P*.

The PI3K family has been subdivided into three classes (Fig. b) – class I, II, and III – based on sequence homology, protein domain organisation, substrate specificity, and mode of regulation. Class I PI3Ks signal downstream of cell surface receptors to control fundamental cellular functions like survival, growth, and proliferation, but also regulate more cell specific tasks such as insulin signalling, immune cell activation, and motility. The class II enzymes have been discovered based on sequence homology to class I and III PI3Ks (MacDougall LK, Curr Biol, 1995; Molz L, J Biol Chem, 1996), but their function and substrate specificity in vivo are poorly defined. Experimental data for example implicate roles in clathrin-mediated endocytosis and insulin signalling (Gaidarov I, Mol Cell, 2001; Falasca M and Maffucci T, Biochem Soc Trans, 2007). The only class III member vacuolar sorting protein 34 (Vsp34) is the prototype PI3K and the only member found in all eukaryots. Vsp34 is involved in endosomal vesicle trafficking, protein synthesis, and autophagy (Backer JM, Biochem J, 2008).

All members of the PI3K family contain a conserved central core composed of a C2, a helical, and a lipid kinase domain. The lipid kinase domain shows homology to protein kinase domains, having a P- (phosphate binding loop), catalytic, and activation loop. Basic residues in the activation loop

influence substrate specificity and their exchange in PI3Kα by the corresponding segments in class II or III enzymes switches inositol lipid specificity in vitro (Pirola L, J Biol Chem, 2001). Class I PI3Ks use PIP_2 as substrate in vivo, but also phosphorylate PtdIns(4)*P* and PI in vitro. They are the only enzymes that generate PI(3,4,5)P_3. Class II PI3Ks phosphorylate PI and PI(4)*P* in vitro, but the preferred in vivo substrate is unclear, while class III PI3K Vsp34 exclusively phosphorylates PI. In contrast to protein kinases, PI3Ks are not regulated by activation loop phosphorylation. In addition to lipid kinase activity, the PI3K catalytic subunit also possesses an intrinsic protein kinase activity. Whether this is of any physiological significance is not known. The C2 domain is supposed to be involved in phospholipid membrane binding (Walker EH, Nature, 1999), while the function of the helical domain is unknown. Class I and III PI3Ks associate with a regulatory subunit (Fig. b), but not class II enzymes, which instead contain N- and C-terminal extensions. Vsp34 activity depends on its regulatory subunit, which is the Ser/Thr kinase p150.

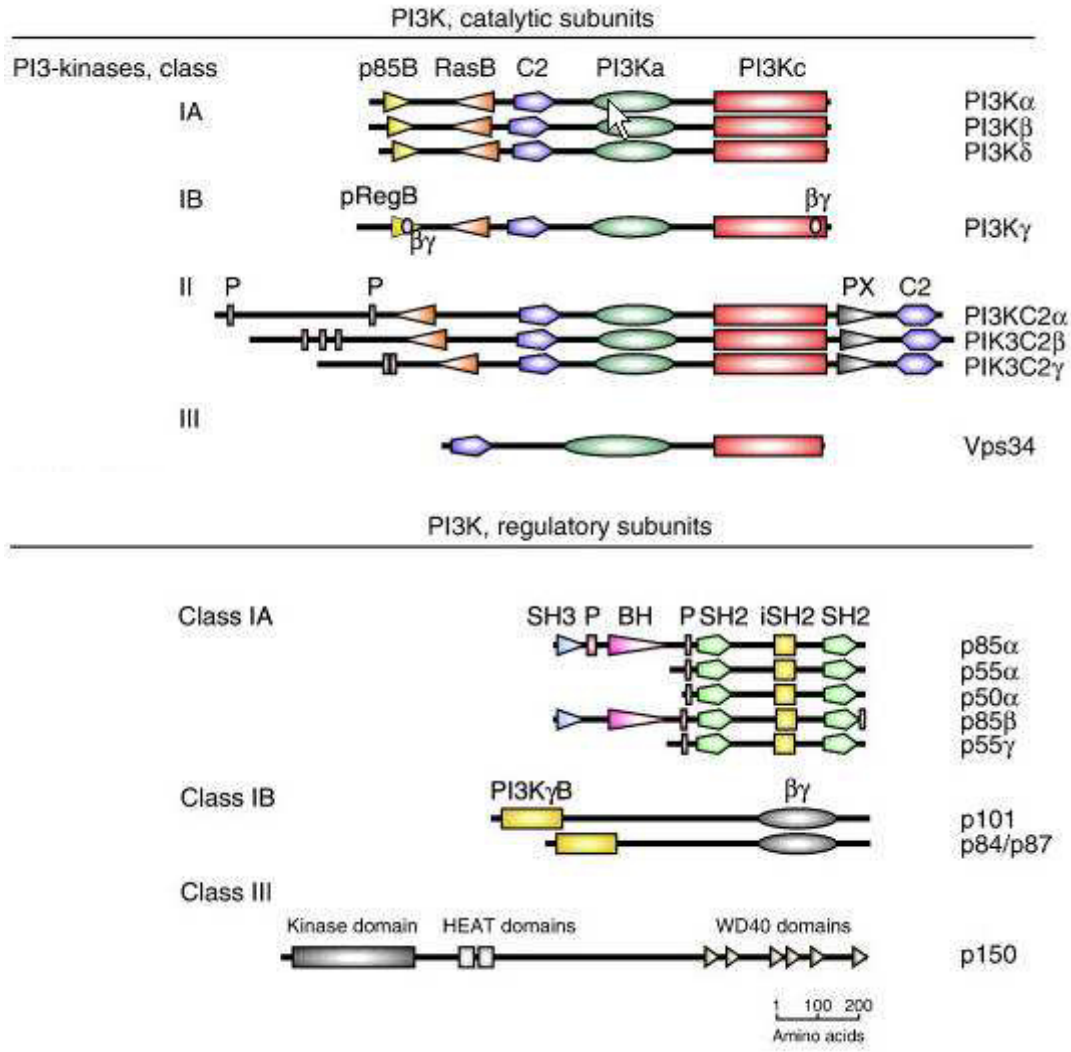

Fig. b: Domain organisation of PI3K catalytic and regulatory proteins. p85B: adaptor binding domain (ABD); RasB: Ras binding domain (RBD); C2: C2 domain; PI3Ka: helical domain; PI3Kc: catalytic domain; SH3: Src homology 3 domain; P: proline-rich region; BH: Bcr homology domain; SH2: Src homology 2 domain; iSH2: inter-SH2 domain (adapted from (Marone R, Biochim Biophys Acta, 2008)).

2.2 Class I PI3Ks

Class I PI3-kinases have been subdivided into the subclasses IA and IB and contain four members. PI3Kα, PI3Kβ, and PI3Kδ belong to the class IA group, while PI3Kγ is the only class IB family member. Class I PI3Ks contain, additional to the C2, helical, and kinase domain, an N-terminal domain (ABD) followed by a Ras-binding domain (RBD). The N-terminal domain of class IA PI3Ks functions as adaptor binding domain (ABD) and tightly interacts with a p85 regulatory subunit family member. In contrast to all other domains, the ABD of class IA PI3Ks shows no similarity the corresponding region in class IB PI3Kγ. Consistantly PI3Kγ does not bind to p85s. The RBDs of PI3Kα and PI3Kγ bind to Ras in vitro and fold into a similar structure as the unrelated RBDs of Raf and RalGDS (Rodriguez-Viciana P, Nature, 1994; Rubio I, Biochem J, 1997; Pacold ME, Cell, 2000; Huang CH, Science, 2007). While studies of engineered PI3K RBD mutants demonstrate physiological importance of this domain, its precise mechanism of action in vivo is obscure (Suire S, Nat Cell Biol, 2006; Kang S, Proc Natl Acad Sci U S A, 2006; Kurig B, Proc Natl Acad Sci U S A, 2009; Gupta S, Cell, 2007).

2.2.1 Class IA PI3Ks

Class IA PI3Ks exist in cells in tight complex with a p85/p55 regulatory protein. These are encoded by three genes, *Pik3r1*, *Pik3r2,* and *Pik3r3*, giving rise to p85α, p55α, and p50α, p85β, and p55γ, respectively. All class IA PI3Ks can bind to any of the p85-related subunits. Knowledge about adaptor preferences and isoform-specificities is scarce. They are required for the stability of the catalytic subunits, regulate membrane localization, PI3K activation, and restrict catalytic activity in quiescent cells. All p85-related subunits contain two Src homology 2 (SH2) domains separated by an intervening coiled-coil domain (iSH2). Full-length p85 additionally possess an N-terminal Src homology 3 (SH3) domain followed by a BCR (breakpoint cluster region) domain (BH domain) that is flanked by two proline-rich regions (Kapeller R, J Biol Chem, 1994). The iSH2 domain binds tightly to the ABD of the catalytic PI3K subunit (Holt KH, Mol Cell Biol, 1994). The SH2 domains bind phosphorylated tyrosine residues (pY) in the tails of activated receptor tyrosine kinases, protein tyrosine kinases, or adaptor proteins (Klippel A, Mol Cell Biol, 1992). The phosphorylated tyrosine has to be part of an immunoreceptor tyrosine-based activation motif (ITAM) of the sequence pYXXM (X any amino acid), but there exist exceptions (HGFR, pYVSV) (Songyang Z, Cell, 1993; Ponzetto C, Mol Cell Biol, 1993). Binding to phosphotyrosine motifs releases inhibitory contacts between p85 and PI3K leading to increased lipid turnover in vitro (Carpenter CL, J Biol Chem, 1993; Miled N, Science, 2007). The precise roles of the p85 SH3 or BH domain are unclear. The SH3 domain mediates binding to proline-rich sequences and has been shown to associate with the adaptor proteins Shc or Cbl (Harrison-Findik D, Oncogene, 1995; Soltoff SP and Cantley LC, J Biol Chem, 1996; Dombrosky-Ferlan PM and Corey SJ, Oncogene, 1997; Hunter S, Mol Endocrinol, 1997). These interactions might regulate membrane localisation and/or activation. The BH domain is highly homologous to the GTPase activation protein (GAP) domain of the breakpoint cluster region (Bcr) protein, but does not have GTPase activity. It has been proposed to interact with the Rho family proteins Cdc42 and Rac (Zheng Y, J Biol Chem, 1994; Tolias KF, J Biol Chem, 1995). Analysis of p85 truncations showed that p85 contains a GTPase-responsive and

inhibitory region (Chan TO, Cancer Cell, 2002). The GTPase-responsive domain is located within the iSH2 domain and stimulates protein kinase B (PKB) activation by active H-Ras or Rac1, which however depends on prior release of PI3K inhibition by the p85 C-terminus (LED(52 amino acids)-cSH2, LED lays over the regulatory square). Interestingly, the PI3K activating influenza virus non-structural protein (NS)1 interacts with p85β at a similar region in the iSH2, including the LED and precedent sequences (Hale BG, Proc Natl Acad Sci U S A, 2010).

2.2.2 Class IB PI3K

The class IB member PI3Kγ can associate with a p101 (*Pik3r5*) or p84 (*Pik3r6*) adaptor protein (Sugimoto Y, Proc Natl Acad Sci U S A, 1984; Suire S, Curr Biol, 2005). Their genes are located next to each other on the same chromosome. p101 and p84 share 30% amino acid sequence identity and 37% sequence similarity. Both adaptors have no sequence similarity with any known protein or protein domain, and are completely different from the p85 adaptors of class IA PI3Ks. Sequence homologies of p101 and p84 are highest in the N- and C-terminal regions, which are also most highly conserved. The middle parts of the two protein sequences vary greatly and may regulate isoform-specific protein interactions and functions. Whereas p101 contains a nuclear localisation signal (NLS) and is localised to nucleus in the absence of PI3Kγ, p84 lacks such a sequence (Brock C, J Cell Biol, 2003; Voigt P, J Biol Chem, 2006). Adaptor protein coexpression is not required for PI3Kγ stability, but enhances PI3Kγ expression levels (Voigt P, J Biol Chem, 2006). On the other hand, p101 is instable in the absence of PI3Kγ, while p84 can be expressed alone.

Discovery of PI3Kγ and p101

PI3Kγ has been discovered by attempts to find the enzyme that catalyzes the fast and large accumulation of PtdIns(3,4,5)P_3 in response to stimulation of neutrophils and myeloid-derived cells (U937) with chemotactic ligands (Stephens L, J Biol Chem, 1993; Stephens L, Cell, 1994; Sugimoto Y, Proc Natl Acad Sci U S A, 1984). These stimuli signal through a subfamily of G protein-coupled receptors (GPCRs) whose activation and chemotactic effects are blocked by *B. Pertussis* Toxin (*P*Tx). As *P*Tx also blocked PIP_3 production indicated to the existence of a G-protein regulated PI3K activity. In support of this, Gβγ-dimers but not heterotrimeric Gα·GDP-Gβγ, presented on artifical lipid vesicles, stimulated PIP_3 production in neutrophil lysates. In contrast to other known G-protein regulated enzymes like phospholipase C (PLC)β, this PI3K activity could only be activated by Gβγ dimers, but not by active GTP-loaded Gα subunits. Moreover, this PI3K activity had to be distinct from the previously identified protein tyrosine kinase (PTK)-sensitive PI3K isoforms, since activity was neither sensitive to phospho-Tyr peptides nor affected by depletion of p85 subunits from neutrophil cytosol. Purification of this PI3K activity from myeloid-derived cells or platelet cytosol yielded a protein complex of 210-220 kDa (Stephens LR, Cell, 1997; Tang X and Downes CP, J Biol Chem, 1997), that was composed of two subunits of ~110 and 101 kDa. This protein fraction was chromatographically and immunologically distinct from known PI3-kinases and was potently activated by Gβγ dimers in vitro. The coding DNA sequences were obtained by PCR-based approaches with degenerate oligonucleotide primers that have either been derived from

conserved regions of PI3Kα or have been deduced from peptide sequences of purified PI3K. The protein was called PI3Kγ (recommended by UniProt) or p110γ (alternative name). The coding sequence of the 101 kDa adaptor subunit was cloned by the peptide sequencing approach.

Regulation of PI3Kγ by Gβγ subunits and p101

Both recombinant PI3Kγ and PI3Kγ/p101 phosphorylate PI(4,5)P_2, PI(4)*P,* and PI on the 3' position of the inositol ring in vitro and are inhibited by Wortmannin (Stoyanov B, Science, 1995; Tang X and Downes CP, J Biol Chem, 1997). However, free and adaptor-associated PI3Kγ show differential preferences for phosphoinositides as well as differential sensitivities towards Gβγs in vitro. In association with p101, PI3Kγ prefers PIP_2 over PI as substrate and is more sensitive to stimulation by Gβγ subunits. While PI3Kγ alone is not, 2-4-, or 20-40-fold activated by recombinant Gβγ subunits in the presence of PIP_2 as substrate (Sugimoto Y, Proc Natl Acad Sci U S A, 1984; Krugmann S, J Biol Chem, 1999; Tang X and Downes CP, J Biol Chem, 1997; Maier U, J Biol Chem, 1999), enzymatic activity is increased 6-7-, 20-40-, or 60-fold by using PI as substrate (Krugmann S, J Biol Chem, 1999; Maier U, J Biol Chem, 1999; Leopoldt D, J Biol Chem, 1998). Differences between these studies likely depend on experimental conditions such as the presence of detergents, kind and location of the protein tag, use of human or porcine PI3Kγ, etc. PI3Kγ complexed to p101 is more sensitive to activation by Gβγ subunits in presence of PIP_2 as substrate as PI3Kγ alone (20-150-fold activation), but only poorly likes PI (3-25-fold stimulation) (Maier U, J Biol Chem, 1999; Krugmann S, J Biol Chem, 1999; Stephens LR, Cell, 1997). Gβγs do not affect the affinity (K_m) of PI3Kγ/p101 for ATP, but increase maximal PIP_2 turnover (V_{max}) (Tang X and Downes CP, J Biol Chem, 1997). In consistence with increased Gβγ-sensitivity in the presence of p101, this adaptor has a much higher affinity for Gβγ subunits than PI3Kγ, as it binds 5 times more Gβγs per mole input protein in binding assays (Stephens LR, Cell, 1997). This better binding efficiency is even more evident following coexpression of Gβγ with p101 or PI3Kγ in HEK293 cells, as Gβγs only promote efficient translocation of GFP-tagged p101 but not PI3Kγ to the plasma membrane (Brock C, J Cell Biol, 2003). Gβγ dimers having a geranylgeranylated Gγ subunit ($G\gamma_{2,\ 10,\ 12,\ 13}$) activate PI3Kγ/p101 much more efficiently (26-fold) than those having a farnesyl isoprenoid moiety (0, 5-6-fold) ($G\gamma_{1,\ 11}$, $G\gamma_{t\ (transducin)}$) (Kerchner KR, J Biol Chem, 2004; Maier U, J Biol Chem, 2000; Stoyanov B, Science, 1995). Farnesylated Gβγs associate equally well with PI3Kγ/p101, but are not able to stimulate enzymatic activity, maybe being compromised in inducing the required conformational changes. Switching of the CAAX-box of $G\gamma_2$ to get a farnesylated instead of geranylgeranylated subunit does not affect maximal PI3Kγ/p101 activation, however slightly decreases efficiency (higher EC_{50}). On the other hand exchange of the farnesyl with a geranylgeranyl isoprenoid moiety of $G\gamma_1$ or $G\gamma_{11}$ creates gain of function mutants that fully activate PI3Kγ/p101, but again with reduced efficiency. Gβγ subunits not only function, through p101, as PI3Kγ membrane translocators, but also allosterically stimulate lipid kinase activity of membrane-targeted PI3Kγ (Brock C, J Cell Biol, 2003). The relative importance of these two

mechanisms on endogenous PI3Kγ activation has not yet been investigated. Many Gβγ effectors such as phospholipase Cβ (PLCβ) are membrane-associated proteins and therefore modulated by allosteric activation. A third activating input into PI3Kγ may further derive from receptor interaction. In contrast to other heterotrimeric G protein regulated proteins, neither free nor dimeric PI3Kγ is substantially (max 1.5x) activated by active Gα subunits from different subfamilies like $G\alpha_{i1-3}$, $G\alpha_{s}$, $G\alpha_{o}$, and $G\alpha_{q}$ (Ramkumar V, J Biol Chem, 1993; Sugimoto Y, Proc Natl Acad Sci U S A, 1984; Tang X and Downes CP, J Biol Chem, 1997; Kerchner KR, J Biol Chem, 2004).
Characterisation of p101 truncation mutants indicates that the N-terminal region of p101 mediates PI3Kγ binding, while the C-terminus interacts with Gβγ subunits of heterotrimeric G-proteins (Voigt P, J Biol Chem, 2005). As the N- and C-terminus are highly conserved in p101, they may constitute new protein-binding domains. However, as the structure of p101 is completely unknown, it can not be excluded that truncations disturb proper protein folding influencing protein interactions indirectly. PI3Kγ is a globular protein with extensive interdomain interactions (Walker EH, Nature, 1999). Here already small deletions interfere with the functional integrity the enzyme. Increasing N-terminal truncations decrease basal activity of PI3Kγ and removal of more than the first 169 amino acids shuts off catalytic activity (Krugmann S, J Biol Chem, 1999). PI3Kγ is therefore not suitable for interaction site mapping by generation of deletion mutants. Since controversial results have been obtained by this method, the interaction site of p101 on PI3Kγ is undefined (Krugmann S, J Biol Chem, 1999; Maier U, J Biol Chem, 1999).
Most studies analysed p101 functions biochemically in vitro or with heterologous expression systems. The physiological importance of p101 could be demonstrated following generation of p101 knock-out mice (Suire S, Nat Cell Biol, 2006). p101 is required for neutrophil migration towards the GPCR-ligands C5a and fMLP. Moreover, neutrophil recruitment in vivo to the inflamed peritoneum also depends on p101 in a model of thioglycollate-triggered aseptic peritonitis.

Regulation of PI3Kγ by Gβγ subunits and p84

Mast cells were found to lack p101 expression, which prompted search for an alternative but homologous adaptor (Calvez R, Diss, 2004, University of Fribourg, Switzerland). p84 was discovered and comparative analysis showed that this adaptor shares several characteristics with p101. Both adaptors associate with PI3Kγ in coimmunoprecipitation assays following coexpression, and are required for fMLP- or Gβγ-induced PIP_3 production in heterologous expression systems (HEK293) (Brock C, J Cell Biol, 2003; Voigt P, J Biol Chem, 2006). However, whereas p101 potentiates PI3Kγ activation by Gβγ subunits in vitro and is translocated by them to the plasma membrane in cells (Stephens LR, Cell, 1997; Brock C, J Cell Biol, 2003), p84 does not share these characteristics (Kurig B, Proc Natl Acad Sci U S A, 2009). In the presence of p84 instead, Gβγ-dependent PI3Kγ activation is sensitive to inhibition of basal Ras activation (Kurig B, Proc Natl Acad Sci U S A, 2009) as well as cholesterol depletion (Bohnacker T, Sci Signal, 2009). Interestingly, cholesterol removal also blocks lysophosphatidic acid (LPA, GPCR ligand) induced PI3K activation in Vero cells, where it regulates PI3K/p85 compartmentalisation (Peres C, FEBS Lett, 2003). Mechanistic basics of p84 action are incompletely understood and require further investigations.

2.3 Transmembrane signal transduction by protein tyrosine kinase- and G protein-coupled receptors

PI3K class I family members couple to cell surface receptors and therefore regulate the conversion of external information into a cellular response. Class IA PI3Ks are canonically activated downstream of protein tyrosine kinase (PTK)-coupled receptors, while class IB member PI3Kγ is regulated by G protein-coupled receptors (GPCRs) (Fig. c).

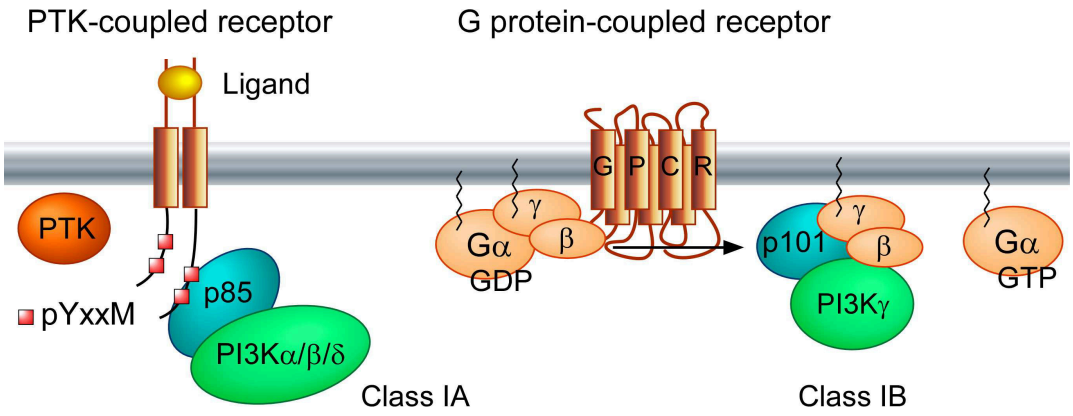

Fig. c: Activation of class I PI3Ks by cell surface receptors

2.3.1 Protein tyrosine kinase (PTK)-coupled receptors

Protein tyrosine kinase (PTK)-coupled receptors are either regulated by an intrinsic protein kinase activity contained in the cytoplasmic receptor tail or by association with an intracellular tyrosine kinase. While most PTK-coupled receptors are monomers, the insulin and insulin-like growth factor receptors are heterotetramers, being composed of two disulfide-linked membrane-spanning β-subunits and two extracellular α-subunits. Ligand binding generally triggers receptor dimerisation leading to kinase-mediated transphosphorylation of receptor tails or associated adaptor proteins. Phosphorylation sites lay in so-called immunoreceptor tyrosine-based activation motifs (ITAMs), which provide docking sites for the activation of downstream signalling proteins. The regulatory subunits of class IA PI3Ks, the "p85"s, specifically bind to phosphorylated YXXM motifs via their SH2 domains (Songyang Z, Cell, 1993). This brings the catalytic subunit in close proximity to the plasma membrane and its lipid substrate. Other domains of the regulatory and catalytic subunits govern further control of PI3K activation. Exact mechanisms regulating lipid kinase activation in vivo are poorly characterised. Examples of receptors that couple to class IA PI3Ks are the platelet-derived growth factor receptor (PDGF), the endothelial growth factor receptor (EGF), and the insulin receptor (IR). While p85 binds directly to the PDGF receptor tails, mechanisms of EGF-mediated PI3K activation are obscure. The IR phosphoryates the adaptor protein IRS1 (insulin receptor substrate 1), which subsequently recruits p85/PI3K.

2.3.2 G protein-coupled receptors (GPCRs)

G protein-coupled receptors (GPCRs) comprise the largest group of cell surface receptors. GPCRs are composed of a seven transmembrane domain and transmit signals through activation of receptor-associated heterotrimeric GTP-binding proteins (Pierce KL, Nat Rev Mol Cell Biol, 2002). Ligand binding triggers conformational changes that stimulate the release of GDP from the Gα subunit, which results in the exchange of the GDP with an abundantly available GTP molecule and the release of the Gα-associated Gβγ subunits. Both the active GTP-loaded Gα subunit as well as the Gβγ dimer are involved in the activation of downstream effector proteins. Some GPCRs stimulate adenylyl cyclase, while others activate phospholipase Cβ (PLCβ) and/or PI3K. Signalling specificity is achieved through the diversity of the Gα, Gβ, and Gγ subunits. All Gγ subunits are posttranslationally modified at the C-terminal CAAX motif by attachement of a 15-carbon farnesyl or 20-carbon geranylgeranyl group, which anchors the Gβγ dimer to membranes. PI3Kγ activation is sensitive to *B. Pertussis* toxin from the bacterium *Bordetella pertussis* (Davies SP, Biochem J, 2000; Sugimoto Y, Proc Natl Acad Sci U S A, 1984), which specifically blocks activation of heterotrimeric G-proteins of the $G_{i/o}$ family through ADP-ribosylation of the alpha subunit (Mangmool S and Kurose H, Toxins (Basel), 2011). Examples of G_i- and PI3Kγ-coupled GPCRs are the N-formyl peptide receptor (FPR) or the C5a complement receptor (C5aR). The FRP can be stimulated experimentally with the synthetic peptide N-formyl-methionyl-leucyl-phenylalanin (f-Met-Leu-Phe, fMLP), and is believed to be physiologically activated by N-formylated peptides derived from bacterial protein degradation or mitochondrial proteins upon tissue damage. fMLP and C5a trigger chemotaxis and oxidative burst in neutrophils in a PI3Kγ-dependent manner (Hirsch E, Science, 2000; Suire S, Nat Cell Biol, 2006).

2.4 Mast cells

2.4.1 Introduction to mast cells

Mast cells are tissue-resident immune cells of hematopoietic origin. They locate to all organs throughout the body such as skin, gut, and respiratory tract. They are particularly abundant around blood vessels and lymphatic microvessels. They have been discovered based on the unique staining of their secretory granules by different dyes. The mast cell is a phylogenetically old cell type and exists in all species with blood circulation. It develops from multipotent stem cells in the bone marrow (Kirshenbaum AS, J Immunol, 1991). Precursors leave the bone and enter the blood stream, from where they colonise the whole body and differentiate into mature cells under the influence of locally generated factors. Under homeostatic conditions, mast cell tissue homing and maintenance exclusively depends on the activation of the mast cell stem cell factor (SCF) receptor Kit by its ligand SCF, expressed as membrane-bound form on stromal cells (Galli SJ, Am J Pathol, 1993). Mice devoid of a functional Kit receptor or defective in SCF expression lack mast cells. Under inflammatory conditions, mast cells are directed to sites of tissue damage or infection via stromal and immune cell released cytokines in a Kit-independent manner. Mast cells are long-lived cells and can proliferate in the tissue. As mast cell maturation depends on the local micro-environment, they are a highly heterogeneous population. Differences occur in number,

morphology, mediator content, and responsiveness to various stimuli (variability of receptor expression). Based on histochemical and morphological properties, rodent mast cells have been classified into two major groups (Gurish MF and Boyce JA, J Allergy Clin Immunol, 2006). Connective tissue mast cells (CTMC) possess safranin-positive granules and reside in the submucosal connective tissue of the skin, peritoneal cavity, and respiratory tract. Mucosal mast cells (MMCs) are safranin-negative and are found the mucosal epithelium of the gastrointestinal tract. In contrast to CMTCs, MMCs develop in a T cell dependent manner, as this mast cell population is absent in athymic mice (Ruitenberg EJ and Elgersma A, Nature, 1976). MMCs expand rapidly upon T cell dependent immune responses to certain intestinal parasites. Further phenotypical differences are found for example in protease expression, serotonin and proteoglycan content, and stimulated eicosanoid release. Evidence of two principle mast cell populations has also been obtained in humans (Metcalfe DD, Physiol Rev, 1997). Here, classification has mainly been based on different protease contents of the secretory granules. While human MC_{TC}s contain tryptase and chymase, human MC_Ts only produce tryptase. In terms of tissue localisation and T cell dependence, MC_{TC}s mostly resemble rodent CTMCs, while MC_Ts are most similar to rodent MMCs.

Rodent and human mast cell characteristics (mod. from (Metcalfe DD, Physiol Rev, 1997)):

RODENTS	*Connective tissue mast cells (CTMC):*	*Mucosal mast cells (MMC):*
Location	submucosal connective tissues (skin, peritoneal cavity, respiratory tract)	mucosal epithelial surfaces (gastrointestinal tract (lamina propria)), mucosal surfaces)
Size	10-20 μm	5-10 μm
Staining	Safranin	Alcian blue
T cell dependence	no	yes
Protease content	Chymase (RMCP I, rat mast cell protease I)	Chymase (RMCP II, rat mast cell protease II)
Proteoglycans	Heparin	Chondroitin sulfate
Eicosanoids	PDG_2	PDG_2, LTC_4
HUMANS	*MC_{TC}*	*MC_T*
Location	skin, small intestine (submucosa), lymph nodes	alveolar tissue, small intestine (mucosa)
T cell dependence	no	yes
Protease content	Tryptase, Chymase, Carboxypeptidase, Cathepsin G	Tryptase

2.4.2 Mast cells are key players in allergy

Under normal physiological conditions, mast cells are thought to regulate tissue repair and remodelling, host defence, and neuroimmunoendocrine processes (Maurer M, Exp Dermatol, 2003). However, mast cells are more famous for their disease promoting roles in allergic and inflammatory diseases. They are key players in allergic rhinitis (hay fever), food allergy, contact dermatitis (eczema), allergic conjunctivitis, and anaphylactic shock and contribute to inflammation

in multiple sclerosis and rheumatoid arthritis (Maruotti N, Clin Rheumatol, 2007). Mast cells are activated in an immunoglobulin E (IgE)-dependent manner through the high-affinity receptor for IgE (FcεRI) or independently of IgE by complement receptors and Toll-like receptors. They mainly act through the plethora of inflammatory mediators and cytokines they can synthesize and secrete. Mast cells thereby modulate the function of blood vessels, smooth muscle, mucus glands, and immune cells (Fig. d).

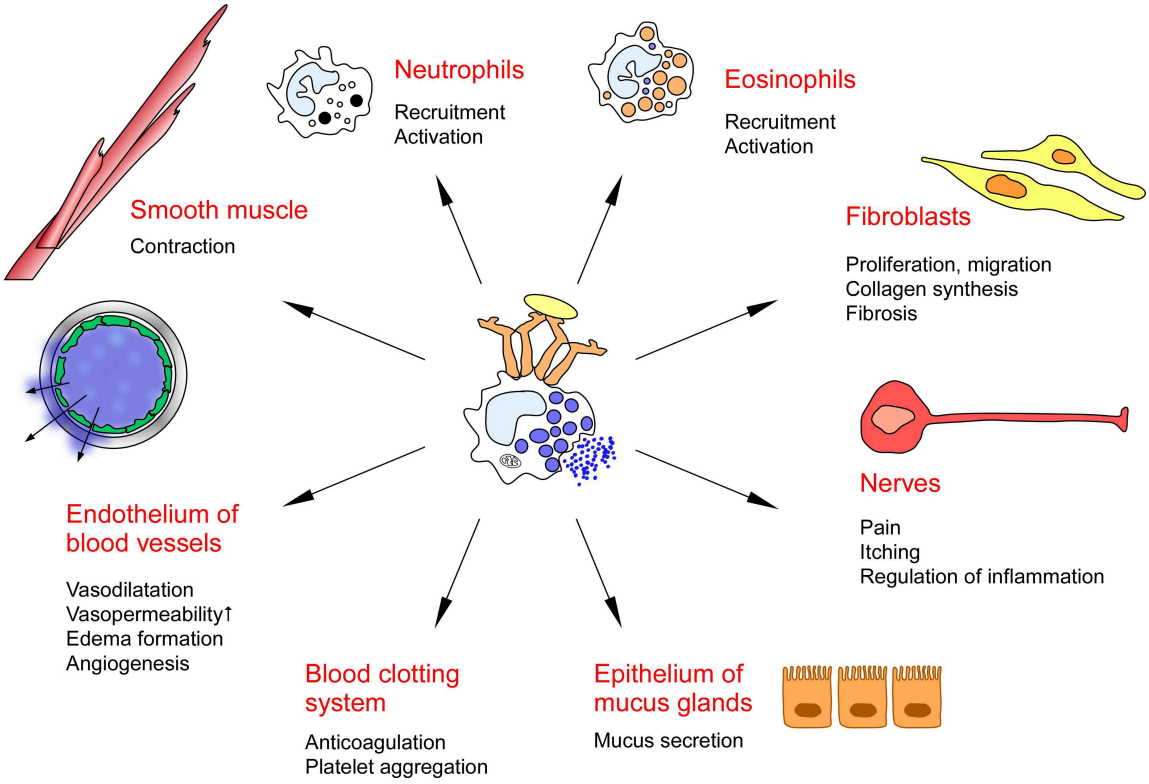

Fig. d: Targets of mast cells

Allergies develop after an inappropriate immune response to a normally harmless environmental agent, leading to the continuous production of IgE by B cells. The IgE binds to its receptor, FcεRI, on the mast cell surface and stimulates the production cytokines that promote mast cell recruitment and proliferation. The allergic response initiates open a second contact with the same allergen, which crosslinks the mast cell bound IgE molecules. This leads to receptor aggregation, triggering activation of intracellular signalling pathways that control the release of preformed proinflammatory mediators from secretory granules and the production of lipid mediators. These immediately released factors set up an inflammatory response, which is characterized by tissue swelling, heat, and redness. Histamine is the most potent granule associated mediator, acting on the endothelium to increase blood vessel diameter and permeability. The immediate reaction is followed by a late phase reaction that depends on the release of newly synthesized cytokines and chemokines. These chemotactic and cell-activating factors coordinate the recruitment of neutrophils and eosinophiles from the blood into the allergen-activated tissue (Fig. e).

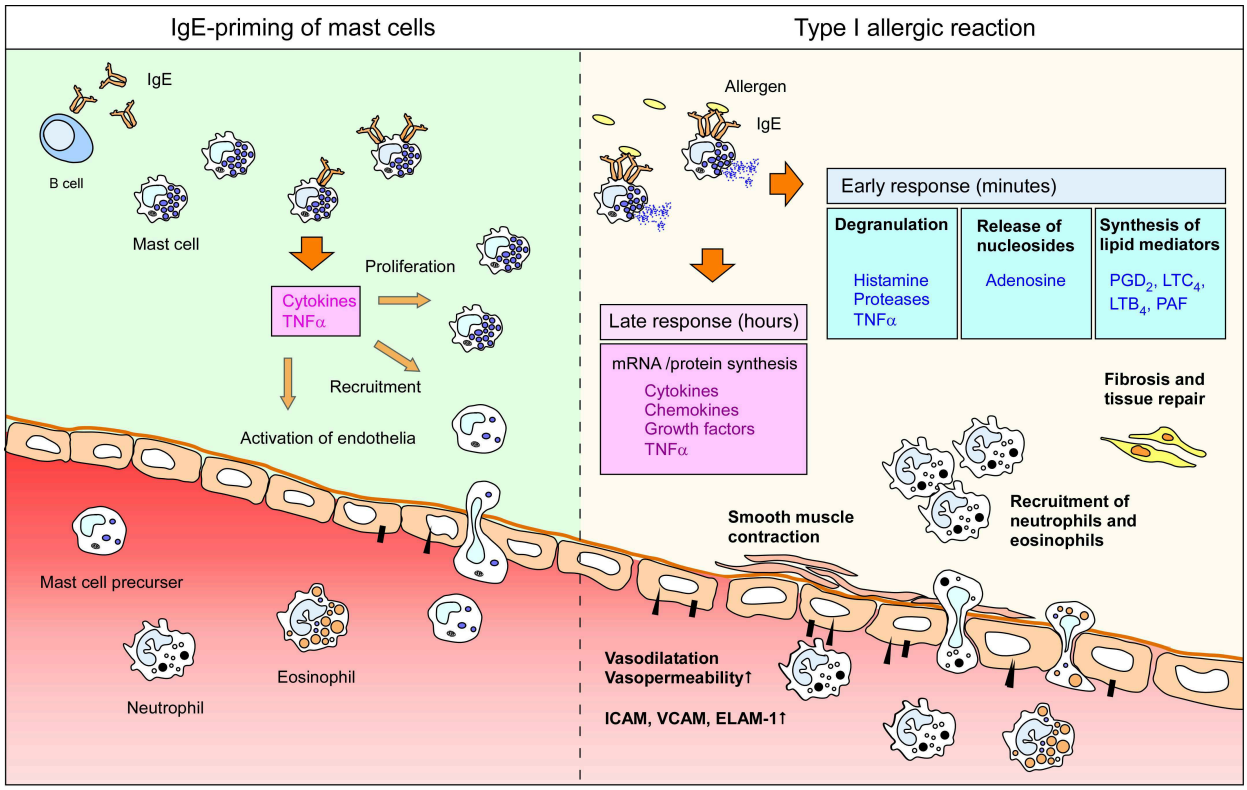

Fig. e: Mast cell activation in allergy.

3. Aims

3.1 Background

3.1.1 PI3K is essential to mast cell degranulation

Allergy is triggered by mast cell activation via the high-affinity IgE receptor (FcεRI). In order to develop new strategies to combat allergic disease, it is of interest to understand how receptor activation is coupled to granule exocytosis. Studies with the natural pan phosphoinositide 3-kinase (PI3K) inhibitor Wortmannin have identified PI3K as central regulator of mast cell degranulation (Marquardt DL, J Immunol, 1996). That the PI3K lipid product PIP_3 is a potent modulator of mast cell degranulation is further reflected by the hyperresponsive phenotype of inositol 5'-phosphatase (SHIP) knock-out mast cells, which degranulate in response to suboptimal antigen concentrations due to the continues, unrestricted accumulation of PIP_3. (Huber M, Proc Natl Acad Sci U S A, 1998). Due to the key role of PI3K in IgE/antigen-triggered signal transduction, it is of interest to understand how this lipid kinase is activated and regulates degranulation. First attempts to this goal delivered information on PI3K isoform-specificity, which became examinable after establishment of techniques to generate transgenic mice.

Analysis of PI3Kγ$^{-/-}$ mice showed that PI3Kγ regulates mast cell activation, immune cell migration, and respiratory burst (Hirsch E, Science, 2000; Sasaki T, Science, 2000; Li Z, Science, 2000; Laffargue M, Immunity, 2002; Del Prete A, EMBO J, 2004). Our group has demonstrated the essentiality of the PI3Kγ PI3K-isoform in mast cell degranulation in vivo in a model of passive systemic anaphylaxis (Laffargue M, Immunity, 2002). This acute life-threatening allergic disease depends on the body-wide activation of mast cells and the release of histamine. Experimentally this can be simulated in wild type mice by intravenous injection of IgE and antigen and the dye Evans blue as marker of endothelial barrier integrity. Whereas wild type mice react with a dramatic increase in vascular permeability, as visualised by leakage of Evans blue into the surrounding tissue, PI3Kγ$^{-/-}$ mice are protected. In order to study the molecular basis of PI3Kγ activation, mast cell degranulation was analysed at the cellular level using bone marrow-derived mast cells (BMMC) developed from wild type and PI3Kγ$^{-/-}$ mice.

3.1.2 PI3Kγ regulates mast cell hyperdegranulation via an autocrine activation loop

Consistent with defective mast cell activation in vivo, PI3Kγ$^{-/-}$ BMMCs also show an impaired degranulation response. As PI3Kγ has been shown to be activated by G protein-coupled receptors (GPCRs) (Stephens LR, Cell, 1997) and as the FcεRI is a protein tyrosine kinase (PTK)-coupled receptor, it has been investigated whether autocrine-paracrine pathways regulate mast cell degranulation. A good candidate GPCR-ligand was adenosine as this agent was known to be released by activated mast cells and tissue, is found at increased levels at inflamed sites of asthmatic people, and stimulates vascular leakage in a mast cell dependent manner after administration to mice (Marquardt DL, Proc Natl Acad Sci U S A, 1984; Forsythe P and Ennis M, Inflamm Res, 1999; Tilley SL, J Clin Invest, 2000). In accordance with these thoughts, PI3Kγ was found to enhance degranulation through adenosine/GPCR-triggered PIP_3 production. PI3Kγ thereby

functions as a mast cell hyperactivator boosting degranulation triggered by IgE/antigen (Laffargue M, Immunity, 2002) (Fig. f).

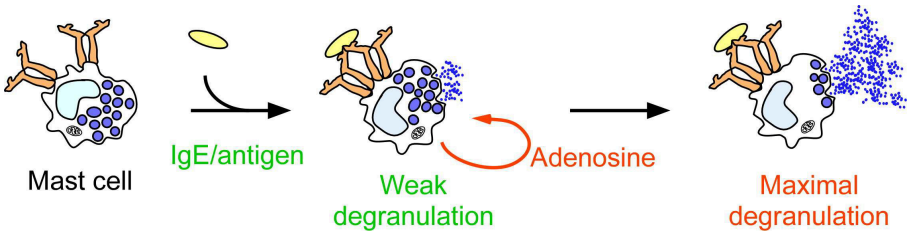

Fig. f: Model of mast cell hyperactivation by adenosine

Based on this and as pan PI3K inhibition completely blocks mast cell degranulation, it has been proposed a model, in which the FcεRI first engages class IA PI3K to trigger a weak degranulation response which is subsequently amplified by class IB PI3Kγ leading to full-scale mediator release. In analogy to B cell receptor signalling (Okkenhaug K, Science, 2002; Clayton E, J Exp Med, 2002; Koyasu S, Biochem Soc Trans, 2004), class IA PI3K has been expected to regulate Ca^{2+} mobilisation downstream of the FcεRI. Whereas inositol 5'-phosphatase SHIP was expected to counterregulate class IA PI3K signalling, PI3Kγ has been thought to escape receptor-proximal PIP_3 inactivation by SHIP (Fig. g) (Wymann MP, Biochem Soc Trans, 2003).

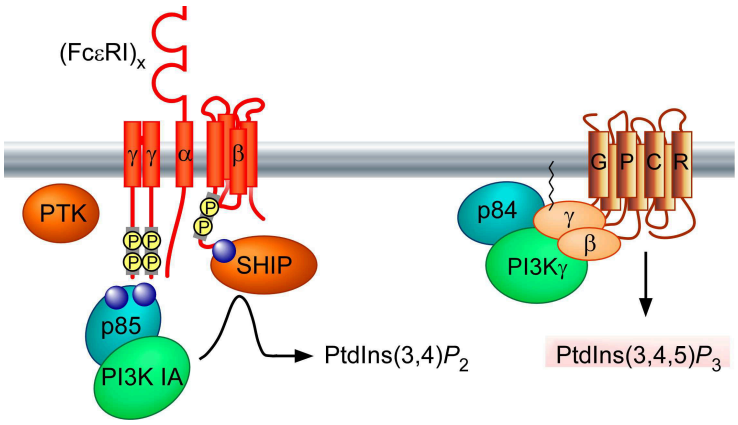

Fig. g: Model of SHIP action in mast cells

3.1.3 PI3Kγ relays more that adenosine/GPCR signalling

Despite PI3Kγ was identified to potentiate mast cell degranulation via adenosine/GPCR pathways, this mechanism does not completely explain the phenotype of PI3Kγ$^{-/-}$ BMMCs. In the study of Laffargue et al. (Laffargue M, Immunity, 2002), an observation remained unexplained: Blockade of GPCR or adenosine signalling interfered only partially with degranulation of wild type BMMCs, resulting in an inhibition that was much less severe than the phenotype of PI3Kγ$^{-/-}$ BMMCs. To take this into account, it must to be thought about other ways of PI3Kγ regulation. Consistently, PI3Kγ is required to relay much more that adenosine signalling, as this nucleoside is not needed for mast degranulation in vivo and in vitro. Whereas A3 adenosine receptor (A_3AR)$^{-/-}$ knock-mice are

resistant to vascular changes after intradermal adenosine injection, they are still sensitive to passive systemic anaphylaxis (Tilley SL, J Clin Invest, 2000). As well, $A_3AR^{-/-}$ BMMCs respond normally to IgE/antigen but not adenosine stimulation. These observations could either be explained by the involvement of other GPCR-ligands than adenosine or the existence of an unknown PI3Kγ activation pathway.

3.2 Starting point

3.2.1 Thapsigargin is a non-canonical PI3Kγ activator

Experiments with Thapsigargin opened the door to the discovery of a novel PI3Kγ activation mechanism. FcεRI aggregation culminates in the mobilisation of intra- and extracellular Ca^{2+} and degranulation. Ca^{2+} mobilising agents like Thapsigargin trigger mast cell degranulation at this receptor-distal step in wild type BMMCs (Fig. h). In contrast, PI3Kγ$^{-/-}$ BMMCs completely fail to degranulate following Thapsigargin stimulation. This was of surprise, as Ca^{2+} mobilisation triggered by the FcεRI was thought to be regulated by class IA PI3K and therefore to occur downstream of PI3K activation. Instead, these results showed essentiality of PI3K at a later/parallel step to Ca^{2+} mobilisation, and that this involves class IB PI3Kγ. Actually, it has already been observed that pan PI3K inhibition blocks degranulation induced by Ca^{2+} mobilising agents (Marquardt DL, J Immunol, 1996), but the significance of this has been inadvertently ignored. Importantly, whereas Thapsigargin triggers PI3K activation, as measured by PKB phosphorylation, in wild type BMMCs, this is also blocked in the absence of PI3Kγ. Thapsigargin therefore turned out to be a convenient tool to address non-canonical PI3Kγ activation in mast cells. Signalling mechanisms can thereby be analysed in a simplified cellular environment decoupled from upstream and other receptor-regulated events.

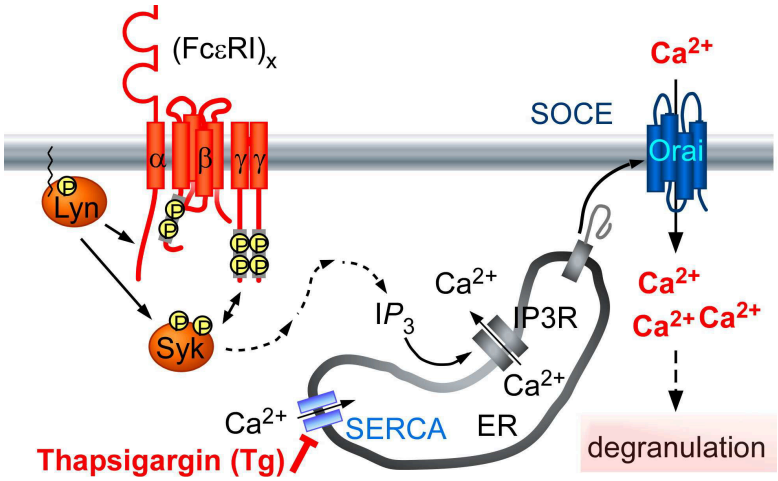

Fig. h: Thapsigargin triggers mast cell degranulation at the step of Ca^{2+} mobilisation (SOCE: store-operated Ca^{2+} entry; ER: endoplasmic reticulum; IP3R: inositol(1,4,5)-trisphosphate receptor; SERCA: sarco/endoplasmic reticulum Ca^{2+} ATPase; Orai: calcium release-activated calcium channel protein 1)

3.2.2 Objective

The goal of this study was to unravel GPCR-independent mechanisms of PI3Kγ activation downstream of the FcεRI. This has been started by the characterisation of Thapsigargin-triggerd PI3Kγ activation in BMMCs by former lab members. Some experimental data thereof are included in the manuscript figure section and are described there. Of most importance, analysis of protein kinase C (PKC)$\beta^{-/-}$ BMMCs showed that PI3K activation is blocked in the absence of this kinase. It was therefore of prior interest to unravel how PKCβ mechanistically connects to PI3Kγ, starting with the analysis whether this involves a direct or indirect mechanism. Contemporaneously, Thapsigargin-based results had to be incorporated into the analysis of FcεRI-mediated signal transduction. Additionally, it was necessary to think about alternative PI3Kγ activation models and to check compatibility with current literature.

To study mast cell signal transduction and exocytosis, bone marrow-derived mast cells (BMMCs) were preferred as model system. As we wanted to analyse PI3K signalling, it was of importance to work with primary cells and not cell lines that harbor mutations that promote constitutive PI3K activation. Activation mechanisms were studied with recombinant proteins in vitro or by exogenous protein expression in cultured cells. Signalling and degranulation were analysed in wild type, PI3K$\gamma^{-/-}$, and PKC$\beta^{-/-}$ BMMCs.

4. Results

Manuscript

Non-canonical Activation of PI3Kγ by Ca^{2+}/PKCβ in Mast Cells

Romy Walser[1], John E. Burke[2], Daniel Hess[3], Katja Björklöf[1,6], Muriel Laffargue[1,7], Michael Leitges[4], Emilio Hirsch[5], Roger L. Williams[2], Matthias P. Wymann[1]

[1]Institute of Biochemistry and Genetics, Department of Biomedicine, University of Basel, Basel, Switzerland;
[2]Medical Research Council, Laboratory of Molecular Biology, Cambridge, United Kingdom;
[3]Friedrich Miescher Institute for Biomedical Research, Basel, Switzerland;
[4]Biotechnology Centre, University of Oslo, Oslo, Norway;
[5]Department of Genetics, Biology and Biochemistry, University of Torino, Torino, Italy;
Present addresses: [6]Amgen Switzerland AG, Zug, Switzerland; [7]INSERM U563, Département Lipoprotéines et Médiateurs Lipidiques, Toulouse, France

Correspondence: romy.walser@unibas.ch

4.1 Abstract

Allergy depends on mast cell mediator release and stimulation of the high-affinity IgE receptor (FcεRI). Receptor clustering activates protein tyrosine kinases that coordinate Ca^{2+} mobilisation and protein kinase C (PKC) activation. Mast cell degranulation is blocked by pan phosphoinositide 3-kinase (PI3K) inhibition or genetic inactivation of class IB PI3Kγ. Adenosine amplifies receptor-triggered degranulation in an autocrine-paracrine manner via G protein-coupled receptor-coupled PI3Kγ. Here we demonstrate direct activation of PI3Kγ by the FcεRI and Ca^{2+} mobilising agents. PI3Kγ activation depends on high Ca^{2+} levels and PKCβ, which phosphorylates PI3Kγ on Ser582 in the helical domain. This is an interesting region as it constitutes a hot-spot of oncogenic PI3Kα mutations. Analysis of phosphorylation-mimicking mutants indicates that Ser582 acts as switch-site for PI3Kγ activation. We determined the PI3Kγ-p84 binding interphase and show that PI3Kγ is active in an adaptor subunit-free manner. Our data provide unexpected new insights into PI3-kinase regulation and underpin PI3Kγ's central role in allergy regulation.

4.2 Introduction

Allergic inflammation is driven by mediator release from mast cells. These immune cells of hematopoietic origin reside in vascularized tissue throughout the body. Allergies develop after an inappropriate immune response to a harmless environmental agent, leading to the production of allergen-specific immunoglobulin E (IgE) by B cells at sites of allergen exposure (Gould HJ and Sutton BJ, Nat Rev Immunol, 2008). Allergens activate mast cells by triggering aggregation of the high-affinity receptor for IgE (FcεRI) through crosslinking of receptor-bound IgE molecules.

FcεRI activation is coupled to the release of preformed pro-inflammatory mediators from secretory granules, the synthesis of lipid mediators, and the translationally or transcriptionally controlled generation of cytokines and chemokines. Mast cell activation in vivo promotes an immediate increase in vascular permeability leading to tissue swelling, which depends on activation of the endothelium by granule-released histamine (Nagai H, Biol Pharm Bull, 1995). Hours later, cytokines and chemokines orchestrate the recruitment of neutrophils and eosinophils from the blood to the affected tissue.

In order to find targets to treat allergic disease it is important to understand how receptor activation is coupled to granule release. The FcεRI is a tetrameric complex composed of the IgE-binding α chain, a β-chain, and two disulfide linked γ-chains (Ravetch JV and Kinet JP, Annu Rev Immunol, 1991). Receptor aggregation is coupled to the activation of membrane-anchored protein tyrosine kinase (PTK) Lyn (Nishizumi H and Yamamoto T, J Immunol, 1997). Lyn phosphorylates tyrosines in immunoreceptor tyrosine-based activation motifs (ITAMs) in the β- and γ-chains and thereby initiates both positive and negative signalling events (Kawakami Y, J Immunol, 2000; Hernandez-Hansen V, J Immunol, 2004; Xiao W, J Immunol, 2005). Phosphorylated ITAMs serve as docking sites for the Src homology 2 (SH2) domains of the tyrosine kinase Syk as well as the inositol-5'-phosphatase SHIP1 (Kimura T, J Biol Chem, 1996; Osborne MA, J Biol Chem, 1996). Syk functions as the master activator of mast cell degranulation, promoting Ca^{2+} mobilisation through coordination of phospholipase Cγ (PLCγ) activation. Syk phosphorylates the adaptor proteins LAT and SLP-76 as well as PLCγ (Costello PS, Oncogene, 1996; Scharenberg AM and Kinet JP, J Allergy Clin Immunol, 1994). Phosphorylated LAT recruits SLP-76, which indirectly binds to LAT via its Grb2/Gads-binding domain (Saitoh S, J Exp Med, 2003; Kambayashi T, Mol Cell Biol, 2010; Zhu M, J Exp Med, 2004). Both of these adaptors, alone and in cooperation, promote the recruitment of phospholipase C (PLC)γ1 and PLCγ2 to the plasma membrane, where PLCγ gets fully activated by phosphorylation (Pivniouk VI, J Clin Invest, 1999; Kettner A, Mol Cell Biol, 2003; Wang D, Immunity, 2000; Wen R, J Immunol, 2002; Saitoh S, Immunity, 2000). PLCγ hydrolyses phosphatidylinositiol(4,5)bisphospate (PI(4,5)P_2) to generate inositol(1,4,5)trisphosphate (IP3) and diacylglycerol (DAG). IP3 promotes Ca^{2+} release from the endoplasmatic reticulum (ER), while DAG and Ca^{2+} regulate protein kinase C (PKC) activation. ER-store depletion is coupled by store-operated Ca^{2+} entry (SOCE) to the influx of extracellular Ca^{2+}. STIM1 thereby serves as luminal Ca^{2+} sensor and triggers assembly of Orai1 into functional plasma membrane Ca^{2+} channels (Baba Y, Nat Immunol, 2008; Vig M, Nat Immunol, 2008). Both Ca^{2+} mobilisation and PKC activation are recognized as central steps in mast cell degranulation. Likewise essential is activation of phosphoinositide 3-kinase (PI3K), which generates the lipid second messenger PI(3,4,5)P_3 (PIP_3). While blockade of PIP_3 production by Wortmannin completely inhibits degranulation (Marquardt DL, J Immunol, 1996; Pendl GG, Int Arch Allergy Immunol, 1997), blockade of PIP_3 degradation promotes hypersensitivity to suboptimal antigen concentrations as well as degranulation by the non-secretagogue stem cell factor (SCF) (Huber M, Proc Natl Acad Sci U S A, 1998). PIP_3 positively modulates mast cell degranulation by enhancing Ca^{2+} mobilisation by recruiting PLCγ and Brutons tyrosine kinase (Btk) to the plasma membrane (Kawakami Y, J Immunol, 2000; Kitaura J, J Exp Med, 2000; Iwaki S, J Biol Chem, 2005). Mast cell degranulation is counterregulated at the step of

PI3K activation by the inositol phosphatase SHIP1, which dephosphorylates PIP_3 to PI(3,4)P_2 (Huber M, Proc Natl Acad Sci U S A, 1998). SHIP1 functions a signal terminator, but also as a "gate-keeper" to prevent degranulation at sub- and supraoptimal antigen concentrations (Gimborn K, J Immunol, 2005). Mast cell degranulation finishes by the docking and fusion of granules to the plasma membrane (Deng Z, Biophys J, 2009). While early signalling events are well characterized, it is not much known about how Ca^{2+}, PKC, and PI3K connect to granule release.

Protein kinases C (PKCs) are serine/threonine kinases that are composed of an N-terminal regulatory and a C-terminal catalytic domain. In quiescent cells they are located in the cytosol in an inactive state, but translocate to plasma membrane upon cell surface receptor stimulation. The family has been grouped into three classes. PKCα, PKCβ, and PKCγ belong to the conventional PKCs (cPKCs) and are activated by Ca^{2+}, DAG, and phospholipid-binding. Of these cofactors, novel PKCs (nPKC; PKCδ, ε, η, θ) do not require Ca^{2+} for activation, while atypical PKCs (aPKC; PKCζ, ι/λ) do not depend on Ca^{2+} nor DAG.

FcεRI activation is followed by translocation of several PKC isoforms (Ozawa K, J Biol Chem, 1993). Despite this, analysis of PKC knock-out mast cells showed so far only a requirement of PKCβ for mast cell degranulation (Nechushtan H, Blood, 2000), while PKCα, PKCδ, or PKCε are dispensable (Fehrenbach K, J Immunol, 2009; Leitges M, Mol Cell Biol, 2002; Lessmann E, Int Immunol, 2006). Although PKCβ is an essential degranulation regulator, its substrates remained obscure. In rat basophilic leukemia (RBL-2H3) cells, antigen or calcium ionophore stimulate the phosphorylation of myosin heavy and light chains at sites, that are found to be targeted by PKC in vitro kinase assays (Ludowyke RI, J Biol Chem, 1989; Ludowyke RI, J Immunol, 1996; Ludowyke RI, J Immunol, 2006). Apart from regulation of cytoskeletal changes, PKC has been speculated to regulate granule-membrane fusion. With respect to this, IgE/antigen was found to trigger SNAP-23 phosphorylation at two residues in rodent mast cells, of which one site is conserved (Hepp R, J Biol Chem, 2005). Despite phosphorylation is sensitive to PKC inhibition, IκB kinase (IKK)β is rather the direct kinase (Suzuki K and Verma IM, Cell, 2008). Consistently, SNAP-23 is a poor substrate for PKC in vitro (Foster LJ, Biochemistry, 1998) in contrast to IKKβ (Suzuki K and Verma IM, Cell, 2008). By now nothing is known about the role of the mentioned sites nor their relevance for degranulation (Bresnick AR, Curr Opin Cell Biol, 1999; Morgan A, Biochem Soc Trans, 2005; Snyder DA, Cell Biochem Biophys, 2006).

Phosphoinositide 3-kinase (PI3K) activation is triggered by diverse cell surface receptors to regulate both homeostatic as well as transient cellular functions. Basal growth factor-induced PI3K signalling regulates cell survival and proliferation, whereas acute PI3K activation is essential to specific cellular tasks, like regulated secretion, adhesion, and chemotaxis (Foukas LC, Proc Natl Acad Sci U S A, 2010; Hirsch E, Science, 2000; Del Prete A, EMBO J, 2004). Through regulation of these processes, PI3K confers a risk to cancer development or chronic inflammation once regulatory mechanisms become inoperative (Samuels Y, Science, 2004; Jaiswal BS, Cancer Cell, 2009; Rudd ML, Clin Cancer Res, 2011; Rommel C, Nat Rev Immunol, 2007).

Receptor-coupled PI3Ks belong to the class I family, being composed of the subgroups IA and IB. The class IA PI3Ks - PI3Kα, β, and δ - are canonically activated by protein tyrosine kinase (PTK)-coupled receptors and associate with a p85/p55 regulatory protein (p85α, p50α, p55α; p85β; p55γ).

The only class IB member PI3Kγ is activated downstream of heterotrimeric G protein-coupled receptors (GPCRs) and interacts with the adaptors p101 or p84 (also known as $p87^{PIKAP}$) (Stephens LR, Cell, 1997; Suire S, Curr Biol, 2005).

PI3Ks are lipid kinases that transfere a phosphate group from ATP to the 3' hydroxyl group of the inositol ring of phosphoinositides. These lipid molecules then serve as docking sites for the recruitment of downstream effectors. Class I PI3Ks catalyse the formation $PI\mathit{P}_3$, and thus transduce downstream signalling through the recruitment of pleckstrin homology (PH) domain containing proteins to the plasma membrane. The best-known downstream effector of PI3K is protein kinase B (PKB), which after its recruitment to the plasma membrane, gets activated by phosphorylation on Thr308 and Ser473. Detection of PKB phosphorylation serves as convenient readout to measure PI3K activation.

PI3Kγ has been discovered to exist in a tight complex with p101 in myeloid-derived cells (Stephens LR, Cell, 1997). p101 sensitises PI3Kγ for activation by Gβγ subunits of trimeric G proteins in vitro and heterologous expression systems, and is essential for chemotaxis of neutrophils towards GPCR-ligands (Stephens LR, Cell, 1997; Brock C, J Cell Biol, 2003; Suire S, Nat Cell Biol, 2006). As mast cells were found to lack p101 expression, a homologous PI3Kγ adaptor, that shared 30% sequence identity with p101, was identified and called p84 (Suire S, Curr Biol, 2005; Bohnacker T, Sci Signal, 2009). Ectopically expressed p84 coimmunoprecipitates with PI3Kγ and supports Gβγ-dependent PtdIns(3,4,5)P_3 production in HEK293 cells (Brock C, J Cell Biol, 2003; Voigt P, J Biol Chem, 2006). However, in contrast to p101, p84 does not potentiate PI3Kγ activation by Gβγ subunits in vitro nor is it translocated by them to the plasma membrane (Kurig B, Proc Natl Acad Sci U S A, 2009). p84 action is incompletely understood, but sensitive to overexpression of the GTPase activating domain of neurofibromin or cholesterol depletion (Kurig B, Proc Natl Acad Sci U S A, 2009; Bohnacker T, Sci Signal, 2009).

While inhibitor based studies identified PI3K to be central to mast cell degranulation, insights into PI3K-isoform specificities awaited availability of isoform-targeted transgenic mice. We have shown that deletion of PI3Kγ in mice blocks FcεRI-dependent mast cell degranulation in vivo (Laffargue M, Immunity, 2002). Analysis of bone marrow-derived mast cells (BMMCs) has shown that PI3Kγ functions as an amplifier of mast cell degranulation in an autocrine-paracrine manner via adenosine signalling through G protein-coupled receptors (GPCRs). However, as this pathway only partially contributes to degranulation, it does not explain the strong degranulation defect of $PI3K\gamma^{-/-}$ BMMCs (Saito H, J Immunol, 1987; Laffargue M, Immunity, 2002; Endo D, Int Arch Allergy Immunol, 2009). Furthermore, despite PI3Kγ is activated by adenosine via the A3 adenosine receptor, A_3AR knockout mice and BMMCs are still sensitive to passive systemic anaphylaxis and antigen-induced degranulation, respectively (Tilley SL, J Clin Invest, 2000; Gao Z, Mol Pharmacol, 2001).

As it must exist another pathway to PI3Kγ in BMMCs, we explored novel activation mechanisms. A convenient tool to that goal turned out to be Thapsigargin, since degranulation induced by this Ca^{2+} mobilising agent was blocked in $PI3K\gamma^{-/-}$ BMMCs. By pharmacological and genetic targeting strategies, we identified that PI3Kγ activation depends on store-operated Ca^{2+} entry and subsequent

PKCβ activation. PKCβ activates PI3Kγ by phosphorylation of Ser582 in an adaptor-independent manner. Coincidentally we determined the p84 binding interphase on PI3Kγ. Our results change our view on PI3K regulation and show for the first time how a PTK-coupled receptor connects to class IB PI3Kγ.

4.3 Results

4.3.1 Thapsigargin-induced mast cell degranulation depends on PI3Kγ, but not Gβγ subunits of heterotrimeric G proteins

Activation of the high-affinity receptor for IgE (FcεRI) on mast cells by IgE and antigen triggers granule exocytosis and the release of proinflammatory mediators. PI3Kγ is essential to mast cell degranulation in mice in a model of passive systemic anaphylaxis as well as in bone marrow-derived mast cells (BMMCs) in vitro (Laffargue M, Immunity, 2002). A central step in signalling to mast cell degranulation is the mobilisation of extracellular Ca^{2+} by store-operated Ca^{2+} entry (SOCE) (Beaven MA, J Biol Chem, 1984; Ma HT and Beaven MA, Crit Rev Immunol, 2009). As Ca^{2+} mobilising agents like Thapsigargin and ionophores trigger degranulation at this step, they are of valuable help to dissect receptor proximal from distal signalling events. In order to delineate PI3Kγ activation in BMMCs, we compared degranulation of wild type and PI3Kγ$^{-/-}$ BMMCs in response to receptor activation and Ca^{2+} influx. Following loading with anti-dinitrophenyl (DNP) specific IgE overnight, FcεRI receptors of wild type and PI3Kγ$^{-/-}$ BMMCs were activated through crosslinking of the bound IgEs with multivalent antigen (DNP_{30-40}-human serum albumin). In the same experiment, BMMCs were also directly stimulated with the plant compound Thapsigargin to trigger SOCE-induced degranulation. Thapsigargin, an inhibitor of the Ca^{2+} influx pumps of the sarco/endoplasmatic reticulum, activates the plasma membrane Ca^{2+} channels indirectly by promoting passive depletion of the intracellular Ca^{2+} stores (Thastrup O, Proc Natl Acad Sci U S A, 1990). Degranulation, as measured by the release of β-hexosaminidase into the cell supernatant, was impaired in PI3Kγ$^{-/-}$ BMMCs both following stimulation with IgE/DNP or Thapsigargin (Figure 1A). Further, PI3Kγ deficiency caused a similar blockade in degranulation as the treatment of wild type BMMCs with the pan PI3K inhibitor Wortmannin (Figure 1A). These observations imply that mast cell degranulation mainly depends on the PI3Kγ PI3K-isoform and that PI3Kγ is activated at a step downstream of Ca^{2+} mobilisation. These results were surprising to us, as PI3Kγ so far has only been reported to be activated downstream of G protein-coupled receptors (GPCRs) (Stephens L, Cell, 1994; Stephens LR, Cell, 1997). How Thapsigargin engages PI3Kγ? Since impaired FcεRI-induced degranulation of PI3Kγ$^{-/-}$ BMMCs has been related to defective PI3Kγ activation by the autocrine released GPCR ligand adenosine (Laffargue M, Immunity, 2002), we analysed whether Thapsigargin-induced degranulation is also potentiated by autocrine-regulated mechanisms. To test this hypothesis we preincubated wild type and PI3Kγ$^{-/-}$ BMMCs with adenosine deaminase (ADA), which inactivates adenosine by converting it to inosine, before stimulation. While IgE/DNP stimulated degranulation was partially reduced in wild type BMMCs in the presence of ADA, Thapsigargin-induced degranulation was insensitive to ADA treatment (Figure 1B). Consistently,

Thapsigargin-induced PI3K activation, as measured by activation of its downstream target protein kinase B (PKB), was also not affected by ADA treatment (Figure 1C, right). In contrast, ADA efficiently blocked PKB phosphorylation following stimulation with adenosine (Figure 1C, left). PI3Kγ activation by GPCRs is blocked by *B. Pertussis* Toxin (*P*Tx) (Stephens L, J Biol Chem, 1993; Laffargue M, Immunity, 2002) that inhibits activation heterotrimeric G-protein of the $G_{i/o}$ family by ADP-ribosylation of the G_α subunit (Mangmool S and Kurose H, Toxins (Basel), 2011). In order to exclude the possibility that Thapsigargin activates PI3Kγ through release of other GPCR-ligands than adenosine, we blocked GPCR signalling by preincubation with *P*Tx. While Thapsigargin-induced PKB activation was insensitive to *P*Tx, adenosine-mediated PI3Kγ activation was abrogated (Figure 1D). Blocked PKB phosphorylation in PI3Kγ$^{-/-}$ BMMCs shows again that Thapsigargin engages exclusively the PI3Kγ PI3K isoform (Figure 1C/D). All in all, these data show that Thapsigargin-induced PI3Kγ activation and degranulation does not depend on GPCR/Gβγ-coupled PI3Kγ. Conclusively it must exist a non-canonical route to PI3Kγ in BMMCs.

4.3.2 Thapsigargin-induced PI3Kγ activation depends on an influx of extracellular Ca^{2+}

To ensure that Thapsigargin-induced PI3Kγ activation depends on its property to trigger Ca^{2+} mobilisation, we performed stimulations under Ca^{2+} free conditions. To capture the calcium ions in the medium, wild type BMMCs were preincubated for 5 min with the Ca^{2+} chelating compound EDTA prior to stimulation. Thapsigargin-induced PKB phosphorylation was blocked the presence of EDTA (Figure 2A, left). As well, PKB phosphorylation triggered by another Ca^{2+} mobilising agent, the calcium ionophore ionomycin, was blocked following Ca^{2+} chelation with EDTA (Figure 2A, right). To evaluate that not only extracellular Ca^{2+}, but also its influx into the cell is required for PI3Kγ activation, BMMCs were incubated with the membrane permeable Ca^{2+} chelator BAPTA/AM to capture mobilised Ca^{2+} intracellularly. Again, PKB activation was blocked by Thapsigargin, but not by interleukin 3 (IL-3) or adenosine (Ade), which activate PI3K by distinct pathways that do not require Ca^{2+} mobilisation (Figure 2B).

Next we determined the intracellular Ca^{2+} concentrations required to trigger PI3Kγ activation. To this end, BMMCs, loaded with the fluorescent Ca^{2+} sensing dye Fura-4F, were stimulated in the presence of different extracellular Ca^{2+} concentrations to modulate maximal stimulus-triggered Ca^{2+} uptake. After stimulation with Thapsigargin, the increase in Fura fluoresence was measured with a photospectrometer, and concomitantly (at 2 min) some cells were removed out of the cuvette and processed for quantification of PKB activation by immunoblotting. PKB phosphorylation was plotted as function of the calculated intracellular Ca^{2+} concentrations $[Ca^{2+}]_i$. Graphical illustration of the data shows, that Thapsigargin-induced PKB activation follows a switch-on kinetic mechanism (Figure 2C). As long as the intracellular Ca^{2+} levels are below ~630 nM PI3Kγ is off, but otherwise on. Panel 2D shows that PI3Kγ activation is blocked at extracellular Ca^{2+} concentrations below physiological levels, and represents a Western blot used to generate the data shown in Fig 2C. While Thapsigargin and IgE/DNP trigger store-operated Ca^{2+} entry (SOCE), GPCR-coupled receptors mobilise Ca^{2+} only from internal stores (Ramkumar V, J Biol Chem, 1993), and therefore do not activate Ca^{2+}-sensitive PI3Kγ. While Thapsigargin triggers an

intracellular Ca^{2+} rise to more than 1 μM, IB-MECA, an A3 adenosine receptor (A_3AR) agonist, reaches maximal levels of only about 160 nM (Figure 2E). GPCR-triggered Ca^{2+} mobilisation is sensitive to *B. Pertussis* toxin (*P*Tx), as it depends on inositoltriphosphate (IP3) production by Gβγ-sensitive phospholipase C β (PLCβ). As expected, Thapsigargin-induced Ca^{2+} mobilisation is not affected by this G protein inhibitor (Figure 2E).

4.3.3 PKCβ relays Ca^{2+} mobilisation to PI3Kγ activation

Next we looked for candidates that may couple Ca^{2+} mobilisation to PI3Kγ activation. One candidate was the protein kinase C (PKC) family, which has been subdivided into three groups based on cofactor requirements for activation. Only conventional PKCs (cPKCs) require Ca^{2+} for activation, but not novel PKCs (nPKCs) or atypical PKCs (aPKCs), which only depend on DAG or neither Ca^{2+} nor DAG, respectively. A further hint for an involvement of PKC in PI3Kγ activation came from our observation that the PKC activator phorbol 12-myristate 13-acetate (PMA) triggers PKB phosphorylation in BMMCs. We tested a panel of PKC-inhibitors for inhibition of PI3K activation in wild type BMMCs. After a 20 min preincubation time with the inhibitors, BMMCs were stimulated with Thapsigargin, PMA, or adenosine, and PI3K activation was analysed by phospho-PKB immunoblotting. Broad-spectrum PKC-inhibitors (Ro318425, Gö6983), a conventional/atypical PKC-inhibitor (Gö6976), and a conventional PKC-inhibitor (PKC412) substantially blocked PKB phosphorylation both in response to stimulation with Thapsigargin or PMA (Figure 3A, Figure S1A). Rottlerin, which selectivity for PKC has been questioned (Davies SP, Biochem J, 2000; Soltoff SP, Trends Pharmacol Sci, 2007) since being published to be a PKCδ-specific inhibitor (Gschwendt M, Biochem Biophys Res Commun, 1994), had no effect on PKB activation. On the other hand, GPCR-dependent PI3Kγ activation by adenosine was resistant to inhibition of PKC (Figure S1B). The reduction in PKB activation in the presence of increasing concentrations of PKC412 correlated well with an inhibition of Thapsigargin- or IgE/DNP-induced mast cell degranulation (Figure 3B).

In order to determine which isotype of conventional PKC is involved in PI3Kγ activation, we analysed BMMCs developed from the bone marrow of PKCα, PKCβ, and PKCγ knock-out mice. Whereas PKB activation was blocked in $PKC\beta^{-/-}$ BMMCs in response to stimulation with PMA or Thapsigargin (Figure 3C), this defect was not observed in $PKC\alpha^{-/-}$ or $PKC\gamma^{-/-}$ BMMCs (Figure S1C). Interestingly phosphorylation of T308 of PKB was completely blocked after PI3K-inhibition with Wortmannin, but not phosphorylation of S473, which was only partially affected (Figure 3C, lane 6 and 9). PKB activation requires phosphorylation at both positions, which is mediated by two different kinases. Phosphorylation of T308 in the activation loop is strictly mediated by phosphoinositide-dependent kinase 1 (PDK1) and depends on its PH-domain that mediates recruitment to PI3K-produced PIP_3. Mechanisms of S473 phosphorylation are less clearly defined, but depend on distinct kinases in different cell types and signalling pathways. In in vitro assays and partially in mast cells, it has been shown that PKCβ2 can function as a S473 kinase (Kawakami Y, J Biol Chem, 2004). Since only T308 phosphorylation is strictly dependent on PIP_3 production, we favoured to use this site as readout for PI3K activation hereinafter. Whereas PMA and

Thapsigargin depend on PKCβ for PI3K activation (Figure 3C), PKB phosphorylation is not impaird in PKCβ$^{-/-}$ BMMCs in response to adenosine which signals through GPCR-coupled PI3Kγ nor the cytokines interleukin-3 (IL-3) or stem cell factor (SCF) which activate class IA PI3K (Figure 3D). FcεRI-triggered degranulation is reported to be impaired both in PI3Kγ$^{-/-}$ and PKCβ$^{-/-}$ BMMCs (Laffargue M, Immunity, 2002; Nechushtan H, Blood, 2000). We herein confirm these findings and additionally show that degranulation is blocked to a similar extent upon knock-out of either protein, both following stimulation with IgE/DNP (Figure 3E) or Thapsigargin (Figure S1D). Since the direct result of PI3Kγ activation is PtdIns(3,4,5)P_3 production, we measured formation of this membrane lipid in PKCβ$^{-/-}$ and PKC-inhibitor treated BMMCs. BMMCs were labelled metabolically with [^{32}P]-orthophosphate for 4 hours, followed by stimulation with adenosine, Thapsigargin, or PMA. Cellular lipids were extracted, deacylated, and analysed by high performance liquid chromatography (HPLC). Both genetic and pharmacological targeting of PKCβ completely blocks PIP_3 production in BMMCs by Thapsigargin or PMA, but not adenosine (Figures 3F, G). Panel 3F shows PIP_3 peaks of representative HPLC chromatograms, and quantifications of PIP_3 production are displayed in graphical form in panel 3G. PIP_3 production in response to PMA occurs very fast and follows transient kinetics, producing a peak of PIP_3 at ~30 seconds after stimulation (Figure 3H).

4.3.4 PKCβ interacts with and phosphorylates PI3Kγ

PKCβ-dependent PIP_3 production occurred quickly and efficiently and was sensitive to long-term genetic and short-term small molecule-based PKC inactivation. As a next step, we examined whether PKCβ functions mechanistically as direct PI3Kγ activatior. To check this hypothesis, we first analysed whether PKCβ and PI3Kγ are interaction partners, which we tested by the means of coimmunoprecipitation assays. We coexpressed PI3Kγ with different PKCβ2 constructs (Figure 4A) in HEK293 cells and immunoprecipitated either PI3Kγ or HA-tagged PKCβ. Upon capturing of PI3Kγ, only the catalytic domain (cat) and the pseudosubstrate deletion mutant (Δps) of PKCβ2 copurified with PI3Kγ, but not the wild type full-length enzyme (Figure 4B, left). Similarly, upon immunoprecipitation of PKCβ2, only the PKCβ2 cat fragment and the Δps deletion mutant copurified PI3Kγ (Figure 4B, right). PKCs are found in an inactive closed conformation in quiescent cells, which is mechanistically mediated through an intraprotein interaction between the pseudosubstrate (ps) domain and the kinase domain (KD). Since PKCβ interacts with PI3Kγ only in its open conformation, indicates that PKCβ has first to be activated by cofactor binding in cells.
Since PKCβ is a protein kinase and PI3Kγ an interaction partner, we wanted to know whether PI3Kγ is a PKC substrate. Recombinant GST-tagged wild type (PI3Kγ wt) and kinase-inactive PI3Kγ (PI3Kγ KR) were incubated in an in vitro kinase assay with recombinant PKCβ2 in the presence of 10 μM ATP and [γ^{32}P]-ATP. After 30 min of incubation, the two proteins were separated by SDS-PAGE and phosphate incorporation into PI3Kγ was quantified by phosphorimager technology. PKCβ phosphorylates both wild type and kinase-dead PI3Kγ (Figure 4C, lanes 5-8). Wild type PI3Kγ autophosphorylates on its C-terminal tail on Ser1101 (Czupalla C,

Rapid Commun Mass Spectrom, 2003), and this activity is seen in lane 1 and 3 of figure 4C. Since PKCβ-mediated phosphorylation was about twice as intense as PI3Kγ autophosphorylation, PI3Kγ is a reasonable substrate for PKCβ.

In order to determine the PKCβ-specific phosphorylation sites, in vitro phosphorylated and trypsin-digested kinase-inactive PI3Kγ was analysed by liquid chromatography tandem mass spectrometry (LC-MSMS). A peptide with the sequence YES(582)LKHPK could be identified both phosphorylated on Ser582 as well as non-phosphorylated. Representative spectra of both peptides are shown in Figure S2A/B. Using a MRM (multiple reaction monitoring) method (Figure S2C) we could clearly show that phosphorylation was not present in the assay without PKCβ or when a PKC-inhibitor was used (Figure 4D, upper half). Furthermore the phosphorylation could also be detected with MRM in vivo after stimulation of BMMCs with PMA or IgE/DNP but not without stimulation (Figure 4D, lower half). Although the stimulation time for IgE/DNP was not optimal (see Figure S3G), the phosphopeptide could be clearly detected.

Inspection of the amino acid residues surrounding S582 shows that this region assorts quite well with a published optimal substrate motif for PKCβ determined by peptide library screening (Figure 4E) (Nishikawa K, J Biol Chem, 1997). Furthermore, S582 is conserved in higher vertebrates such as mammals and birds (Figure 4F). Mast cells have been found in all classes of vertebrates including as well amphibians and fish (Mulero I, Proc Natl Acad Sci U S A, 2007). Interestingly, only mast cells from an evolutionarily advanced phylogenetic order of fish, the Perciformes, store histamine in their granules und use it as inflammatory mediator (Mulero I, Proc Natl Acad Sci U S A, 2007). Other fish species and also amphibians lack histamine (or serotonin) and do not respond to histamine administration. The PKC-PI3Kγ pathway might therefore have evolved at about the same time as histamine started to regulate immunity. Sequence comparison of class I PI3Ks shows that S582 is an isoform-specific regulatory site, as only PI3Kγ contains a phosphorylatable amino acid residue at this position (Figure S2D).

4.3.5 PI3Kγ phosphorylation depends on Ca^{2+} and PKCβ and S582 positively regulates PI3Kγ's lipid kinase activity

To be able to monitor PI3Kγ phosphorylation in vivo, we requested the production of phospho-Ser582 specific polyclonal antibodies by commercial ways. To validate specificity of the antibodies, we mutated Ser582 of PI3Kγ to alanine and analysed whether epitop recognition was lost. GFP-tagged PI3Kγ wt and a S582A mutant were transfected into wild type BMMCs and the cells were stimulated with PMA. PI3Kγ was immunoprecipitated from cell lysates with an anti-PI3Kγ antibody and phosphorylation of S582 was detected by immunoblotting. Only GFP-PI3Kγ wt (and endogenous PI3Kγ), but not the S582A mutant was specifically phosphorylated upon PMA stimulation (Figure S3A). Next we analysed whether PI3Kγ phosphorylation is regulated in a stimulus-specific manner. PMA, Thapsigargin, and IgE/DNP all triggered PI3Kγ S582 phosphorylation in BMMCs, but not adenosine, in agreement with its different mode of PI3Kγ activation (Figure 5A). Consistent with impaired PKB activation in the absence of Ca^{2+}

mobilisation, phosphorylation of PI3Kγ on S582 by IgE/DNP was also blocked by EDTA, EGTA, and BAPTA/AM (Figure 5B). Phosphorylation of PI3Kγ is mainly mediated by PKCβ, as this was greatly impaired in PKCβ$^{-/-}$ BMMCs in response to PMA or IgE/DNP stimulation (Figure 5C).

Serine 582 is located at the beginning of the helical domain of PI3Kγ. The helical domain (also called PIK domain or accessory domain) is conserved in PI3- and PI4-kinases, but its function is unknown. Certainly it is important for the structural integrity of these kinases, as being involved in extensive interdomain interactions (Walker EH, Nature, 1999). Interestingly, the beginning of the helical domain constitutes a hot-spot region of activating PI3Kα mutation found in various types of tumours (Samuels Y, Science, 2004). PI3Kα helical domain mutants have increased activity in vitro, promote PKB activation and oncogenic transformation in cell culture models, and induce tumour growth of xenograft transplants in vivo (Zhao JJ, Proc Natl Acad Sci U S A, 2005; Kang S, Proc Natl Acad Sci U S A, 2005; Ikenoue T, Cancer Res, 2005; Isakoff SJ, Cancer Res, 2005; Pang H, Cancer Res, 2009). To check whether the activity of PI3Kγ is regulated at the level of the helical domain, we compared the activity of recombinant wild type PI3Kγ, a Ser582 to Ala and a phosphorylation mimicking Ser582 to Glu mutant of PI3Kγ in an in vitro lipid kinase assay. Recombinant proteins were purified from baculovirus infected Sf9 cells by the means of a C-terminal His6-tag, and the enzymes activities were assessed in the presence of PIP_2-containing mixed lipid vesicles. The lipid kinase activity of the PI3Kγ S582E mutant was enhanced two-fold (Figure 5D), which is an increase in activity similar to that reported for PI3Kα mutants (Miled N, Science, 2007; Carson JD, Biochem J, 2008; Gymnopoulos M, Proc Natl Acad Sci U S A, 2007). Moreover, PI3Kγ S582E also showed higher activity when phosphatidylinositol (PI) was added as substrate (Figure 5E). Besides lipid kinase activity, PI3Kγ also possesses autophosphorylation activity, which was also increased 2-fold by mutation of Ser582 to Glu (Figure S3B).

In order to analyse signalling of PI3Kγ S582 mutants in a physiologically relevant environment, we exogenously expressed them in PI3Kγ$^{-/-}$ BMMCs. Surprisingly, while PI3Kγ wild type and PI3Kγ S582A were efficiently expressed, expression of the phosphorylation mimicking mutants, S582E and S582D, was strongly downregulated early after transfection (Figure 5F). A similar downregulation was also observed for the GFP-tagged S582E/D mutants (not shown). While instability hampered further analysis of these mutants in vivo, this characteristic on the other hand might be an indirect sign of increased activity. Oncogenic PI3Kα mutants for example are poorly expressed in Sf9 cells, but this can be overcome by addition of a PI3K inhibitor (Mandelker D, Proc Natl Acad Sci U S A, 2009) or expression as kinase inactive form (Hon WC, Oncogene, 2012). In contrast to BMMCs, expression of PI3Kγ S582E/D was not affected in HEK293, which are devoid of endogenous PI3Kγ, but expression was also reduced in Sf9 cells (4-5-fold) compared to wild type PI3Kγ (not shown).

Activation of class I PI3Ks inside cells is regulated by modulation of catalytic activity as well as membrane and substrate binding. Regulation occurs through adaptor subunits but also through the catalytic subunit itself either in cooperation with the adaptor or not. Furthermore, PI3K activation can depend only, partially, or not on adaptor-mediated or artificial plasma membrane-targeting, which has been shown for example by analysis of artificially membrane-anchored PI3K, deletion of

the adaptor-binding domain, or analysis of gain-of-function mutations (Costa C, Proc Natl Acad Sci U S A, 2007; Aoki M, J Biol Chem, 2000; Zhao JJ, Proc Natl Acad Sci U S A, 2005; Zhao L and Vogt PK, Proc Natl Acad Sci U S A, 2008; Zhao L and Vogt PK, Cell Cycle, 2010). While GPCR-activated PI3Kγ is regulated by binding of the adaptor p101 to Gβγ subunits (Stephens LR, Cell, 1997), FcεRI couples to p101-free PI3Kγ as this adaptor is not expressed in mast cells (Bohnacker T, Sci Signal, 2009). In neutrophils, both p101-dependent and -independent PI3Kγ effector functions strictly depend on a functional Ras binding domain (RBD), as genetic manipulation thereof causes a PI3Kγ$^{-/-}$ phenotype (Suire S, Nat Cell Biol, 2006). Results presented here and published data show that PI3Ks can be regulated at the level of the helical as well as the RBD domain (Samuels Y, Science, 2004; Ikenoue T, Cancer Res, 2005; Suire S, Nat Cell Biol, 2006; Zhao L and Vogt PK, Cell Cycle, 2010). Interestingly, we found that PKCβ not only phosphorylates PI3Kγ on S582 but simultaneously also on S257 in the Ras binding domain (RBD). Mass spectrometric analysis of in vitro phosphorylated trypsin-digested human PI3Kγ revealed a second phosphopeptide with the sequence KKS^{P}(257)LMDIPESQSEQDFVLR and two non-modified peptides with the sequences KSLMDIPESQSEQDFVLR and SLMDIPESQSEQDFVLR. Representative spectra of the first two peptides are shown in Figure S3C/D. As for S582, S257 phosphorylation was detected in vitro and in vivo by MRM (Figure S3E/F) and site-specific antibodies (Figure S3G and data not shown). Phosphorylation of S257 is triggered in response to IgE/DNP, PMA and Thapsigargin stimulation (Figure S3G and data not shown). It therefore may be possible that in cells both phosphorylations are required to promote PI3Kγ activation. We did not observe increased activation of S257 phosphorylation mimicking mutants (S257E, S257D) of recombinant PI3Kγ in vitro nor additional activation of a double S257E, S582E mutant (Figure S3H). Still it should be kept in mind that detection of PI3K activation is limited by the already high activity state of this enzyme in vitro. As for S582, the sequence around S257 matches well with a PKCβ specific substrate motif (Figure S3I), and S257 is well conserved (Figure S3J). Comparison of the primary and secondary structure around S257 and published RBD inactivating mutations (Suire S, Nat Cell Biol, 2006; Kang S, Proc Natl Acad Sci U S A, 2006) with the corresponding region of the other class I PI3Ks, shows a stretch of very low homology and different conformation (Figure S3K). Isoform-specific regulation of PI3Ks may therefore be regulated, beyond other mechanisms, at the level of the RBD. Depending on the PI3K isoform and signalling pathway this may involve interaction with a Ras-like protein, a lipid molecule and/or phosphorylation thereby regulating allosteric activation of catalytic elements (Pacold ME, Cell, 2000) or membrane binding. Of note, FcεRI-triggered degranulation does not depend on Ras activation (Graham TE, J Immunol, 1998; Fujimoto M, Eur J Pharmacol, 2009; Mor A, Inflammation, 2011), and Thapsigargin does not activate Ras in BMMCs (Figure S3L). Whether S257 regulates PI3Kγ functions in mast cells is unknown and needs further investigation.

4.3.6 Activation of PI3Kγ by phosphorylation requires p84-free PI3Kγ

We found that mast cells are devoid of the PI3Kγ adaptor p101, but express a homologous adaptor protein, called p84 or p87^{PIKAP} (Gen Bank entry AY753194, (Bohnacker T, Sci Signal, 2009)).

Unexpectedly, phosphorylation of exogenously expressed PI3Kγ by PMA stimulation was gradually blocked by coexpression of increasing concentrations of p84 in PI3Kγ$^{-/-}$ BMMCs (Figure 6A, lanes 4-6). As p84 efficiently coimmunoprecipitated with exogenously expressed PI3Kγ, access to S582 is likely sterically blocked by p84. To further investigate whether S582 lies in the PI3Kγ-p84 interphase, we analysed binding of p84 to PI3Kγ S582 point mutants by coimmunoprecipitation. We coexpressed wild type and mutated PI3Kγ with p84 in PI3Kγ$^{-/-}$ BMMCs und immunoprecipitated PI3Kγ from cell lysates. Whereas p84 efficiently bound to PI3Kγ wild type and the S582A mutant, the affinities of p84 for the phosphorylation-micking mutants, S582E and S582D, were much lower (Figure 6B). Similarly, when we coexpressed the same proteins in HEK293 cells, we found weaker association of p84 with PI3Kγ S582E and S582D than with PI3Kγ wild type or S582A, both upon immunoprecipitation of either p84 or PI3Kγ (Figure 6C). These experiments therefore revealed the helical domain of PI3Kγ to be part of the p84 binding site.

Whereas wild type and S582A PI3Kγ could be expressed in PI3Kγ$^{-/-}$ BMMCs very efficiently in the presence (Figure 6B) and absence of p84 (Figure 5F), expression of the phosphorylation-mimicking mutants was only possible by cotransfection of p84. Despite association strength of p84 is greatly reduced for the S582E and S582D mutants (Figure 6B), continual low affinity on and off binding of p84 in side cells probably prevents degradation through inhibition of these activated mutants.

Since endogenous PI3Kγ is phosphorylated very efficiently in wild type BMMCs by PMA stimulation, endogenous p84 does not block activation of endogenous PI3Kγ (Figure 6A, lane 1). Consistently endogenous PI3Kγ coimmunoprecipitates only low amounts of endogenous p84 (Figure 6A, lane 1). Despite low association by coimmunoprecipitation, endogenous p84 expression depends partially on PI3Kγ in mast cells, neutrophils, and splenocytes, as expression of this adaptor is reduced in corresponding PI3Kγ$^{-/-}$ cells (Bohnacker T, Sci Signal, 2009). We performed additional coimmunoprecipitation experiments to more deeply characterise the interaction behaviour of endogenous and plasmid-expressed PI3Kγ and p84. Whereas exogenously expressed PI3Kγ coimmunoprecipitates both transfected p84 and the low amount of endogenous p84 found in PI3Kγ$^{-/-}$ BMMCs, endogenous PI3Kγ pulls endogenous p84 very inefficiently down (Figure 6D). Furthermore, whereas exogenously expressed GFP-PI3Kγ binds to endogenous p84 from wild type BMMCs, endogenous PI3Kγ fails to do so (Figure 6E). p84-PI3Kγ binding not only varies between endogenous and exogenous proteins, but also in mast cell lines. While endogenous p84 and PI3Kγ form a stable complex in the human mast cell line HMC-1, they do this poorly in rat basophilic leukaemia cells (RBL-2H3) (not shown). Currently, the reasons for these disparate interaction affinities are unclear.

4.3.7 PI3Kγ interacts with p84 mainly through the beginning of the helical domain

To understand the structural reasons by which p84 blocks PI3Kγ S582 phosphorylation, we performed deuterium exchange mass spectrometry (DXMS) to map the PI3Kγ-p84 binding interface. DXMS has become a powerful method for examining protein folding, protein-protein contacts, protein-ligand binding, and conformational changes (Engen JR, Anal Chem, 2009). We

have previously applied this methodology to map the interface of the catalytic subunit of class IA PI3Kδ with its p85 regulatory subunit and lipids (Burke JE, Structure, 2011). This technique relies on the fact that amide hydrogens exchange with solvent at a rate dependent on their conformation and solvent accessibility. Location and extent of deuterium uptake are analysed by peptide mass determination following proteolysis. We first optimized protein digestion conditions and were able to identify 202 peptide fragments from the PI3Kγ catalytic subunit that covered >90% of the primary sequence (Figure S4, Table S1). Deuterium incorporation into free and p84-complexed PI3Kγ was analysed at seven time points from 3 to 3000 seconds. The presence of p84 caused decreases in deuterium exchange greater than 0.5 Da in peptides that spanned the N-terminal, C2, and helical domain of PI3Kγ (Figure 7B, Figure S5). Greatest exchange changes in the presence of p84 were mapped onto the crystal structure of PI3Kγ lacking the N-terminal domain (PDB ID: 2CHX, residues 144-1093) to visualize the p84 binding area (Figure 7A, Figure S5). The peptides that showed the greatest decrease in deuterium incorporation (>1.0 Da) clustered to three specific regions, the RBD-C2 linker, C2-helical domain linker, and the helical domain. To visualize the areas that have the largest changes in deuterium incorporation in the presence of p84, we integrated the average differences in exchange at all seven time points (Figure 7C). This analysis showed that PI3Kγ interacts with p84 predominantly with the helical domain, and that p84 protection clusters around S582. We did not map the interacting surface on p84, due to difficulties in expressing and purifying free p84 in a sufficient quantity for these studies.

We were surprised to find that p84 interacts with PI3Kγ predominantly through the helical domain, as it has been postulated that this adaptor binds to the N-terminus of PI3Kγ, in analogy to p85 binding to class IA PI3K. However, this assumption has never been analysed experimentally by means of N-terminal PI3Kγ truncation mutants. We generated a deletion mutant of PI3Kγ lacking the first 130 amino acids. Coimmunoprecipitation experiments using either HA-p84 (Figure 7D, left) or PI3Kγ (right) show that wild type GST-tagged PI3Kγ and GST-tagged truncated (Δ130) PI3Kγ interact equally well with p84. The N-terminus is therefore not directly involved in p84 binding. We do find a slight decrease in deuterium incorporation for two peptides in the N-terminal domain of PI3Kγ (59-70 and 107-113) in the presence of p84, this interaction however seems to be dispensable for p84 binding. Untagged truncated (Δ130) PI3Kγ, in contrast to GST-Δ130-PI3Kγ, interacts only weakly with p84, and also much less efficiently than untagged full-length PI3Kγ. The N-terminus of PI3Kγ is therefore required for the structural integrity of PI3Kγ and the p84 binding region. GST-tag attachment can complements this function, rescuing p84 binding.

4.4 Discussion

PI3Kγ is a key regulator of allergy controlling IgE/antigen-dependent mast cell degranulation (Laffargue M, Immunity, 2002). In order to develop new strategies to treat allergic disease it is of interest to understand how this lipid kinase is regulated. PI3Kγ has been shown to regulate mast cell hyperactivation by boosting PIP_3 production by autocrine and paracrine released adenosine (Laffargue M, Immunity, 2002). Because the PI3Kγ$^{-/-}$ phenotype is not recapitulated by genetic and

pharmacological inhibition of adenosine and GPCR signalling in mice and cells (Saito H, J Immunol, 1987; Endo D, Int Arch Allergy Immunol, 2009; Laffargue M, Immunity, 2002), PI3Kγ activation by the FcεRI is incompletely understood. We found that Thapsigargin triggers degranulation in a PI3Kγ-dependent but GPCR-independent manner. We thereby run across a convenient tool to address non-canonical PI3Kγ activation in BMMCs. FcεRI-triggered granule exocytosis depends on store-operated Ca^{2+} entry and Thapsigargin directly triggers degranulation at this receptor-distal step. We show that PI3Kγ activation occurs downstream of Ca^{2+} mobilisation and that PKCβ relays Ca^{2+} signalling to PI3Kγ activation. We thereby unravelled for the first time a mechanism by which a protein tyrosine kinase (PTK)-coupled receptor activates PI3Kγ.

That PI3K activation occurs downstream of Ca^{2+} mobilisation is reflected by several lines of evidence. First, studies with the PI3K-inhibitor Wortmannin have shown that initial PLCγ activation, inositol trisphosphate (IP3) production, and Ca^{2+} mobilisation are not affected by this drug (Tkaczyk C, J Biol Chem, 2003). Second, in the absence of Ca^{2+}, FcεRI crosslinking fails to promote protein kinase B (PKB) phosphorylation (T308), which is strictly controlled by PI3K-derived PIP_3. Third, PI3K activation absolutely depends on PKCβ2, which requires Ca^{2+} for its activation. Fourth, if PI3K activation would occur upstream of Ca^{2+} mobilisation, Thapsigargin or ionophores would be expected trigger degranulation in a PI3K-independent manner (this study and (Marquardt DL, J Immunol, 1996)). In disagreement with this study, we initially observed defective Ca^{2+} mobilisation in PI3Kγ$^{-/-}$ BMMCs in response to IgE/DNP (Laffargue M, Immunity, 2002) or Thapsigargin (not shown) stimulation. This however, we found to be caused by Fura-2 release into the medium due to its property to partition into granules, leading to artificial Ca^{2+} signals in wild type BMMCs (Almers W and Neher E, FEBS Lett, 1985; Di Virgilio F, Cell Calcium, 1990; Vorndran C, Biophys J, 1995). In later experiments with other fluorescent Ca^{2+} chelators like Fura-4F or Fura-FF no differences between wild type and PI3Kγ$^{-/-}$ BMMCs were observed (not shown).

When mast cell degranulation was discovered to be Wortmannin-sensitive, it has been anticipiated that PTK-coupled FcεRI couples to class IA PI3K. By now PI3Kγ turned out to be the key PI3K, and also many other observations disfavour involvement of class IA PI3K. The most ubiquitously expressed class IA PI3K regulatory subunit p85α is not required for IgE-dependent mast activation in vivo in a model of passive systemic anaphylaxis and in BMMCs (Fukao T, Nat Immunol, 2002; Tkaczyk C, J Biol Chem, 2003). Moreover, p85α-p55α-p50α$^{-/-}$ fetal liver-derived mast cells (FLMCs) and p85β$^{-/-}$ BMMCs degranulate normally (Lu-Kuo JM, J Biol Chem, 2000; Tan BL, Blood, 2003; Tkaczyk C, J Biol Chem, 2003). Consistently, FcεRI regulatory chains do not contain consensus p85 binding motifs (YXXM) (Songyang Z, Cell, 1993). Despite the Gab2 adaptor protein was suggested to function as alternative p85 anchor in mast cell exocytosis (Gu H, Nature, 2001), other studies do not support this finding and connect Gab2 with other functions. FcεRI-triggered Gab2 tyrosine phosphoryation is only evident in serum-starved BMMCs, and the presence of serum is sufficient to fully trigger Gab2 tyrosine phosphorylation (compare (Gu H, Nature, 2001; Yu M, J Immunol, 2006) with (Hernandez-Hansen V, J Immunol, 2004)). Gab2 controls chemokine mRNA induction both at suboptimal and optimal antigen concentrations or FcεRI occupancy (Gonzalez-Espinosa C, J Exp Med, 2003). Furthermore, degranulation is not affected by siRNA-mediated

downregulation of Gab2 in BMMCs (Barbu EA, J Biol Chem, 2010). Analysis of PI3Kδ kinase dead BMMCs (D910A/ D910A) showed that PKB is readily activated following stimulation of the FcεRI in contrast to PI3Kγ$^{-/-}$ BMMCs (Ali K, Nature, 2004). Moreover, Thapsigargin or PMA trigger normal PKB phosphorylation in PI3Kδ$^{D910A/D910A}$ BMMCs (not shown). In vivo, decreased mast cell degranulation in the ear of PI3Kδ $^{D910A/D910A}$ mice correlates with the reduction in mast cell numbers at this location (Ali K, Nature, 2004).

Despite protein kinase C (PKC) activation is known to be a key event to mast cell degranulation, its function and substrates remained obscure. By analysis of BMMCs derived from isoform-specific knock-out mice, PKCβ was identified to be essential for FcεRI- and ionomycin-triggered mast cell degranulation (Nechushtan H, Blood, 2000). We herein unravelled that PKCβ functions as PI3Kγ regulator in this process. We additionally show that direct activation of PKCβ by phorbol ester is sufficient trigger PI3K and PKB activation in mast cells. PMA by itself however does not trigger granule exocytosis, as membrane fusion in mast cells is additionally controlled by Ca^{2+}-regulated steps. Interestingly, PKCβ-dependent PI3K activation depends on relatively high Ca^{2+} concentrations lying in the low micromolar range. With respect to this, in vitro studies have identified a special high Ca^{2+} requirement for the activation of PKCβ2 compared with PKCβ1 or PKCα (Keranen LM and Newton AC, J Biol Chem, 1997). Whereas PKCβ2 required a 40-fold greater Ca^{2+} concentration for half-maximal activation than membrane binding, this difference was only 10- and 2-fold for PKCβ1 and PKCα, respectively. Apart from PKCβ2, BMMCs also express high amounts of PKCα. Despite these two PKCs share high homology and substrate sequence specificity, PKCα can not complement for PKCβ. Of the two splice variants of PKCβ, mast cells express much more PKCβ2 than PKCβ1 (own observations, (Kawakami Y, J Immunol, 2000)). PKCβ1 and PKCβ2 differ only in their last 50-52 amino acids, but the specific role of the C-termini is unknown. As diacylglycerol (DAG) analogs enhance granule exocytosis or directly stimulate release in some exocytotic cell types, PKC has been proposed to regulate granule-membrane fusion (Morgan A, Biochem Soc Trans, 2005). However by now, other phorbol ester sensitive membrane fusion regulators have been identified, like e.g. the Munc-13 proteins (Kazanietz MG, Mol Pharmacol, 2002). FcεRI triggers phosphorylation of synaptosomal-associated protein 23 (SNAP-23) in mast cells. Despite sensitive to PKC-inhibitors and PKCβ deficiency ((Hepp R, J Biol Chem, 2005), own observations), inhibitor of NF-κB kinase β (IKKβ) is rather the direct kinase (Suzuki K and Verma IM, Cell, 2008). As only one of the two identified sites is conserved in humans, and SNAP-23 phosphorylation is only reported in this cell type, the relevance of this finding is currently unclear. Of note, the exocytotic machinery seems to be intact in PKCβ$^{-/-}$ BMMCs, as costimulation of the FcεRI with Kit rescues defective antigen-induced degranulation (Fehrenbach K, J Immunol, 2009).

Characterisation of recombinant PI3Kγ phosphorylation site mutants identified S582 as a switch site for PI3K activation. Unfortunately, we could not directly address increased PI3K signalling in vivo in a physiological environment, as it was impossible to express the phosphorylation-mimicking mutants at adequate levels in BMMCs. However, the strong expression defect of these mutants

likely results from a gain of function trait, as oncogenic PI3K mutants also showed impaired expression in several instances. Since nucleofection of BMMCs is not a gentle method for exogenous protein expression, we also tried lentivirus-based approaches. This unfortunately was hampered by the fast loss of transgene expression as well as toxicity problems with high viral titers. While exogenous expression of PI3Kγ activating mutants was severely and moderately impaired in BMMCs and Sf9 cells, respectively, expression was normal HEK293 cells. PI3K activation therefore depends on a second input that is provided by the cellular environment. To take account of cell type specific protein regulation, functional studies should therefore be preferentially done in physiologically relevant cell types. The most frequently occurring mutations in PI3Kα in cancer cluster to three hotspots, E542 and E545 in the helical and H1047 in the kinase domain (Samuels Y, Science, 2004). These mutations have been reported to promote PKB activation only in certain cell types like mammary epithelial cells (Zhao JJ, Cancer Cell, 2003; Zhao JJ, Proc Natl Acad Sci U S A, 2005; Isakoff SJ, Cancer Res, 2005; Pang H, Cancer Res, 2009) or some fibroblasts (Kang S, Proc Natl Acad Sci U S A, 2005; Zhao L and Vogt PK, Proc Natl Acad Sci U S A, 2008; Ikenoue T, Cancer Res, 2005), but not in HEK293 cells.

S582 of PI3Kγ lays at the beginning of the helical domain, and is therefore located in the same domain region as most oncogenic helical domain-associated mutations found in PI3Kα (P539, Glu542, Glu545, and Q546) (Samuels Y, Science, 2004; Samuels Y and Velculescu VE, Cell Cycle, 2004). These sites and other oncogenic PI3Kα mutations lie near or within the last four helices of the catalytic domain (Zhang X, Mol Cell, 2011). These helices form a square that surrounds the activation and catalytic loops. Reported mutations might therefore affect catalysis or lipid binding by allosteric mechanisms. The PI3Kγ helical domain folds into a stack of five A/B pairs of antiparallel helices (Walker EH, Nature, 1999). S582 sits in the B helix of the first helical pair. As the intrahelical loop of this helix pair contacts the regulatory helices of the catalytic domain, it might forward conformational changes resulting from S582 phosphoryation. Despite located at slightly distinct positions than S582, helical domain mutations of PI3Kα might affect lipid kinase activation by a similar mechanism. Whether these mutations induce structural changes, has not yet been investigated by X-ray crystallography.

As S582 points inward of the crystal structure of PI3Kγ Δ143, the helical domain beginning, at least in the phosphorylated state, must adopt a different conformation. Since we found that untagged N-terminally truncated PI3Kγ (Δ130) is structurally impaired with respect to p84 binding compared to full-length PI3Kγ, it might be that PI3Kγ Δ143 folds improperly. Additionally, PI3Kγ Δ143 has a ten fold lower in vitro Ras binding affinity and probably also less basal activity, as it is expressed at highly elevated levels in BMMCs and Sf9 cells ((Pacold ME, Cell, 2000), and own observations). Whereas the catalytic loop of crystallised PI3Kγ Δ143 is locked in an inactive conformation (Walker EH, Nature, 1999; Pacold ME, Cell, 2000), active site loop residues of PI3Kδ (ΔABD) and Vsp34 (ΔC2) are oriented in a catalytically competent manner (Berndt A, Nat Chem Biol, 2010; Miller S, Science, 2010). Further, it is also feasible that PKCβ binding induces a conformational change that exposes S582. As endogenous PI3Kγ does not interact with p84 in BMMCs, it might be possible that PI3Kγ adopts different conformations in distinct cell types.

In vitro data show that PI3Kα helical domain mutations relieve inhibitory contacts between the N-terminal SH2 domain (nSH2) of p85 and PI3Kα. This has been derived from investigation of charge-reversal mutations of PI3Kα and p85α and analysis of the crystal structure of the PI3Kα H1047R/p85α-niSH2 complex (Miled N, Science, 2007; Mandelker D, Proc Natl Acad Sci U S A, 2009). Whereas the niSH2 fragment of p85 blocks the activity of monomeric wild type PI3Kα 2-fold, PI3Kα helical domain hot spot mutants are not inhibited by p85 nor further activated by phosphopeptides (Miled N, Science, 2007; Carson JD, Biochem J, 2008). The relative importance of the release of p85-inhibition for net PI3Kα activation is not yet clear, as monomeric helical domain mutants are more active that monomeric wild type PI3Kα. Recombinant PI3Kα is less active that the helical domain mutants in vitro, and N-terminally truncated p85 binding defective PI3Kα is less oncogenic than the mutants in vivo, despite absence of p85-inhibition (Ikenoue T, Cancer Res, 2005; Gymnopoulos M, Proc Natl Acad Sci U S A, 2007; Miled N, Science, 2007; Zhao L and Vogt PK, Proc Natl Acad Sci U S A, 2008). These mutations therefore not only relieve p85-binding but also inherently modulate PI3K activity.

Apart from S582, PI3Kγ concomitantly also phosphorylates S257 in the Ras binding domain (RBD). The RBD is important for PI3Kγ regulation, as artificially engineered PI3Kγ RBD mutants are functionally dead in vivo (Suire S, Nat Cell Biol, 2006; Kang S, Proc Natl Acad Sci U S A, 2006; Kurig B, Proc Natl Acad Sci U S A, 2009). As the RBD around S257 is divergent in all class I PI3Ks, it is likely that this region modulates isoform-specificities. Consistently, also RBD mutants of PI3Kα and PI3Kβ as well as Dictyostelium or Drosophila PI3K show functional defects under certain conditions (Zhao L and Vogt PK, Proc Natl Acad Sci U S A, 2008; Zhao L and Vogt PK, Cell Cycle, 2010; Kang S, Proc Natl Acad Sci U S A, 2006; Sasaki AT, J Cell Biol, 2004; Orme MH, Nat Cell Biol, 2006). Whether S257 coregulates PI3Kγ activation in mast cells is unclear at the moment and needs further investigation.

As PI3Kγ complexed to p84 could not be phosphorylated on S582, we unexpectedly obtained information on the p84 interaction site. We show that p84 binds to PI3Kγ through the helical domain beginning and not the N-terminal region, as has been anticipated in analogy to adaptor interaction in class IA PI3K. Despite the N-terminus of PI3Kγ is not involved in p84 binding, it is required for the structural integrity of the p84 binding site. Addition of a GST-tag compensates this function. It is possible that p101 also interacts with the helical domain of PI3Kγ, because our results are in consent with previous publications analysing the interaction of PI3Kγ with p101. Krugmann et al. showed reduced binding of p101 to different long (Δ122-Δ369) N-terminal deletion mutants of Myc- or His-tagged PI3Kγ, but they did not analyse mutants with a bulky GST-tag (Krugmann S, J Biol Chem, 1999). This however was done by Maier et al., who efficiently copurified p101 with both full-length and truncated (Δ97) GST-PI3Kγ from baculovirus-infected Sf9 cells (Maier U, J Biol Chem, 1999).

PI3Kγ has been discovered by attempts to find the enzyme that makes the PIP_3 downstream of G protein-coupled receptors (GPCRs) in myeloid cells (Stephens L, Cell, 1994; Stephens LR, Cell, 1997; Stephens LR, Cell, 1997). It was found there to coexist in tight association with the adaptor

p101, which functions as PI3Kγ's Gβγ-sensor (Stephens LR, Cell, 1997; Brock C, J Cell Biol, 2003; Suire S, Nat Cell Biol, 2006). Mast cells were the first cells discovered to express PI3Kγ but not p101 (Bohnacker T, Sci Signal, 2009), and therefore have to engage PI3Kγ differently – for example through the adaptor p84 or PKCβ. Besides mast cells, endothelial cells also express PI3Kγ but not p101 (Hsieh SN, Diss, 2003, Friedrich Schiller University, Jena, Germany), and therefore might also rely on PKC. Of note, PI3Kγ can also be regulated in a p101-independent manner in cells expressing p101. In neutrophils, p101 is required for migration towards fMLP or C5a, but is dispensable for reactive oxygen species (ROS) production (Suire S, Nat Cell Biol, 2006). PKC activation by phorbol ester also promotes PI3K/PKB activation in cell types other than mast cells, like 3T3-L1 adipocytes or primary human blood-derived B cells (Nave BT, Biochem J, 1996; Barragan M, J Leukoc Biol, 2006). These examples illustrate that PKC-PI3K pathways will likely be discovered to regulate more functions in more cells.

4.5 Experimental procedures

Cell Culture

Bone marrow-derived mast cells (BMMCs) were developed from femoral bone marrow of 8-12 week old C57BL/6J (Jackson Laboratories), PKCβ$^{-/-}$ (Leitges M, Science, 1996; Standaert ML, Endocrinology, 1999), and PI3Kγ$^{-/-}$ mice (Hirsch E, Science, 2000) (both on a C57BL/6J genetic background). Cells were cultured in IMDM supplemented with 10% heat-inactivated FCS, 2 mM L-glutamine, 100 units/ml penicillin, 100 µg/ml streptomycin, 50 µM β-mercaptoethanol, and 2 ng/ml recombinant murine IL-3 (Peprotech). SCF (5 ng/ml) was added once after starting bone marrow culture, while IL-3 was readded every 2nd to 3rd day. BMMCs were used after 4 weeks of culture until generally 8 or maximally 16 weeks. c-Kit and FcεRI expression was followed by flow cytometry. HEK293 cells were cultured in DMEM supplemented with 10% FCS, Pen/Strep, and L-Gln.

Transfections

HEK293 cells were seeded into 6 cm dishes and were transfected with JetPEI^{TM} (Polyplus-transfection) using 2.5 µg of total plasmid DNA. BMMCs were transfected by nucleofection (Amaxa) using solution T and PI3Kγ (1-3 µg) and p84 (0.2-2 µg) expression plasmids where indicated. Total DNA concentrations were adjusted to 10 µg with pcDNA3 vector.

Stimulation of BMMCs

For stimulation of the FcεRI, BMMCs were passively sensitized with 100 ng/ml anti-dinitrophenyl (DNP)-specific immunoglobulin E (SPE-7, Sigma) overnight in complete growth medium. Degranulation was triggered by the addition of DNP coupled to human serum albumin (DNP_{30-40}-HSA) at concentrations between 5 and 100 ng/ml. For analysis of PKB phosphorylation, BMMCs were IL-3 starved in growth medium containing 2% or 10% FCS, and stimulations were stopped on ice, the cells immediately collected by centrifugation for 1 min at 2000 g, and lysed in 1x Laemmli

sample buffer. Other stimuli used were Thapsigargin (0.03125-1 μM, Sigma), phorbol 12-myristate 13-actetate (PMA) (50-200 ng/ml, Alexis), adenosine (1 μM, Sigma), stem cell factor (SCF) (10 ng/ml, Peprotech), and interleukin-3 (IL-3) (10 ng/ml, Peprotech). Stimulations were done at 37°C for the indicated times.

(Co-)Immunoprecipitation

Transfected HEK293 cells were washed with phosphate buffered saline (PBS) and lysed with NP-40 lysis buffer [50 mM Tris/HCl pH 7.4, 138 mM NaCl, 2.7 mM KCl, 5% glycerol, 1% NP-40] supplemented with protease inhibitors [20 μM leupeptin, 18 μM pepstatin, 5 μg/ml aprotinin, phenylmethylsulfonylfluorid (PMSF)], phosphatase inhibitors [40 mM NaF, 2 mM Na_3VO_4], 0.5 mM EDTA, and 0.5 mM EGTA for 15 min on ice. Insoluble material was pelleted by centrifugation and one-tenth of clarified lysate was mixed with Laemmli sample buffer for overall protein expression examination. The remainder of lysate was incubated with anti-PI3Kγ (ascites fluid, 641, corresponds to Jena Bioscience ABD-027) or anti-HA.11 (Covance) antibodies for 1 hour at 4°C on a rotating wheel, followed by incubation with 25 μl of a 50% slurry of GammaBind Plus Sepharose (Amersham Biosciences) or protein G agarose (Millipore) for additional 2 hours. Immune complexes were washed 3x with NP-40 lysis buffer, 1x with 0.1 M Tris/HCl pH 7.4, 0.5 M $LiCl_2$, 0.2% NP-40, 1x again with NP-40 lysis buffer, and eluted by the addition of Laemmli sample buffer.

BMMCs were collected by centrifugation and lysed in NP-40 lysis buffer supplemented with protease inhibitors, phosphatase inhibitors [40 mM NaF, 10 mM β-glycerophosphate, 5 mM sodium pyrophosphate], 2 mM EDTA, and 2 mM EGTA for 15 min on ice. Cell debris was removed by centrifugation and endogenous or transfected PI3Kγ was immunoprecipitated from the cleared lysate with anti-PI3Kγ (ascites fluid, 641) antibodies (1-2 hours) and protein A or G agarose beads (2-5 hours). Immune complexes were washed as describe above before resuspension in 1x Laemmli sample buffer. Lysates and immunoprecipitations were analysed by Western blotting.

Western blotting and quantification

Protein samples were heated to 95°C, centrifuged, separated by SDS-PAGE, and transferred to polyvinylidene fluorid (PVDF)-membranes (Millipore) by semi-dry transfer. Membranes were blocked with 5% (w/v) milk powder (Migros) in TBS-T buffer [20 mM Tris/HCl, pH 7.6, 137 mM NaCl, 0.1% (v/v) Tween 20 (Fluka)]. Blots were incubated overnight at 4°C with the primary antibody, followed by incubation with horseradish peroxidase (HRP)-coupled secondary goat anti-mouse or anti-rabbit antibodies (Sigma). Protein bands were visualized by enhanced chemiluminescence (Millipore). Developed X-ray films (Fuji) were scanned on an Epson Perfection scanner (4990 Photo) as 16-bit grayscale images without adjustments and inverted band intensities quantified with ImageJ 1.42q software (NIH) using the rectangle tool. Band pixel values were background corrected using an area above or below the selected band. Levels of protein phosphorylation were normalised to relative total protein levels and expressed in correlation to a freely chosen stimulated sample that was set to 1.

β-Hexosaminidase release

Mast cell degranulation was assessed by measuring the release of β-hexosaminidase into cell supernatants (Schwartz LB, J Immunol, 1979; Ozawa K, J Biol Chem, 1993). Stimulations were done for 20 min in PIPES-buffered solution [25 mM PIPES pH 7.4, 119 mM NaCl, 5 mM KCl, 5.6 mM glucose, 1 mM $CaCl_2$, 0.4 mM $MgCl_2$, 0.1 % fatty-acid free, low endotoxin bovine serum albumin (LE-BSA, Sigma)] in 24 well plates having 0.5 Mio cells in a volume of 500 µl. Plates were centrifuged at 4°C for 5 min and 100 µl aliquots (triplicate) of supernatant were transferred to 96 well plates. Samples for measurement of total β-hexosaminidase were obtained by lysis of cells in unstimulated wells with PIPES-buffered solution/0.1% Triton X-100, and 100 µl aliquots were transferred to the 96 well plate. β-hexosaminidase activity was assessed by incubation with 100 µl of substrate solution [100 mM p-nitrophenyl-N-acetyl-β-D-glucosaminidine (p-NAG) in 0.1 M sodium acetate pH 4] for 1 h at 37°C. The reaction was stopped with 100 µl of 0.15 M $Na_2CO_3/NaHCO_3$ and generated p-nitrophenol was quantified by measurement of absorbance at 410 nm on a spectrophotometer (Spectramax 340). Background values were derived from lysed unstimulated cell pellets incubated without p-NAG. β-hexosamidinase release was calculated by the formula: Release (R) [%] = $(A_{Stimulated} - A_{Unst.})/(A_{Total\ unst.} - A_{Total\ background})*100$.

Cytosolic Ca^{2+} concentrations

BMMCs were washed with and resuspended in HEPES buffer [10 mM HEPES/NaOH pH 7.5, 137 mM NaCl, 2.7 mM KCl, 5 mM glucose, 1 mM $CaCl_2$, 1 mM $MgCl_2$, 0.1 % fatty acid free BSA]. Cells were loaded with 4 µM Fura-4F/AM for 10 min, washed twice, and resuspended in HEPES buffer containing different Ca^{2+} concentrations ($[Ca^{2+}]_{e\ (extracellular)}$ = 0 - 1 mM). Cells were stimulated in a continuously stirred cuvette at 37° in a fluorescence spectrometer (Perkin Elmer LS50B). The excitation wavelength was alternated between 340 and 380 nm and fluorescence emission was measured at 510 nm. Calibration and calculation of intracellular Ca^{2+} concentrations were done as described in the supplements.

Cellular PdtIns(3,4,5)P_3 measurements

Cellular PtdIns(3,4,5)P_3 levels have been measured as described (Arcaro A and Wymann MP, Biochem J, 1993) with some modifications. BMMCs were cultured for 2 hours in phosphate-free RPMI medium/2% FCS, and labelled metabolically with 1 mCi/ml [^{32}P]-orthophosphate for 4 h. Cells were washed, stimulated, and lysed by the addition of chloroform/methanol (1:2, v/v, with butylated hydroxytoluene and carrier phosphoinositides). Lipids were extracted, deacylated, and separated by high performance liquid chromatography (HPLC).

Production of recombinant PI3Kγ

Recombinant human PI3Kγ was expressed as N-terminal GST- or C-terminal His_6-tagged-fusion protein in Sf9 cells by infection with recombinant baculoviruses. Plasmid (pAcG2T-PI3Kγ, codons 38-1102) and baculovirus for GST-PI3Kγ have been described (Stoyanov B, Science, 1995). Coding

sequences for full-length PI3Kγ-His_6 and point mutants were inserted into pVL1393 (BD Biosciences), and recombinant baculoviruses were obtained by cotransfection of Sf9 cells with BaculoGold DNA (BD Biosciences). Baculovirus-infected Sf9 cells were harvested 2-2.5 days postinfection, were washed with PBS, und lysed with either GST- or His-lysis buffer [GST: 50 mM Tris/HCl pH 7.5, 150 mM NaCl, 5 mM EDTA, 1 mM NaF, 1 mM DTT, 1% Triton-X100; His: 50 mM $NaH_2PO_4 \cdot 2H_2O$/NaOH, pH 8, 300 mM NaCl, 20 mM imidazol, 5% glycerol, 1% NP-40] containing protease inhibitors. GST-PI3Kγ was purified on glutathione sepharose 4B (Amersham Biosciences) and eluted with 50 mM Tris/HCl pH 7.5, 150 mM NaCl, 5 mM EDTA, 1 mM DTT, 5% glycerol, 20 mM glutathione after extensive washing. PI3Kγ-His6 was purified over Ni^{2+}-NTA agarose (Qiagen) and eluted with 50 mM $NaH_2PO_4 \cdot 2H_2O$/NaOH, pH 8, 300 mM NaCl, 250 mM imidazol. Proteins were mixed 1:1 with 2x storage buffer [80 mM HEPES/NaOH pH 7.4, 4 mM EDTA, 2 mM DTT, 20 mM benzamidine, ~90% ethylenglycol] and kept at -20°C. Protein concentrations were quantified by Coomassie-staining in SDS-PAGE gels using the Odyssey infrared imaging system (LI-COR Biosciences). Bovine serum albumin served as standard.

In vitro protein kinase assay

Recombinant wild type (wt) and kinase inactive (K833R) GST-PI3Kγ was incubated at an equal molar ratio with recombinant PKCβ2 (40 ng) (Invitrogen) in 1x kinase buffer (KB) [50 mM HEPES pH 7.4, 10 mM $MgCl_2$, 1 mM $CaCl_2$, 1 mM DTT, 0.03% Triton X-100] in the presence of 10 µM ATP and 5 µCi of [γ^{32}P]-ATP (Perkin Elmer) for 30 min at 30°C. Some samples included phosphatidylserine (PS, Sigma) lipid vesicles (0.1 mg/ml) containing 1-oleoyl-2-acetyl-sn-glycerol (OAG, 0.01 mg/ml, Cayman Chemical). Reactions were terminated by the addition of Laemmeli sample buffer, and proteins were resolved by SDS-PAGE, and stained with Coomassie dye (Serva blue G). Gels were dried on a Whatmann paper, exposed to X-ray films and storage phosphor screen, and ^{32}P-incorporation quantified with ImageQuant TL Software (Amersham Biosciences). As standard served a dilution series of the radioactive ATP-mix spotted onto the Whatmann paper.

In vitro lipid kinase assay

PI3Kγ-His_6 (200 ng) was incubated with PtdIns(4.5)P_2-containing lipid vesicles, 10 µM ATP, and 4 µCi of [γ^{32}P]-ATP in buffer (LKB) [40 mM HEPES pH 7.4, 150 mM NaCl, 4 mM $MgCl_2$, 1 mM DTT, 0.1 mg/ml fatty-acid free BSA] for 10 min at 30°C. Composition of the lipid vesicles has been chosen to mimic relative mole ratios found in the inner leaflet of the plasma membrane (PE/PS/PC/SM/PIP_2 = 30/20/10/4.5/1.2). Lipids dissolved in $CHCl_3$/MeOH (2:1) were combined in a glass tube, dried under a steam of nitrogen gas, and resuspended in 1x LKB without BSA by tip sonication (f. c. in assay: 130 µM PE, 87 µM PS, 43 µM PC, 20 µM SM, 5 µM PIP_2). Alternatively PtdIns/PS vesicles (~200 µM each) were used. Reactions were terminated by addition of 1 M HCl and $CHCl_3$/MeOH. Lipids were isolated by chloroform extraction, separated by TLC, and quantified with phosphoimager technology.

Mass spectrometry

Coomassie-stained PI3Kγ was excised from the SDS-PAGE gel and digested with trypsin. Resultant peptides were analyzed by LC-MSMS. To identify phosphosites, peptide MS-MS spectra were analysed with Mascot searching the protein sequence database UNIPROT_15.6. Selective detection of the S582 and S257 phospho- and non-phosphopeptides was done later on with multiple reaction monitoring (MRM) analysing the transitions shown in Figure S2C and S3F.

Deuterium exchange measurement

Recombinant PI3Kγ alone or copurified with p84 was diluted into a D_2O solution. Amide hydrogen/deuterium exchange was allowed to proceed for 7 time periods. Samples were injected into the pepsin-column and resulting peptides separated by HPLC and analysed by mass spectrometry and DXMS software (Sierra Analytics).

4.6 Figures

Figure 1 Walser *et al.*

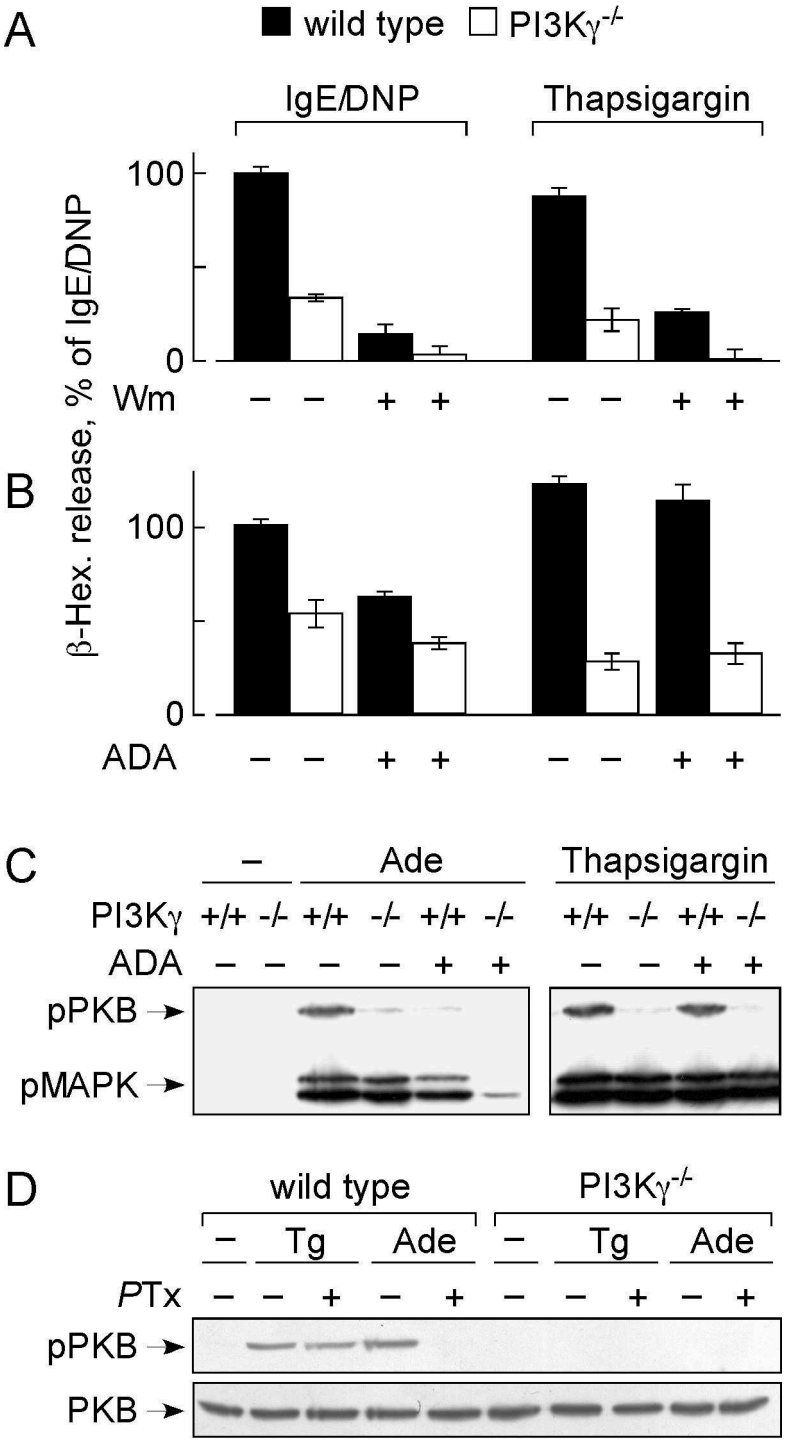

Figure 2 Walser *et al.*

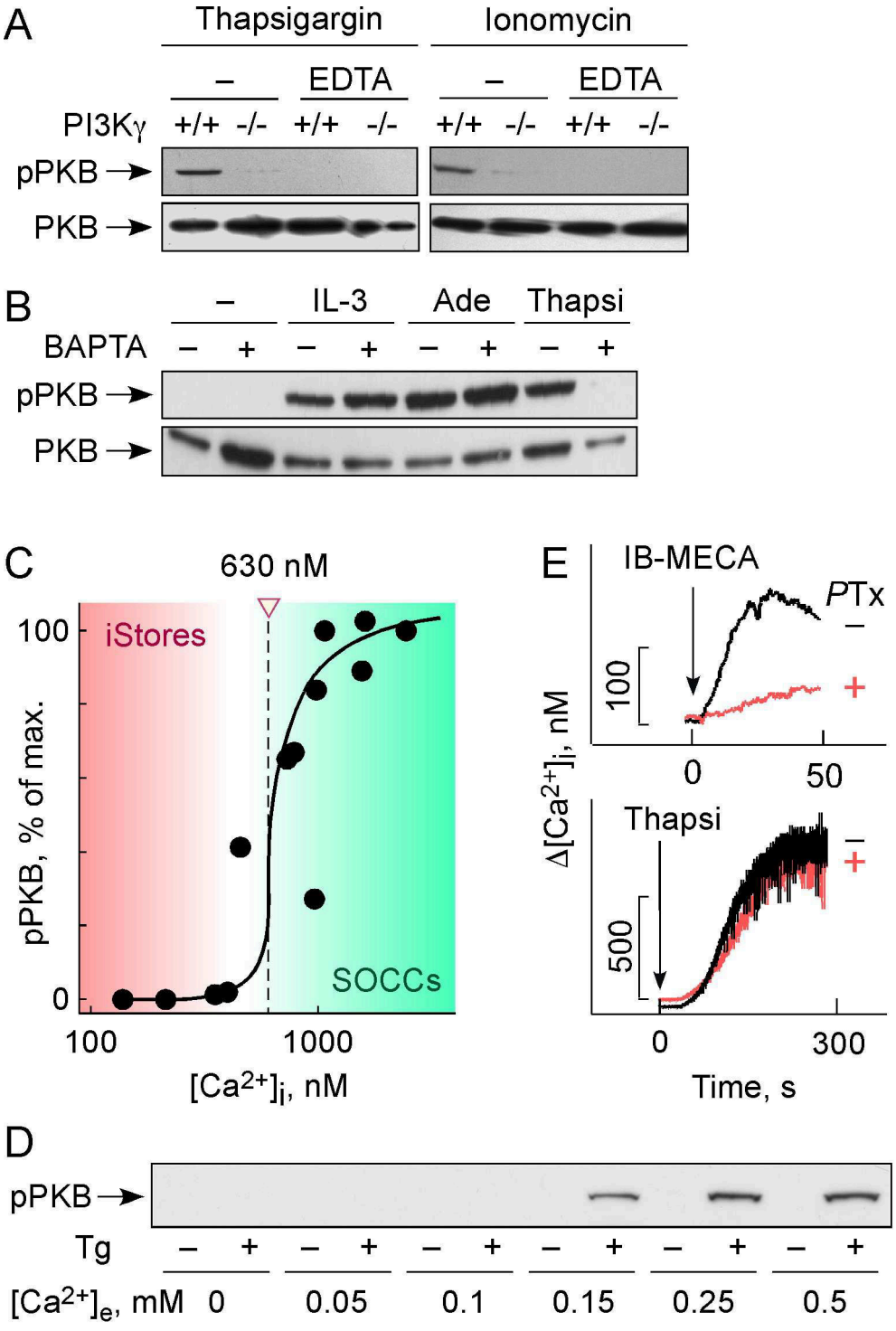

Figure 3 Walser *et al.*

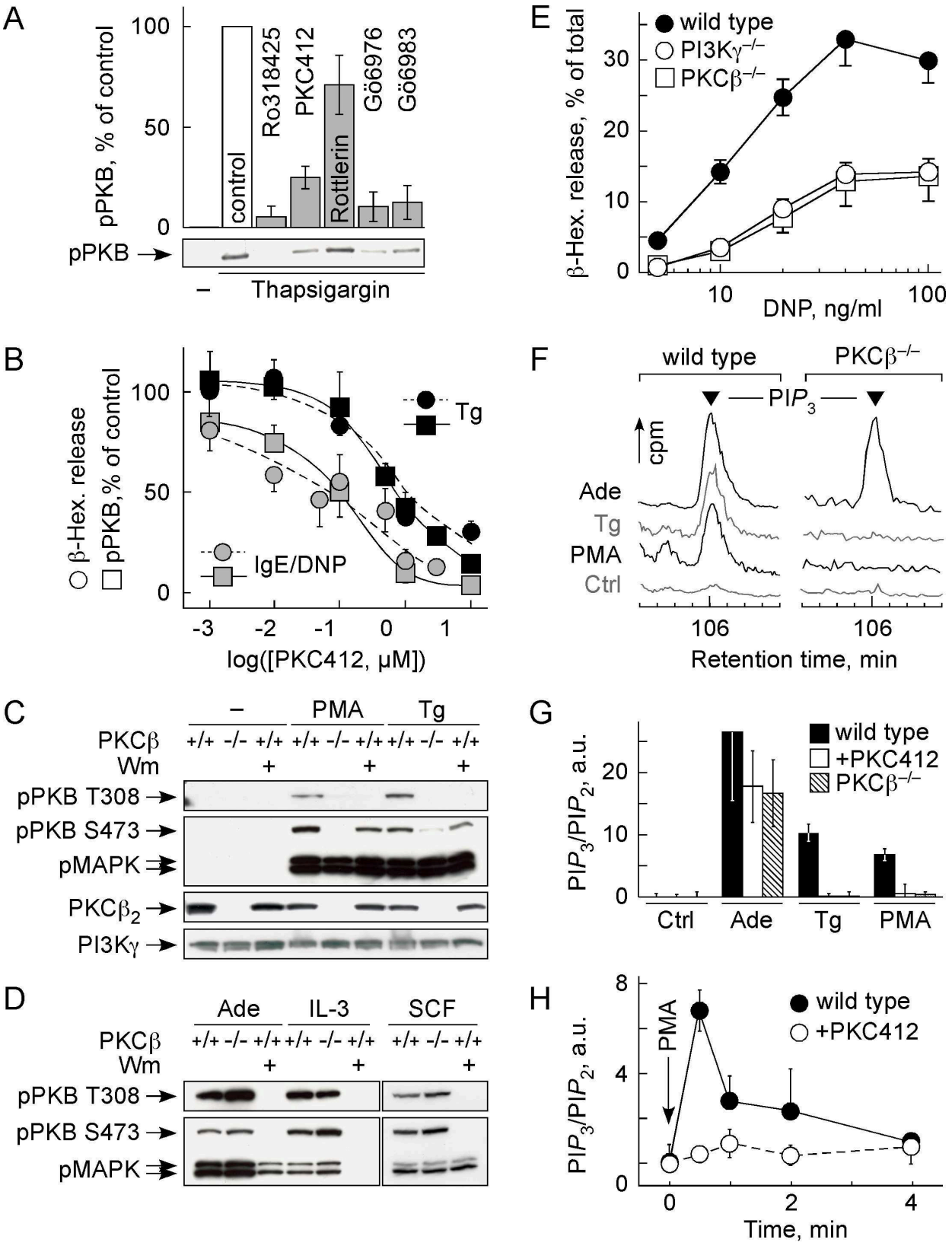

Figure 4

Walser *et al.*

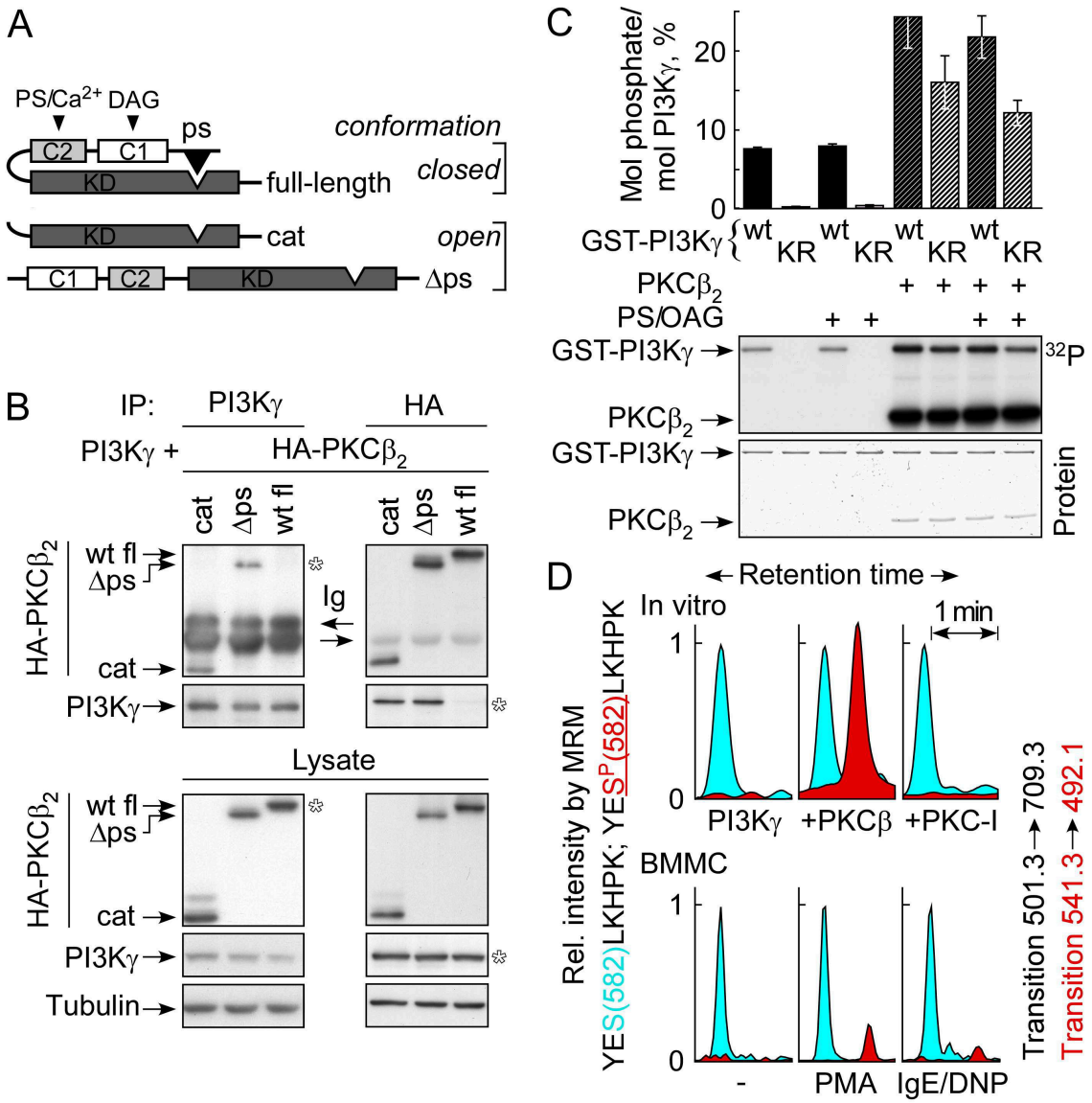

Figure 5 Walser *et al.*

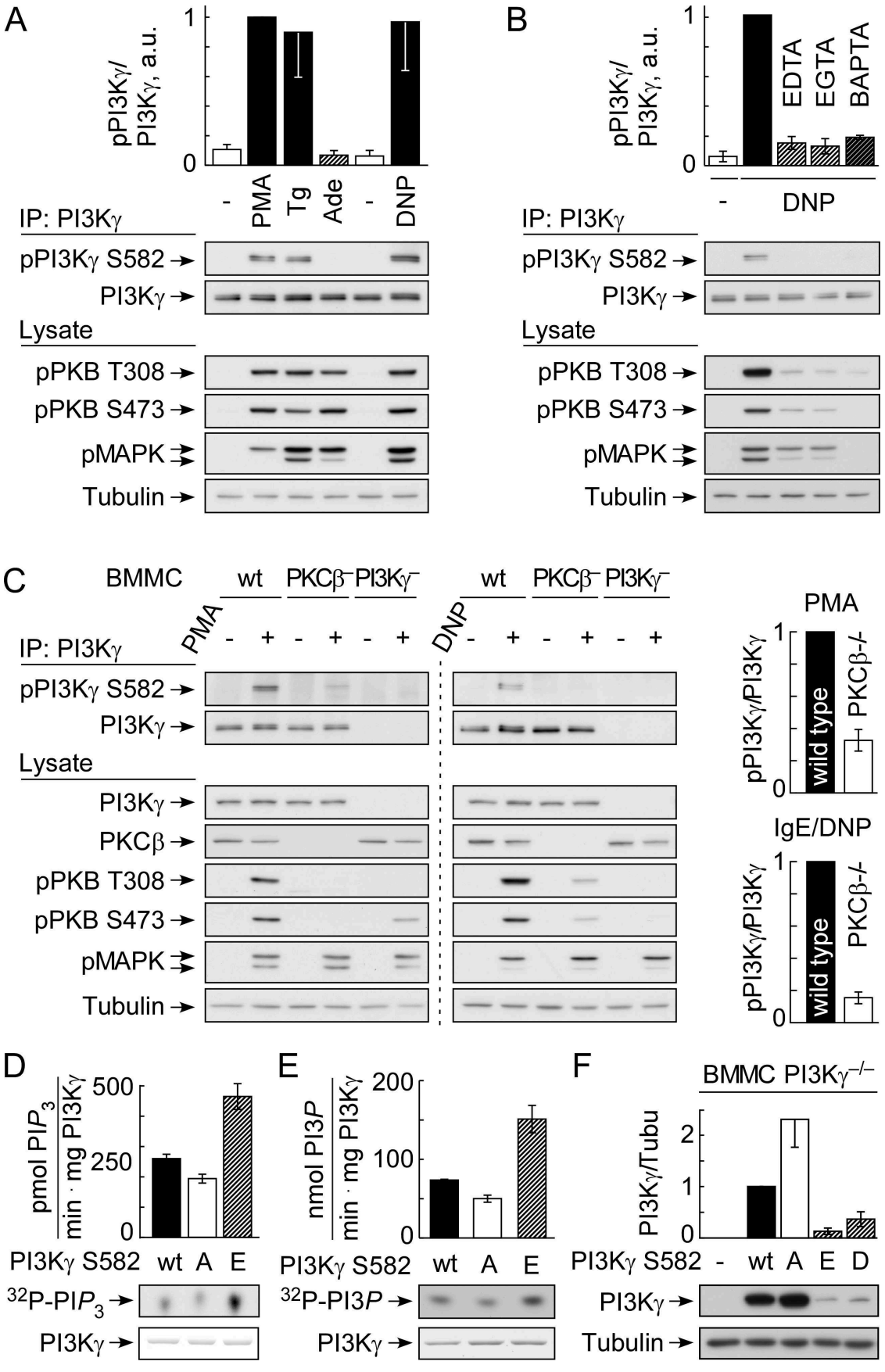

Figure 6 Walser *et al.*

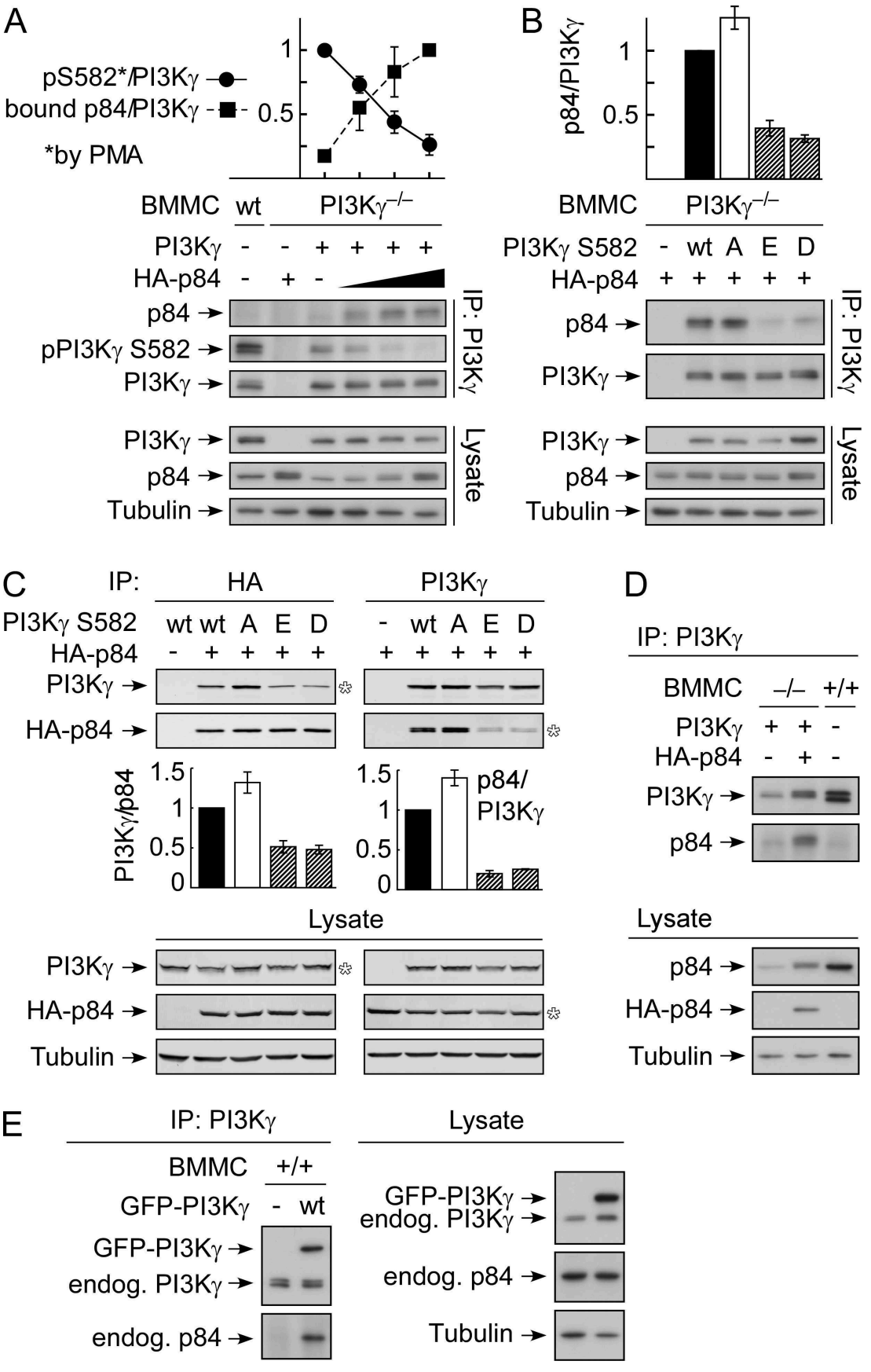

Figure 7 Walser *et al.*

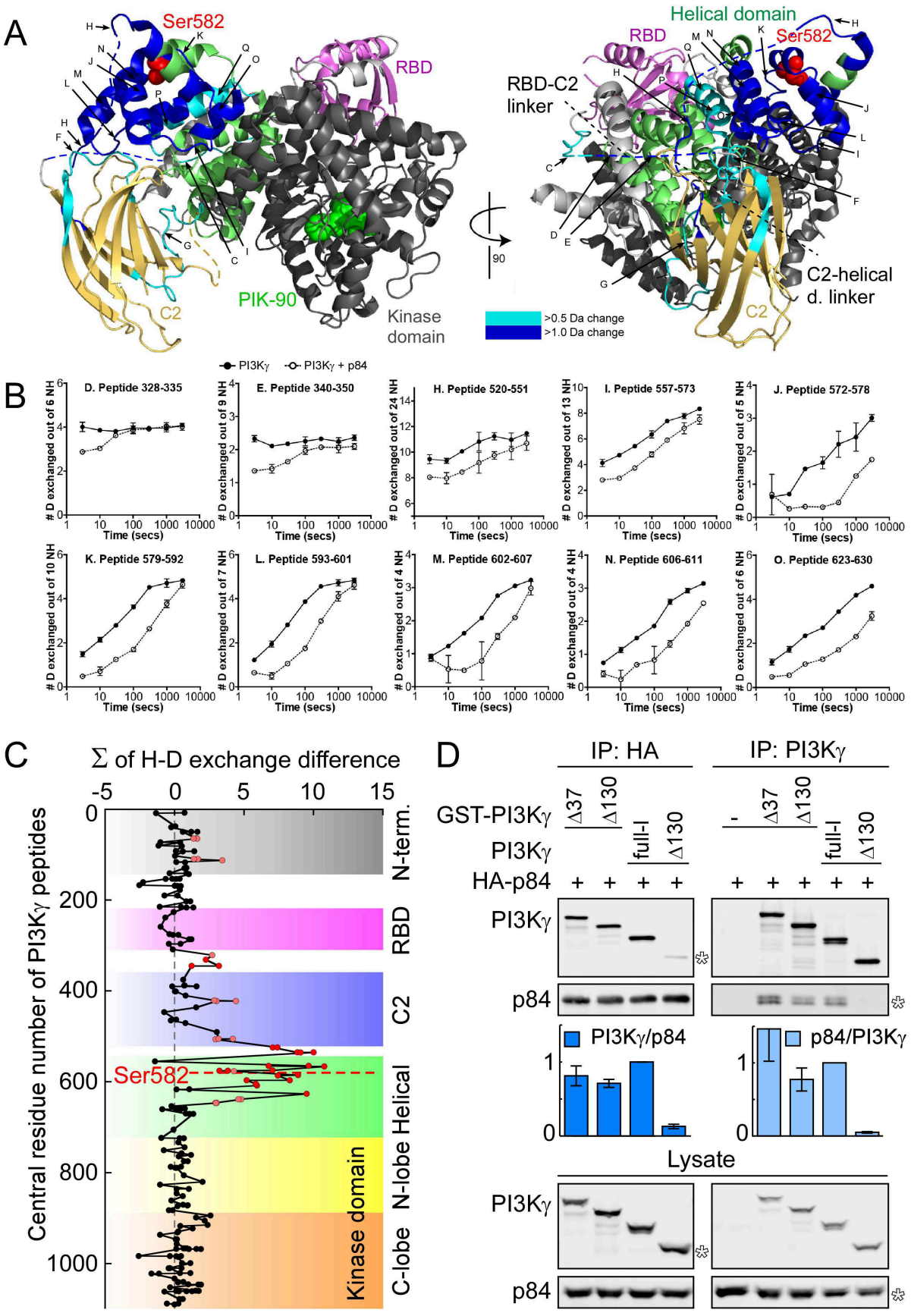

4.7 Figure legends

Figure 1. PI3Kγ controls Thapsigargin-induced mast cell degranulation in a GPCR-independent manner.

(A) Granule release of PI3Kγ$^{-/-}$ BMMCs was compared with wild type BMMCs by measuring the release of β-hexosaminidase into cell supernatants. BMMCs were resuspended in PIPES-buffered solution and pretreated for 15 min with 100 nM Wortmannin where indicated. Degranulation was triggered by crosslinking of IgE (100 ng/ml, overnight) occupied FcεRIs with DNP (10 ng/ml) or the addition of Thapsigargin (1 μM). Data are the mean ± SEM of three experiments (n = 3).

(B) Granule release was assessed following 1 min preincubation with 10 units/ml adenosine deaminase (ADA). Stimulations and statistics were done as in (A).

(C) Wild type or PI3Kγ$^{-/-}$ BMMCs were stimulated with adenosine (1 μM) or Thapsigargin (1 μM) for 2 min, and PKB S473 phosphorylation was analysed by Western blotting. Before stimulation, BMMCs were IL-3 starved in medium/2% FCS for 3 hours, and pretreated with ADA for 1 min where indicated.

(D) Heterotrimeric G proteins were inactivated by preincubation with 100 ng/ml *B. Pertussis* toxin (*P*Tx) for 4 hours. Wild type or PI3Kγ$^{-/-}$ BMMCs were stimulated and analysed as in (C).

Figure 2. Thapsigargin-triggered PI3Kγ activation depends on an influx of extracellular Ca^{2+} and follows a switch-on kinetic mechanism.

(A) BMMCs were IL-3 starved in medium/2% FCS for 3 hours and preincubated for 5 min where indicated with 5 mM EDTA before stimulation with 1 μM Thapsigargin or 1 μM ionomycin. PKB S473 phosphorylation was analysed by Western blotting.

(B) BMMCs cultured as in (A) were pretreated for 10 min with the cell-permeable Ca^{2+} chelator BAPTA/AM (10 μM) and stimulated either with 10 ng/ml IL-3, 1 μM adenosine, or 1 μM Thapsigargin. PKB activation was analysed as in (A).

(C) BMMCs were loaded with 4 μM Fura-4F/AM for 10 min in HEPES buffer containing 1 mM Ca^{2+}. Washed cells were resuspended in the same buffer but in the presence of different Ca^{2+} concentrations (extracellular Ca^{2+}, $[Ca^{2+}]_e$) to modulate maximal stimulation-induced intracellular Ca^{2+} levels ($[Ca^{2+}]_i$). Cells were stimulated with 0.5 μM Thapsigargin and intracellular Ca^{2+} increase and PKB activation were measured by Fura fluoresence or Western blotting, respectively. pPKB S473 levels are displayed as a function of $[Ca^{2+}]_i$. Data points come from two independently performed experiments.

(D) Representative Western blot that was used to quantify phospho-PKB levels in panel (C).

(E) Intracellular Ca^{2+} concentrations were measured in wild type BMMCs following stimulation with the A3 adenosine receptor agonist IB-MECA or Thapsigargin. *B. Pertussis* Toxin (100 ng/ml) was added 4 hours before stimulation where indicated.

Figure 3. PKCβ relays Thapsigargin-induced PI3Kγ activation.

(A) Effect of different protein kinase C (PKC)-inhibitors on Thapsigargin-induced PKB phosphorylation (S473) was analysed by Western blotting and quantified with Image J software. Wild type BMMCs were starved in IL-3 free medium/2%FCS and preincubated with the inhibitors for 20 min before stimulation. pan-PKC inh.: Ro318425, Gö9683. cPKC-inh.: PKC412 (CPG41251). c/aPKC-inh.: Gö6976. Rottlerin: broad acting inhibitor, not PKC-specific.

(B) Granule release and PKB activation (S473) in response to Thapsigargin (1 μM) or IgE/DNP (100 ng/ml IgE overnight, 10 ng/ml DNP) was measured in the presence of increasing concentrations of the cPKC inhibitor PKC412. Starved cells as in (A) were stimulated and analysed for PKB phosphorylation by Western blotting or were resuspended in PIPES-buffered solution and used in a β-hexosaminidase release assay. Data are averages of three independent experiments (n = 3) with different BMMC batches (error bars indicate SEM).

(C) PKB activation in response to 100 nM PMA or 1 μM Thapsigargin (2 min) was analysed in wild type and PKCβ$^{-/-}$ BMMCs. Cells were starved as in (A) and were pretreated where indicated with 100 nM Wortmannin (Wm) for 15 min before stimulation. Cell lysates were analysed by Western blotting for phoshorylation of PKB (T308 and S473) and MAPK (Thr183/Tyr185).

(D) Wild type and PKCβ$^{-/-}$ BMMCs were stimulated with 1 μM adenosine, 10 ng/ml IL-3, or 10 ng/ml SCF under conditions as described in (C).

(E) FcεRI-triggered degranulation of wild type, PKCβ$^{-/-}$, and PI3Kγ$^{-/-}$ BMMCs (cultured for 4-7 weeks) was compared following stimulation with different DNP concentrations. BMMCs were saturated with IgE overnight (100 ng/ml) in complete growth medium, and were stimulated in PIPES-buffered solution in 24 well plates at a concentration of 1 Mio cells/ml. Data are the average of five independent experiments (error bars indicate SEM).

(F/G) Intracellular PtdIns(3,4,5)P_3 levels were measured in untreated (Ctrl) and cPKC-inhibitor (PKC412) treated wild type BMMCs as well as PKCβ$^{-/-}$ BMMCs after stimulation with 0.5 μM Thapsigargin, 200 ng/ml PMA, or 5 μM adenosine for 30 seconds. BMMCs were cultured for 2 hours in phosphate-free medium/2%FCS and then metabolically labelled with 1 mCi/ml [^{32}P]-orthophosphate for 4 h. Cell stimulations were stopped by the addition of $CHCl_3$/MeOH and lipids were extracted, deacylated, and separated by HPLC. Panel (F) shows representative elution peaks of PIP_3 of the HPLC chromatograms. (G) Relative levels of PIP_3 production were quantified by integration of the peak areas of PIP_3 and PIP_2 and expressed as ratio of PIP_3/PIP_2 (data show mean ± SEM, n = 4-6).

(H) Intracellular PIP_3 production was measured over time in wild type BMMCs the presence or absence of the cPKC inhibitor PKC412 in response to PMA (200 nM) stimulation. Data are averages of three independent experiments ± SEM.

Figure 4. PKCβ interacts with and phosphorylates PI3Kγ.

(A) Schematic representation of the PKCβ2 constructs used for transfection into HEK293 cells (displayed without N-terminal HA-tag). Wild type full-length PKCβ2: amino acids (aa) 1-673, catalytic domain (cat): aa 302-673, pseudosubstrate deletion mutant (Δps): deletion of aa 19-31.

Intramolecular inhibition of wild type PKCβ by the pseudosubstrate domain (ps) is relieved in cells upon cofactor binding (Ca^{2+}, phosphatidylserine (PS), diacylglycerol (DAG)). The two deletion mutants are in an open conformation as they lack the ps domain.

(B) HEK293 cells were cotransfected with plasmids encoding full-length PI3Kγ and HA-tagged PKCβ2 constructs (illustrated in (A)). Cells were lysed and a sample thereof was removed to control for proper protein expression (lower part). PI3Kγ or HA-PKCβ2 was immunoprecipitated with anti-PI3Kγ or anti-HA antibodies, respectively, from the rest of the lysate (upper part). Immuncomplexes were captured on protein G beads, washed, separated by SDS-PAGE, and analysed by Western blotting with antibodies against PI3Kγ, HA-tag, and β-tubulin. Ig: Immunoglobulin heavy chain of mouse anti-PI3Kγ or anti-HA antibody.

(C) Recombinant GST-PI3Kγ wild type (wt) or kinase inactive mutant (KR, Lys 833 mutated to Arg) were incubated with recombinant PKCβ2, 10 μM ATP, and 5 μCi of [γ^{32}P]-ATP in kinase buffer for 30 min. The reaction was stopped by the addition of Laemmeli sample buffer and the proteins were separated by SDS-PAGE. The dried gel was stained with Coomassie dye and exposed to X-ray films and storage phosphor screen. Shown are an autoradiograph and quantifications done with phosphorimager technology. Data represent the mean ± SEM of three experiments (n = 3).

For optimal PKC activation, reaction mixtures contained 1 mM Ca^{2+}. Where indicated, samples also contained phosphatidylserine (PS) vesicles containing the DAG analog 1-oleoyl-2-acetyl-sn-glycerol (OAG). Their presence did not further increase PKCβ autophosphorylation or trans-phosphorylation. Addition of Triton X-100 was sufficient (own observation) to fully potentiate kinase activity of recombinant PKCβ, which already has a high inherent basal activity.

(D) In vitro and in vivo phosphorylation of PI3Kγ on S582 as analysed by LC-MRM. S582 non-phospho- and phospho-peptides were detected in the multiple reaction monitoring mode (MRM), quantifying the transition 501.1 to 709.3 for the non-modified peptide (blue) and 541.3 to 492.1 for the phospho-peptide (red). Data were normalised to the transition of the non-modified peptide, which was set to 1. Upper part: Recombinant human kinase dead GST-PI3Kγ (2 μg) was incubated alone, together with PKCβ2, or PKCβ2 and PKC-inhibitor (Ro318425, 2 μM) in the presence of 100 μM ATP and PS/OAG vesicles in kinase buffer for 30 min. After SDS-PAGE and Coomassie staining, PI3Kγ was excised from the gel and prepared for LC-MRM. Lower part: Wild type mouse BMMCs (300 Mio/stimulation) were starved for 4 hours in IL-3 free medium/2% FCS and were left unstimulated or were treated for 2 min with 50 nM PMA or for 4 min with 10 ng/ml DNP (preloaded with 100 ng/ml IgE overnight). Endogenous PI3Kγ was immunoprecipitated from cell lysates, resolved by SDS-PAGE, and analysed with LC-MRM.

(E) Comparison of the sequence around S582 with a PKCβ substrate motif determined by screening of a peptide library (Nishikawa K, J Biol Chem, 1997). Values in parentheses indicate relative selectivities for the amino acids (1 corresponds to no selectivity).

(F) Alignment of the sequences adjacent to S582 of PI3Kγ from different species (obtained by protein blast).

Figure 5. Phosphorylation of PI3Kγ is Ca^{2+}/PKCβ-dependent and regulates enzymatic activity.
(A) Phosphorylation of endogenous PI3Kγ was analysed in wild type BMMCs in response to stimulation with 100 nM PMA, 1 μM Thapsigargin, 1 μM adenosine, or 20 ng/ml DNP for 2 min. If necessary, BMMCs were loaded with IgE (100 ng/ml) overnight (lanes 5, 6). Before stimulation, BMMCs were resuspended in IL-3 free growth medium. PI3Kγ was immunoprecipitated from lysates with an anti-PI3Kγ antibody and protein A agarose beads. Lysate samples and immunoprecipitations were analysed by Western blotting with the indicated antibodies. PI3Kγ phosphorylation was quantified with ImageJ software, normalised to total PI3Kγ levels, and expressed as fold of the signal obtained by PMA. Data are the mean of three experiments (n = 3) ± SEM.
(B) IgE (100 ng/ml, overnight) loaded BMMCs were resuspended in growth medium without IL-3. Cells were pretreated for 5 min with 0.5 mM EDTA or EGTA, or for 10 min with 10 μM BAPTA/AM to capture either extracellular or intracellular Ca^{2+}, respectively. Cells were stimulated for 30 s with DNP (100 ng/ml) and PI3Kγ phosphorylation and PKB activation were analysed as in (A) (n = 3, error bars indicate SEM).
(C) Phosphorylation of PI3Kγ was compared between wild type and PKCβ$^{-/-}$ BMMCs. PI3Kγ$^{-/-}$ BMMCs were included into the experiment as negative control. Experimental settings were as in (A) and stimulations were done with 50 nM PMA or 20 ng/ml DNP. Western blots of one experiment are shown on the left. Bar graphs on the right show the quantification of PI3Kγ phosphorylation in PKCβ$^{-/-}$ BMMCs relative to wild type BMMCs (PMA n = 4, DNP n = 3, error bars indicate SEM).
(D) Lipid kinase activities of recombinant PI3Kγ wild type (wt) and phosphorylation site mutants (S582A, S582E) were analysed in the presence of mixed phospholipid vesicles containing PtdIns(4,5)P_2 as substrate (PE/PS/PC/SM/PI*P*2 = 30/20/10/4.5/1.2). PIP_3 production was detected by autoradiography after extraction of the lipids and separation by thin layer chromatography. Shown are autoradiographs, quantifications done with phosphoimager system, and Coomassie stained SDS-PAGE gels of samples where no lipids but Laemmeli sample buffer was added instead. Data shown are the mean ± SEM of three experiments (n = 3) each done in triplicate.
(E) Lipid kinase activity of recombinant PI3Kγ wt, S582A, and S582E towards phosphatidylinositol (PI) was measured using PI-phosphatidylserine (PS) vesicles. PI3*P* production was quantified and data represented as described in (D). Data are the mean of a triplicate experiment.
(F) Expression plasmids of PI3Kγ wild type (wt) and S582 point mutants were transfected into PI3Kγ$^{-/-}$ BMMCs by nucleofection (Amaxa). Next day (2x) or after 8 hours (1x) cell lysates were prepared and protein expression analysed by SDS-PAGE and immunoblotting. PI3Kγ expression levels were quantified with ImageJ software, normalised to α-tubulin, and expressed as fold of wild type (wt) PI3Kγ (mean ± SEM, n = 3).

Figure 6. S582 phosphorylation requires adaptor-free PI3Kγ.

(A) PI3Kγ and increasing amounts of p84 plasmids were transfected into PI3Kγ$^{-/-}$ BMMCs by nucleofection (Amaxa). Wild type and transfected PI3Kγ$^{-/-}$ BMMCs were stimulated with 200 nM PMA for 30 s. PI3Kγ was immunoprecipitated from cell lysates with an anti-PI3Kγ antibody and protein G beads. p84 binding and S582 phosphorylation were detected by Western blotting, quantified with ImageJ software, normalised to PI3Kγ protein levels, and plotted as fold of maximal values, which were set to 1. Proper exogenous protein expression was analysed by Western blotting of cell lysates (bottom). Data show mean ± SEM of n = 2 experiments.

(B) PI3Kγ wild type, S582A, and phosphorylation mimicking mutants (S582E, S582D) were expressed together with p84 in PI3Kγ$^{-/-}$ BMMCs by cotransfection of 1.5 μg of each plasmid DNA. PI3Kγ was immunoprecipitated from cell lysates and p84 binding was analysed by Western blotting and quantification with ImageJ software. Data were normalised to PI3Kγ wt and represented as mean ± SEM of n = 3 experiments.

(C) Same plasmids as used in (B) were transfected into HEK293 cells and PI3Kγ-p84 association was analysed by co-immunoprecipitation assays, Western blotting, and Odyssey infrared imaging system. Results from PI3Kγ wt and HA-p84 transfections were set to 1. Data are shown as mean ± SEM (left: IP of HA-p84, n = 4, 4, 8, 3; right: IP of PI3Kγ, n = 2 all lanes).

(D) PI3Kγ-p84 interactions were analysed in wild type and transfected PI3Kγ$^{-/-}$ BMMCs. Exogenously expressed or endogenous PI3Kγ was immunoprecipitated from cell lysates and p84 binding was analysed by Western blotting. Shown are representative blots of a quadruplet experiment.

(E) Wild type BMMCs were mock-transfected or with GFP-PI3Kγ. Endogenous and GFP-PI3Kγ were immunoprecipitated from cell lysates and interaction with endogenous p84 was analysed by Western blotting. Shown are representative blots of a triplicate experiment.

Figure 7. p84 interacts primarily with the helical domain of PI3Kγ.

(A) Changes in deuteration levels between free and p84-bound PI3Kγ are mapped onto the crystal structure of PI3Kγ (PDB ID: 2CHX). Regions that are covered by peptides of PI3Kγ (labelled A-Q) that showed greater than 0.5 or 1.0 Da changes in deuteration are colored light or dark blue, respectively. The greatest difference in exchange observed at any time was used for the mapping. Ser582 is highlighted as red spheres. The ATP competitive inhibitor PIK-90 in the crystal structure is shown in green as a reference point for the kinase domain. The linker regions between the RBD and the C2 domain and the C2 and the helical domain are shown as dashed lines. Domain coloring was done the following: RBD: purple, C2 domain: light brown, helical domain: green, kinase domain: dark grey.

(B) The number of incorporated deuteriums in the absence (•) and presence (o) of p84 at seven time points are shown for peptides with more than 1.0 Da exchange difference. Data represent mean ± SD of two independent experiments.

(C) The deuterium exchange differences between free and p84-bound PI3Kγ were summed up over all seven time points for every identified peptide (x-axis), which were graphed according to their central residue number (y-axis).
(D) p84 was coexpressed with GST-tagged or untagged PI3Kγ constructs in HEK293 cells. N-terminal deletions of 37 or 130 amino acids are denoted Δ37 or Δ130, respectively. HA-p84 (left) or PI3Kγ (right) was immunoprecipitated from cell lysates with anti-HA or anti-PI3Kγ antibodies and protein G beads. PI3Kγ-p84 interactions were analysed by Western blotting and Odyssey infrared imaging system and expressed as fold of untagged, full-length PI3Kγ-p84 association. Data show mean ± SEM (left: n = 4, 6, 6, 6; right: n = 2, 4, 4, 4).

4.8 Supplemental figures

Figure S1 *Suppl. to Figure 3*

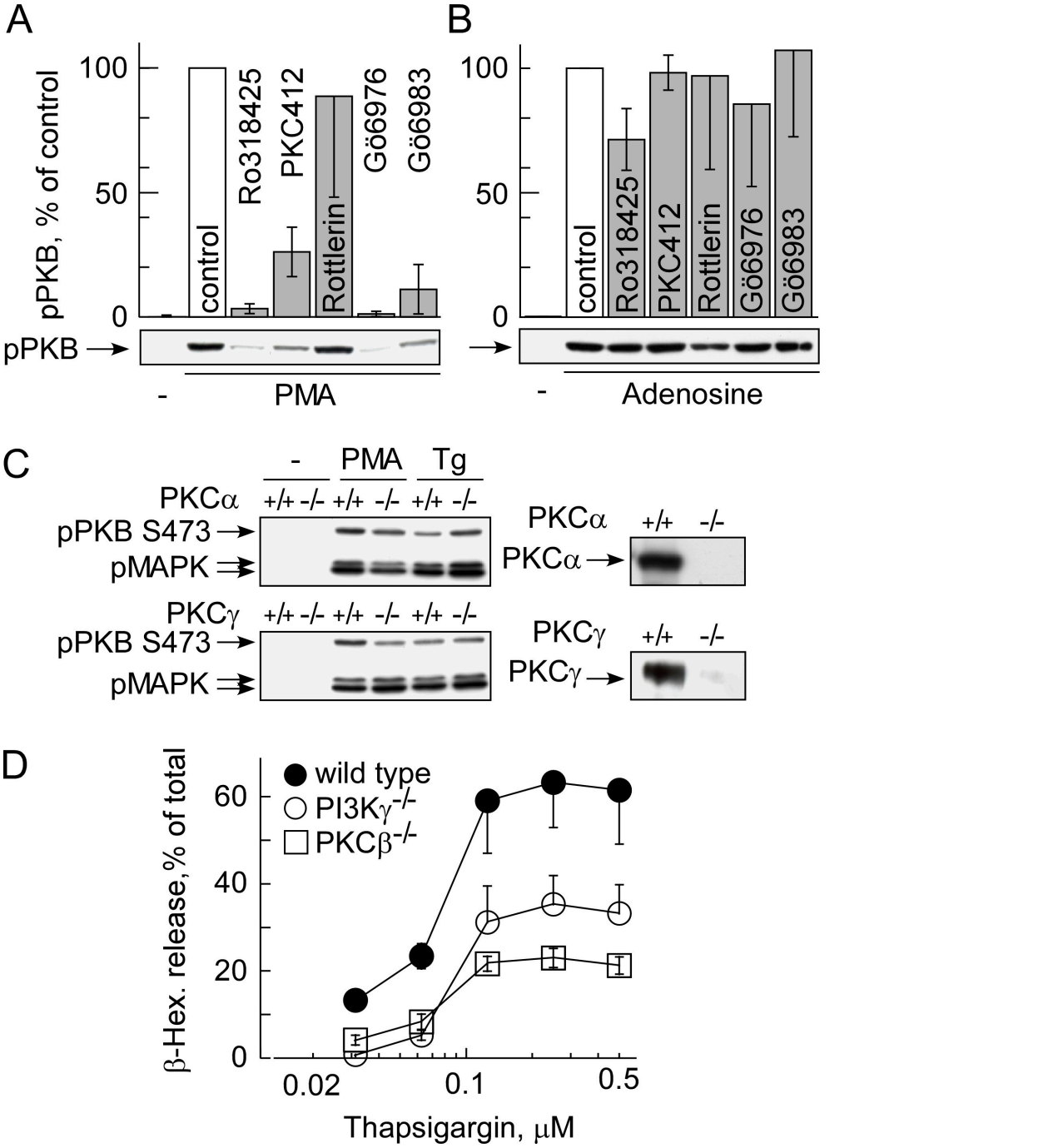

Figure S2

Suppl. to Figure 4

A

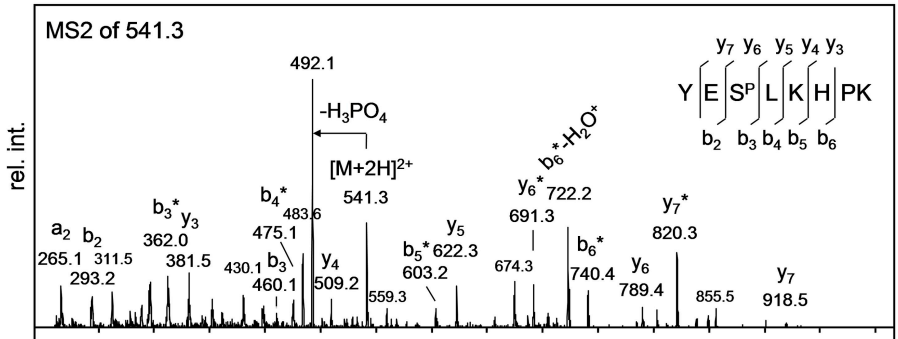

B

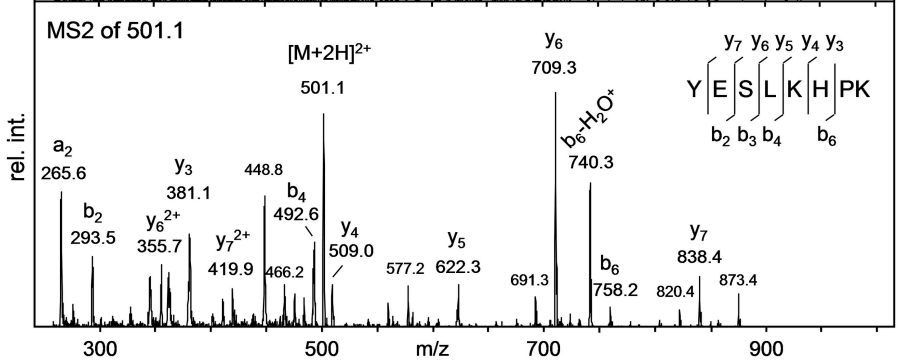

C

Peptide	Precursor m/z	Fragment m/z	Time min	Dwell time ms	Collision energy
$Y_{580}ES^{P}LKHPK$	541.3	492.1	16.8	200	40
$Y_{580}ESLKHPK$	501.1	709.3	16.0	100	30

* α-helix
T turn
t bend
d disordered

D S582

```
                    Hα1A                  Hα1B      Hα1B'      Hα2A          Hα2B          Hα2B'
                ************ TTT     *********t******t ttt******      *************  ******
Hs_PI3Kγ  548 PNQLRKQLEAIIATDPLNPLTAEDKELLWHFRYESLKH PKAYPKLFSSVKWGQQEIVAKTYQLLARREVWDQSA

                 ********    TTTT  **********t******t t********      **************
Hs_PI3Kα  524 RENDKEQLKAISTRDPLSEITEQEKDFLWSHRHYCVTI PEILPKLLLSVKWNSRDEVAQMYCLVKDW

                 ******       TT   **********t*******    ********      *************
Mm_PI3Kβ  525 GKKFLAVLKEILDRDPLSQLCENEMDLIWTLRQDCRENFPQSLPKLLLSIKWNKLEDVAQLQALLQIW

                dddddddd***** dddd   *********t*******    ********      **************
Mm_PI3Kδ  505  EEEQLQLREILERRGSGELYEHEKDLVWKMRHEVQEHFPEALARLLLVTKWNKHEDVAQMLYLLCSW
```

Figure S3

Suppl. to Figure 5

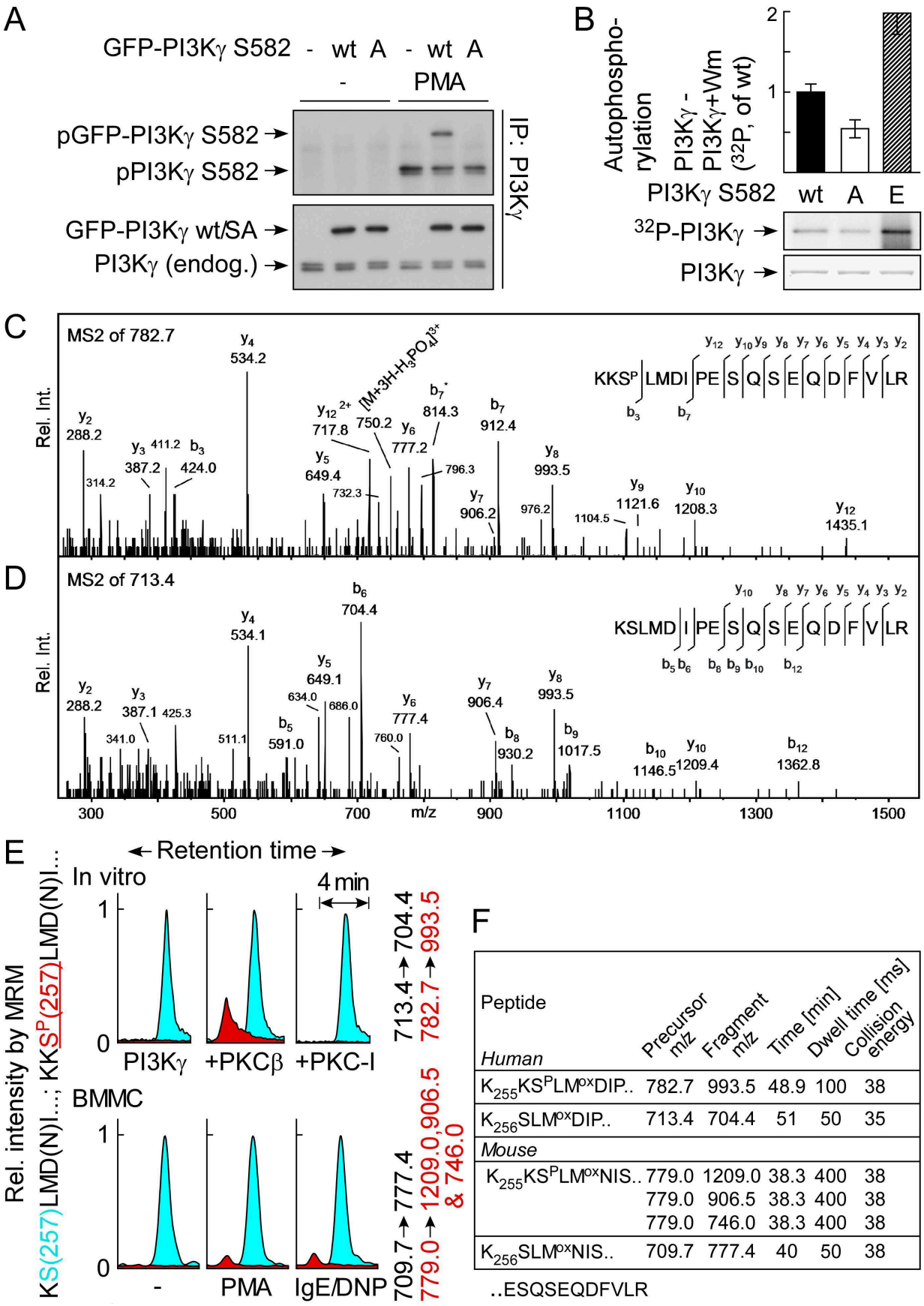

Peptide	Precursor m/z	Fragment m/z	Time [min]	Dwell time [ms]	Collision energy
Human					
$K_{255}KS^{P}LM^{ox}DIP..$	782.7	993.5	48.9	100	38
$K_{256}SLM^{ox}DIP..$	713.4	704.4	51	50	35
Mouse					
$K_{255}KS^{P}LM^{ox}NIS..$	779.0	1209.0	38.3	400	38
	779.0	906.5	38.3	400	38
	779.0	746.0	38.3	400	38
$K_{256}SLM^{ox}NIS..$	709.7	777.4	40	50	38

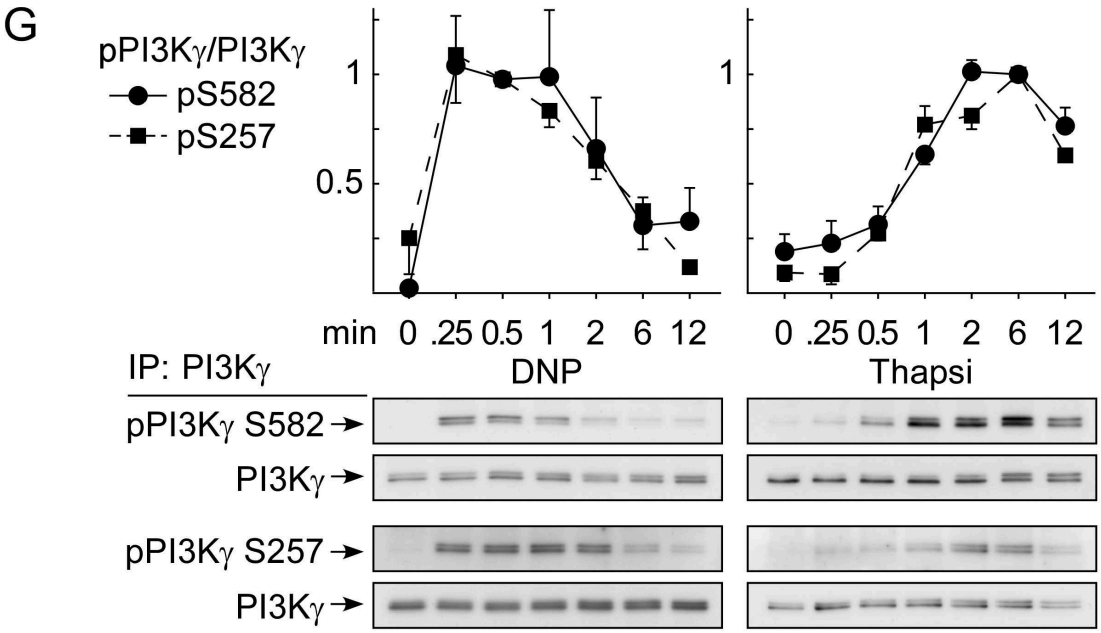

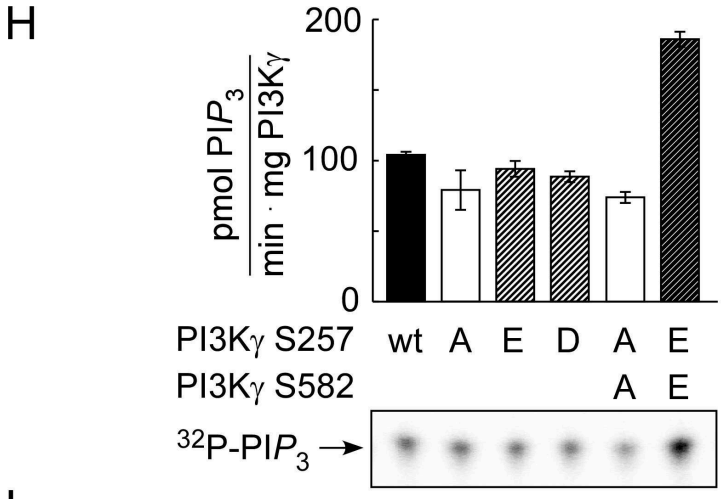

I

Residue position	-7	-6	-5	-4	-3	-2	-1	0	1	2	3	4	5
Peptide Residues	Y(1.8)	K(1.6)	L(1.9) F(1.8)	K(1.9) R(1.6)	R	K(2.7) Q(2.0) E(1.5)	G(2.1) K(1.8) M(1.7)	**S**	F(3.0) M(2.1) L(1.8)	K(3.0) R(2.0) F/M(1.5)	K(2.6) Y(1.7) F/R(1.5)	K(1.9) F(1.5)	A(1.7) F/K(1.6) M(1.5)
PI3Kγ	T	K	M	A	K	K	K	**S257**	L	M	H	P	K

J

		S257
Mammals	Homo sapiens	AILQSFFTKMAKKK**S**LMDIPESQSEQDFV
	Pan troglodytes	AILQSFFTKMAKKK**S**LMDIPESQSEQDFV
	Macaca mulatta	TILQSFFTKMAKKK**S**LMDIPESQSEQDFV
	Equus caballus	TILQSFFTKMAKKK**S**LMDIPESQNEQDFV
	Bos taurus	TILQSFFTKMAKKK**S**LMDIPESQNEQDFV
	Sus scrofa	TILQSFFTKMAKKK**S**LMDIPESQNERDFV
	Canis familiaris	AILRSFFAKMAKKKALMGIPEGQSERDFV
	Rattus norvegicus	TILQSFFTKMAKKK**S**LMNIPESQSEQDFV
	Monodelphis domestica	TILQSFFTKMAKKK**S**LMDIPESQSELDFV
	Mus musculus	TILQSFFTKMAKKK**S**LMNIPESQSEQDFV
Bird	Gallus gallus	MILHSFFTKMAKKK**S**LMDIPEDHSELDFV
	Taeniopygia guttata	MILHSFFTKMAKKK**S**LMDIPEDHSELDFV
Amphibian	Xenopus tropicalis	VILHSFFTKMAKKK**S**LLDISEENSELDFV
Fish	Danio rerio	QVLQSFFAKITNKRALLGISEDVSESDFV

K

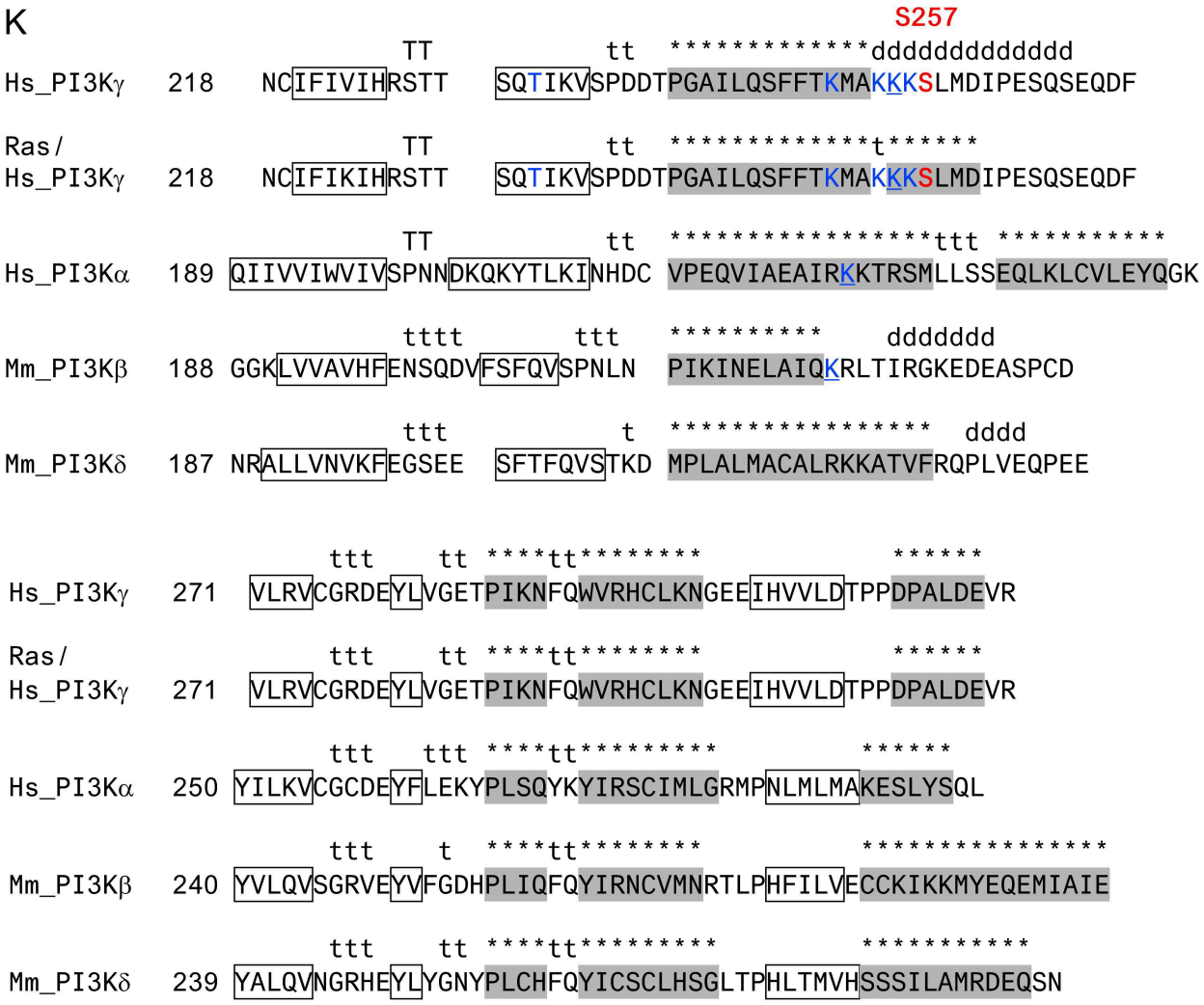
S257
Hs_PI3Kγ 218 NCIFIVIHRSTT SQTIKVSPDDTPGAILQSFFTKMAKKKSLMDIPESQSEQDF
Ras/
Hs_PI3Kγ 218 NCIFIKIHRSTT SQTIKVSPDDTPGAILQSFFTKMAKKKSLMDIPESQSEQDF
Hs_PI3Kα 189 QIIVVIWVIVSPNNDKQKYTLKINHDC VPEQVIAEAIRKKTRSMLLSSEQLKLCVLEYQGK
Mm_PI3Kβ 188 GGKLVVAVHFENSQDVFSFQVSPNLN PIKINELAIQKRLTIRGKEDEASPCD
Mm_PI3Kδ 187 NRALLVNVKFEGSEE SFTFQVSTKD MPLALMACALRKKATVFRQPLVEQPEE
Hs_PI3Kγ 271 VLRVCGRDEYLVGETPIKNFQWVRHCLKNGEEIHVVLDTPPDPALDEVR
Ras/
Hs_PI3Kγ 271 VLRVCGRDEYLVGETPIKNFQWVRHCLKNGEEIHVVLDTPPDPALDEVR
Hs_PI3Kα 250 YILKVCGCDEYFLEKYPLSQYKYIRSCIMLGRMPNLMLMAKESLYSQL
Mm_PI3Kβ 240 YVLQVSGRVEYVFGDHPLIQFQYIRNCVMNRTLPHFILVECCKIKKMYEQEMIAIE
Mm_PI3Kδ 239 YALQVNGRHEYLYGNYPLCHFQYICSCLHSGLTPHLTMVHSSSILAMRDEQSN
α-helix
β-sheet
T turn
t bend
d disordered

L

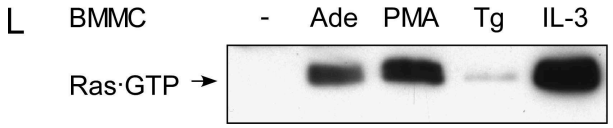
BMMC
-
Ade
PMA
Tg
IL-3
Ras·GTP

Figure S4

Suppl. to Figure 7

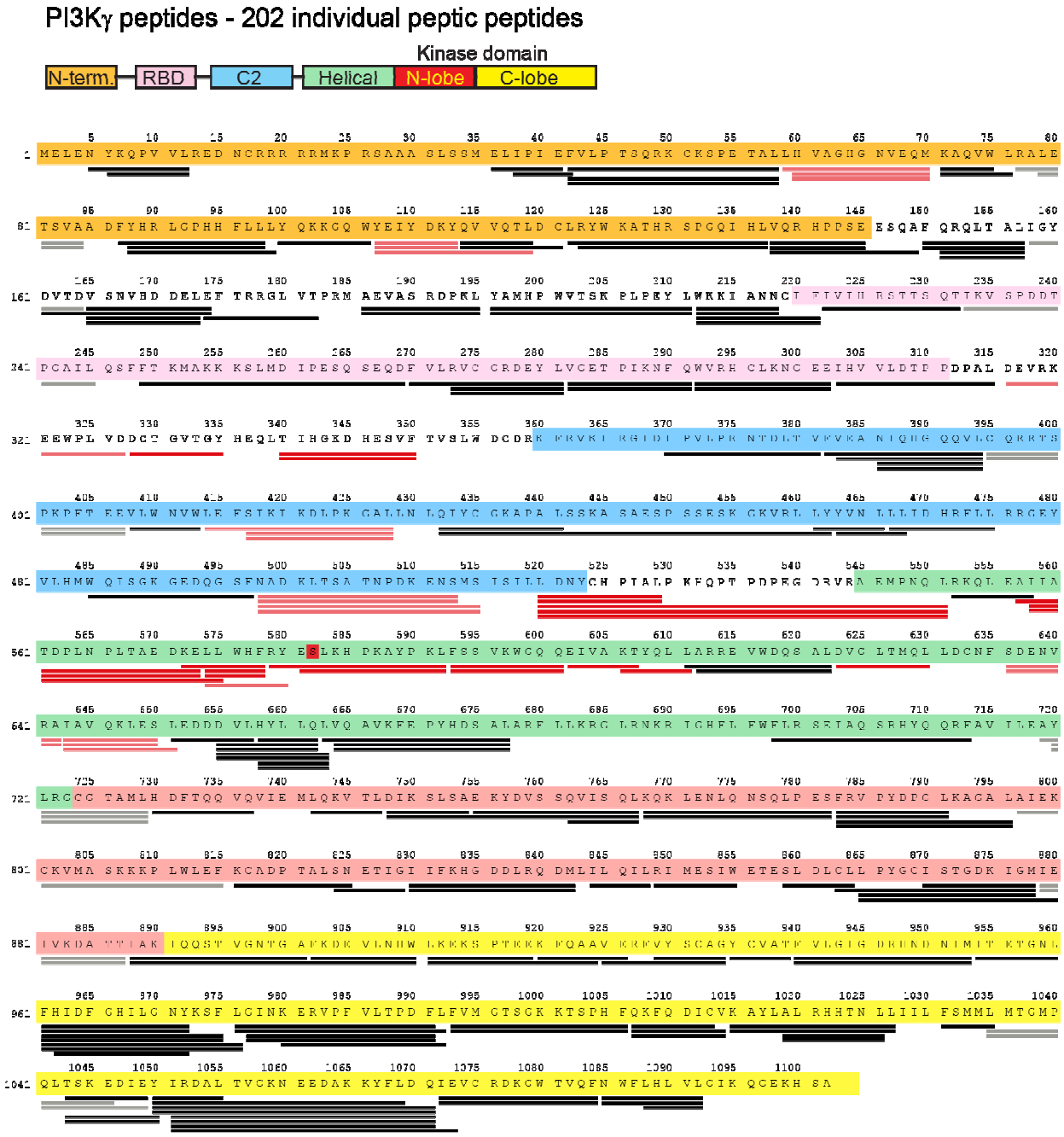

Figure S5

Suppl. to Figure 7

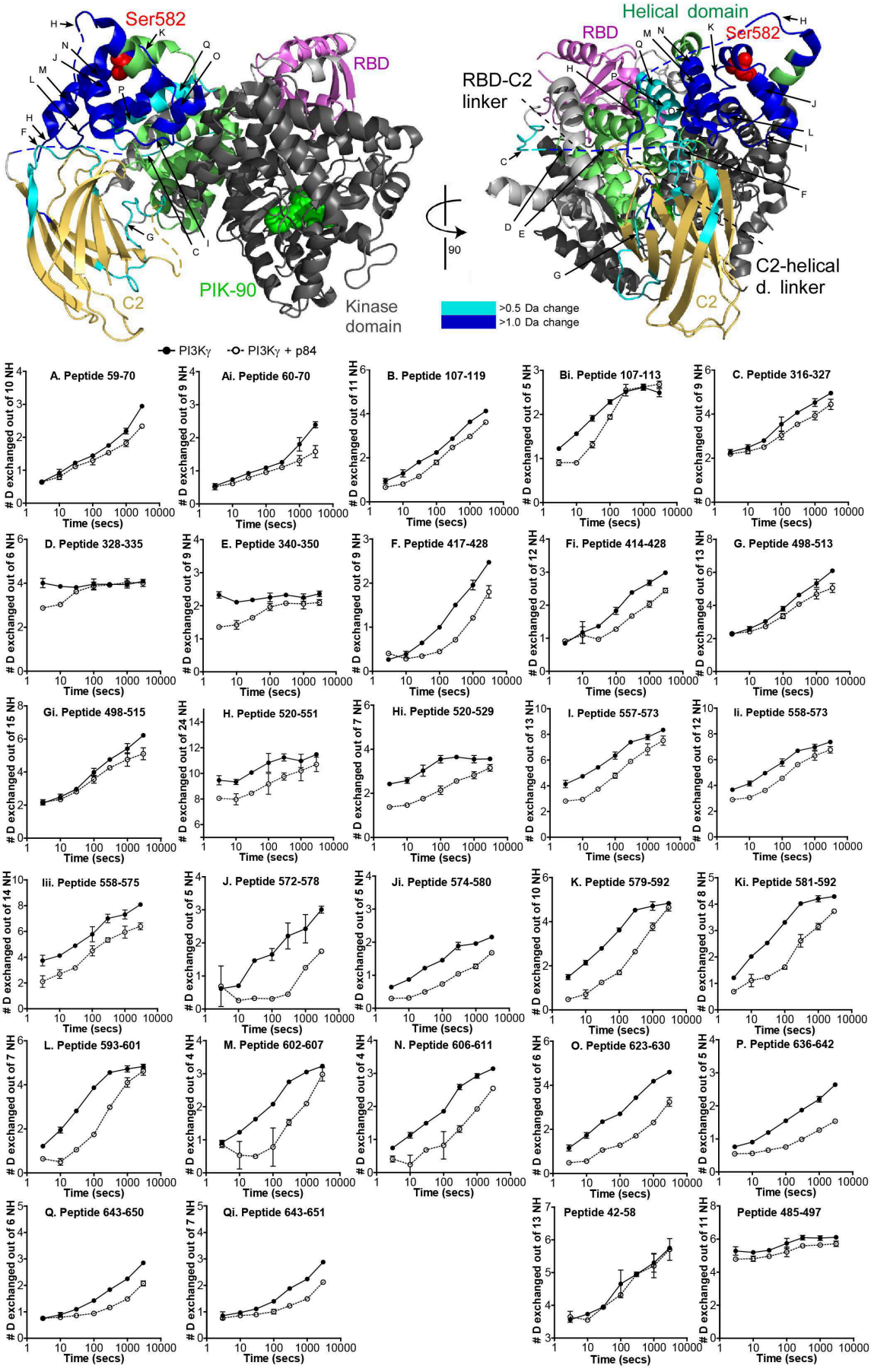

4.9 Supplemental figure legends

Figure S1. Related to Figure 3.

(A/B) Effect of different protein kinase C (PKC)-inhibitors on PMA or adenosine induced PKB phosphorylation (S473) was analysed by Western blotting and quantified with Image J software. Wild type BMMCs were starved for 3 hours in IL-3 free medium/2%FCS and preincubated with the inhibitors for 20 min before stimulation. pan-PKC inh.: Ro318425, Gö9683. cPKC-inh.: PKC412 (CPG41251). c/aPKC-inh.: Gö6976. Rottlerin: broad acting inhibitor, not PKC-specific.

(C) PKB activation in response to 100 nM PMA or 1 μM Thapsigargin (2 min) was analysed in wild type, PKC$\alpha^{-/-}$, and PKC$\gamma^{-/-}$ BMMCs. Before stimulation cells were starved as in (A/B). Cell lysates were analysed for PKB (S473) and MAPK (Thr183/Tyr185) phosphorylation by Western blotting.

(D) Wild type, PKC$\beta^{-/-}$, and PI3K$\gamma^{-/-}$ BMMCs (cultured for 4-7 weeks) were stimulated with different concentrations of Thapsigargin and degranulation was quantified by measuring release of β-hexosaminidase into cell supernatants. Data are the average of three independent experiments ± SEM.

Figure S2. Related to Figure 4.

(A/B) Identification of PI3Kγ phosphorylation sites by MS. Recombinant kinase-inactive GST-PI3Kγ (amino acids 38-1102) was phosphorylated in vitro by recombinant PKCβ in the presence of 100 μM ATP/[γ^{32}P]-ATP. Proteins were separated by SDS-PAGE and trypsin-digested PI3Kγ was analysed by LC-MSMS. (A) Enhanced product ion spectra of the tryptic phospho-S582-peptide of PI3Kγ. The y- and b-fragments detected are indicated in the sequence. Fragments showing a H_3PO_4 loss are marked with an asterisk. The b_2, y_6, and y_7 fragments allow assignment of the phosphorylation to serine 3 in the peptide. (B) Enhanced product ion spectra of the non-phosphorylated form of this peptide.

(C) Relevant information for the MRM analysis of the peptides containing Ser582. The amino acid numbering is as in Swiss-Prot entry P48736.

(D) Sequence alignment of the beginning of the helical domain of class I PI3Ks. Alignments were done by inspection of the crystal structures of PI3Kγ (1E8Y), PI3Kα (3HHM), PI3Kβ (2Y3A), and PI3Kδ (2WXR). Secondary structure elements are labelled as indicated in the legend. S582 is colored red, while cancer-associated PI3Kα mutations are marked as blue.

Figure S3. Related to Figure 5.

(A) Wild type BMMCs were transfected with empty vector or expression plasmids for GFP-PI3Kγ wild type or GFP-PI3Kγ S582A. Next day cells were stimulated with 200 nM PMA for 45 seconds, and PI3Kγ was immunoprecipitated from cell lysates. Specificity of the anti-phospho-S582 antibodies was validated by Western blotting.

(B) Autophosphorylation of recombinant wild type PI3Kγ-His6 and S582 mutants was analysed in the presence of 10 μM ATP/[^{32}P]-ATP in kinase buffer. For background measurement, reactions were also performed the presence of 0.5 μM Wortmannin (Wm). Band intensities were quantified

with phosphoimager technology and data are expressed as fold of autophosphorylation of PI3Kγ wt. Data represent two triplicate experiments ± SEM.

(C/D) Identification of PI3Kγ phosphorylation sites by MS. Recombinant kinase-inactive GST-PI3Kγ (residues 38-1102) was phosphorylated in vitro by recombinant PKCβ2 in the presence of 100 μM ATP/[γ^{32}P]-ATP. Proteins were separated by SDS-PAGE and trypsin-digested PI3Kγ was analysed by LC-MSMS. (C) Enhanced product ion spectra of the tryptic phospho-S257-peptide of PI3Kγ. The y- and b-fragments detected are indicated in the sequence. Fragments showing a H_3PO_4 loss are marked with an asterisk. The b3, b7, y10, and y12 fragments allow assignment of the phosphorylation to serine 3 in the peptide. (D) Enhanced product ion spectra of the non-phosphorylated peptide that starts with KSLM... Shown fragmentations are derived from precursors with oxidized methionine.

(E) In vitro and in vivo phosphorylation of PI3Kγ on S257 as analysed by LC-MRM. Data come from the same protein samples used to measure S582 phosphorylation (see figure 4D). Upper part: In vitro phosphorylated recombinant human PI3Kγ. The transitions 713.4 to 704.4 for the non-modified peptide (blue) and 782.7 to 993.5 for the phosphopeptide (red) are shown. Lower part: In vivo phosphorylated mouse PI3Kγ. Monitored were the transition from 709.7 to 777.4 for the non-modified peptide (blue) and the transitions from 779.0 to 1209.0, 906.5, and 746.0 for the phosphopeptide (red). Transitions of the non-modified peptides were set to 1 and used to normalize the data.

(F) Relevant information for the MRM analysis of the peptides containing Ser257. The amino acid numbering is as in Swiss-Prot entries P48736 and Q9JHG7.

(G) Kinetics of PI3Kγ phosphorylation on S257 and S582 were analysed with respect to time. BMMCs were IL-3 starved for 1 hour and stimulated with either 100 ng/ml DNP (pretreated with 100 ng/ml IgE overnight) or 1 μM Thapsigargin. PI3Kγ was immunoprecipitated from cell lysates and phosphorylation was analysed by Western blotting and quantification with ImageJ software. Data were normalised to phospho-PI3Kγ/PI3Kγ values of 0.5 min stimulation with DNP or 6 min with Thapsigargin, which were set to 1. Data are mean values ± SEM of three separate experiments (n = 3).

(H) Lipid kinase activities of recombinant PI3Kγ wild type, S257 mutants, and S257/S582 double mutants were measured by an in vitro kinase assay using mixed phospholipid vesicles containing PIP_2 as substrate. Extracted lipids were separated by thin layer chromatography and PIP_3 production was quantified by phosphoimager technology. Data represent mean ± SEM of a triplicate experiment.

(G) Comparison of the sequence around S257 with a PKCβ substrate motif determined by screening of a peptide library (Nishikawa K, J Biol Chem, 1997). Values in parentheses indicate relative selectivities for the amino acids (1 corresponds to no selectivity).

(H) Alignment of the sequences adjacent to S257 of PI3Kγ from different species (obtained by protein blast).

(I) Sequence alignment of the Ras binding domain (RBD) of class I PI3Ks near to S257 of PI3Kγ. Secondary structure assignments were done by inspection of the crystal structures of PI3Kγ (1E8Y,

1HE8), PI3Kα (3HHM), PI3Kβ (2Y3A), and PI3Kδ (2WXR), and are labelled as indicated in the legend. S257 is colored red. Mutated residues of published engineered inactivating PI3K RBD mutants are colored blue (DASAA) (Suire S, Nat Cell Biol, 2006) or are underlined (e.g. PI3Kγ K255E) (Kang S, Proc Natl Acad Sci U S A, 2006).

(J) BMMCs were stimulated with 5 μM adenosine, 200 nM PMA, 0.5 μM Thapsigargin, or 10 ng/ml IL-3 for 2 min. Cleared lysates were incubated with recombinant GST-RBD (of Raf) to capture active GTP-loaded endogenous Ras. Copurified Ras was detected by immunoblotting with a mix of anti-H-, anti-K-, anti-N-, and anti-pan-Ras antibodies.

Figure S4. Related to Figure 7.

PI3Kγ domain order and peptide coverage after pepsin digestion. Identified and analyzed peptides are shown under the primary sequence of PI3Kγ, which has been colored according to the domain boundaries shown above. Light or dark red lines represent peptides with greater than 0.5 or 1.0 Da changes in deuteration in the absence and presence of p84, respectively. Gray bars indicate peptides continued in the next line of the sequence.

Figure S5. Related to Figure 7.

Changes in deuteration levels of PI3Kγ in the presence of p84. Peptides spanning PI3Kγ (labelled A-Q) that showed greater than 0.5 Da changes in deuteration in the presence and absence of p84 were mapped onto the crystal structure of PI3Kγ (PDB ID: 2CHX, residues 144-1093). The greatest difference in exchange observed at any time was used for the mapping. Ser582 is shown as red balls. The ATP competitive inhibitor PIK-90 is shown in green as a reference point for the kinase domain. The linker regions between the RBD and the C2 domain and the C2 and helical domain are shown as dashes lines. Domain coloring was done the following: RBD: purple, C2 domain: light brown, helical domain: green, kinase domain: dark grey. The graphs are showing the number of incorporated deuteriums in the presence (o) and absence (•) of p84 at seven time points for peptides with more than 0.5 Da exchange difference. The last two graphs represent peptides with <0.5 Da deuteration changes. Data represent mean ± SD of two independent experiments.

4.10 Supplemental table and legend

				PI3Kγ							PI3Kγ + p84						
				Time													
Z	#D	S	E	3	10	30	100	300	1000	3000	3	10	30	100	300	1000	3000
1	5	5	12	85%	86%	86%	89%	90%	94%	86%	86%	84%	85%	85%	87%	89%	85%
1	4	6	12	76%	74%	75%	77%	75%	74%	75%	81%	78%	80%	79%	80%	80%	80%
1	3	36	41	3%	4%	5%	7%	11%	16%	19%	4%	4%	5%	6%	11%	14%	17%
1	3	38	42	2%	4%	6%	6%	5%	7%	6%	9%	4%	3%	3%	4%	12%	9%
2	13	42	58	28%	30%	31%	37%	39%	41%	45%	28%	27%	30%	33%	38%	41%	44%
3	13	42	58	27%	29%	31%	36%	39%	41%	44%	27%	26%	30%	33%	37%	40%	42%
4	13	42	58	27%	29%	30%	36%	38%	41%	44%	28%	27%	30%	33%	38%	40%	44%
2	10	59	70	6%	9%	12%	14%	18%	22%	29%	6%	8%	11%	13%	15%	18%	23%
1	9	60	70	6%	7%	10%	12%	14%	19%	26%	6%	7%	9%	12%	13%	15%	18%
2	9	60	70	5%	7%	9%	12%	14%	19%	25%	5%	6%	8%	10%	12%	15%	18%
1	3	71	75	2%	3%	2%	3%	2%	3%	5%	6%	7%	4%	7%	8%	12%	11%
1	4	71	76	3%	2%	3%	4%	6%	8%	9%	3%	2%	3%	4%	4%	5%	6%
1	6	77	84	51%	50%	51%	51%	50%	50%	50%	54%	52%	54%	53%	53%	54%	54%
1	4	79	84	48%	61%	65%	74%	76%	76%	78%	47%	55%	62%	72%	76%	76%	76%
3	9	87	98	4%	5%	3%	7%	8%	8%	11%	5%	4%	7%	5%	8%	6%	9%
2	8	88	98	6%	8%	9%	11%	12%	14%	17%	5%	6%	7%	8%	10%	10%	12%
3	9	88	99	4%	5%	6%	7%	8%	8%	11%	4%	4%	5%	6%	7%	7%	9%
1	5	100	106	32%	40%	52%	57%	56%	57%	59%	32%	37%	48%	56%	58%	60%	61%
1	5	107	113	25%	31%	38%	46%	50%	52%	50%	18%	18%	26%	39%	51%	53%	54%
2	5	107	113	25%	29%	37%	45%	51%	52%	54%	18%	21%	29%	40%	50%	54%	55%
2	11	107	119	9%	12%	16%	20%	26%	33%	37%	6%	7%	11%	16%	22%	27%	33%
1	4	114	119	0%	-1%	-1%	-1%	0%	2%	7%	0%	-2%	-2%	-2%	-2%	6%	3%
1	6	114	121	19%	19%	19%	20%	21%	25%	30%	14%	16%	20%	20%	22%	23%	26%
2	13	122	137	4%	5%	8%	13%	17%	19%	21%	4%	4%	6%	10%	16%	20%	21%
3	12	123	137	7%	8%	9%	13%	18%	21%	25%	6%	7%	9%	12%	17%	20%	26%
1	4	138	145	4%	4%	4%	8%	13%	21%	24%	6%	7%	6%	9%	14%	21%	25%
2	4	138	145	6%	6%	10%	10%	18%	23%	47%	6%	6%	6%	8%	12%	18%	43%
2	8	138	149	33%	37%	39%	50%	52%	54%	56%	33%	33%	39%	46%	51%	53%	52%
1	6	150	157	-1%	-1%	0%	4%	11%	17%	24%	-1%	-1%	0%	6%	13%	17%	23%
2	6	150	157	3%	4%	5%	8%	14%	25%	28%	3%	4%	6%	9%	14%	20%	25%
1	5	151	157	5%	3%	5%	10%	18%	22%	28%	4%	3%	5%	9%	17%	24%	27%
2	5	151	157	4%	4%	5%	9%	17%	30%	34%	6%	5%	6%	11%	23%	31%	35%
1	5	158	164	11%	13%	15%	24%	36%	45%	53%	21%	16%	22%	31%	44%	51%	59%
2	12	161	174	20%	26%	28%	33%	37%	41%	46%	25%	28%	32%	35%	41%	45%	47%
1	7	165	173	13%	22%	26%	32%	33%	32%	34%	18%	21%	27%	30%	32%	32%	32%
2	7	165	173	15%	24%	27%	32%	37%	36%	36%	19%	22%	28%	30%	37%	34%	33%
1	8	165	174	17%	24%	26%	31%	33%	35%	38%	18%	22%	26%	28%	32%	36%	36%
1	7	174	182	2%	2%	3%	4%	8%	13%	16%	2%	3%	2%	3%	5%	11%	14%
1	7	186	195	11%	19%	19%	25%	32%	40%	47%	15%	19%	21%	25%	34%	43%	47%
2	7	186	195	11%	17%	20%	25%	32%	40%	48%	13%	15%	19%	24%	32%	41%	47%
2	11	196	211	22%	25%	29%	35%	39%	42%	47%	23%	23%	29%	32%	37%	42%	45%
3	11	196	211	22%	25%	28%	35%	38%	42%	46%	22%	23%	28%	31%	36%	41%	44%
1	5	212	218	39%	45%	51%	60%	67%	69%	71%	47%	48%	55%	61%	69%	72%	72%
2	5	212	218	43%	50%	55%	66%	72%	74%	76%	45%	46%	55%	63%	70%	73%	75%
1	8	212	221	20%	26%	30%	41%	49%	53%	57%	19%	21%	27%	35%	48%	52%	56%
2	8	212	221	25%	31%	28%	43%	52%	55%	56%	24%	29%	26%	42%	50%	54%	54%
1	9	222	232	28%	27%	27%	29%	30%	33%	36%	28%	27%	28%	29%	30%	33%	35%
2	9	233	245	8%	9%	10%	14%	18%	21%	25%	10%	10%	10%	14%	19%	22%	27%
4	18	249	269	48%	48%	48%	51%	50%	50%	52%	49%	47%	50%	49%	52%	52%	53%
2	10	270	281	-11%	-12%	-10%	-10%	-8%	-8%	-6%	-9%	-9%	-11%	-10%	-9%	-7%	-7%
1	7	273	281	1%	2%	3%	4%	6%	5%	7%	3%	1%	4%	6%	2%	3%	5%
2	7	273	281	2%	2%	2%	2%	3%	4%	5%	3%	3%	3%	4%	3%	3%	4%
1	7	282	291	10%	9%	9%	10%	10%	11%	15%	8%	7%	7%	6%	9%	9%	13%
2	7	282	291	6%	8%	9%	10%	10%	11%	14%	7%	6%	6%	7%	8%	8%	11%
2	9	292	302	5%	11%	15%	21%	21%	21%	23%	6%	8%	16%	19%	21%	21%	22%
3	9	292	302	5%	11%	15%	21%	21%	21%	23%	7%	10%	17%	21%	23%	22%	22%
2	8	303	315	12%	9%	13%	17%	20%	23%	22%	12%	9%	16%	16%	20%	22%	24%
2	9	316	327	25%	28%	31%	39%	45%	50%	55%	24%	26%	28%	34%	39%	44%	49%
1	6	328	335	67%	64%	64%	66%	66%	66%	68%	48%	51%	60%	65%	65%	67%	67%
2	9	340	350	26%	23%	24%	25%	26%	25%	26%	15%	16%	18%	22%	23%	23%	23%
3	9	340	350	25%	23%	23%	24%	24%	24%	25%	17%	17%	20%	23%	25%	24%	27%
2	9	370	381	31%	35%	39%	47%	55%	56%	58%	33%	33%	38%	46%	53%	56%	57%
2	11	382	394	9%	13%	15%	17%	19%	21%	25%	10%	11%	14%	15%	18%	20%	23%
2	10	383	394	8%	13%	14%	16%	18%	21%	25%	9%	11%	14%	15%	18%	20%	22%
1	7	386	394	15%	21%	23%	26%	30%	35%	41%	15%	17%	21%	23%	26%	32%	37%
2	7	386	394	16%	24%	25%	28%	31%	34%	41%	21%	24%	24%	25%	30%	34%	42%
2	9	395	407	11%	13%	16%	22%	25%	28%	32%	13%	13%	17%	20%	25%	29%	31%
3	9	395	407	11%	13%	15%	22%	26%	28%	32%	12%	13%	17%	20%	25%	29%	32%
1	4	408	413	15%	27%	32%	37%	42%	52%	62%	13%	19%	29%	35%	42%	51%	57%
2	12	414	428	7%	10%	11%	15%	20%	22%	25%	8%	9%	8%	11%	14%	17%	20%
2	9	417	428	3%	5%	8%	13%	19%	23%	30%	3%	2%	4%	5%	6%	11%	21%
3	9	417	428	3%	4%	7%	11%	17%	22%	27%	4%	3%	4%	5%	8%	13%	20%
2	7	432	441	45%	43%	45%	50%	54%	55%	54%	42%	40%	43%	45%	48%	53%	53%
4	27	432	462	31%	30%	32%	34%	35%	35%	36%	30%	31%	32%	35%	35%	37%	35%
1	4	461	466	0%	0%	0%	0%	0%	1%	0%	-1%	-1%	0%	0%	0%	1%	-1%
1	4	463	468	0%	1%	1%	5%	14%	20%	21%	5%	4%	2%	5%	11%	15%	25%
2	7	467	475	1%	1%	7%	7%	13%	14%	14%	2%	1%	2%	8%	11%	11%	11%
2	11	485	497	48%	47%	48%	52%	55%	55%	56%	44%	44%	45%	47%	51%	51%	52%
2	13	498	513	17%	20%	23%	29%	35%	41%	47%	17%	18%	21%	25%	31%	36%	38%
3	13	498	513	18%	21%	24%	30%	36%	42%	47%	18%	18%	21%	25%	31%	34%	38%
2	15	498	515	14%	17%	20%	26%	31%	35%	41%	14%	15%	18%	23%	28%	32%	34%
3	15	498	515	14%	16%	19%	26%	31%	36%	41%	14%	15%	18%	23%	28%	31%	34%
1	7	520	529	33%	35%	41%	51%	52%	50%	51%	19%	21%	25%	31%	36%	37%	40%
2	7	520	529	35%	37%	43%	51%	52%	51%	51%	20%	21%	25%	31%	37%	40%	45%
3	24	520	551	39%	39%	42%	45%	47%	46%	48%	34%	34%	36%	39%	41%	43%	45%
4	24	520	551	39%	39%	42%	45%	47%	46%	48%	34%	33%	35%	38%	41%	42%	45%
5	24	520	551	35%	36%	39%	42%	43%	42%	45%	29%	30%	32%	35%	38%	37%	42%
2	5	552	558	15%	15%	19%	18%	18%	24%	26%	19%	18%	17%	25%	36%	23%	25%
2	13	557	573	32%	36%	42%	49%	57%	60%	64%	22%	23%	29%	37%	45%	53%	58%
2	12	558	573	31%	35%	41%	48%	56%	58%	61%	24%	25%	30%	38%	47%	53%	56%
2	14	558	575	27%	29%	35%	41%	50%	52%	58%	15%	19%	23%	32%	38%	42%	46%
2	5	572	578	12%	14%	29%	33%	44%	49%	60%	14%	5%	6%	6%	9%	25%	35%
1	3	574	578	9%	11%	15%	19%	27%	32%	37%	-1%	0%	1%	2%	5%	13%	22%
2	3	574	578	17%	21%	25%	29%	37%	43%	48%	5%	5%	8%	9%	13%	21%	31%
2	5	574	580	13%	17%	24%	29%	38%	39%	43%	6%	6%	10%	15%	21%	25%	34%
2	10	579	592	15%	21%	28%	36%	45%	47%	48%	5%	7%	12%	17%	26%	38%	47%
3	8	581	592	15%	25%	32%	41%	50%	52%	54%	9%	14%	15%	20%	33%	39%	47%
1	7	593	601	17%	28%	40%	55%	65%	67%	69%	9%	7%	15%	25%	43%	59%	66%
2	7	593	601	18%	22%	39%	53%	64%	65%	66%	6%	13%	25%	27%	56%	60%	64%
1	4	602	607	23%	31%	41%	52%	69%	76%	81%	21%	8%	12%	20%	38%	52%	75%
1	4	606	611	19%	28%	37%	46%	65%	73%	79%	10%	6%	17%	21%	33%	48%	64%

				PI3Kγ							PI3Kγ + p84						
				Time													
Z	#D	S	E	3	10	30	100	300	1000	3000	3	10	30	100	300	1000	3000
2	10	611	622	50%	54%	54%	56%	57%	57%	59%	52%	51%	53%	53%	56%	56%	56%
2	9	612	622	51%	53%	52%	55%	54%	54%	55%	53%	51%	53%	52%	55%	54%	54%
1	6	623	630	19%	29%	39%	45%	57%	70%	77%	8%	9%	18%	21%	28%	38%	54%
1	5	636	642	15%	19%	25%	32%	38%	45%	53%	12%	12%	14%	16%	22%	28%	32%
2	5	636	642	15%	18%	24%	31%	37%	44%	53%	11%	11%	13%	15%	20%	25%	31%
1	6	643	650	13%	14%	19%	23%	30%	35%	45%	12%	13%	15%	15%	18%	24%	34%
2	6	643	650	12%	15%	18%	24%	31%	37%	48%	13%	13%	14%	16%	19%	25%	35%
2	7	643	651	12%	14%	16%	20%	27%	32%	41%	11%	12%	13%	14%	18%	21%	30%
1	5	651	657	3%	3%	4%	6%	9%	13%	18%	3%	2%	3%	4%	9%	19%	20%
1	6	655	662	12%	11%	8%	14%	24%	31%	39%	11%	11%	7%	11%	20%	32%	38%
2	6	655	662	1%	3%	5%	10%	20%	30%	36%	3%	3%	4%	9%	20%	29%	37%
1	7	655	663	2%	2%	3%	8%	20%	25%	31%	1%	2%	1%	7%	15%	25%	31%
2	7	655	663	1%	2%	4%	9%	18%	27%	32%	1%	1%	3%	7%	16%	26%	32%
1	3	658	662	4%	6%	8%	13%	24%	31%	33%	4%	4%	6%	10%	19%	29%	32%
1	4	658	663	0%	1%	1%	4%	17%	25%	25%	1%	1%	1%	4%	17%	25%	21%
2	4	658	663	-3%	-2%	0%	7%	15%	20%	22%	4%	4%	4%	7%	16%	21%	26%
3	12	663	677	3%	4%	5%	6%	7%	7%	9%	3%	3%	4%	5%	6%	6%	7%
2	11	664	677	3%	4%	6%	7%	8%	9%	10%	2%	2%	5%	6%	7%	7%	8%
3	11	664	677	4%	5%	6%	8%	8%	9%	10%	2%	3%	4%	5%	8%	7%	8%
4	14	698	713	4%	5%	6%	9%	12%	17%	20%	4%	4%	5%	8%	13%	17%	21%
1	9	719	729	0%	1%	3%	7%	10%	16%	25%	-1%	0%	4%	8%	12%	21%	29%
1	8	720	729	2%	6%	9%	12%	14%	19%	27%	3%	3%	6%	9%	12%	19%	28%
2	8	720	729	3%	5%	9%	13%	16%	24%	31%	4%	4%	7%	10%	15%	22%	33%
1	6	730	737	1%	1%	1%	1%	1%	1%	1%	1%	0%	0%	0%	0%	1%	1%
1	4	742	747	9%	17%	28%	40%	51%	61%	69%	7%	12%	23%	38%	48%	60%	68%
1	5	748	754	69%	69%	71%	75%	76%	77%	81%	77%	74%	75%	75%	77%	77%	78%
2	18	748	767	64%	62%	63%	64%	66%	64%	66%	64%	62%	63%	64%	64%	65%	65%
2	11	755	767	64%	68%	69%	66%	70%	73%	74%	61%	65%	68%	68%	69%	70%	72%
1	4	762	767	3%	4%	4%	6%	8%	11%	24%	9%	2%	2%	4%	7%	12%	17%
2	12	768	782	30%	37%	46%	62%	67%	67%	69%	31%	35%	46%	58%	66%	67%	66%
3	12	768	782	30%	39%	45%	59%	64%	64%	66%	31%	34%	45%	56%	64%	65%	65%
1	5	783	791	2%	1%	2%	3%	7%	11%	13%	0%	1%	1%	2%	5%	10%	11%
2	5	783	791	-3%	-1%	1%	3%	5%	6%	10%	0%	1%	5%	2%	5%	7%	8%
2	10	783	796	3%	3%	3%	6%	12%	18%	22%	3%	3%	3%	7%	12%	18%	22%
3	10	783	796	3%	3%	5%	7%	12%	18%	21%	4%	3%	3%	6%	12%	18%	21%
4	16	797	815	7%	7%	10%	13%	15%	16%	18%	6%	7%	8%	11%	15%	17%	17%
1	7	816	825	36%	41%	49%	60%	65%	67%	69%	34%	36%	45%	55%	61%	63%	65%
1	4	824	829	30%	38%	43%	52%	55%	56%	60%	38%	40%	51%	56%	55%	56%	63%
2	11	830	842	4%	6%	10%	15%	18%	19%	21%	3%	3%	8%	13%	16%	19%	21%
3	11	830	842	2%	5%	8%	13%	16%	20%	21%	2%	3%	7%	13%	19%	19%	20%
1	3	844	848	4%	3%	6%	7%	16%	5%	4%	1%	6%	6%	7%	9%	6%	5%
1	5	849	855	1%	1%	0%	0%	5%	6%	3%	0%	0%	0%	-1%	6%	-1%	1%
1	4	859	864	0%	0%	1%	4%	1%	1%	1%	7%	0%	1%	1%	1%	2%	1%
2	13	863	878	4%	4%	4%	8%	13%	17%	21%	4%	4%	4%	6%	12%	16%	21%
2	12	865	878	4%	5%	5%	8%	11%	14%	17%	4%	4%	4%	6%	9%	12%	16%
2	14	865	880	3%	6%	6%	8%	8%	11%	12%	3%	3%	3%	7%	8%	11%	12%
1	7	870	878	5%	6%	6%	10%	15%	18%	22%	6%	5%	6%	8%	14%	18%	21%
1	7	879	887	22%	31%	37%	45%	50%	53%	55%	26%	31%	36%	45%	51%	54%	56%
2	7	879	887	26%	34%	39%	44%	53%	52%	54%	28%	41%	40%	41%	48%	52%	54%
2	12	888	901	46%	45%	47%	51%	54%	58%	63%	43%	43%	45%	48%	50%	55%	59%
4	21	888	910	23%	25%	28%	29%	32%	34%	38%	23%	24%	27%	28%	31%	34%	36%
1	7	902	910	7%	9%	9%	11%	17%	21%	23%	5%	5%	6%	7%	11%	14%	17%
3	6	911	919	9%	9%	8%	11%	15%	19%	22%	6%	4%	5%	6%	8%	11%	16%
3	11	911	924	14%	16%	19%	23%	27%	32%	41%	15%	13%	18%	22%	27%	33%	40%
1	5	920	926	4%	11%	12%	13%	12%	16%	20%	4%	4%	4%	7%	8%	14%	21%
1	8	925	934	3%	2%	1%	1%	2%	1%	3%	3%	1%	0%	2%	1%	0%	2%
1	4	929	934	1%	1%	1%	2%	2%	2%	2%	1%	2%	1%	2%	-1%	1%	0%
1	3	935	939	-4%	-4%	-4%	-4%	-4%	-4%	-4%	0%	1%	2%	2%	2%	1%	-1%
2	12	940	953	2%	1%	2%	3%	5%	7%	9%	2%	1%	2%	3%	5%	7%	8%
3	12	940	953	1%	1%	2%	2%	4%	7%	9%	1%	1%	2%	2%	4%	7%	8%
1	5	954	960	4%	7%	10%	18%	22%	25%	28%	4%	5%	10%	17%	22%	25%	28%
2	10	961	972	29%	30%	31%	34%	36%	35%	38%	29%	28%	31%	31%	34%	34%	36%
3	10	961	972	27%	29%	30%	33%	35%	34%	37%	28%	27%	30%	31%	33%	34%	36%
2	13	961	975	32%	33%	33%	36%	38%	37%	40%	33%	33%	36%	35%	37%	37%	37%
3	13	961	975	35%	34%	34%	37%	37%	37%	40%	34%	32%	33%	33%	36%	36%	38%
2	14	961	976	38%	39%	40%	42%	44%	43%	46%	38%	37%	39%	39%	41%	42%	43%
3	14	961	976	38%	39%	40%	41%	43%	42%	44%	38%	37%	40%	39%	41%	42%	43%
2	9	962	972	34%	36%	38%	41%	42%	43%	45%	35%	35%	37%	40%	40%	42%	44%
3	12	976	991	8%	8%	9%	13%	16%	15%	18%	10%	10%	17%	15%	19%	18%	20%
3	13	976	992	12%	11%	12%	16%	19%	18%	21%	13%	11%	14%	16%	19%	19%	21%
2	11	977	991	12%	11%	14%	17%	20%	20%	21%	12%	11%	12%	16%	20%	20%	21%
3	11	977	991	13%	13%	14%	18%	20%	22%	24%	14%	13%	13%	17%	20%	23%	22%
2	9	980	992	3%	4%	6%	8%	11%	12%	12%	3%	2%	4%	8%	12%	10%	14%
2	11	993	1006	16%	15%	16%	20%	22%	23%	27%	16%	15%	16%	20%	21%	23%	22%
3	11	993	1006	21%	20%	19%	22%	26%	28%	31%	18%	19%	18%	22%	26%	25%	29%
1	5	1007	1013	3%	3%	2%	3%	4%	3%	5%	7%	4%	6%	0%	5%	3%	6%
1	6	1007	1014	2%	3%	3%	3%	4%	4%	5%	2%	2%	1%	1%	4%	2%	4%
2	6	1007	1014	0%	0%	-2%	-1%	0%	4%	1%	3%	2%	-1%	-1%	2%	1%	1%
2	11	1015	1027	1%	2%	2%	3%	6%	8%	9%	1%	1%	1%	2%	5%	8%	9%
3	11	1015	1027	3%	3%	4%	5%	8%	10%	13%	2%	2%	2%	3%	6%	9%	10%
1	6	1019	1026	8%	10%	11%	13%	17%	24%	24%	13%	16%	13%	17%	25%	20%	21%
2	6	1019	1026	7%	7%	7%	10%	15%	17%	19%	11%	11%	10%	15%	20%	23%	19%
1	3	1031	1035	-3%	-2%	-2%	-2%	-1%	1%	2%	-2%	-1%	-1%	-1%	-1%	0%	-1%
2	9	1035	1046	7%	12%	13%	16%	17%	20%	25%	7%	9%	12%	14%	17%	20%	24%
2	12	1035	1049	30%	34%	37%	44%	50%	52%	56%	31%	31%	36%	43%	49%	54%	56%
1	5	1043	1049	27%	33%	36%	45%	54%	61%	64%	30%	29%	32%	37%	51%	58%	62%
1	6	1043	1050	21%	23%	31%	39%	49%	57%	62%	20%	18%	25%	33%	44%	54%	59%
2	6	1043	1050	22%	23%	28%	38%	47%	52%	56%	22%	20%	23%	31%	41%	49%	52%
1	4	1050	1055	1%	2%	1%	0%	-1%	-1%	-1%	9%	1%	1%	0%	0%	-1%	0%
3	18	1050	1069	11%	10%	10%	12%	12%	14%	18%	11%	10%	9%	9%	10%	12%	17%
3	20	1050	1071	9%	10%	10%	11%	12%	14%	16%	9%	9%	10%	9%	11%	12%	14%
4	20	1050	1071	10%	11%	11%	13%	14%	15%	17%	10%	10%	11%	12%	14%	15%	18%
2	19	1051	1071	11%	11%	11%	13%	13%	14%	17%	11%	11%	10%	11%	12%	13%	15%
3	19	1051	1071	10%	11%	10%	12%	12%	13%	16%	11%	10%	11%	11%	12%	12%	15%
4	19	1051	1071	10%	10%	11%	12%	13%	13%	16%	11%	10%	11%	10%	11%	14%	15%
4	21	1051	1073	9%	9%	10%	11%	12%	12%	14%	11%	10%	11%	11%	12%	12%	13%
2	11	1072	1084	12%	17%	23%	34%	41%	41%	42%	13%	15%	23%	33%	40%	41%	42%
3	11	1072	1084	12%	16%	21%	32%	39%	41%	44%	11%	13%	22%	32%	38%	41%	42%
1	6	1085	1092	31%	38%	49%	58%	57%	59%	58%	31%	34%	44%	55%	61%	59%	62%
2	6	1085	1092	22%	39%	57%	66%	69%	68%	66%	23%	34%	55%	69%	72%	72%	71%
1	3	1088	1092	37%	63%	69%	74%	74%	73%	75%	43%	53%	68%	73%	75%	76%	77%

Relative % deuteration: 0% 5% 10% 15% 20% 25% 30% 35% 40% 45% 50% 55% 60% 65% 70%-95%

Table S1. Related to Figure 7.

Deuterium exchange data of all analysed peptides (202 peptides) of PI3Kγ in the absence or presence of p84 are summarized in tabular form. Percent hydrogen deuterium exchange was calculated for each of the seven time points and colored according to the legend. Data show the mean of two independent experiments. The charge state (Z), maximal number of exchangeable amide hydrogens (#D), starting residue number (S), and ending residue number (E) are displayed for every peptide.

5. Discussion

5.1 Allergy depends on PI3K

In allergy mast cells are activated through the high-affinity receptor for IgE (FcεRI). Receptor crosslinking by IgE/allergen engages the mast cells full mediator release program, leading to granule exocytosis and the production of lipid mediators, cytokines, and chemokines. Preformed granule stored histamine and both stored and newly synthesized TNFα exert very broad and potent effector functions. Through activation of the H1 receptor, histamine induces vascular leakage, tissue swelling, smooth muscle contraction, and cytokine production. TNFα on the other hand upregulates and activates adhesion molecules on blood vessels and thereby promotes the recruitment of neutrophils and eosinophils, and as well, stimulates cytokine production. Pharmacological targeting of these molecules or cognate receptors has proofed useful to combat allergy-associated symptoms. However, their dedication is limited to some inflammatory conditions, and more powerful drugs that for example already interfere with mediator secretion would be beneficial. Since early on it has been recognized that phosphoinositide 3-kinase (PI3K) is essential to antigen-induced mast cell activation, making it to an interesting drug target. However the mechanisms of PI3K activation and regulation by the FcεRI are incompletely understood and controversial. This study confirms PI3Kγ's central role in mast cell degranulation and opens insight into novel regulation mechanisms.

5.2 Ca^{2+} mobilisation triggers PI3K activation in mast cells

We have shown that the class IB PI3K isoform PI3Kγ controls mast cell activation in vivo by IgE/antigen in a model of passive systemic anaphylaxis (Laffargue M, Immunity, 2002). By analysis of PI3K$\gamma^{-/-}$ bone marrow-derived mast cells (BMMCs), we found that PI3Kγ partially controls mast cell degranulation by integrating autocrine and paracrine GPCR-derived signals into the FcεRI pathway. Synergistic signalling readily allows intracellular barriers to be overcome, leading to massive mast cell degranulation. Here we showed that the FcεRI also directly couples to PI3Kγ independently of GPCRs. Signalling to degranulation requires to overcome a threshold concentration of intracellular Ca^{2+}. Thapsigargin and other Ca^{2+} mobilising agents are widely used to trigger exocytosis at this receptor-distal step. We show that PI3K$\gamma^{-/-}$ BMMCs fail to degranulate in response to Thapsigargin, and thereby identify the step of PI3Kγ activation to be downstream of the Ca^{2+} signal. Thapsigargin thereby activates PI3Kγ independently of autocrine-released adenosine and other GPCR-ligands, since Thapsigargin-induced degranulation is insensitive to the treatment with adenosine deaminase or *B. Pertussis* Toxin (Figure 1). Initially we observed reduced Ca^{2+} mobilisation in PI3K$\gamma^{-/-}$ BMMCs in response to IgE/DNP (Laffargue M, Immunity, 2002, Fig. 1A) or Thapsigargin (not shown). This however, we found to be derived from artificial Ca^{2+} signals in wild type BMMCs caused by Fura-2's property to partition into granules leading to dye release into the medium upon stimulation (Almers W and Neher E, FEBS Lett, 1985; Di Virgilio F, Cell Calcium, 1990; Vorndran C, Biophys J, 1995). In later experiments with other fluorescent Ca^{2+} chelators like Fura-4F or Fura-FF no differences between wild type and PI3K$\gamma^{-/-}$ BMMCs were

observed (PI3K in signalling and disease, abstract, 2003, Katja Björklöf). As Thapsigargin does not activate PI3Kγ in the presence of Ca^{2+} chelators, Ca^{2+} influx is the trigger that activates PI3Kγ (Figure 2A, B). Interestingly, threshold levels for PI3Kγ activation lay in the low micromolar range (Figure 2C), which cells only can achieve by the uptake of external Ca^{2+}. Other receptors, like some GPCRs, that promote low Ca^{2+} signals by internal store depletion can not couple to "Ca^{2+}-sensitive" PI3Kγ (Figure 2E). FcεRI crosslinking triggers a strong and sharp rise of intracellular Ca^{2+} followed by a plateau phase of sustained decayed Ca^{2+} influx (reviewed in (Ma HT and Beaven MA, Crit Rev Immunol, 2009)). Several evidence indicate that PI3K activation by the FcεRI occurs downstream of the initial peak of Ca^{2+} mobilisation. First, in the absence of Ca^{2+}, FcεRI crosslinking fails to promote protein kinase B (PKB) activation, which is strictly controlled by PI3K-derived PIP_3 (Figure 5B). Second, studies with the PI3K-inhibitor Wortmannin have shown that initial PLCγ activation, inositol trisphosphate (IP3) production, and Ca^{2+} mobilisation are not affected by this drug (Tkaczyk C, J Biol Chem, 2003). In some studies reduced Ca^{2+} mobilisation was reported owing to Fura-2-dependent artefacts (Lam RS, Cell Physiol Biochem, 2008). Third, PI3K activation absolutely depends on PKCβ2 (Figure 3), which requires Ca^{2+} for its activation. Fourth, if PI3K activation would occur upstream of Ca^{2+} mobilisation, degranulation triggered by Thapsigargin or ionophores should be Wortmannin-insensitive and PI3K-independent which is not the case (Figure 1) (Marquardt DL, J Immunol, 1996). FcεRI-induced Ca^{2+} mobilisation is regulated by PLCγ, which is cooperatively activated by Syk, LAT1, and SLP-76 (Kambayashi T, Mol Cell Biol, 2010). LAT1 anchors PLCγ directly but also recruits it through SLP-76 (Saitoh S, J Exp Med, 2003). Impaired LAT1 signalling is partially rescued through LAT2 redistribution into the LAT1 compartment leading to recruitment of SLP-76-PLCγ by this adaptor. LAT1-LAT2 double knockout BMMCs show a complete block of PLCγ activation and Ca^{2+} mobilisation (Zhu M, J Exp Med, 2004; Kambayashi T, Mol Cell Biol, 2010). Data on PKB activation in LAT deficient BMMCs have been published only in two studies. Unexpectedly, Roget K. et al. reported unimpaired PKB activation in both $LAT1^{-/-}$ and $LAT1\text{-}LAT2^{-/-}$ BMMCs (stimulation time, DNP concentration unknown) (Roget K, J Immunol, 2008). But also unexpectedly, these cells as well as the wild type BMMCs showed a $SHIP^{-/-}$ or $Lyn^{-/-}$ like phenotype, at least insofar as degranulation was not inhibited at supraoptimal antigen concentrations (Gimborn K, J Immunol, 2005; Hernandez-Hansen V, J Immunol, 2004). Concurrently they also reported a role for LAT in negative signalling (Malbec O, J Immunol, 2004; Roget K, J Immunol, 2008). The route of PI3K activation has not been analysed in these studies. Reduced SHIP activation with concomitant continued PIP_3 accumulation might have been responsible for PKB activation. Consistently, in another report, PKB activation was greatly reduced at 2 min in $LAT1^{-/-}$ BMMCs, but was normal at late timer points (Kambayashi T, Immunol Rev, 2009). Alternatively, these cells might have gained the ability to activate PI3K by other means. In studies done by other groups, LAT deficient BMMCs showed normal inhibition of degranulation at supraoptimal antigen concentrations (Saitoh S, Immunity, 2000; Saitoh S, J Exp Med, 2003; Zhu M, J Exp Med, 2004). Whether reduced degranulation correlates with reduced PI3K activation has not been investigated in these reports. It can be speculated that the different behaviour of $LAT^{-/-}$ BMMCs of distinct groups is related to the age of

the mast cells, which over prolonged culture time loose inhibitory control mechanisms or gain new functions. Whatsoever, it would be important to analyse PKB activation at optimal antigen concentrations and at early time points, when PIP_3 levels are not influenced by defects in SHIP activation. Furthermore, interpretation of adaptor knock-out phenotypes is complicated by the multifunctionality of these proteins. In this respect, analysis of LAT knock-in BMMCs harboring specific protein binding site mutations would be interesting.

5.3 PI3Kδ, p85 regulatory subunits, Gab2, and Fyn are not direct regulators of the FcεRI

While PI3K is accepted as an essential controller of FcεRI-induced mast cell degranulation, the role of individual family members and their mode of activation have been controversial. Apart from PI3Kγ, PI3Kδ has been reported to control mast cell degranulation (Ali K, Nature, 2004). Additionally, there has been provided evidence, but also disproof, for a role of tyrosine kinase Fyn and the adaptor protein Gab2 as PI3K and degranulation regulators (Parravicini V, Nat Immunol, 2002; Gu H, Nature, 2001).

In vivo the most ubiquitously expressed class IA PI3K regulatory subunit p85α is not required for IgE-dependent mast activation in a model of passive systemic anaphylaxis (Fukao T, Nat Immunol, 2002). Consistently, p85α$^{-/-}$ BMMCs also degranulate normally (Fukao T, Nat Immunol, 2002; Tkaczyk C, J Biol Chem, 2003). It might be possible that p85α function is compensated by another "p85" regulatory subunit. However, p85α-p55α-p50α$^{-/-}$ fetal liver-derived mast cells (FLMCs) also readily degranulate, despite class IA PI3K expression and PI3K activation, as assessed by loss of proliferation and migration in response to stem cell factor (SCF), is severely compromised in these cells (Lu-Kuo JM, J Biol Chem, 2000; Tan BL, Blood, 2003). Importantly, PIP_3 downregulation by SHIP seems to be intact, as these cells do not show a phenotype of exaggerated PKB activation. As for p85α, genetic deletion of p85β also does not impair degranulation of BMMCs (Lu-Kuo JM, J Biol Chem, 2000; Tkaczyk C, J Biol Chem, 2003).

In vivo mast cell degranulation in the ear of PI3Kδ kinase inactive (D910A/D910A) as well as Gab2$^{-/-}$ mice is reduced by half compared with wild type mice, which correlates well with the reported 50% reduction in mast cell numbers at this location (Ali K, Nature, 2004; Yu M, J Biol Chem, 2006; Nishida K, Blood, 2002). Peculiarly, degranulation has been reported being reduced by 50% in PI3Kδ$^{D910A/D910A}$ BMMCs, despite PKB was readily activated in these cells in response to stimulation of the FcεRI. In regard of these in vivo and in vitro results, unambiguous interpretation of PI3Kδ function is not possible and needs further investigation.

Gab2 is a widely expressed adaptor protein with an N-terminal PIP_3-selective PH domain, several tyrosine and serine/threonine phosphorylation sites, and two proline-rich motifs. Gab2 has been implicated in growth factor and cytokine signalling in cultured cells (Gu H, Mol Cell, 1998; Nishida K, Blood, 1999), but its concrete physiological roles in vivo are unknown, and Gab2$^{-/-}$ mice have been reported to be generally healthy (Gu H, Nature, 2001). Gab2 functions have mainly been studied in mast cell, yielding to controversial results. Whereas IgE/antigen-induced PI3K activation and mast cell degranulation have been reported to be reduced in Gab2$^{-/-}$ BMMCs (Gu H, Nature,

2001), Gab2 downregulation by siRNA had no effect on degranulation (Barbu EA, J Biol Chem, 2010). In agreement with a role of Gab2 in FcεRI signalling, stimulation of wild type BMMCs induced or increased Gab2 phosphorylation (Gu H, Nature, 2001; Yu M, J Immunol, 2006; Parravicini V, Nat Immunol, 2002). However, in another study, where stimulation was done in serum-containing medium, no change of Gab2 phosphorylation following FcεRI activation was reported (Hernandez-Hansen V, J Immunol, 2004). Interestingly, Gab2 has been shown to control chemokine mRNA (MIP-1α/β, MCP-1) induction both at suboptimal and optimal antigen concentrations and FcεRI occupancy (Gonzalez-Espinosa C, J Exp Med, 2003). Further, transcription of the *MCP-1* gene has also been observed to be induced in IgE loaded mast cells (Saitoh S, Immunity, 2000). As Gab2 phosphorylation and signalling in vitro seems to be influenced by mast cell starvation and stimulation conditions, Gab2 might affect FcεRI signalling through mast cell steady state and well-being modulation. Overall, the discussed publications rather ascribe a minor role of Gab2 to mast cell degranulation, as observed impairments likely result from indirect effects (reduced mast cell numbers in vivo, serum starvation in vitro).

While having an controversial role in FcεRI signalling, PI3Kδ, p85α, and Gab2, all regulate in some way mast cell homing to certain body locations (Ali K, Nature, 2004; Fukao T, Nat Immunol, 2002; Gu H, Nature, 2001; Nishida K, Blood, 2002; Yu M, J Biol Chem, 2006). In the corresponding knock-out or knock-in mice, mast cell numbers in the peritoneal cavity and intestine are severely reduced and reach only half-normal levels in the ear dermis. Additionally, p85α and $Gab2^{-/-}$ mice also have almost no mast cells in the stomach, which is less affected in $PI3K\delta^{D910A/D910A}$ mice. Mast cell homing and maintenance in vivo depends on Kit receptor activation by stem cell factor (SCF) (reviewed in (Galli SJ, Am J Pathol, 1993)). Activated Kit autophosphorylates on several tyrosine residues and thereby switches on diverse effector pathways, which separately or in cooperation regulate mast cell survival, proliferation, migration, and adhesion (Serve H, EMBO J, 1995; Timokhina I, EMBO J, 1998; Kissel H, EMBO J, 2000; Kimura Y, Proc Natl Acad Sci U S A, 2004). PI3Kδ is the principal Kit-coupled PI3K isoform, being recruited mainly by p85 binding to phosphorylated tyrosine 719 on Kit (Yee NS, J Biol Chem, 1994). How and whether Gab2 connects to Kit is unknown at present. Since SCF-induced PI3K activation in not affected in $Gab2^{-/-}$ BMMCs (Yu M, J Biol Chem, 2006), this adaptor might control Kit responses by a separate or downstream pathway. PI3Kδ and p85α control mast cell adhesion, chemotaxis, and proliferation (Ali K, Nature, 2004; Ali K, J Immunol, 2008; Lu-Kuo JM, J Biol Chem, 2000; Fukao T, Nat Immunol, 2002; Tan BL, Blood, 2003). While Gab2 also regulates mast cell proliferation, especially at high SCF concentrations (Nishida K, Blood, 2002; Yu M, J Immunol, 2006), a possible role in movement has not been investigated yet. The mechanism by which Gab2 regulates mast cell tissue homing is unknown, but might involve Kit signalling and/or growth factor-induced gene transcription in mast or tissue cells. All in all, current knowledge collectively assigns important roles to PI3Kδ in Kit signalling, whereas GPCRs and the FcεRI mainly couple to PI3Kγ.

While Lyn controls the phosphorylation of the FcεRI β- and γ-chains and thereby initiates Syk activation and Ca^{2+} mobilisation (Nishizumi H and Yamamoto T, J Immunol, 1997), another protein tyrosine kinase, Fyn, has been suggested to control PI3K activation in mast cells (Parravicini

V, Nat Immunol, 2002). Follow-up studies however reported conflicting results ranging from zero to an essential role in PI3K activation as well as in vitro and in vivo mast cell degranulation (Barbu EA, J Biol Chem, 2010; Odom S, J Exp Med, 2004; Kambayashi T, Immunol Rev, 2009). The reason for these discrepancies has not been unravelled. But as Ca^{2+} mobilisation is sufficient to activate PI3K in mast cells, there seems to be no need for a separate pathway. While Thapsigargin-induced degranulation is blocked in PI3K$\gamma^{-/-}$ BMMCs (Figure 1), Fyn$^{-/-}$ BMMCs degranulate normally in response to this agent (Sanchez-Miranda E, Biochem Biophys Res Commun, 2010), and therefore Fyn should be dispensable for PI3Kγ activation.

Despite PI3K is essential for mast cell degranulation, its effector pathways are vaguely characterised. Potential PIP_3 effectors are the PH-domain containing proteins PKB, PLCγ, Btk, and Vav. PLCγ and Btk controlled sustained Ca^{2+} mobilisation (Kawakami Y, J Immunol, 2000; Deng Z, Biophys J, 2009; Iwaki S, J Biol Chem, 2005) could regulate activation of the Ca^{2+}-sensing component of the fusion machinery (Baram D, Immunol Rev, 2001). It is possible that a PKB catalyzed phosphorylation event is essential for degranulation, or that recruitment of another PH-domain-containing protein is required. A degranulation regulator downstream of PI3K is phospholipase D (Lin P and Gilfillan AM, Eur J Biochem, 1992; Cissel DS, J Pharmacol Exp Ther, 1998). Its product diacylglycerol (DAG) might regulate granule-plasma membrane fusion via DAG-sensitive Munc13 proteins (Elstak ED, Blood, 2011; Brose N and Rosenmund C, J Cell Sci, 2002). Cytoskeletal rearrangements might be regulated by the guanine nucleotide exchange factor Vav which mediates Rac activation (Crespo P, Nature, 1997).

5.4 PKCβ emerges to be a novel PI3Kγ activator

Protein kinase C (PKC) activation is a key event to mast cell degranulation. Despite this, PKC's function and substrates remained obscure. By analysis of BMMCs derived from isoform-specific knock-out mice, PKCβ was identified to be essential for FcεRI and ionomycin triggered mast cell degranulation (Nechushtan H, Blood, 2000). We confirm this (Figure 3E, Figure S1D) and show that PKCβ regulates degranulation by PI3Kγ activation (Figure 3-5). Additionally, we also show that direct activation of PKCβ by phorbol myristate acetate (PMA) is sufficient trigger PI3K and PKB activation in mast cells (Figure 3C, 3F-H, 5A/C). PMA by itself however does not trigger mast cell degranulation, because granule-membrane fusion is additionally controlled by Ca^{2+}-regulated events. Interestingly, PKCβ-dependent PI3K activation depends on relatively high Ca^{2+} concentrations, lying in the low micromolar range (Figure 2C). With respect to this, in vitro studies have identified a special high Ca^{2+} requirement for the activation of PKCβ2 compared with PKCβ1 or PKCα (Keranen LM and Newton AC, J Biol Chem, 1997). Whereas PKCβ2 required a 40-fold greater Ca^{2+} concentration for half-maximal activation than membrane binding, this difference was only 10- and 2-fold for PKCβ1 and PKCα, respectively. Apart from PKCβ2, BMMCs also express high amounts of PKCα. Despite these two PKCs share high homology and substrate sequence specificity, PKCα can not complement for PKCβ. Of the two splice variants of PKCβ, PKCβ2 is expressed at much higher levels than PKCβ1 (own observations, (Kawakami Y, J Immunol, 2000)),

and therefore likely dominates signalling in mast cells. PKCβ1 and PKCβ2 only differ in their last 50-52 amino acids. The specific role of the PKCβ's C-termini is currently unknown.

So far three PKC targets have been identified in mast cells: myosin heavy and light chain und the vesicle fusion protein SNAP-23 (Ludowyke RI, J Biol Chem, 1989; Ludowyke RI, J Immunol, 1996; Ludowyke RI, J Immunol, 2006; Hepp R, J Biol Chem, 2005). Whether these phosphorylation sites play a physiological role in mast cells and beyond is not yet known. Therefore, the function of PKC in mast cell degranulation is still enigmatic. While myosin regulates the reorganisation of actin filaments, SNAP proteins are part of the cell's membrane fusion machinery. Mast cell degranulation is accompanied by the disassembly of the cortical F-actin ring, subsequent increased actin polymerisation, and rearrangement of the tubulin network (Pfeiffer JR, J Cell Biol, 1985; Apgar JR, Mol Biol Cell, 1994; Hajkova Z, J Immunol, 2011). Whereas actin filament stabilizing or destabilizing agents only minimally affect degranulation by Ca^{2+} mobilising agents (Sasaki J, J Exp Med, 2005), microtubule modifying drugs completely block histamine release (Urata C and Siraganian RP, Int Arch Allergy Appl Immunol, 1985). A possible regulation of the actin-myosin network by PKC should therefore not be a prerequisite for exocytosis. Apart from regulation of cytoskeletal dynamics, PKC has been proposed to regulate granule-membrane fusion (reviewed in (Morgan A, Biochem Soc Trans, 2005)). This assumption originated from the observation that diacylglycerol (DAG) analogs trigger granule release in some exocytotic cell types. However by now, other phorbol ester sensitive proteins which regulate membrane fusion have been identified, like e.g. the Munc-13 proteins. FcεRI triggers phosphorylation of SNAP-23 in mast cells. Despite sensitive to PKC-inhibitors and PKCβ deficiency ((Hepp R, J Biol Chem, 2005), own observations), IKKβ is rather the direct kinase (Suzuki K and Verma IM, Cell, 2008). As only one of the two identified sites is conserved in humans, the relevance of this finding is unclear. SNAP-23 phosphorylation in other cell types has not yet been reported. Of note, costimulation of the FcεRI with Kit or adenosine rescues defective antigen-induced degranulation of PKCβ$^{-/-}$ BMMCs ((Fehrenbach K, J Immunol, 2009) and not shown, one experiment). The exocytotic machinery seems therefore to be intact in these cells, which corroborates our finding that PKCβ acts at an earlier step in the degranulation pathway. In some cell types, protein kinase D (PKD) is another PKC downstream target. In mast cells PKD activation is not blocked by PKC-inhibitors und also not required for degranulation ((Murphy TR, J Immunol, 2007), own observations).

Within this study we unravelled a key function of PKC in mast cells. We identified PKCβ to be the direct activator of class IB PI3Kγ downstream of the FcεRI. In this novel pathway, store-operated Ca^{2+} influx activates PKCβ, which interacts with and activates PI3Kγ by phosphorylation (Figures 2-5). Mass spectrometry identified the PKCβ-targeted sites to lie at two very critical regions within PI3Kγ. Serine 582 lays at the beginning of the helical domain, while S257 sits in the Ras binding domain (RBD). The helical domain beginning is famous for harbouring activating mutations of PI3Kα in cancer (Samuels Y, Science, 2004). But also the RBD domain is interesting. PI3Kγ with an artificially mutated RBD (PI3Kγ DASAA) is functionally dead in vivo, as mutant and knock-out neutrophils are equally impaired (Suire S, Nat Cell Biol, 2006). Further overexpressed PI3Kγ needs a functional RBD to transform chicken fibroblasts, which however additionally depends on the

presence of serum, but not on an artificial membrane tag (Kang S, Proc Natl Acad Sci U S A, 2006). In vitro characterisation of recombinant PI3Kγ phosphorylation site mutants identified S582 as a switch site for activation. The activity of the phosphoserine-mimicking PI3Kγ mutant (S582E) was increased 2-fold compared with wild type PI3Kγ (Figure 5D, E), which is an increase similar to that published for activated PI3Kα mutants (Miled N, Science, 2007, (Suppl); Carson JD, Biochem J, 2008; Gymnopoulos M, Proc Natl Acad Sci U S A, 2007, (Suppl)). On the other hand, mutation of S257 had no effect on PI3Kγ's in vitro lipid kinase activity (Figure S3H). Still it should be kept in mind that detection of PI3K activation is limited by the already high activity state of this enzyme in vitro. Excited by the gain of activity of the helical domain mutant, we focused further experimental work on the analysis of S582. This strategy was further substantiated by the fact that the function of the RBD of PI3Ks is unknown at present and therefore tricky to investigate. Despite engineered PI3K RBD mutants showed functional defects in several studies (Zhao L and Vogt PK, Proc Natl Acad Sci U S A, 2008; Zhao L and Vogt PK, Cell Cycle, 2010; Gupta S, Cell, 2007; Suire S, Nat Cell Biol, 2006; Kang S, Proc Natl Acad Sci U S A, 2006; Kurig B, Proc Natl Acad Sci U S A, 2009; Sasaki AT, J Cell Biol, 2004; Orme MH, Nat Cell Biol, 2006), a prove for the claimed direct (or even indirect) involvement of Ras is missing. Other regulatory functions of the RBD should therefore be considered with equal plausibility, and may for example involve the interaction with another protein or membrane lipid. Importantly, we did not observe Ras activation by Thapsigargin (Figure S3L), and others showed no inhibition of FcεRI-mediated mast cell degranulation by Ras prenylation inhibitors (farnesyltransferase inhibitors) (Fujimoto M, Eur J Pharmacol, 2009; Mor A, Inflammation, 2011).

Characterisation of S582 showed that its phosphorylation in BMMCs depends on p84-free PI3Kγ, as this site is not accessible in the exogenously expressed PI3Kγ-p84 complex (Figure 6A). In accordance with this, endogenous PI3Kγ coimmunoprecipitates, both, endogenous or exogenous p84 much less efficiently than exogenously expressed PI3Kγ (Figure 6D, E). PI3Kγ-p84 binding also varies within mast cell lines. While PI3Kγ efficiently associates with p84 in the human mast cell line HMC-1, it does this poorly in rat basophilic leukaemia cells (RBL-2H3) (not shown). Currently the reason for these disparate interaction affinities is unclear. We also observed that endogenous PI3Kγ is the better substrate for S582 phosphorylation than exogenous wild type PI3Kγ (Fig 6A, and not shown). This may be caused by the observed association of endogenous p84 with exogenous PI3Kγ, but also might arise from the reduced responsiveness of the transfected pool of cells (transfection efficiency ~75%). BMMCs transfected by nucleofection (Amaxa) are poorly viable and partially refractory to stimulation. If expressed at around physiological levels (1-2-fold of endogenous), transiently expressed wild type PI3Kγ (without or with p84) only partially complements PKB activation in PI3Kγ$^{-/-}$ BMMCs compared with wild type BMMCs (Thesis Figure 1A and 2). This might derive from different localisation or processing of endogenous than exogenous PI3Kγ and/or disturbed functional integrity of the cell by the harsh transfection method (plasmid DNA gets "injected" in the nucleus). Upon several fold overexpression of PI3Kγ in PI3Kγ$^{-/-}$ BMMCs, PMA or Thapsigargin trigger levels of PKB phosphorylation as seen in wild type BMMCs (Thesis Figure 3). The relevance of this finding has however to be interpreted with

precaution as being dependent on unphysiological presets. In fact, overexpressed PI3Kγ can be oncogenic in vivo (Kang S, Proc Natl Acad Sci U S A, 2006) overcoming cell inherent control mechanisms.

Despite the limited applicability of nucleofection of BMMCs for functional assays, expression of PI3Kγ S582 point mutants in PI3Kγ$^{-/-}$ BMMCs identified two things. First, co-immunoprecipitation studies showed reduced binding of the phosphorylation site-mimicking mutants PI3Kγ S582E or S582D to p84 compared to wild type PI3Kγ or PI3Kγ S582A (Figure 6B). This result could be confirmed by expression of the same constructs and pulldown assays in HEK293 cells (Figure 6C), and showed that S582 lays at the interphase of PI3Kγ and p84. This conclusion is in consent with the finding that S582 is inaccessible for phosphorylation if PI3Kγ is bound to p84 (Figure 6A). We additionally characterised the p84-PI3Kγ binding interphase by deuterium exchange mass spectrometry, which confirmed that p84 interacts with the helical domain beginning (Figure 7). Second, while wild type PI3Kγ and the S582 mutants were expressed at similar levels in PI3Kγ$^{-/-}$ BMMCs if coexpressed with p84 (Figure 6B), expression of the PI3Kγ constructs alone differed quantitatively (Figure 5F). Whereas wild type and the S582A mutant of PI3Kγ were strongly expressed in the absence of p84, expression of the two phosphorylation site-mimicking mutants was strongly downregulated early after transfection (Figure 5F). This might be a sign of increased activity of these mutants, as cells often downregulate expression of harmfully activated proteins. In contrast to BMMCs, expression of PI3Kγ S582E or S582D was not affected in HEK293, which are devoid of endogenous PI3Kγ. But expression was also reduced in Sf9 cells (4-5-fold), which also downregulate constitutively active PI3Kα (H1047R/L, C420R, E545K; p85a: N564D) (Mandelker D, Proc Natl Acad Sci U S A, 2009; Hon WC, Oncogene, 2012). Since this instability in BMMCs made it impossible to compare signalling between the mutants in a physiological environment, and because of the mentioned disadvantages of nucleofection, we tried to generate stably transfected BMMCs by lentivirus-based approaches. Unfortunately, this was hampered by two reasons. On one hand, high viral titers that effectively promoted GFP expression, were toxic to BMMCs, and secondly, cells, infected with either low or high titer virus supernatants, very quickly lost transgene expression. More intense characterisation of the PKCβ phosphorylation sites in BMMCs was therefore not possible to us by technical reasons. Despite this, our analyses showed that non-canonical, PKCβ-activated PI3Kγ operates in an adaptor-free manner, and is regulated by phosphorylation of S582. Contemporaneously we identified S582 to lie centrally in the p84-binding region of PI3Kγ, which we mapped to the helical domain beginning.

As PKCβ interacts with and phosphorylates PI3Kγ, our data support a model of direct activation of PI3Kγ by PKCβ. There exists the possibility that PKCβ potentiates PI3Kγ activation by phosphorylation of another protein, thereby generating a docking site for PI3Kγ translocation. In view of our finding that the N-terminal domain is not involved in p84 binding, but would be free for an unknown recruitment function, in analogy to class IA PI3K targeting by p85, this hypothesis merits warranty. Despite expression of membrane-anchored PI3K generally promotes constitutive PKB activation in cell lines, the sole addition of a membrane-targeting tag is not sufficient for full PI3K activation in primary cells or in vitro assays (Costa C, Proc Natl Acad Sci U S A, 2007; Zhao

JJ, Proc Natl Acad Sci U S A, 2005; Krugmann S, Biochem J, 2002). Accordingly, we did not observe PKB phosphorylation following transfection of PI3Kγ-CAAX into PI3Kγ$^{-/-}$ BMMCs (one experiment) (Thesis Figure 4A). Moreover, PKB activation induced by helical domain mutations in PI3Kα depends on a functional Ras binding domain (RBD) and is not affected by deletion of the N-terminal adaptor-binding domain (ABD) (Zhao L and Vogt PK, Proc Natl Acad Sci U S A, 2008; Zhao L and Vogt PK, Cell Cycle, 2010).

We think that PKCβ mainly targets the plasma-membrane located pool of PI3Kγ, which has been determined to constitute 5-8% of total PI3Kγ in neutrophils (Suire S, Curr Biol, 2002). Part of PI3Kγ also locates to the membrane in macrophages, where it reaches similar levels to PI3Kγ-CAAX in knock-in macrophages (Costa C, Proc Natl Acad Sci U S A, 2007). As the expression level of membrane-anchored PI3K is likely limited due to space-constraints, such restrictions may also influence total levels of membrane-located PI3K in wild type cells. Interestingly, the relative level of PI3Kγ S582 phosphorylation by PMA in wild type BMMCs was 1.5-fold of S582 phosphorylation of PI3Kγ-CAAX transfected into PI3Kγ$^{-/-}$ BMMCs (one experiment) (Thesis Figure 4B). In addition to cells, PI3Kγ also spontaneously associates with lipid vesicles in vitro. Here, membrane binding is promoted by inclusion of a high ratio of negatively charged phospholipids like PtdIns(4,5)P_2 or phosphatidylethanolamine (PE) and prevented by an excess of neutral lipids like phosphatidylcholine (PC) (Krugmann S, Biochem J, 2002). Additionally to activity regulation, PI3Kγ phosphorylation might also influence the affinity to membranes and orientation. While we found evidence for S582 to regulate catalytic activity, it might be possible that phosphorylation of S257 affects plasma membrane binding. Apart from PI3Kγ activation, it is also conceivable that PKCβ carries additional PI3Kγ to the plasma membrane, as activated PKCβ interacts with PI3Kγ in coimmunoprecipitation assays (Figure 4B). As both proteins are highly expressed in BMMCs, an encounter would be statistically favoured. PI3K translocation is very difficult to detect by microscopy or membrane fractionation techniques. Therefore, people generally prefer to monitor PIP_3 production by means of translocation of engineered GFP-PH-domain fusion constructs (Voigt P, J Biol Chem, 2006). Studies quantifying PI3K translocation in cells reported translocation of only a minority total PI3K (~5%) (Domin J, J Biol Chem, 1996). Bulk PI3K translocation seems therefore not to be required for signal propagation. Future experiments will be required to address such aspects in more detail.

Whereas adenosine activates PI3Kγ in a Gβγ-dependent manner in BMMCs (Bohnacker T, Sci Signal, 2009), antigen, Thapsigargin, and PMA activate PI3Kγ through PKCβ. Besides mast cells, endothelial cells (HUVEC, BREC, HBMEC, HMEC-1) also express PI3Kγ but not p101 (Hsieh SN, Diss, 2003, Friedrich Schiller University, Jena, Germany). It would therefore be interesting to analyse whether PI3Kγ is also regulated by PKC in these cells. Furthermore, PI3Kγ can also be regulated in a p101-independent manner in cells expressing p101. In neutrophils for example, p101 is required for migration towards fMLP or C5a, but is dispensable for reactive oxygen species (ROS) production, which may be regulated by PI3Kγ in an adaptor-free or p84-dependent manner (Suire S, Nat Cell Biol, 2006). PMA also promotes PKB activation in cell types other than mast cells like 3T3-L1 adipocytes or primary human blood-derived B cells (Nave BT, Biochem J, 1996;

Barragan M, J Leukoc Biol, 2006). All in all these examples illustrate that future work will likely reveal further important roles of the PKC-PI3K pathway additional to mast cell degranulation.

5.5 Regulation of PI3Kγ by the helical domain

Serine 582 is located at the beginning of the helical domain of PI3Kγ and is conserved in higher vertebrates such as mammals and birds (no blastp entry available for reptiles) (Figure 4F). Mast cells have been found in all classes of vertebrates including as well amphibians and fish (Mulero I, Proc Natl Acad Sci U S A, 2007). Intriguingly, only mast cells from an evolutionarily advanced phylogenetic order of fish, the Perciformes, store histamine in their granules and use it as inflammatory mediator. Other fish species and also amphibians (frog, newt) lack histamine or serotonin, and do not respond to histamine administration (Mulero I, Proc Natl Acad Sci U S A, 2007). The PKC-PI3Kγ pathway might therefore have evolved at about the same time as histamine started to regulate immunity. However, as IgE is exclusively produced in mammals, degranulation must be triggered by a different stimulus in other classes.

The helical domain (also called PIK domain or accessory domain) is conserved in PI3- and PI4-kinases, but its function is not known. Certainly it is important for the proteins structural integrity, as being involved in extensive interdomain interactions. The PI3Kγ helical domain folds into a stack of five A/B pairs of antiparallel helices (Walker EH, Nature, 1999). The surface formed by the A helices interacts with the catalytic domain, while the "B surface" is mainly solvent exposed. Further interactions by the helical domain are mediated by loops contacting the C2 and Ras-binding domain (RBD). S582 sits in the B helix of the first helical pair, which intrahelical loop contacts regulatory helices in the C-terminal lobe of the kinase domain (Thesis Figure 5). As S582 points inward of the published crystal structure, this region, at least in the phosphorylated state, must adopt a different conformation. Since we found that untagged PI3Kγ Δ143 is structurally impaired with respect to p84 binding compared to GST-Δ143-PI3Kγ and full-length PI3Kγ (Figure 7D), it is likely that truncated PI3Kγ folds improperly. With respect to this, it might be of note to mention that the catalytic loop of PI3Kγ Δ143 is locked in an inactive conformation in published crystal structures (Walker EH, Nature, 1999; Pacold ME, Cell, 2000). For comparison, active side amino acids in the catalytic loop of PI3Kδ (ΔABD) or Vsp34 (ΔC2) are oriented in a catalytic competent manner (Walker EH, Nature, 1999; Berndt A, Nat Chem Biol, 2010; Miller S, Science, 2010). It is also feasible that PKCβ binding induces a conformational change that exposes S582, because PMA could stimulate some phosphorylation of PI3Kγ Δ143 in BMMCs. But whether phosphorylation efficiency equalls that of wild type PI3Kγ is unclear, as N-terminal truncated PI3Kγ was expressed at a much higher level than full-length PI3Kγ, despite of transfection of equal amounts of plasmid DNA (one experiment) (Thesis Figure 1B).

Interestingly, all known activating helical domain-associated mutations found in PI3Kα in cancer lay, as S582, at the beginning of the helical domain (P539, Glu542, Glu545, and Q546) (marked by stars in Thesis Figure 5) (Samuels Y and Velculescu VE, Cell Cycle, 2004). Among all identified oncogenic mutations in PI3Kα, two helical domain, E545K and E542K, and a C-terminal mutation, H1047R, occur most frequently. These mutations cause an approximate 2-fold gain of

enzymatic activity in vitro, promote PKB activation and oncogenic transformation in cell culture models, and induce tumour growth of xenograft transplants in vivo (Zhao JJ, Proc Natl Acad Sci U S A, 2005; Resnick AC, Proc Natl Acad Sci U S A, 2005; Isakoff SJ, Cancer Res, 2005; Pang H, Cancer Res, 2009). Increased PKB activation has been reported in immortalized, genetically engineered (HMEC) (Zhao JJ, Cancer Cell, 2003; Zhao JJ, Proc Natl Acad Sci U S A, 2005), spontaneously immortalized (MCF-10A) (Isakoff SJ, Cancer Res, 2005), and breast cancer-derived (MDA-MB-231) (Pang H, Cancer Res, 2009) human mammary epithelial cells, as well as in primary chicken embryo (Resnick AC, Proc Natl Acad Sci U S A, 2005; Zhao L and Vogt PK, Proc Natl Acad Sci U S A, 2008) and NIH-3T3 fibroblasts (Ikenoue T, Cancer Res, 2005). Unfortunately, it has not been published whether these mutations also promote PI3K activation in standard cell lines such as HEK293 or COS-7 cells. It is likely that increased PI3K signalling depends on a second signalling input, which is not shut on in every cell line and cell type.

It is thought that the helical domain mutations in PI3Kα relieve inhibitory contacts between the nSH2 of p85 and PI3Kα. This has been derived from in vitro data analysing charge-reversal mutations of PI3Kα and p85α biochemically, and analysis of the crystal structure of the PI3Kα H1047R/p85α-niSH2 complex (fragment 322-694 of p85α) (Miled N, Science, 2007; Mandelker D, Proc Natl Acad Sci U S A, 2009). While the niSH2 fragment of p85 blocks the activity of monomeric wild type PI3Kα 2-fold, the PI3Kα helical domain hot spot mutants are already fully active and neither inhibited by p85 nor further activated by phosphopeptides (Miled N, Science, 2007; Carson JD, Biochem J, 2008). Whether these in vitro results directly apply in vivo has not been investigated, presumably due to difficulties to address this experimentally. Additional studies indicate that helical domain mutations also regulate PI3Kα activity by an inherent and not only p85-dependent mechanism. Monomeric mutant PI3Kα is more active than monomeric wild type PI3Kα both in vitro and in cultured cells ((Ikenoue T, Cancer Res, 2005; Gymnopoulos M, Proc Natl Acad Sci U S A, 2007); (Miled N, Science, 2007) (Suppl; vitro); (Zhao L and Vogt PK, Proc Natl Acad Sci U S A, 2008), (cells)). In cellular studies, effects of the binding of endogenous p85 to transfected PI3Kα can be prevented by the use of N-terminally truncated PI3Kα (Δ72) (Zhao L and Vogt PK, Proc Natl Acad Sci U S A, 2008). Whether oncogenic PI3Kα helical domain mutations induce structural changes, for example in the kinase domain, is unknown, as there are no crystal structures available.

Since PI3Kα activity can be modulated at the level of the helical domain, we wanted to know whether this also applies for PI3Kγ and S582. Analysis of the phosphorylation-mimicking PI3Kγ S582E mutant showed that this is indeed the case, as its enzymatic activity was increased 2-fold in vitro compared with wild type PI3Kγ. Unfortunately, we could not directly address increased PI3K signalling in vivo, as it was impossible to express the phosphorylation-mimicking mutants at adequate levels in BMMCs. However, as already mentioned, the strong downregulation of these mutants likely derives from a gain of function trait.

Apart from the helical domain, activating PI3Kα mutations lie within or near the last four helices of the catalytic domain. They form a regulatory square that holds the activation and catalytic loop in place (Zhang X, Mol Cell, 2011). Since the loop of the helical domain beginning directly contacts

the regulatory square, it might regulate catalysis by forwarding conformational changes. Therefore, despite located at distinct positions of the same helix, S582 of PI3Kγ and E542 or E545 of PI3Kα might affect lipid kinase activity by a similar allosteric way.

Characterisation of PI3Kα helical domain mutants in chicken embryo fibroblasts (CEFs) showed that PKB activation and cellular transformation is dependent on functional Ras binding domain (RBD). Mutation of lysine 227 to glutamate in the RBD abrogates E545K-dependent cellular outcomes (Zhao L and Vogt PK, Proc Natl Acad Sci U S A, 2008). While RBD mutations interfered with signalling of bovine and human PI3Kα E545K, PKB activation induced by the H1047R mutation was blocked only by modification of the human but not bovine RBD (Zhao L and Vogt PK, Proc Natl Acad Sci U S A, 2008; Zhao L and Vogt PK, Cell Cycle, 2010). In these studies, the functional role of the RBD has not been investigated. As the cells were serum-starved only, stimulus-triggered signalling events should not play a role. Rather appropriate steady-state signalling might be of importance. So far PI3Kα helical and Ras binding domain double mutants have only been investigated in CEFs but not other cell types. It is therefore premature to conclude that the gain of activation induced by helical domain mutations depends on RBD coregulation in every case. Yet such observations show, that PI3K activation inside cells can depend on more than one upstream signal and domain. Interestingly, we not only found phosphorylation of S582 of PI3Kγ by PKCβ in vitro or BMMCs but also concomitant phosphorylation of S257 in the RBD (Figure S3C-E, G). It is therefore tempting to speculate that in cells both phosphorylations are required to promote PI3Kγ activation. For example, phosphorylation of S257 might impact PI3Kγ-plasma membrane or -coregulator binding, and its possible role are under investigation.

5.6 Regulation of PI3Kγ by the Ras binding domain

Despite the Ras binding domain (RBD) is essential to PI3Kγ function in vivo (Suire S, Nat Cell Biol, 2006; Kang S, Proc Natl Acad Sci U S A, 2006) its mechanism of action is unclear. The RBD of PI3K has little sequence homology with the RBD of Raf or RalGEF and therefore constitutes a different domain group. Despite this, the RBDs of all three groups fold into a similar structure. Interestingly, S257 lays in a region in the RBD (amino acids 255-265) that is disordered in the crystal structure of PI3Kγ, but is ordered in the structure of PI3Kγ complexed to Ras (Walker EH, Nature, 1999; Pacold ME, Cell, 2000). S257 lays at the edge of the Ras-PI3Kγ interphase, is largely solvent exposed, and not buried in the interface (Thesis Figure 6). The serine side chain hydroxyl group lies at bonding distance to Gln 25 of Ras, but this interaction does not seem to be essential for complex formation. Whether S257 phosphorylation is of physiological importance we do not know. As S257 is located at the border of the Ras binding site, phosphorylation might have no effect on Ras binding or may regulate its dislocation. With respect to mast cell degranulation, S257 may regulate PI3Kγ activation in concert with S582. It is conceivable that the RBD regulates PI3Kγ function by different independent mechanisms. Depending on the context, phosphorylation or activator protein interaction may be involved.

PI3Kγ (Δ143, V223K)-Ras (H-Ras·GMPPNP) crystals were obtained with a PI3Kγ mutant having increased Ras binding affinity (V223K). Since recombinant PI3Kγ Δ143 has a 10-fold lower in vitro

Ras binding affinity than GST-PI3Kγ (Pacold ME, Cell, 2000), it might be possible that the N-terminal region is not only important for the structural integrity of the helical (Figure 7D) but also the Ras binding domain. As Ras-PI3Kγ binding is mediated by hydrogen bond and salt bridge interactions (beyond the farnesyl moiety), association force depends on the ionic strength of the microenvironment. Ras not only interacts with the RBD of PI3Kγ but also contacts the catalytic domain. Ras-PI3Kγ binding induces conformational changes in the C2 domain and the C-terminal lobe of the kinase domain. PI3Kγ substrate binding and catalysis might be enhanced by the movement of backbone helices that hold the activation loop in place.

In vitro and ectopic expression experiments have identified several interesting characteristics of Ras-PI3K interaction. These data contribute to the elucidation of RBD functions, stimulate ideas, and help to design future experiments. In vitro, recombinant PI3Kγ interacts in a GTP-dependent manner with unmodified bacterially expressed Ras (uRas) (Rubio I, Biochem J, 1997; Rubio I, Eur J Biochem, 1999; Pacold ME, Cell, 2000). In contrast to uRas, farnesylated Ras (mRas, m: modified) can bind PI3Kγ both in the GTP- and GDP-loaded state, but binding efficiency is much better for GTP-loaded Ras at low Ras concentrations (10 nM (far below K_d) vs. 1 μM Ras) (Rubio I, Eur J Biochem, 1999). Additionally, PI3Kγ also forms a high stringency complex with mRas-GTP that is inaccessible to the activity of GTPase-activation protein (GAP) (H-Ras 10-20%, K-Ras4B 50%). Despite PI3Kγ binds to u- and mRas, only mRas enhances lipid kinase activity in vitro. Ras binding probably increases the affinity for PIP_2, as PI3Kγ activation by mR-Ras-GTPγS is most notably increased at PIP_2 concentrations below 10 μM, but is only minimally (1.5 fold) affected at high PIP_2 concentrations (above 50 μM) (Suire S, Curr Biol, 2002). In vitro and in heterologous expression systems, active Ras does not promote PI3Kγ membrane translocation (Suire S, Curr Biol, 2002). Ras therefore likely activates PI3Kγ by an allosteric mechanism. In vivo activation of PI3Kγ by constitutively active Ras might be direct or indirect, because active Ras also promotes cytokine release in cultured cells (Ancrile B, Genes Dev, 2007; Sparmann A and Bar-Sagi D, Cancer Cell, 2004). Furthermore it is also possible that PI3Kγ is activated in vivo by another farnesylated protein or another Ras family member, and that in vitro association with classical Ras represents crossreaction. Indeed, the Ras proteins constitute a big protein family which member-functions are mostly undefined. PI3Kγ might interact with its physiological binding partner with much higher affinity. Raf for example has a much higher Ras binding strength than PI3K or RalGEF, which likely explains why Ras only promotes plasma membrane translocation of Raf but not PI3K. Moreover, only the RBD of Raf is suited for Ras·GTP pulldown assays. Ras-PI3K interaction is experimentally difficult to detect, as it is not possible to copurify the complex at an equal stochiometric ratio. Whereas precipitated Ras or PI3K is easily visible by Coomassie dye staining, detection of the copurified binding partner requires Western blotting.

Examination of the structure of the RBD of class I PI3Ks identifies a region of no homology between β-sheet 2 and 3. In PI3Kγ (PDB: 1E7U), part of this region is disordered (amino acids 255-265), but folds into an ordered loop containing a small α-helix when cocrystallized with Ras (PDB: 1HE8) (Pacold ME, Cell, 2000) (Figure S3K). The corresponding region in PI3Kα is

ordered and folds after a turn into a long α-helix (aa 237- 247) (PDB: 2RD0, 3HHM) (Huang CH, Science, 2007; Mandelker D, Proc Natl Acad Sci U S A, 2009). In comparison with PI3Kγ, PI3Kα also shows different in vitro Ras binding characteristics. Recombinant PI3Kα binds both to uRas and mRas in a strictly GTP-dependent manner (Rodriguez-Viciana P, Nature, 1994). On the other hand, activation is as well dependent on posttranslational modification (Rodriguez-Viciana P, EMBO J, 1996). Further, Ras pulldown assays work efficiently with a RBD containing construct (aa 133-314) of PI3Kα, but not with the corresponding fragment of PI3Kγ (aa 220-311).

All in all, current evidence strongly suggests that PI3Kγ is physiologically regulated at the level of the RBD. Whether this involves Ras, a Ras-like protein, and/or phosphorylation on S257 requires further investigation. The RBD might not only regulate stimulus-induced PI3K activation, but might also promote constitutive PI3K membrane association through a growth/survival factor activated farnesylated protein. Because of distinct structure and behaviour among PI3Ks, the RBD likely, beyond other mechanisms, regulates isoform-specificity. Whether interaction with Ras itself plays a physiological role in this process is not yet clear (Karasarides M, J Biol Chem, 2001).

5.7 Regulation of PI3Kγ by adaptor proteins

PI3Kγ interacts with two adaptor subunits, p101 or p84, which expression is regulated in a cell type-specific manner. While mast cells only express p84, neutrophils and monocytes express both adaptors, and lymphocytes mainly p101 (Bohnacker T, Sci Signal, 2009). p84 and p101 share 30% sequence identity and 37% sequence similarity (Suire S, Curr Biol, 2005) and exhibit several identical characteristics. Both adaptors associate with PI3Kγ in coimmunoprecipitation assays following coexpression, and are required for fMLP- or Gβγ-induced PIP_3 production in heterologous expression systems (HEK293) (Brock C, J Cell Biol, 2003; Voigt P, J Biol Chem, 2006). However, whereas p101 potentiates PI3Kγ activation by Gβγ subunits in vitro and is translocated by them to the plasma membrane in cells (Stephens LR, Cell, 1997; Brock C, J Cell Biol, 2003), p84 does not share these characteristics (Kurig B, Proc Natl Acad Sci U S A, 2009). In the presence of p84 instead, Gβγ-dependent PI3Kγ activation is sensitive to expression of the GTPase activation domain of neurofibromin 1 (GAP_{NF1}) (Kurig B, Proc Natl Acad Sci U S A, 2009) as well as cholesterol depletion (Bohnacker T, Sci Signal, 2009). GAP_{NF1} inhibits basal Ras activation in HEK293 cells but likely also acts on other targets. In neutrophils, in contrast to HEK293 cells (Kurig B, Proc Natl Acad Sci U S A, 2009), p101-regulated PI3Kγ activation also depends on an intact Ras binding domain (Suire S, Nat Cell Biol, 2006). Despite mechanistic basics are incompletely understood, these data show that coactivators and adaptor proteins regulate PI3Kγ activation in versatile ways.

As PI3Kγ complexed to p84 was resistant to S582 phosphorylation (Figure 6A), we unexpectedly obtained information on the p84 binding site. Our data show that p84 binds to PI3Kγ through the helical domain beginning (Figure 7A-C) and not the N-terminal region (Figure 7D) as has been anticipated in analogy to adaptor binding in class IA PI3K. In fact, the interaction site between p84 and PI3Kγ has not yet been characterised experimentally. We show here that N-terminally truncated (Δ130) GST-tagged PI3Kγ interacts with p84 equally well as full-length PI3Kγ (Figure

7D). Despite the N-terminus of PI3Kγ is not involved in p84 binding, it is required for the structural integrity of the p84 binding site, as untagged N-terminally truncated PI3Kγ (Δ130) fails to interact with p84. The GST-tag therefore acts as protein stabilizer rescuing p84 binding.

It is likely that also p101 interacts with the helical domain of PI3Kγ, since our results are in consent with previous publications analysing the interaction of PI3Kγ with p101. Krugmann et al. showed reduced binding of p101 to different long (Δ122-Δ369) N-terminal deletion mutants of Myc- or His-tagged PI3Kγ, but they did not analyse GST-tagged deletion mutants (Krugmann S, J Biol Chem, 1999). This however was done by Maier et al. who observed equal association of p101 with GST-PI3Kγ and GST-PI3Kγ Δ97 upon copurification from baculovirus-infected Sf9 cells (Maier U, J Biol Chem, 1999).

Untagged PI3Kγ Δ130 is functionally dead in vivo, as it does not support PKB activation in BMMCs (one experiment) (Thesis Figure 1). Additionally it is expressed at much higher levels than full-length PI3Kγ following transfection of equal amounts of plasmid DNA. Decreased degradation might be caused by lower inherent basal activity and structural changes affecting proteasom recognition. Similar to PI3Kγ Δ130 in BMMCs, PI3Kγ Δ143 is expressed at much higher levels in Sf9 cells. In vitro, recombinant GST-tagged PI3Kγ Δ130 was found to have increased lipid kinase and autophosphorylation activity than "full-length" GST-PI3Kγ (Δ37) und reacted efficiently with Wortmannin (Stoyanova S, Biochem J, 1997). This shows that GST-tagging not only rescues p84 binding but also positively affects lipid kinase activity. While there is no information available on the in vitro activity of untagged PI3Kγ Δ130, two groups reported normal basal activity of C-terminally His-tagged PI3Kγ Δ143 (Krugmann S, Biochem J, 2002; Walker EH, Nature, 1999). However, as enzymatic properties have not been characterized in detail, differences to wild type PI3Kγ might not have come to light. While increasing N-terminal truncations reduce basal lipid kinase activity at least in vivo, PI3Kγ is catalytically dead following removal of more than 169 amino acids (Krugmann S, Biochem J, 2002). Crystallisation of PI3Kγ Δ143 secured a shapshot of PI3Kγ with the catalytic loop in an inactive conformation. For comparison, in the structures of PI3Kδ (ΔABD) or Vsp34 (ΔC2), active site amino acids in the catalytic loop are oriented in a catalytic competent manner (Walker EH, Nature, 1999; Berndt A, Nat Chem Biol, 2010; Miller S, Science, 2010). Because of the observations, that p84 fails to interact with PI3Kγ Δ143 and that the regulatory S582 points inward of the crystal structure, it would be interesting to know whether the helical domain beginning folds differently in the full-length enzyme.

Following ectopic expression in cell lines, PI3Kγ and p84 form a stable complex that can be efficiently coimmunoprecipitated (Figure 6A-E, 7D) (Suire S, Curr Biol, 2005; Voigt P, J Biol Chem, 2006). Association is not required for stability as either protein is also expressed efficiently alone, but cotransfection augments expression levels. p101 interacts more strongly with PI3Kγ and is less stable than p84 in the absence of PI3Kγ. Analysis of endogenous p84 expression in PI3Kγ$^{-/-}$ cells showed stable expression in the bone marrow, but downregulation in bone marrow-derived mast cells and macrophages, neutrophils, and splenocytes (Bohnacker T, Sci Signal, 2009). As p84 levels were normal in cells expressing kinase-dead PI3Kγ (PI3Kγ$^{KR/KR}$), p84 expression is positively

influenced by the presence of this kinase. Despite of this interdependence, endogenous PI3Kγ and p84 coimmunoprecipitate from BMMCs only poorly and much less efficiently than the exogenously expressed proteins. Because of this and as PKCβ only targets p84-free PI3Kγ, it would be interesting to know, whether PI3Kγ levels exceed that of p84. Some PI3Kγ/p84 would then be available for activation by GPCRs, while single PI3Kγ is available for PKCβ. Alternatively, free PI3Kγ might localise to a region in cells that is not accessible for p84, or is processed in way that prevents p84 binding. Whether PI3Kγ activation by PKCβ occurs completely independent on p84 or requires its presence indirectly, we do not know, as investigation of this would require the availability of $p84^{-/-}$ BMMCs. Actually, it might be possible that p84 not only blocks PI3Kγ activation by PKCβ but also by GPCRs, as it does not serve as Gβγ recruitment adaptor for PI3Kγ as p101 (Kurig B, Proc Natl Acad Sci U S A, 2009). Furthermore, sequence identity of both adaptors is quite low. Consistently, BMMCs, which do not express p101, are resistant to stimulation by several GPCR ligands. So far adenosine is the only known ligand that triggers PI3Kγ activation in a GPCR-dependent manner in BMMCs (Bohnacker T, Sci Signal, 2009). It would therefore be important to analyse, whether adenosine-stimulated PI3Kγ activation depends on endogenously expressed p84. It has been proposed that adenosine- and p84-dependent PI3Kγ activation depends on coactivation by a Ras family member (Kurig B, Proc Natl Acad Sci U S A, 2009). Since Ras targets the RBD of PI3Kγ and not p84, the function of this adaptor is unclear in this model. Additionally, GFP-tagged PI3Kγ or p84 do not translocate in a microscopically detectable manner in complemented and stimulated $PI3K\gamma^{-/-}$ BMMCs or transfected HEK293 cells. It might be possible that growth factor or constitutively activated Ras locates some PI3Kγ at the plasma membrane, where it is accessible to allosteric activation by the receptor and Gβγ subunits. In HEK293 cells for example, both the fMLP receptor and Gβγ subunits potentiate activation of PI3Kγ-CAAX (Brock C, J Cell Biol, 2003).

5.8 Regulation of class I PI3Ks by phosphorylation

We discovered a new mechanism of PI3K regulation. We identified the serine/threonine kinase PKC to regulate PI3K activation by phosphorylation. The regulatory sites in PI3Kγ could be mapped to S582 and S257. Some other serine/threonine phosphorylation sites of PI3K and the p85 adaptor have been published. These are however targeted by the PI3K's inherent protein serine kinase activity. In contrast to lipid kinase activity, protein kinase activity of class IA PI3K is Mn^{2+}-dependent in vitro. On the other hand, class IB PI3Kγ operates with both Mn^{2+} and its physiological cofactor Mg^{2+}. Recombinant PI3Kγ and PI3Kδ autophosphorylate themselves in their C-termini – PI3Kγ on Ser1101 and PI3Kδ on Ser1039 (Stoyanova S, Biochem J, 1997; Vanhaesebroeck B, Proc Natl Acad Sci U S A, 1997). Whereas autophosphorylation does not affect lipid kinase activity of PI3Kγ, the activity of PI3Kδ is decreased. PI3Kα transphosphorylates its tightly bound adaptor subunit, p85α or p85β, at the end of the interSH2 domain on S608 (Carpenter CL, Mol Cell Biol, 1993; Dhand R, EMBO J, 1994). In the crystal structure of PI3Kα (2Y3A), S608 is located in a disordered stretch that folds over the catalytic site. Phosphorylation is

therefore facilitated by vicinity, which explains why PI3Kα only phosphorylates tightly bound p85. In contrast to PI3Kα, PI3Kβ and PI3Kδ do not phosphorylate p85. Whereas S608 is conserved in p85α, this is not true for p85β. It was shown that phosphorylated PI3Kα/p85 has a 2-fold decreased basal activity in vitro (Dhand R, EMBO J, 1994). Since S608 is prephosphorylated to a great extent in cell lines (Domin J, J Biol Chem, 1996), it has been hypothesized that this helps to keep PI3Kα at low basal state in quiescent cells (Dhand R, EMBO J, 1994). Whether mutation of S608 would relieve some inhibition of endogenous PI3Kα in vivo is unknown. However, baculovirus-expressed wild type and mutated p85 inhibit PI3Kα lipid kinase activity identically in in vitro assays using PtdIns as substrate. Analysis of phosphorylation of coexpressed PI3Kα-p85α in Sf9 cells by in vivo labelling with [^{32}P]-orthophosphate revealed p85α to contain phospho-serine and -threonine and PI3Kα to contain phospho-serine (Dhand R, EMBO J, 1994). Following activation of T lymphocytes by the T cell antigen receptor (TCR)/CD3 complex or activation of PKC by phorbol ester, p85α-associated PI3K gets rapidly and exclusively phosphorylated on serine residues (Reif K, J Biol Chem, 1993). On the other hand, p85α basal serine phosphorylation does not change during T cell activation, but p85β gets phosphorylated on threonine residues. The identity of the phosphorylation sites, whether they are targeted by PKC, and whether they regulate PI3K activation in vivo is unknown.

Additional to serine/threonine residues, p85 regulatory subunits have also been reported to become tyrosine phosphorylated on several and distinct residues in a stimulus-specific fashion. p85 is phosphorylated by the Src family kinases Lck and Abl on tyrosine 688 in vitro or after their overexpression in COS-7 cells (von Willebrand M, J Biol Chem, 1998). Y688 is conserved in p85α, β (Y686), and γ (Y422) and is located in the cSH2 domain of p85. It has been proposed that phosphorylation Y688 releases inhibition of PI3K by p85 (Cuevas BD, J Biol Chem, 2001; Zhang X, Mol Cell, 2011). Insulin stimulates phosphorylation of exogenously expressed p85α at Y368, Y580, and Y607 in Chinese hamster ovary (CHO) cells overexpressing the human insulin receptor (IR). While recombinant IR phosphorylates recombinant full-length p85 only on Y607, p85 truncation mutants were phosphorylated at all three sites. Metabolic labelling experiments showed that platelet-derived growth factor (PDGF) stimulates in vivo phosphorylation of p85 on tyrosine residues in NIH-3T3 cells, while phospho-serine content remained unchanged (Domin J, J Biol Chem, 1996). Recombinant PDGF receptor phosphorylates recombinant p85 on S508 in vitro. Mutation of S508 to phenylalanine abrogates phosphopeptide detection by two-dimensional chromatography, both in the in vitro assay or following PDGF-stimulation of p85-transfected COS-6M cells (Kavanaugh WM, Biochemistry, 1994). Despite identification of all these serine/threonine and tyrosine phosphorylation sites, evidence for a physiological role in vivo is so far missing.

5.9 Notes

Dose response behaviour of LAT$^{-/-}$ BMMCs

Dose response intact: LAT1$^{-/-}$ LAT1$^{-/-}$, 1YF, 2YF, 3YF, 4YF (Retroviral compl.) LAT2$^{-/-}$ (LAT1$^{-/-}$ degr. only) LAT1$^{-/-}$, LAT2$^{-/-}$	 Saitoh S, Immunity, 2000 Saitoh S, J Exp Med, 2003 Volná P, J Exp Med, 2004 Zhu M, J Exp Med, 2004
Degranulation at supraoptimal antigen concentrations: LAT1$^{-/-}$, LAT2$^{-/-}$, DKO (mice from Volná) LAT1$^{-/-}$, LAT-YYYY, FYYY, YFFF, FFFF (knock-in) (FFFF degranul., but Ca^{2+}↓)	 Roget K, J Immunol, 2008 Malbec O, J Immunol, 2004
Dose response not analysed: LAT1$^{-/-}$, LAT2$^{-/-}$, DKO; SLP-76$^{-/-}$ (DNP until 30 ng) (text only: pPKB mentioned to be normal) LAT1$^{-/-}$, SLP-76$^{-/-}$, Fyn-SLP-76$^{-/-}$	 Kambayashi T, Mol Cell Biol, 2010 Kambayashi T, Immunol Reviews, 2009

Effect of serum starvation on Gab2 phosphorylation in BMMCs

Stimulated pGab2	Starving and stimulation conditions (*no serum!)	Reference
yes	2 μg/ml IgE, 4 h (in what?) Resuspension in Tyrode's buffer* before stimulation 10 ng/ml DNP (2, 5, 10 min)	Gu H, Nature, 2001
yes	IgE-containing hybridoma supernatant, ON Starved in IMDM/1%BSA* 3-4 h Resuspension in Tyrode's buffer* before stimulation 10 ng/ml DNP (5, 10 min)	Yu M, J Immunol, 2006 (same group as Gu H, 2001)
RBL-2H3: increased phosphorylation BMMCs: increase over basal (Fig. 2a, Fig. 1d unclear)	SCF starvation ON 1 μg/ml IgE in IL-3 free medium Resuspension in Tyrode's buffer* (washed twice) Stimulation with 10-100 ng/ml DNP	Parravicini V, Nat Immunol, 2002
no (already phosphorylated)	RPMI 1640 complete w/o IL-3, 1 μg/ml IgE ON 10 ng/ml DNP-BSA	Hernandez-Hansen V, J Immunol, 2004

Cell lines supporting helical domain mutation-dependent PKB activation

Reference	Cells	Mutations	Activity in vitro	P-PKB in cells
Zhao JJ, Caner Cell, 2003	Engineered HMEC (hTERT, SV 40 LT, endog. cMyc↑)	Myr-Flag-PI3Kα	–	P-PKB induction
Zhao JJ, PNAS, 2005	Engineered HMEC (hTERT, SV 40 LT, endog. cMyc↑)	HA-tagged, H1047R, E545K	–	P-PKB induction, (more than Myr-)
Kang S, 2005 (Vogt lab)	RCAS vector transfeced primary chicken embryo fibroblasts (passaged 3 times) (40 h 0.5% FCS/0.1% chicken serum, 2 h no serum at all)	E542K, E545K, H1047R (tagged?)	IP: PI3Kα, PI as substrate, activity↑ *(p85 binding not shown)**	P-PKB induction
Gymnopoulos M, 2007 (Vogt lab)	RCAS vector transfeced primary chicken embryo fibroblasts, (40 h 0.5% FCS/0.1% chicken serum, 2 h no serum at all)	Rare mutations (incl. E545A, E545G, H1047L)	IP: PI3Kα, PI as substrate, activity 2-3-fold↑ (Suppl)	Increased PKB (over PI3Kα wt)
Zhao L, 2008 (Vogt lab)	RCAS vector-transfeced primary chicken embryo fibroblasts (passaged 3 times) (40-44 h 0.25% FCS/0.05% chicken serum, 2 h no serum at all)	E542K, E545K, H1047R (Δp85, K227)	–	P-PKB induction
Ikenoue T, 2005	Stably transfected NIH-3T3, 12 h 0.1% serum	E542K, E545K, H1047R	IP: Myc (from starved HEK293T), PI as substrate, activity↑	Increased P-PKB (NIH-3T3)
Pang, H, Cancer Res, 2009	Stably transfected MDA-MB-231, starved 4 h (knockdown of human, expr. of bovine PI3Kα)	E545K, H1047R, C-terminal Myc-tag	–	P-PKB induction (further increased by EGF)
Isakoff SJ, Cancer Res, 2005	Stable MCF-10A& (Puro). Starved 24 h in growth medium w/o EGF, insulin. &Spontaneously immortalized breast/mammary epithelial cells.	HA-PI3Kα E545K, H1047R (bovine)		Increase P-PKB, growth-factor ind. P-PKB

*Miled: Myc-PI3Kα (bovine) wt, E542K, E545K, Q546K. with PIP_2?

Mast cell homing and function

	p85α$^{-/-}$ (p55-p50α$^{+/+}$)	Gab2$^{-/-}$	PI3Kδ^{D910A}
Mast cell numbers:			
Peritoneum	24% (FACS) (1)	0%(ns), ~5% (ab), ~5% (ns)	8% (ab-s)
Dermis: Ear Back Thigh Skin Back: Dermis Back: Hypodermis	65% (tb) 77% nd	100% (tb) (ns); ~43% 50-70% (ns) 50-70% (ns) 60% (ab) ~67% (tb) (not signif.) ~50% (tb)	53% (tb) 86% (not signif.) (tb)
Stomach Mucosa Subm. Muscularis Forestomach Glandular stomach	0% (tb, ab-s, chest) 0% (2) 0%	 ~8% (ab) ~5% (ab)	90% (not signif.) (tb) 57% (tb) 57% (tb)
Jejunum (low # Ileum in wt) Colon	0% (2) 0% 0%	nd	26% (tb) 5% (not signif.) (tb) 0% (tb)
Mice responses:			
PSA	ok (Evans b., plasma hist., survival)	↓↓ (plasma hist.)	nd
PCA	nd	55% (dorsal ear, Evans b.)	Ear: 20% (E. b.); 40% Back: 60% (Evans b.)
BMMC responses:			
BMMC culture	IL-3	2-4 ng/ml IL-3; IL-3 supernatant; 4 ng/ml IL-3	10 ng/ml IL-3 + 20 ng/ml SCF; both 20 ng/ml
Proliferation	IL-3 ok; SCF ↓↓ (3) IL-3: 10 ng/ml, SCF: 200 ng/ml IL-3+SCF: ok (4)	nd; IL-3 ~ok (0.5-20 ng/ ml); SCF low (50 ng/ml) ok, SCF high (200) ↓↓; SCF (50 ng/ml) 30-70%	IL-3 (5), SCF, IL-3+SCF: no prolif. (^{3}H-Thymidine). No PIP$_3$ in response to SCF; nd
Survival (growth factor deprivation)	IL-3 ok; SCF ok	nd; ok; nd	nd; nd
PKB activation SCF IL-3	~70% (almost ok) nd	nd; ↓ (100 ng/ml); ok ↓ (Gu, not shown); nd; nd	↓↓; ↓↓ slightly ↓; nd
Adhesion SCF Migration SCF	discussion part: no polarity in chemotaxis assay, but infiltration in vivo	nd	↓↓ (1-20 ng/ml); blocked ↓↓; nd
Degranulation	ok (β-Hexo) 4 h 1 µg/ml IgE w/o IL-3 10 ng/ml DNP	↓ (^{3}H-Serotonin) 6 h 1 µg/ml IgE 3, 10, 30, 100 ng/ml DNP	55% (β-Hexo), still sensitive to Ly294002. 100 ng/ml IgE/200 ng/ml DNP com-plexes. Diff. much less with 10 ng/ml DNP; 50% (β-Hexo), (100 ng/ml IgE, 30 ng/ml DNP)
Other notes			
References:	(Fukao T, Nat Immunol, 2002), review in (Koyasu S, Novartis Found Symp, 2005)	(Gu H, Nature, 2001), (Nishida K, Blood, 2002) (diff. mice), (Yu M, J Biol Chem, 2006)	(Ali K, Nature, 2004), (Ali K, J Immunol, 2008)

tb: toluidine blue ab: alcian blue s: safranin bs: beberine-sulfate chest: chloroacetate esterase activity

ok: normal response nd: not determined ns: not shown ↓: reduced ↓↓ greatly reduced

Kit^{Y567F}	Kit^{Y569F}	$Kit^{Y567F, Y569F}$	KIT^{Y719F}	$Gab2^{-/-}$-KIT^{Y719F}
Mast cell numbers:				
2% (tb, ab-s, bs) ↓↓	↓↓	~0%	27% (tb); 42% (tb, ab-s, bs, images in Agosti et al), ~25% (ns)	0% (ns)
Dorsal skin mast cells: 100% Tail dermis: ok	Tail dermis: ok	Tail dermis: ~0%	Ear: ~63%; dorsal skin mc: 100% (tb); dors. skin mc: 100% ~100% (tb) ~100% (tb)	~15% (tb) 60% (tb) ~0% (tb)
↓↓ ~ok	↓↓ ~60%	~0% 0%!	nd	nd
nd	nd	nd	nd	nd
Mice responses:				
nd	nd	nd	nd	nd
nd	nd	nd	nd	nd
BMMC responses:				
–, IL-3 supern.	–	–	IL-3 supern.; IL-3 supern.	4 ng/ml IL-3
nd SCF: ok (↓ reduced at ≤10 ng/ml) (6)	nd	nd	SCF: 60% (200 ng/ml); 70% (50 ng/ml) IL-3: nd (6)	SCF: 20%
nd SCF: ok (6)	nd	nd	SCF: 40% (200 ng/ml); nd IL-3: ok (6)	nd
nd	nd	nd	SCF: ↓↓ (residual) ↓↓ PKB kinase acti-vity (H2B) (but also high signal in unst. cells)	SCF: 0%
nd	nd	nd	nd	nd
nd	nd	nd	nd	nd
SCF: pY719, p85 binding ok		Mega-stomach, -colon (but not in W mice)	↓↓ JNK activity (GST-Jun)	↓↓↓ JNK activity (GST-Jun)
(Kimura Y, Proc Natl Acad Sci U S A, 2004), (Agosti V, J Exp Med, 2004)	(Kimura Y, Proc Natl Acad Sci U S A, 2004)	(Kimura Y, Proc Natl Acad Sci U S A, 2004)	(Kissel H, EMBO J, 2000), (Agosti V, J Exp Med, 2004), (Yu M, J Biol Chem, 2006)	(Yu M, J Biol Chem, 2006)

Remarks:

(1) Restoration by i. p. injection of BMMCs. Normal maturation there, since normal response to bacterial infection (TNF-α release).

(2) Restoration by i. v. injection of bone marrow, but not BMMCs (-> environmental defects, requirement of other BM-derived cells). But recruitment of injected BMMCs to small intestine after previous subcutaneous infection with worm (*S. venezuelensis*) (inflammation-induced migration). But only Th2-preconditioned BMMCs (with IL-4, IL-10) can combat infection (impaired cytokine production by mesenteric p85α$^{-/-}$ lymphocytes in response to soluble worm antigen).

(3) PKB activation only slightly reduced (by 30%). PI3Kδ expression levels normal (PI3Kα greatly reduced). Reduced proliferation may result from reduced JNK activation. Proliferative defect by SCF completely rescue in the presence of IL-3.

(4) p85α-p55α-p50α$^{-\backslash-}$ fetal liver-derived mast cell (Lu-Kuo JM, J Biol Chem, 2000): Reduced expression of PI3Kα, PI3Kβ, and PI3Kδ. Normal growth in IL-3 containing medium. Cells survive in the presence of SCF, but do not proliferate (cell#, ^{3}H-Thymidine). PKB phosphorylation in response to SCF only slightly reduced *(blot unclear)* (IgE/MAR induced PKB activation normal).

(5) Reduced degranulation (~50%) in response to SCF, normal in response to rat IgE (5, 20 µg/ml)/MAR (= F(ab')$_2$ anti-rat IgG, 25 µg/ml) (10 Mio cells/ml)**. Degranulation (β-hexo) abrogated by LY294002. *(**SHIP activation intact? → likely yes: no increased pPKB)*

(6) FLMCs degranulate in response to SCF**. p85α is expressed at much higher levels than p85β, and is responsible for the major p85-associated PI3K activity. FLMCs express p85α and p50α (p55α not detectable). p85α-p55α-p50α$^{-\backslash-}$ fetal liver-derived mast cell (Tan BL, Blood, 2003): Greatly reduced migration to fibronectin coated transwells in response to SCF.

(7) Personal comment: But BMMCs develop normally from bone marrow!

(8) W^{sh}/W^{sh} BMMCs transduced with Kit Y567F, Y719F, or Y567F/Y719F (Timokhina I, EMBO J, 1998; Serve H, EMBO J, 1995):
Proliferation, SCF: Y567F: ~50% Y719F: ~70% Y567F/Y719F: ~0%
Apoptosis, SCF: Y567F: ~50% Y719F: ~50% Y567F/Y719F: ~100%
IL-3: both ok. SCF + Wm: ~30% + PP1: 60%
Single mut, Wort, PP1: reduced JNK activation (IKA, GST-Jun). Double mut, Wort/PP1: greatly reduced.
Adhesion, SCF: Y719F: 50% SCF + Wm: 0%

5.10 Thesis figures

Thesis Figure 1

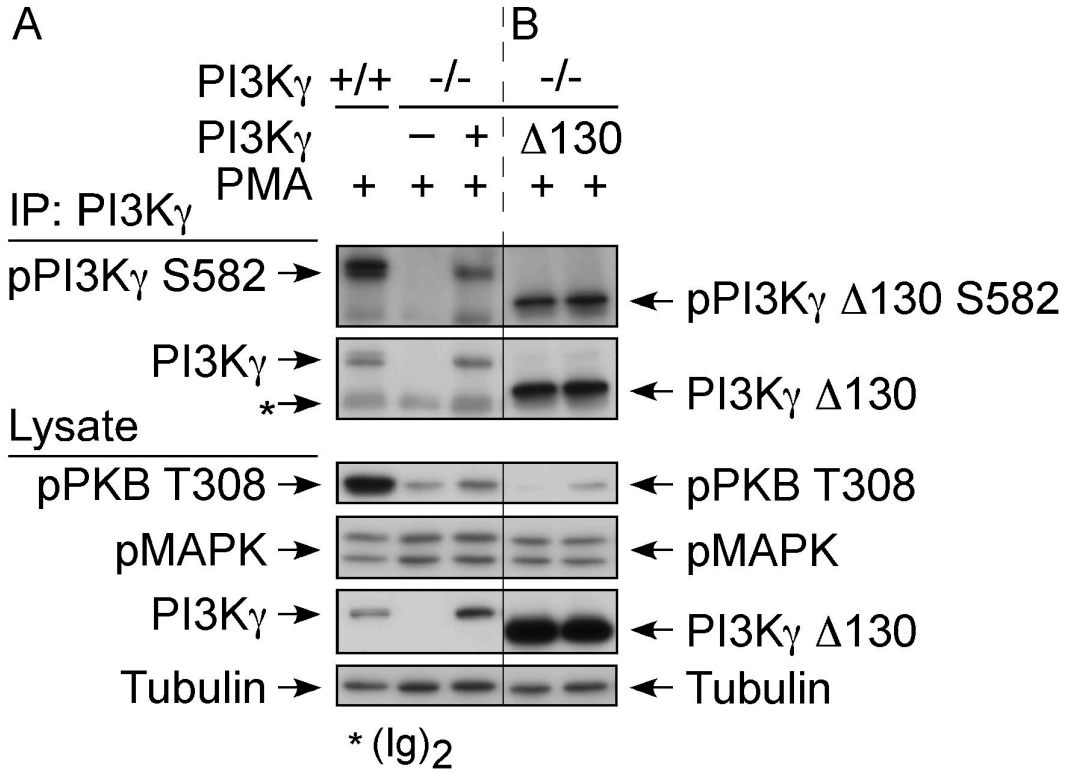

Thesis Figure 2

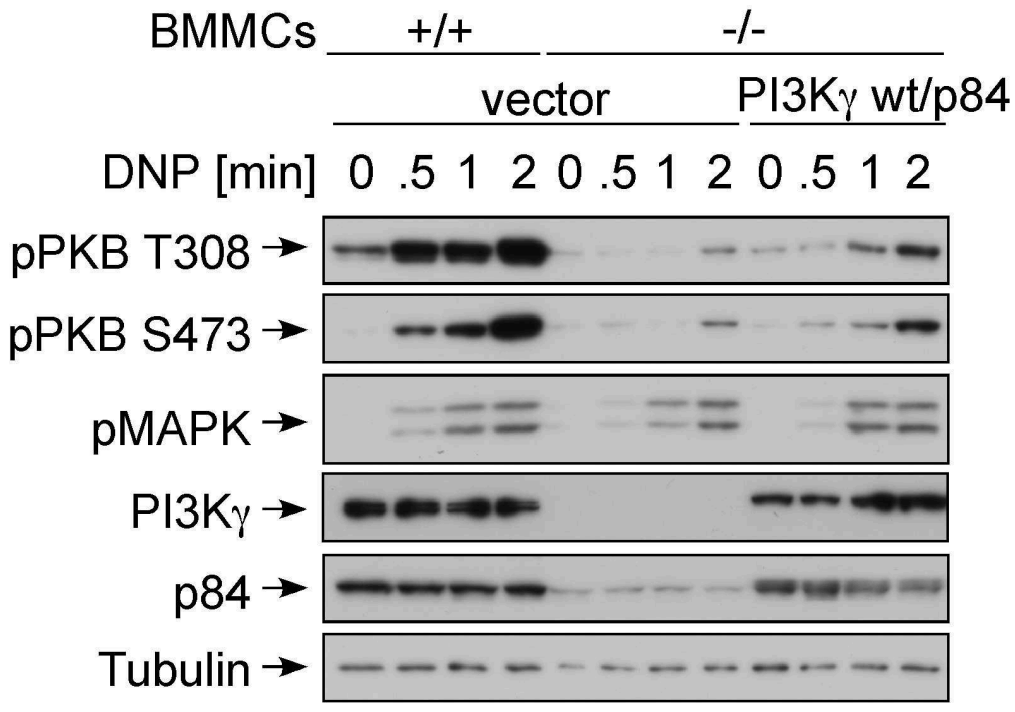

Thesis Figure 3

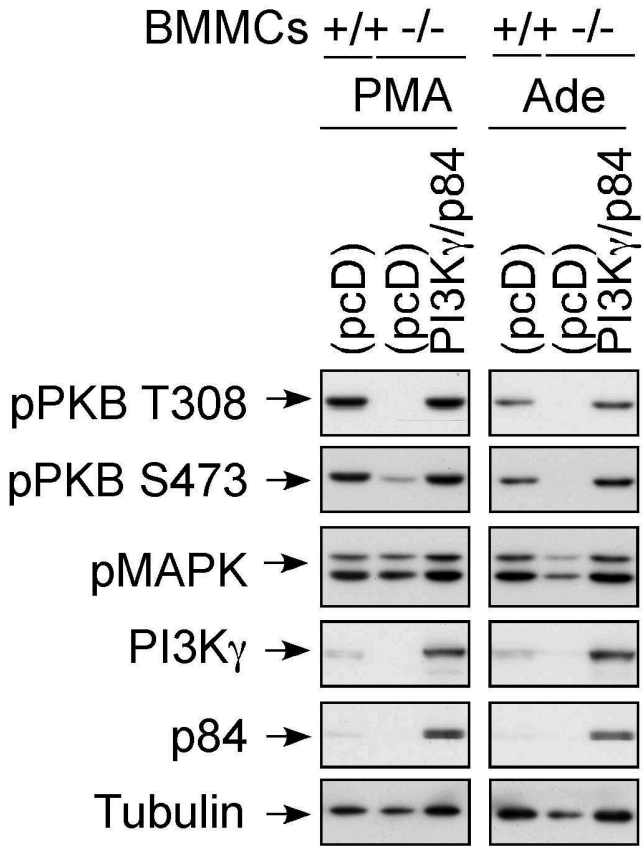

Thesis Figure 4

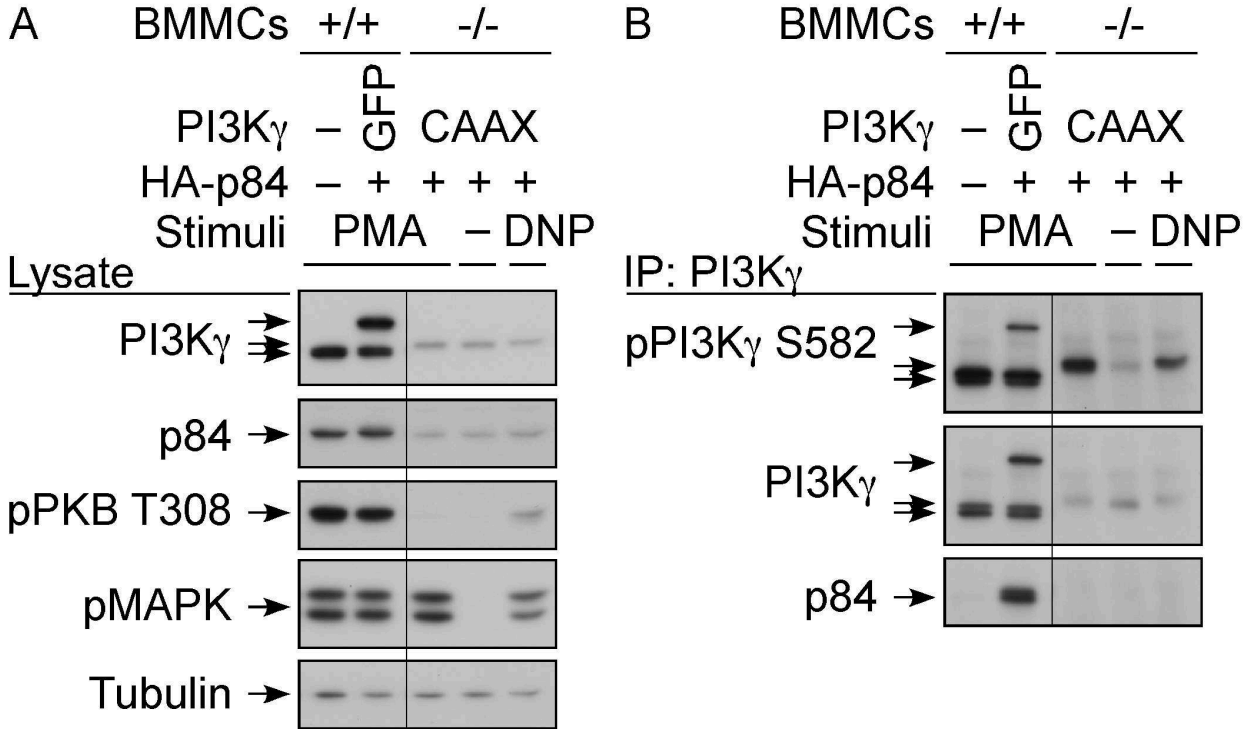

Thesis Figure 5

A

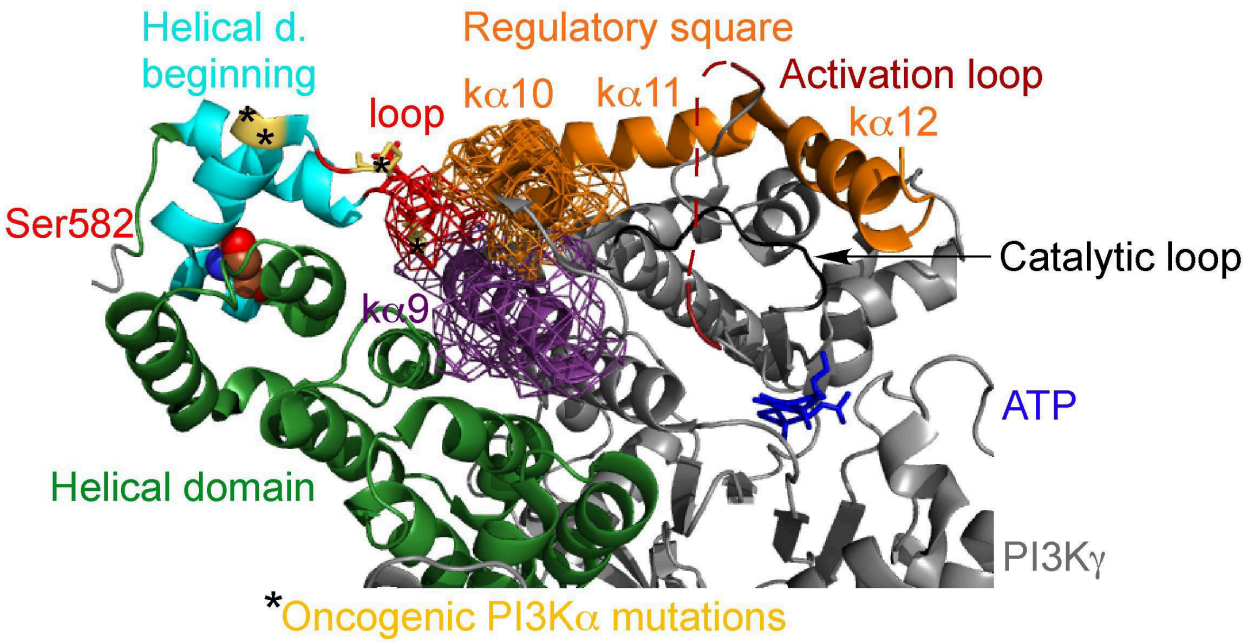

B

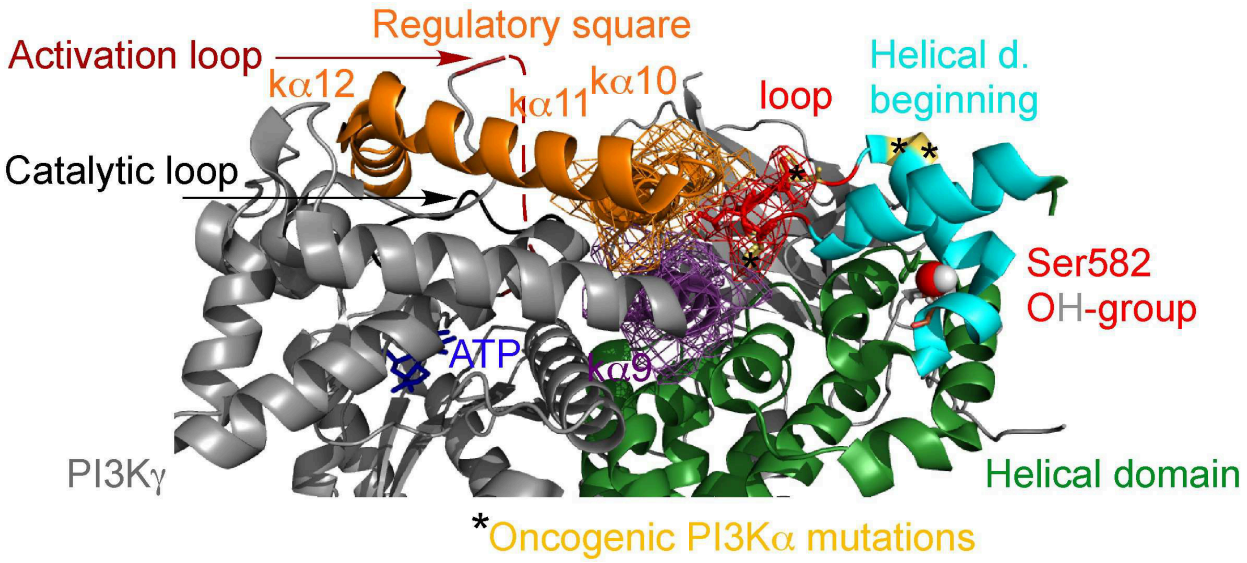

C

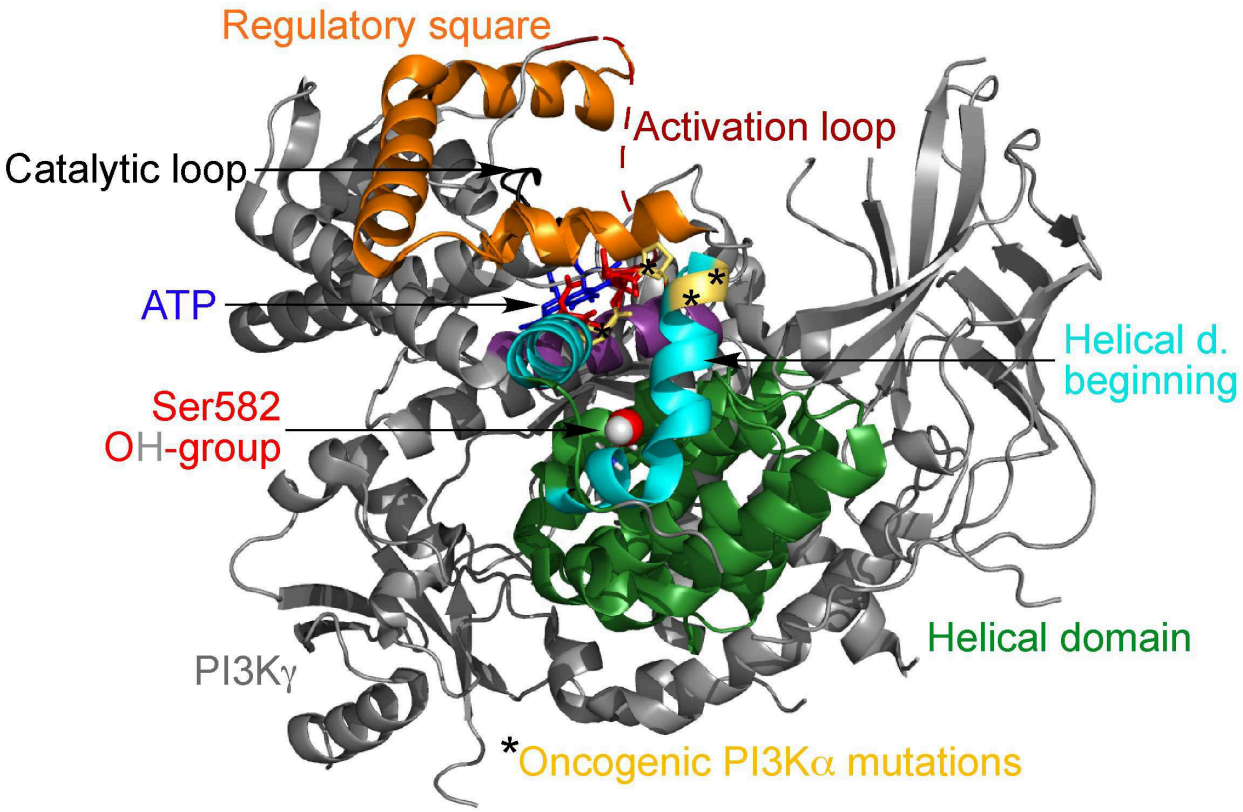

Thesis Figure 6

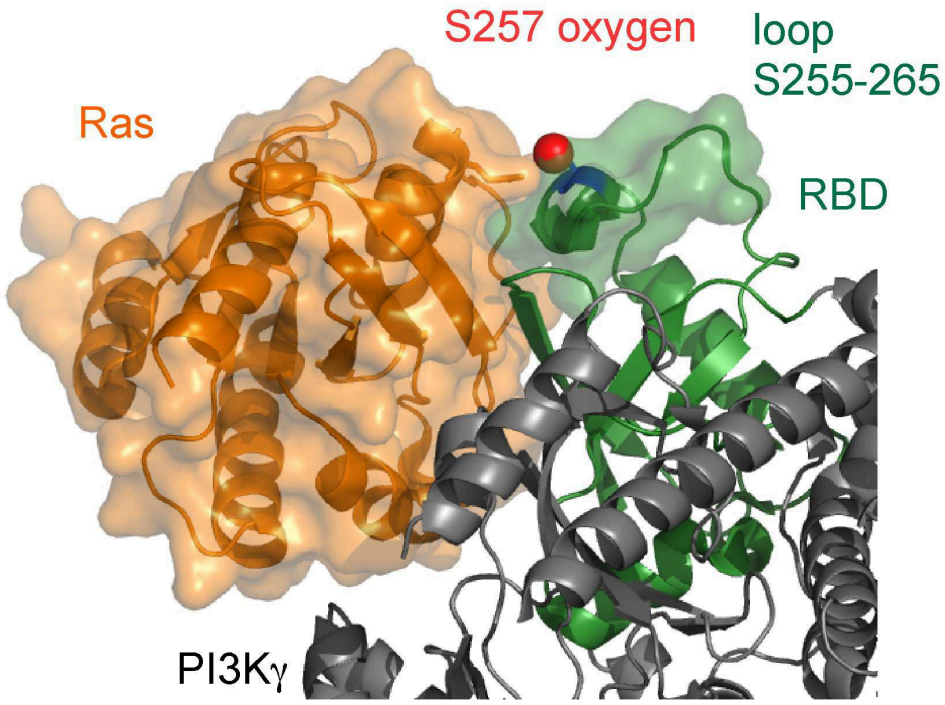

Figure legends to "Thesis figures"

Thesis Figure 1. (A) Exogenously expressed PI3Kγ can not fully complement endogenous PI3Kγ. Wild type or PI3Kγ$^{-/-}$ BMMCs were transfected with vector or 3 μg of PI3Kγ expression plasmid (totally 10 μg plasmid DNA). Next day, cells were IL-3 starved for 1 hour and stimulated with 200 nM PMA for 30 s. PI3Kγ immunoprecipitations and cell lysates were analysed by Western blotting with the indicated antibodies.
(B) N-terminal truncated PI3Kγ is highly overexpressed and does not support PKB activation. PI3Kγ$^{-/-}$ BMMCs were transfected with 0.75 μg of PI3Kγ Δ130 expression plasmid (totally 10 μg plasmid DNA) and stimulated and analysed as described in (A).

Thesis Figure 2. Exogenously expressed PI3Kγ can not fully complement endogenous PI3Kγ. Wild type or PI3Kγ$^{-/-}$ BMMCs were transfected with vector or 1 μg of PI3Kγ and 1 μg of p84 expression plasmids (totally 10 μg plasmid DNA). Cells were incubated with 100 ng/ml IgE overnight and starved next day for 2.5 hours in IL-3 free medium. Stimulations (16 ng/ml DNP) were stopped with ice-cold medium and cells were immediately centrifuged and lysed with 1x Laemmeli sample buffer. PKB phosphorylation and exogenous protein expression were analysed by immunoblotting.

Thesis Figure 3. Several fold overexpression of PI3Kγ complements PKB phosphorylation. Wild type or PI3Kγ$^{-/-}$ BMMCs were transfected with 13 μg of vector or 4 μg of PI3Kγ and 4 μg of p84 expression plasmids (totally 13 μg plasmid DNA). Cells were starved for 3 hours in growth medium/2% FCS and stimulated with 50 nM PMA or 2 μM adenosine. Stimulations were stopped on ice and cells were harvested by centrifugation and lysed with 1x Laemmeli sample buffer. PKB phosphorylation and exogenous protein expression were analysed by immunoblotting.

Thesis Figure 4. (A) Artificially membrane-attached PI3Kγ is inactive in BMMCs.
(B) Level of endogenous PI3Kγ S582 phosphorylation (1.5-fold over PI3Kγ-CAAX) lies in the range of PI3Kγ-CAAX expression, assuming the later gets fully phosphorylated.
(A/B) Wild type BMMCs were transfected with vector DNA or 0.5 μg of expression plasmids of EGFP-PI3Kγ and p84. PI3Kγ$^{-/-}$ BMMCs were transfected with 2 μg of PI3Kγ-CAAX and 0.5 μg of p84 expression plasmids (totally 8 μg plasmid DNA). Cells were incubated overnight with 100 ng/ml IgE and IL-3 starved before stimulation with 200 nM PMA or 100 ng/ml DNP for 45 s. Cell lysates (A) and anti-PI3Kγ immunoprecipitations (B) were analysed by Western blotting with the indicated antibodies.

Thesis Figure 5. Model of PI3Kγ activation by Ser582 phosphorylation.
(A) S582 (O: red, C: brown, N: blue balls) lies in the B helix of the first antiparallel A/B helix pair (light blue) of the helical domain (green) of PI3Kγ. The intrahelical loop (red) of this helix pair interacts with the C-terminal lobe of the kinase domain, including helix kα10 of the regulatory square (orange) and helix kα9 (violet). As these two helices build a wall of the pocket that surrounds the activation and catalytic loops, S582 phosphorylation might trigger PI3Kγ activation by inducing a conformational change in the catalytic centre. In the crystal structure of PI3Kγ Δ143 (PDB ID: 1E7U), S582 is slightly buried looking more inside than outside of the structure. Because of this and other reasons it is likely that the beginning of the helical domain adopts a different conformation in the full-length enzyme and in the phosphorylated state. S582 lays in the same region as oncogenic helical domain-associated mutations in PI3Kα. For comparative purpose the corresponding residues in PI3Kγ have been marked by yellow colour and a star (*). For better view on kα9, kα10, and the loop, the C2 domain has been deleted from the shown structure.
(B) Same structure as in (A) but viewed from the opposite side and including the C2 domain. Ser582 side chain hydroxyl group: O: red, H: gray.
(C) Side view on Ser582. 90° rotation with respected to (B).

Thesis Figure 6. Ser257 is located at the edge between PI3Kγ and Ras in the crystal structure.
Section of the crystal structure of PI3Kγ with Ras (PDB ID: 1HE8). The surfaces of Ras and the loop of the PI3Kγ that gets ordered upon Ras binding are shown. The Ras binding domain (RBD) is coloured green. The S257 residue is coloured blue and the hydroxyl group oxygen is coloured red.

6. Material and methods

6.1 Plasmids

Full-length untagged human PI3Kγ was expressed from pcDNA3 (Invitrogen) (Bondeva T, Science, 1998) and S582 and S257 point mutations were introduced by polymerase chain reaction (PCR) using the overlap extension technique (Ho SN, Gene, 1989). Mouse PKCβ2 cDNA was obtained from Jae-Won Soh (PKClab.org) and inserted BamHI-BstEII-XhoI into pcDNA3 containing a Kozak translation initiation sequence and the human influenza hemagglutinin (HA)-tag between HindIII and BamHI (pcDNA3-kzHA). The catalytic part of PKCβ2 (PKCβ2-CAT) including amino acids 302-673, was amplified from full-length PKCβ2 with the forward primer 5'-ccgcaGGATCCcagaagtttgagagagccaagattg and the reverse primer 5'-ggcgTCTAGAttagctcttgacttcag-gttttaaaaattc and inserted BamHI-XbaI into pcDNA3-kzHA. The pseudosubstrate deletion mutant of PKCβ2 was produced by the overlap extension technique with primers lacking the coding sequence for amino acids 19-31 of PKCβ2 (forward: 5'-gagcacagtgcacgaggtgaagaaccacaaattcac, reverse: 5'-cacctcgtgcactgtgctctcctcgccc) and two helper primers. The baculovirus transfer plasmid encoding GST-PI3Kγ (pAcG2T-PI3Kγ, codons 38-1102) has been described (Stoyanov B, Science, 1995). The transfer plasmid for baculovirus-mediated expression of C-terminal His-tagged full-length human PI3Kγ has been derived from pVL1393 (Invitrogen) containing codons 144-1102 of human PI3Kγ (kindly obtained from R. Williams, (Pacold ME, Cell, 2000)) by inclusion of codons 1-143 by PCR. Serine 582 or S257 mutations were introduced into this construct by insertion of a PciI-EcoRI or BstEII-EcoRI fragment from mutant PI3Kγ in pcDNA3, respectively. All constructs were confirmed by sequencing.

6.2 Mice

C57BL/6J mice were from Jackson Laboratories. PKCβ (Leitges M, Science, 1996; Standaert ML, Endocrinology, 1999) and PI3Kγ knock-out mice (Hirsch E, Science, 2000) have been described and were both on a pure C57BL/6J genetic background. Experiments were carried out in accordance with institutional guidelines and national legislation.

6.3 Cell Culture

Mouse bone marrow-derived mast cells (BMMCs) were developed from progenitor cells by culturing femoral bone marrow of 8-12 week old mice in the presence of 2 ng/ml IL-3 for 4 weeks. Femurs were cut off at both ends and the marrow collected by centrifugation. Cells were resuspended in Icove's modified Dulbecco's medium (IMDM) (Sigma) supplemented with 10% heat-inactivated fetal calf serum (HI-FCS), 2 mM L-glutamine, 100 units/ml penicillin, 100 μg/ml streptomycin, 50 μM β-mercaptoethanol, 2 ng/ml recombinant murine IL3 (Peprotech), and 5 ng/ml SCF and cultured at 37°C, 5% CO_2. IL3 (but not SCF) was readded every second or third day. Non-adherent cells were transferred to new flasks and diluted weekly to 0.5 Mio/ml using 80% of fresh and 20% of conditioned medium. Differentiation of BMMCs was confirmed by measuring

expressing of c-Kit and IgE receptors by flow cytometry. BMMCs were used for experiments after 4 weeks of culture until maximally 16 weeks.
The human embryonic kidney 293 (HEK293) cell line was grown in Dulbecco's modified essential medium (DMEM) supplemented with 10% HI-FCS, 2 mM L-glutamine, 100 units/ml penicillin, and 100 µg/ml streptomycin at 37°C, 5% CO2.
Spodoptera frugiperda *(*Sf9) cells were grown in IPL-41 medium (Genaxxon Bioscience) supplemented with 10% HI-FCS (Sigma-Aldrich), 2% yeastolate, 1% lipid concentrate, 50 µg/ml gentamicin (all Invitrogen), and 2.5 µg/ml amphotericin B (Genaxxon Bioscience). Sf9 cells were cultured as adherent or suspension culture at 27°C. Suspension cells were grown in Erlenmeyer flasks in a shaking incubator at 75-90 rpm.

6.4 Transfection of HEK293 cells

HEK293 cells were seeded into 6 cm dishes (1.32 Mio/dish). Next day, cells were transfected with JetPEI™ (Polyplus-transfection) using 2.5 µg of total plasmid DNA. DNA concentrations were kept constant by the addition of empty pcDNA3 vector (Invitrogen). Cells were incubated with the transfection mixture for 5-8 hours, then the medium was exchanged and the cells left in the incubator overnight.

6.5 Stimulation of BMMCs

For stimulation of BMMCs through the Fc epsilon receptor I (FcεRI), cells were passively sensitized with 100 ng/ml anti-dinitrophenyl (DNP)-specific immunoglobulin E (SPE-7, Sigma) overnight in complete growth medium. Next day, cells were centrifuged for 5 min at 146 g and resuspended IL-3 free growth medium containing 2% or 10% FCS. Degranulation was induced by the addition of DNP coupled to human serum albumin (DNP_{30-40}-HSA) (Sigma) at concentrations between 5 and 100 ng/ml. Other stimuli used to trigger BMMC activation were Thapsigargin (0.03125-1 µM, Sigma), phorbol 12-myristate 13-actetate (PMA) (50-200 ng/ml, Alexis), adenosine (1 µM, Sigma), stem cell factor (SCF) (10 ng/ml, Peprotech), and interleukin-3 (IL-3) (10 ng/ml, Peprotech). Stimulations were done at 37°C for the indicated times. Preincubation with *B. Pertussis Toxin* (*P*Tx) (100 ng/ml, Sigma) was done for 4 hours, and adenosine deaminase (ADA) (10 units/ml, Sigma) was added 1 min before stimulation. Pretreatment time was 15 min for Wortmannin (100 nM) and 20 min for the PKC inhibitors (Ro318425 (1 µM), Gö9683 (0.5 µM), Gö6976 (0.5 µM), Rottlerin (10 µM) (all Calbiochem), PKC412 (CPG41251) (1 µM, Novartis)). For Western blot analysis of PKB and MAPK phosphorylation, stimulations were stopped on ice and the cells were collected by centrifugation for 1 min at 2000 g at 4°C and immediately lysed in 1x Laemmli sample buffer [62.5 mM Tris/HCl pH 6.8, 2% SDS, 10% glycerol, 5% β-mercaptoethanol, bromophenolblue].

6.6 (Co-)Immunoprecipitation (IP)

Transfected HEK293 cells were washed with 3 ml of phosphate buffered saline (PBS) and lysed with 500 µl of NP-40 lysis buffer [50 mM Tris/HCl, pH 7.4, 138 mM NaCl, 2.7 mM KCl, 5%

glycerol, 1% NP-40] supplemented with protease inhibitors [20 μM leupeptin, 18 μM pepstatin, 5 μg/ml aprotinin, phenylmethylsulfonylfluorid (PMSF)], phosphatase inhibitors [40 mM NaF, 2 mM Na_3VO_4 (Fluka)], 0.5 mM EDTA, and 0.5 mM EGTA (both Fluka) for 15 min on ice. Insoluble material was pelleted by centrifugation at 16'000 g for 10 min at 4°C. 50 μl of clarified lysate was mixed with 5x Laemmli sample buffer and used to examine exogenous protein expression. The remainder of lysate was incubated with either anti-PI3Kγ (6.4.1) or anti-HA (HA.11, Covance) antibodies for 1 hour at 4°C on a rotating wheel, followed the incubation with 25 μl of GammaBind Plus Sepharose (50 % slurry) (Amersham Biosciences) for another 2 hours. Immuncomplexes were washed 3x with NP-40 lysis buffer containing NaF and $NaVO_3$, 1x with 0.1 M Tris/HCl pH 7.4, 0.5 M $LiCl_2$, and 1x with phosphate buffered saline pH 7.4. Bound proteins were eluted by the addition of 62.5 μl 1x Laemmli sample buffer, heated to 95°C for 3 min, and stored at -80°C until SDS-PAGE analysis.

Unstimulated and stimulated BMMCs were collected by centrifugation and lysed in NP-40 lysis buffer supplemented with protease inhibitors, phosphatase inhibitors [40 mM NaF, 10 mM β-glycerophosphate, 5 mM sodium pyrophosphate (all Fluka)], 2 mM EDTA, and 2 mM EGTA for 15 min on ice. After removal of cell debris, lysates were precleared with 10 μl of protein A or G agarose beads (50% slurry) (Millipore, Amersham) for 30 min at 4°C. Supernatants were then transferred to new tubes and an aliquot (termed lysate) saved to analyse cell stimulation. Rest of the cleared lysate was incubate with anti-PI3Kγ (6.4.1) antibodies for 1-2 hours at 4°C, followed by additional incubation for 2-5 hours with 25 μl of protein A or G-agarose beads (50% slurry). Bead-PI3Kγ complexes were washed 2x with NP-40 lysis buffer, 2x with 0.1 M Tris/HCl pH 7.4, 0.5 M $LiCl_2$, 0.2% NP-40, and again 1x with NP-40 lysis buffer before resuspension in 1x Laemmli sample buffer. Lysates and immunoprecipitates were analysed by Western blotting.

6.7 Western Blotting

Protein samples were heated to 95°C for 5 min, centrifuged for 2 min at 16'000g, separated by SDS-polyacrylamide gel electrophoresis (PAGE), and transferred to polyvinylidene fluorid (PVDF)-membranes (Millipore) by semi-dry transfer. Membranes were blocked with 5% (w/v) milk powder (Migros, Schweiz) in TBS-T buffer [20 mM Tris/HCl, pH 7.6, 137 mM NaCl, 0.1% (v/v) Tween 20 (Fluka)]. Blots were incubated overnight at 4°C with the primary antibody, followed by incubation with horseradish peroxidase (HRP)-coupled secondary goat anti-mouse or anti-rabbit antibodies (Sigma). Protein bands were visualized by enhanced chemiluminescence (ECL) (Millipore). Phospho-specific antibodies were kept in TBS-T/1% BSA (w/v) [P-PKB S473 (Sigma, 4058), P-PKB T308 (Sigma, 4056 or 9275), P-MAPK (Sigma, M8159 or Promega, V8031), P-PI3Kγ S582 or S257 (antisera against phospho-peptide, affinity-purified, Eurogentec or AMS Biotechnology)], all others in TBS-T/1% (w/v) milk powder [PI3Kγ (raised against amino acids 97-335, ascites by Eurogentec), PKCβ2 (Santa Cruz, sc-210), PKCα (sc-208), PKCγ (sc-211), β-Tubulin (Boehringer Mannheim), α-Tubulin (Sigma, T9026), HA (Covance, MMS-101R), p84 (rabbit antisera produced by Zymed, (Bohnacker T, Sci Signal, 2009)), PKB (gift from B. Hemmings)].

Quantifications of Western blots have been done which ImageJ 1.42q software (NIH) after scanning of developed X-ray films (Fuji) on an Epson Perfection scanner (4990 Photo) as a 16-bit grayscale images without adjustments. Scanned images were inverted with ImageJ and bands were selected with the rectangle tool. Pixel values of the band and a background area above or below the selected band were used to calculate final intensities. Levels of protein phosphorylation were normalised to the total level of the protein and expressed in correlation to the signal obtained by a freely chosen stimulated sample.

6.8 β-Hexosaminidase release assay

Mast cell degranulation was assessed by measuring the release of β-hexosaminidase into cell supernatants (Schwartz LB, J Immunol, 1979; Ozawa K, J Biol Chem, 1993). BMMCs were cultured at 0.8-1 Mio cells/ml in complete growth medium overnight and were, if required, sensitized with 100 ng/ml IgE. Cells were wash ones and resuspended in PIPES-buffered solution [25 mM PIPES pH 7.4, 119 mM NaCl, 5 mM KCl, 5.6 mM glucose, 1 mM $CaCl_2$, 0.4 mM $MgCl_2$, 0.1 % fatty-acid free, low endotoxin bovine serum albumin (LE-BSA, Sigma)]. 0.5 Mio cells were stimulated with DNP or Thapsigargin in a total volume of 500 µl in 24 well plates. Following incubation at 37°C for 20 min, plates were centrifuged at 4°C at 330 g for 5 min. 100 µl aliquots (triplicate) of supernatant were transferred to 96 well plates. For determination of total β-hexosaminidase, unstimulated cells were lysed by the addition of PIPES-buffered solution/0.1% Triton X-100 for 10 min, and 100 µl aliquots (triplicate) were transferred to the 96 well plate. β-hexosaminidase activity was assessed by incubation with 100 µl of substrate solution [100 mM p-nitrophenyl-N-acetyl-β-D-glucosaminidine (p-NAG) in 0.1 M sodium acetate pH 4] for 1 h at 37°C. The reaction was stopped with 100 µl of 0.15 M $Na_2CO_3/NaHCO_3$, and the amount of produced p-nitrophenol was assessed by measuring absorbance at 410 nm on a spectrophotometer (Spectramax 340). Background values were obtained from lysates of unstimulated cells incubated without p-NAG. The amount of β-hexosamidinase released was calculated by using the formula: Release (R) [%] = $(A_{Stimulated} - A_{Unstimulated})/(A_{Total\ unstimulated} - A_{Total\ background})*100$

6.9 Cytosolic Ca^{2+} concentrations

BMMCs were washed with and resuspended in HEPES buffer [10 mM HEPES/NaOH pH 7.5, 137 mM NaCl, 2.7 mM KCl, 5 mM glucose, 1 mM $CaCl_2$, 1 mM $MgCl_2$, 0.1 % fatty acid free BSA]. Cells were loaded with 4 µM Fura-4F/AM for 10 min, washed twice, and resuspended in HEPES buffer containing different Ca^{2+} concentrations ($[Ca^{2+}]_{e\ (extracellular)}$ = 0 - 1 mM) in order to modulate maximal stimulated Ca^{2+} uptake ($[Ca^{2+}]_i$). Cells were stimulated in final volume of 3 ml (0.5 Mio/ml) in a continuously stirred cuvette at 37° in a fluorescence spectrometer (Perkin Elmer LS50B). The excitation wavelength was alternated between 340 and 380 nm and fluorescence emission was measured at 510 nm. Data points were recorded every 200 ms. Samples were run first for 1 min to record the baseline and were then treated with 0.5 µM Thapsigargin for 5 min. Ca^{2+} levels were then adjusted to 2 mM and maximal Fura fluorescence (F_{max}) was determined after cell permeabilisation with 0.1% Triton X-100. Minimal fluorescence (F_{min}) values were obtained after

addition of 4 mM EGTA. After subtraction of autofluorescence, $[Ca^{2+}]_i$ was calculated using the equation of Grynkiewicz et al, 1985 ($[Ca^{2+}]_i = K_d[(R - R_{min})/(R_{max} - R)](F_{380\ EGTA}/F_{380\ Triton})$, $R = F_{340}/F_{380}$). To correlate intracellular Ca^{2+} concentrations with PKB phosphorylation, $[Ca^{2+}]_i$ levels between 2 min and 2 min and 2 seconds were averaged and plotted against relative levels of phosphorylated PKB (S473). Phospho-PKB levels were obtained from cells (1.5 ml) taken out of the cuvette 2 min after stimulation. Lysed cells were analysed by Western blotting and PKB phosphorylation was quantified by intensity measurements with ImageJ software.

6.10 Cellular PdtIns(3,4,5)*P*$_3$ measurements

Cellular PtdIns(3,4,5)P_3 levels have been measured as described (Arcaro A and Wymann MP, Biochem J, 1993) with some modifications. BMMCs were cultured for 2 hours in phosphate-free RPMI medium/2% FCS at 37°C and 5% CO_2, followed by labelling with 1 mCi/ml [^{32}P]-orthophosphate for 4 h. Cells were washed, stimulated, and lysed by the addition of chloroform/methanol (1:2, v/v, with butylated hydroxytoluene and carrier phosphoinositides). Lipids were extracted, deacylated, and separated by high pressure liquid chromatography (HPLC).

6.11 Production of recombinant PI3Kγ

Recombinant human PI3Kγ was expressed as glutathione S-transferase (GST)-fusion protein (N-terminal) or was tagged C-terminal with six histidines. PI3Kγ protein was expressed in Sf9 cells by infection with recombinant baculoviruses. The recombinant baculovirus for the expression of GST-PI3Kγ (amino acids 38-1102) has been described (Stoyanov B, Science, 1995). Recombinant baculoviruses expressing wild type or mutant (S582A, S582E) PI3Kγ-His6 have been obtained by cotransfection of 2 μg of transfer plasmid and 0.25 μg of BaculoGold DNA (BD Biosciences) into Sf9 cells as described by the manufacturer.

For protein production, infected Sf9 cells were harvested 2-2.5 days postinfection, were washed twice wish PBS, und lysed in either GST- or His-lysis buffer [GST-buffer: 50 mM Tris/HCl, pH 7.5, 150 mM NaCl, 5 mM EDTA, 1 mM NaF, 1 mM DTT, 1% Triton-X100; His-buffer: 50 mM $NaH_2PO_4 \cdot 2H_2O$/NaOH, pH 8, 300 mM NaCl, 20 mM imidazol, 5% glycerol, 1% NP-40] containing protease inhibitors. GST-tagged PI3Kγ was purified on glutathione sepharose 4B (Amersham Biosciences) beads and eluted with 50 mM Tris/HCl, pH 7.5, 150 mM NaCl, 5 mM EDTA, 1 mM DTT, 5% glycerol, 20 mM glutathione after extensive washing. PI3Kγ-His6 was purified by using nickel-nitrilotriacetic acid (Ni-NTA) superflow agarose beads (Qiagen) and was eluted with 50 mM $NaH_2PO_4 \cdot 2H_2O$/NaOH, pH 8, 300 mM NaCl, 250 mM imidazol. Proteins were mixed 1:1 with storage buffer [80 mM HEPES/NaOH pH 7.4, 4 mM EDTA, 2 mM DTT, 20 mM benzamidine, ~90% ethylenglycol] and stored at -20°C, or alternatively, kept at 4°C in elution buffer/2 mM EDTA/1 mM DTT/10 mM benzamidine. Protein concentrations were quantified by Coomassie-stained SDS-PAGE gels with the Odyssey infrared imaging system and Odyssey v.2.1 software (LI-COR Biosciences) using bovine serum albumin (BSA) as standard. Purified proteins were diluted to equal concentrations and quantified once more.

6.12 In vitro kinase assay

Recombinant GST-PI3Kγ wild type (wt) or kinase inactive mutant (KR, Lys833 mutated to Arg) were incubated at an equal molar ratio with recombinant PKCβ2 (40 ng) (Invitrogen) in 1x kinase buffer (KB) [50 mM HEPES pH 7.4, 10 mM $MgCl_2$, 1 mM $CaCl_2$, 1 mM DTT, 0.03% Triton X-100] in the presence of 10 µM adenosine 5'-triphosphate (ATP) and 5 µCi of [γ^{32}P]-ATP [Perkin Elmer, 6000 Ci/mmol] per sample in a final volume of 40 µl. Kinase reactions were prewarmed for 2 min at 30°C, started by the addition of 4 µl of ATP-mix (in H_2O) in 20 second intervals, and incubated at 30°C for 30 min on an heat block with shaking (1200 min^{-1}). Reactions were terminated by the addition of 5x Laemmeli sample buffer and the proteins were resolved by SDS-PAGE. Gels were stained with Coomassie brilliant blue (Serva blue G) and dried onto a Whatmann paper. ^{32}P-incorporation was visualized by autoradiography. For quantification, gels were exposed to a storage phosphor screen (GP, Kodak), which was scanned with a phosphoimager (Typhoon 9400). Band intensities were quantified with ImageQuant TL Software (Amersham Biosciences). As standard, a dilution series of the ATP/[γ^{32}P]-ATP-mix was spotted onto the Whatmann paper.
Some of the samples were incubated in the presence phosphatidylserine (PS, Sigma) lipid vesicles (0.1 mg/ml) containing 1-oleoyl-2-acetyl-sn-glycerol (OAG, 0.01 mg/ml, Cayman Chemical). PS in $CHCl_3$/MeOH 2:1 was mixed with OAG in acetonitril in a Eppendorf tube, dried by a stream of nitrogen gas, and resuspended in 1x KB by sonication.

6.13 In vitro lipid kinase assay

Assays were performed in a final volume of 50 µl in 1.5 ml Eppendorf tubes in 1x lipid kinase buffer (LKB) [40 mM HEPES, pH 7.4, 150 mM NaCl, 4 mM $MgCl_2$, 1 mM DTT, 0.1 mg/ml fatty-acid free BSA] in the presence of PtdIns(4.5)P_2-containing lipid vesicles, 10 µM adenosine 5'-triphosphate (ATP), and 4 µCi of [γ^{32}P]-ATP [Perkin Elmer, 6000 Ci/mmol] per sample. Phospholipid composition of the lipid vesicles has been chosen to mimic relative mole ratios found in the inner leaflet of the plasma membrane (PE/PS/PC/SM/PIP_2 = 30/20/10/4.5/1.2-4.6). Lipids dissolved in $CHCl_3$/MeOH (2:1) were combined in a glass tube [f. c. in assay: 130 µM PE, 87 µM PS, 43 µM PC, 20 µM SM, 5-20 µM PIP_2], dried under a steam of nitrogen gas, and resuspended in 1x LKB without BSA by sonication (3x 15 seconds at an amplitude of 30%) on ice with a tip sonicator (U200S, IKA Labortechnik). Recombinant wild type or mutant PI3Kγ-His6 (200 ng/reaction) were diluted into 1x LKB and added (8 µl) to 4 µl of mastermix [1xLKB, but with 1.05 mg/ml BSA] followed by the addition of 30 µl of lipid mix. Samples were mixed and kept on ice for additional 20 min, were then warmed up to 30°C for 2 min on a heat block before starting the reaction by the addition of 8 µl of ATP-mix in 1x LKB without BSA. Samples were incubated for 10 min at 30°C with shaking (1200 min^{-1}) on a heat block. The reaction was stopped by the addition of 100 µl 1 N HCl and the lipids were extracted by the addition of 200 µl $CHCl_3$/MeOH 1:1 and vortexing. Phases were separated by centrifugation for 2 min at 9300 g, the lower organic phase was transferred to a new tube, and the lipids dried under a low heat vacuum in a Speed-Vac (Univapo 150H). Lipids were redissolved in $CHCl_3$/MeOH 4:1 and loaded onto a

potassium oxalate-pretreated silica gel 60 W F254S plate (Merck) for separation by thin layer chromatography (TLC) in a horizontal tank using $CHCl_3$/acetone/MeOH/acetic acid/H_2O (80/30/26/24/14 v/v) as mobile phase. Dried plates were exposed to Fuij Super RX X-ray films and phosphoimager screen and quantified by phosphoimager technology.

L-α-phosphatidylcholine from chicken egg (PC), sphingomyelin from porcine brain (SM), and L-α-phosphatidylinositol(4,5)bisphosphate from porcine brain, triammonium salt (PIP_2) were purchased from Avanti Polar Lipids, while L-α-phosphatidylserine (PS) from bovine brain and L-α-phosphatidylethanolamine from egg yolk, type III (PE) were obtained from Sigma-Aldrich.

6.14 Mass spectrometry

The PI3Kγ protein band was excised from the gel, reduced with 10 mM DTT, alkylated with 55 mM iodoacetamide, and cleaved with porcine trypsin (Promega, Madison, USA) in 50 mM ammonium bicarbonate (pH 8.0) at 37°C overnight (Shevchenko A, Anal Chem, 1996). The extracted peptides were analyzed by capillary liquid chromatography tandem mass spectrometry (LC-MSMS) using a Magic C18 100 μm x 10 cm HPLC column (SwissBioanalytics, Switzerland) connected on line to a 4000 Q Trap (MDS Sciex, Concord, Ontario, Canada) as described earlier (Vichalkovski A, Oncogene, 2010). Data analysis was done with Mascot (Perkins DN, Electrophoresis, 1999) searching the protein sequence database UNIPROT_15.6. from Feb 2010 (9421896 sequences; 1248797668 residues). Relative quantification of the peptides was done with multiple reaction monitoring (MRM) using the same instruments and identical chromatographic conditions. The approach was described earlier (Hess D, J Biol Chem, 2008).

6.15 Protein expression and purification for deuterium exchange studies

The PI3Kγ alone and PI3Kγ/p84 complex were expressed in Sf9 cells using the pFastBac system (Invitrogen). Cells were resuspended in sonication buffer (50 mM Tris/HCl pH 8, 100 mM NaCl, 1 mM PEFA, 25 mM imidazole) and lysed by sonication on ice for 10 minutes. The lysates were ultracentrifuged at 35'000 rpm for 45 minutes at 4 °C in a Ti45 rotor. The soluble cell lysate was filtered through a 0.45 μM filter. Subsequently, the lysate was passed over a Ni-NTA 5 ml Fast Flow column (GE Healthcare) and eluted with an imidazole concentration gradient from 25 to 200 mM. The protein was further purified by ion-exchange HiTrap Q (5ml), Heparin agarose (5ml), and Superdex 200 (16/60) gel-filtration chromatography. The protein was eluted from the gel filtration column in 20 mM Tris pH 7.5, 100 mM NaCl, 5 mM DTT, and 1 mM $(NH_4)_2SO_4$.

6.16 Deuterium exchange sample preparation

5 μl of stock protein solutions (Hs_PI3Kγ-His_6: 30 μM; Hs_PI3Kγ-His_6/Mm_p84-His_6: 35μM) were prepared in 20 mM Tris pH 7.5, 100 mM NaCl, 5 mM DTT, and 1 mM ammonium sulfate. Exchange reactions were initiated by addition of 25 μl of a 98% D_2O solution containing 10 mM HEPES pH 7.2, 50 mM NaCl, and 2 mM DTT, giving a final concentration of 82% D_2O. Deuterium exchange reactions were allowed to carry on for seven time periods, 3, 10, 30, 100, 300, 1000, and 3000 seconds at 23ºC. On-exchange was stopped by the addition of 40 μl of quench

buffer containing 1.2% formic acid and 0.833 M guanidine-HCl, which lowered the pH to 2.6. Samples were then immediately frozen in liquid nitrogen until mass analysis.

6.17 Protein digestion and peptide identification

Different digestion conditions were employed to optimize the peptide digestion map. These optimizations included changing denaturant concentration, flow rate over pepsin, and denaturation time. Peptide identification was performed by running tandem MS/MS experiments using a Sciex QStar Pulsar hybrid QqTOF (Applied Biosystems). Data was analyzed using Mascot software v. 2.2 (Matrix Science) to identify all peptides based on fragmentation and peptide mass, and these identifications were then manually validated using DXMS software (Sierra Analytics) to test for correct m/z state, and the presence of overlapping peptides.

6.18 Measurement of deuterium incorporation

Samples were thawed rapidly on ice and then injected onto an online HPLC system that was immersed in ice. The protein was run over an immobilized pepsin column (Applied Biosystems, Poroszyme®, 2-3131-00) at 50 µl/min, and collected over a 1.7 µm particle C18 peptide trap (2.1 mm x 8 mm, Waters Van-guard) for five minutes. The trap was then switched in line with a 1.7 µm particle, 1 mm x100 mm C18 column (Waters Acquity UPLC) with a vanguard pre-column and peptides were eluted by a 5-45% gradient of buffer A (0.1% formic acid) and buffer B (80% acetonitrile, 20% H_2O, 0.02% formic acid) over 22 minutes and injected onto a Sciex QStar Pulsar hybrid QqTOF (Applied Biosystems) which collected mass spectra from a range of 350 to 1300 m/z.

Mass analysis of the peptide centroids was performed as described previously using the software DXMS (Sierra Analytics) (Burke JE, Biochemistry, 2008; Burke JE, Structure, 2011). Briefly, all selected peptides passed the quality control threshold of the software, and were then manually examined for accurate identification and deuterium incorporation. Results are shown as relative levels of deuteration with no correction for back exchange as described previously (Iacob RE, Proc Natl Acad Sci U S A, 2009). The real level of deuteration will be ~25-35% higher than what is shown, based on tests performed with fully deuterated standard peptides. All experiments were repeated in duplicate, and we found that the average error was less than 0.2 Da. For this reason we consider all changes greater than 0.5 Da that occur at more than one time point as significant. The resulting deuterium incorporation was graphed versus the on-exchange time. All deuterium exchange data for all peptides analyzed (202 peptides) is shown in tabular form (Table S1).

7. Plasmid list

7.1 Plasmids engineered during this study

Number	Plasmid Name	Insert
971	pcDNA3<kzNHA>#971	HA-Tag
972	pcDNA3<CHA>#972	HA-Tag
973	pcDNA3<kzNGST>#973	GST
974	pcDNA3<CGST>#974	GST
975	pcDNA3<CYFP>#975	EYFP
976	pcDNA3<CHA><kzPKCβ2 REG>#976	PRKCB, PKCb, REG
977	pcDNA3<kzNHA><PKCβ2 CAT>#977	PRKCB, PKCb, CAT
978	pcDNA3<kzNHA><PKCβ2 WT>#978	PRKCB, PKCb, AA1-673
979	pcDNA3<CGST><kzPKCβ2 REG>#979	PRKCB, PKCb, REG, AA1-301
980	pcDNA3<kzNGST><PKCβ2 CAT>#980	PRKCB, PKCb, CAT, AA302-673
981	pcDNA3<kzNGST><PKCβ2 WT>#981	PRKCB, PKCb, AA1-673
982	pcDNA3<CYFP><kzPKCβ2 REG>#982	PRKCB, PKCb, REG, AA1-301
983	pEYFP-C1<PKCβ2 CAT>#983	PRKCB, PKCb, CAT, AA302-673
990	pcDNA3-tkGST<PKCβ2 CAT>#990	PRKCB, PKCb, AA302-673
991	pcDNA3-tkGST<PKCβ2 WT>#991	PRKCB, PKCb, AA1-673
992	pcDNA3<kzNHA><PKCβ2 CAT-KR>#992	PRKCB, PKCb, CAT, AA302-673
994	pcDNA3<kzNHA><hsPI3Ka>#994	PI3K alpha, PI3Ka, p110a, HA
995	pcDNA3<hsPI3Ka>#995	PI3K alpha, PI3Ka, p110a
996	pVL1393<hsPI3Ka>#996	PI3K alpha, PI3Ka, p110a
997	pcDNA3<kzNHA><Mm_PKCb1 WT>#997	PRKCB1, PKCb1, PKCb
998	pcDNA3<kzNHA><PKCβ2 ΔPS>#998	PRKCB, PKCb, DPS (ΔAA19-31)
1036	pcDNA3<kzNHA><PKCβ2 ΔPS-KR>#1036	PRKCB, PKCb, DPS
1037	pEYFP-C1<PKCβ2 ΔPS>#1037	PRKCB, PKCb, DPS
1038	pEYFP-C1<PKCβ2 ΔPS-KR>#1038	PRKCB, PKCb, DPS
1042	pEYFP-C1<PKCb2 CAT-KR>#1042	PRKCB, PKCb, CAT
1043	pVL1393<Mm_p87-(His)6>#1043	p87 PIKAP, His6
1053	pVL1393<kzNHA><PKCb2 WT>#1053	PRKCB, PKCb
1054	pVL1393<kzNHA-PKCb2 DPS>#1054	PRKCB, PKCb, DPS (unstable expr.)
1055	pVL1393<kzNHA-PKCb2 CAT>#1055	PRKCB, PKCb, CAT
1066	pVL1393<Hs_PI3Kg WT>#1066	PI3Kg, p110g
1067	pVL1393<Hs-PI3Kg KR>#1067	PI3Kg, p110g
1068	pcDNA3<Hs_PI3Kg WT>#1068	PI3Kg, p110g
1069	pVL1393<Hs_p87>#1069	p87 PIKAP
1117	pCR4Blunt-TOPO<Hs_p101>#1117	p101
1124	pcDNA3.1zeo<kzVenus[1]-Mm_PKCβ2 WT-CHA>#1124	PRKCB, PKCb
1125	pcDNA3.1zeo<kzNHA-MmPKCβ2 WT-Venus[1]>#1125	PRKCB, PKCb
1126	pcDNA3.1zeo<kzVenus[1]-Mm_PKCβ2 ΔPS-CHA>#1126	PRKCB, PKCb, DPS
1127	pcDNA3.1zeo<kzNHA-MmPKCβ2 ΔPS -Venus[1]>#1127	PRKCB, PKCb, DPS
1128	pcDNA3<kzVenus[2]-Hs_PI3Kg-CHA>#1128	PI3Kg, p110g
1129	pcDNA3<kzNHA-Hs_PI3Kg-Venus[2]#1129	PI3Kg, p110g
1131	pEGFP-C1<Mm_PKCβ2 WT>#1131	PRKCB, PKCb

1132	pEGFP-C1<Mm_PKCβ2 ΔPS>#1132	PRKCB, PKCb, DPS
1133	pEGFP-C1_with NotI&XbaI	EGFP
1134	pEGFP-C1<Hs_p101>#1134	p101
1135	pEGFP-C1<Hs_p87>#1135	p87 PIKAP
1158	pVL1393<Hs_PI3Kg KR-GST>#1158	PI3Kg, p110g, GST
1159	pVL1393<Hs_PI3Kg KR S257A-GST>#1159	PI3Kg, p110g, GST
1164	pcDNA3<Hs_PI3Kg-EGFP>#1164	PI3Kg, p110g
1165	pcDNA3<Hs_PI3Kg S257A-EGFP>#1165	PI3Kg, p110g
1166	pcDNA3<Hs_PI3Kg S257E-EGFP>#1166	PI3Kg, p110g
1167	pcDNA3<Hs_PI3Kg S257D-EGFP>#1167	PI3Kg, p110g
1168	pVL1393<Hs_PI3Kg S257A-GST>#1168	PI3Kg, p110g
1202	pVL1932<His-Mm_PKCb2 CAT>#1202	PRKCB, PKCb, CAT
1203	pVL1392<His-Mm_PKCb2 WT>#1203	PRKCB, PKCb
1204	pVL1932<His-Mm_PKCb2 CAT KR>#1204	PRKCB, PKCb, CAT
1205	pVL1392<His-Mm_PKCb2 KR>#1205	PRKCB, PKCb
1216	pVL1393<Hs_PI3Kg WT-His>#1216	PI3Kg, p110g, His6
1217	pVL1393<Hs_PI3Kg KR-His>#1217	PI3Kg, p110g
1218	pVL1393<Hs_PI3Kg S257A WT-His>#1218	PI3Kg, p110g
1219	pVL1393<Hs_PI3Kg S257A KR-His>#1219	PI3Kg, p110g
1220	pVL1393<Hs_PI3Kg S257E WT-His>#1220	PI3Kg, p110g
1221	pVL1393<Hs_PI3Kg S257D WT-His>#1221	PI3Kg, p110g
1222	pVL1393<Hs_PI3Kg S582A WT-His>#1222	PI3Kg, p110g
1223	pVL1393<Hs_PI3Kg S582A KR-His>#1223	PI3Kg, p110g
1224	pVL1393<Hs_PI3Kg S582E WT-His>#1224	PI3Kg, p110g
1225	pVL1393<Hs_PI3Kg S257A S582A WT-His>#1225	PI3Kg, p110g
1226	pVL1393<Hs_PI3Kg S257A S582A KR-His>#1226	PI3Kg, p110g
1227	pVL1393<Hs_PI3Kg S257E S582E WT-His>#1227	PI3Kg, p110g
1233	pLenti CMV MCSmod#1233	-
1234	pcDNA3<Hs_PI3Kg WT 3'UTR>#1234	PI3Kg, p110g
1235	pcDNA3<Hs_PI3Kg S257A WT 3'UTR>#1235	PI3Kg, p110g
1236	pcDNA3<Hs_PI3Kg S257E WT 3'UTR>#1236	PI3Kg, p110g
1237	pcDNA3<Hs_PI3Kg S257D WT 3'UTR>#1237	PI3Kg, p110g
1238	pcDNA3<Hs_PI3Kg S582A WT 3'UTR>#1238	PI3Kg, p110g
1239	pcDNA3<Hs_PI3Kg S582E WT 3'UTR>#1239	PI3Kg, p110g
1240	pcDNA3<Hs_PI3Kg S257A S582A WT 3'UTR>#1240	PI3Kg, p110g
1241	pcDNA3<Hs_PI3Kg S257E S582E WT 3'UTR>#1241	PI3Kg, p110g
1242	pEGFP-C1<Hs_PI3Kg S257A WT>#1242	PI3Kg, p110g
1243	pEGFP-C1<Hs_PI3Kg S257E WT>#1243	PI3Kg, p110g
1244	pEGFP-C1<Hs_PI3Kg S257D WT>#1244	PI3Kg, p110g
1245	pEGFP-C1<Hs_PI3Kg S582A WT>#1245	PI3Kg, p110g
1246	pEGFP-C1<Hs_PI3Kg S582E WT>#1246	PI3Kg, p110g
1247	pEGFP-C1<Hs_PI3Kg S257A S582A WT>#1247	PI3Kg, p110g
1248	pEGFP-C1<Hs_PI3Kg S257E S582E WT>#1248	PI3Kg, p110g
1249	pLenti CMV<Hs_PI3Kg WT>#1249	PI3Kg, p110g
1250	pLenti CMV<Hs_PI3Kg S257A WT>#1250	PI3Kg, p110g
1251	pLenti CMV<Hs_PI3Kg S257E WT>#1251	PI3Kg, p110g

1252	pLenti CMV<Hs_PI3Kg S257D WT>#1252	PI3Kg, p110g
1253	pLenti CMV<Hs_PI3Kg S582A WT>#1253	PI3Kg, p110g
1254	pLenti CMV<Hs_PI3Kg S582E WT>#1254	PI3Kg, p110g
1255	pLenti CMV<Mm_PKCb2 WT>#1255	PRKCB, PKCb
1256	pLenti CMV<Mm_PKCb1 WT>#1256	PRKCB1, PKCb1
1278	pcDNA3<Hs_PI3Kg S582D WT 3'UTR>#1278	PI3Kg, p110g
1279	pEGFP-C1<Hs_PI3Kg S582D WT>#1279	PI3Kg, p110g
1280	pLenti CMV<Hs_PI3Kg S582D WT>#1280	PI3Kg, p110g
1281	pVL1393<Hs_PI3Kg S582D WT>#1281	PI3Kg, p110g
1282	pLenti CMV EGFP#1282	EGFP
1338	pSYFP1-C1#1338	SYFP1
1339	pTurquoise-C1#1339	mTurquoise
1350	pSYFP1-C1<Mm_PKCb2 WT>	PRKCB, PKCb
1351	pSYFP1-C1<Mm_PKCb2 KR>#1351	PRKCB, PKCb
1352	pSYFP1-C1<Mm_PKCb2 DPS>#1352	PRKCB, PKCb, DPS
1353	pSYFP1-C1<Mm_PKCb2 DPS-KR>#1353	PRKCB, PKCb, DPS
1354	pSYFP1-C1<Mm_PKCb2 CAT>#1354	PRKCB, PKCb, CAT
1355	pTurquoise<Mm_PKCb2 WT>#1355	PRKCB, PKCb
1356	pTurquoise<Mm_PKCb2 DPS>#1356	PRKCB, PKCb, DPS
1357	pTurquoise<Mm_PKCb2 CAT>#1357	PRKCB, PKCb, CAT
1358	pLenti CMV SYFP1#1358	SYFP1
1359	pLenti CMV mTurquoise#1359	mTurquoise
1360	pSYFP1-C1<Mm_PKCb2 S660A>#1360	PRKCB, PKCb
1361	pcDNA3<kNHA><Mm_PKCb2 T500E>#1361	PRKCB, PKCb
1362	pcDNA3<kNHA><Mm_PKCb2 DPS T500E>#1362	PRKCB, PKCb, DPS
1363	pcDNA3<kNHA><Mm_PKCb2 CAT T500E>#1363	PRKCB, PKCb, CAT
1371	pLenti CMV SYFP1<Hs_PI3Kg>#1371	PI3Kg, p110g
1372	pLenti CMV mTurquoise<Hs_PI3Kg>#1372	PI3Kg, p110g
1376	pcDNA3-tkGST<Hs_PI3Kg wt>#1376	PI3Kg, p110g
1377	pcDNA3-tkGST<Hs_D130-PI3Kg>#1377	PI3Kg, p110g
1378	pcDNA3<Hs_D130-PI3Kg>#1378	PI3Kg, p110g

7.2 Other plasmids entered into the database

Number	Name	Gene
942	GST-pmt2<PKCβ2-CAT>#942	PRKCB, PKCb, CAT
943	GST-pmt2<PKCβ2-REG>#943	PRKCB, PKCb, REG
1039	pIRES2-EGFP#1039	-
1040	pIRES2-EGFP<rRack1>#1040	rack1, rack, Gnb
1041	pRevTRE<rRack1>#1041	rack1, rack, Gnb
1044	pVL1392#1044	-
1045	pVL1393#1045	-
1200	pVL1393<Hs_D143-PI3Kg-His>#1200	PI3Kg, p110g, His6
1228	pLenti CMV MCS	-
1229	pLenti EF DsRed	DsRed
1230	pMDL g-p RRE	

1231	lenti REV vector	
1232	lenti VSV-G vector	
1334	pSYFP1-C1<Hs_PI3Kg>#1334	PI3Kg, p110g
1335	pTurquoise-C1<Hs_PI3Kg>#1335	PI3Kg, p110g
1336	pSYFP1-C1<Hs_PKCb2>#1336	PRKCB, PKCb
1337	pTurquoise-C1<Hs_PKCb2>#1337	PRKCB, PKCb

8. References

Agosti V, Corbacioglu S, Ehlers I, Waskow C, Sommer G, Berrozpe G, Kissel H, Tucker CM, Manova K, Moore MA, Rodewald HR and Besmer P (2004). Critical role for Kit-mediated Src kinase but not PI 3-kinase signaling in pro T and pro B cell development. J Exp Med *199(6)*, 867-878.

Ali K, Bilancio A, Thomas M, Pearce W, Gilfillan AM, Tkaczyk C, Kuehn N, Gray A, Giddings J, Peskett E, Fox R, Bruce I, Walker C, Sawyer C, Okkenhaug K, Finan P and Vanhaesebroeck B (2004). Essential role for the p110delta phosphoinositide 3-kinase in the allergic response. Nature *431(7011)*, 1007-1011.

Ali K, Camps M, Pearce WP, Ji H, Ruckle T, Kuehn N, Pasquali C, Chabert C, Rommel C and Vanhaesebroeck B (2008). Isoform-specific functions of phosphoinositide 3-kinases: p110 delta but not p110 gamma promotes optimal allergic responses in vivo. J Immunol *180(4)*, 2538-2544.

Almers W and Neher E (1985). The Ca signal from fura-2 loaded mast cells depends strongly on the method of dye-loading. FEBS Lett *192(1)*, 13-18.

Ancrile B, Lim KH and Counter CM (2007). Oncogenic Ras-induced secretion of IL6 is required for tumorigenesis. Genes Dev *21(14)*, 1714-1719.

Aoki M, Schetter C, Himly M, Batista O, Chang HW and Vogt PK (2000). The catalytic subunit of phosphoinositide 3-kinase: requirements for oncogenicity. J Biol Chem *275(9)*, 6267-6275.

Apgar JR (1994). Polymerization of actin in RBL-2H3 cells can be triggered through either the IgE receptor or the adenosine receptor but different signaling pathways are used. Mol Biol Cell *5(3)*, 313-322.

Arcaro A and Wymann MP (1993). Wortmannin is a potent phosphatidylinositol 3-kinase inhibitor: the role of phosphatidylinositol 3,4,5-trisphosphate in neutrophil responses. Biochem J *296 (Pt 2)*, 297-301.

Baba Y, Nishida K, Fujii Y, Hirano T, Hikida M and Kurosaki T (2008). Essential function for the calcium sensor STIM1 in mast cell activation and anaphylactic responses. Nat Immunol *9(1)*, 81-88.

Backer JM (2008). The regulation and function of Class III PI3Ks: novel roles for Vps34. Biochem J *410(1)*, 1-17.

Baram D, Mekori YA and Sagi-Eisenberg R (2001). Synaptotagmin regulates mast cell functions. Immunol Rev *179*, 25-34.

Barbu EA, Zhang J and Siraganian RP (2010). The limited contribution of Fyn and Gab2 to the high affinity IgE receptor signaling in mast cells. J Biol Chem *285(21)*, 15761-15768.

Barragan M, de Frias M, Iglesias-Serret D, Campas C, Castano E, Santidrian AF, Coll-Mulet L, Cosialls AM, Domingo A, Pons G and Gil J (2006). Regulation of Akt/PKB by phosphatidylinositol 3-kinase-dependent and -independent pathways in B-cell chronic lymphocytic leukemia cells: role of protein kinase C{beta}. J Leukoc Biol *80(6)*, 1473-1479.

Beaven MA, Rogers J, Moore JP, Hesketh TR, Smith GA and Metcalfe JC (1984). The mechanism of the calcium signal and correlation with histamine release in 2H3 cells. J Biol Chem *259(11)*, 7129-7136.

Berndt A, Miller S, Williams O, Le DD, Houseman BT, Pacold JI, Gorrec F, Hon WC, Liu Y, Rommel C, Gaillard P, Ruckle T, Schwarz MK, Shokat KM, Shaw JP and Williams RL (2010). The p110delta structure: mechanisms for selectivity and potency of new PI(3)K inhibitors. Nat Chem Biol *6(2)*, 117-124.

Bohnacker T, Marone R, Collmann E, Calvez R, Hirsch E and Wymann MP (2009). PI3Kgamma adaptor subunits define coupling to degranulation and cell motility by distinct PtdIns(3,4,5)P3 pools in mast cells. Sci Signal *2(74)*, ra27.

Bondeva T, Pirola L, Bulgarelli-Leva G, Rubio I, Wetzker R and Wymann MP (1998). Bifurcation of lipid and protein kinase signals of PI3Kgamma to the protein kinases PKB and MAPK. Science *282(5387)*, 293-296.

Bresnick AR (1999). Molecular mechanisms of nonmuscle myosin-II regulation. Curr Opin Cell Biol *11(1)*, 26-33.

Brock C, Schaefer M, Reusch HP, Czupalla C, Michalke M, Spicher K, Schultz G and Nurnberg B (2003). Roles of G beta gamma in membrane recruitment and activation of p110 gamma/p101 phosphoinositide 3-kinase gamma. J Cell Biol *160(1)*, 89-99.

Brose N and Rosenmund C (2002). Move over protein kinase C, you've got company: alternative cellular effectors of diacylglycerol and phorbol esters. J Cell Sci *115(Pt 23)*, 4399-4411.

Burke JE, Karbarz MJ, Deems RA, Li S, Woods VL Jr and Dennis EA (2008). Interaction of group IA phospholipase A2 with metal ions and phospholipid vesicles probed with deuterium exchange mass spectrometry. Biochemistry *47(24)*, 6451-6459.

Burke JE, Vadas O, Berndt A, Finegan T, Perisic O and Williams RL (2011). Dynamics of the phosphoinositide 3-kinase p110δ interaction with p85α and membranes reveals aspects of regulation distinct from p110α. Structure *19(8)*, 1127-1137.

Calvez R. Roles of phosphoinositide 3-kinase γ catalytic and regulatory subunits in inflammation. University of Fribourg, Switzerland: 2004. p. Dissertation.

Carpenter CL, Auger KR, Chanudhuri M, Yoakim M, Schaffhausen B, Shoelson S and Cantley LC (1993). Phosphoinositide 3-kinase is activated by phosphopeptides that bind to the SH2 domains of the 85-kDa subunit. J Biol Chem *268(13)*, 9478-9483.

Carpenter CL, Auger KR, Duckworth BC, Hou WM, Schaffhausen B and Cantley LC (1993). A tightly associated serine/threonine protein kinase regulates phosphoinositide 3-kinase activity. Mol Cell Biol *13(3)*, 1657-1665.

Carson JD, Van Aller G, Lehr R, Sinnamon RH, Kirkpatrick RB, Auger KR, Dhanak D, Copeland RA, Gontarek RR, Tummino PJ and Luo L (2008). Effects of oncogenic p110alpha subunit mutations on the lipid kinase activity of phosphoinositide 3-kinase. Biochem J *409(2)*, 519-524.

Chan TO, Rodeck U, Chan AM, Kimmelman AC, Rittenhouse SE, Panayotou G and Tsichlis PN (2002). Small GTPases and tyrosine kinases coregulate a molecular switch in the phosphoinositide 3-kinase regulatory subunit. Cancer Cell *1(2)*, 181-191.

Cissel DS, Fraundorfer PF and Beaven MA (1998). Thapsigargin-induced secretion is dependent on activation of a cholera toxin-sensitive and phosphatidylinositol-3-kinase-regulated phospholipase D in a mast cell line. J Pharmacol Exp Ther *285(1)*, 110-118.

Clayton E, Bardi G, Bell SE, Chantry D, Downes CP, Gray A, Humphries LA, Rawlings D, Reynolds H, Vigorito E and Turner M (2002). A crucial role for the p110delta subunit of phosphatidylinositol 3-kinase in B cell development and activation. J Exp Med *196(6)*, 753-763.

Costa C, Barberis L, Ambrogio C, Manazza AD, Patrucco E, Azzolino O, Neilsen PO, Ciraolo E, Altruda F, Prestwich GD, Chiarle R, Wymann M, Ridley A and Hirsch E (2007). Negative feedback regulation of Rac in leukocytes from mice expressing a constitutively active phosphatidylinositol 3-kinase gamma. Proc Natl Acad Sci U S A *104(36)*, 14354-14359.

Costello PS, Turner M, Walters AE, Cunningham CN, Bauer PH, Downward J and Tybulewicz VL (1996). Critical role for the tyrosine kinase Syk in signalling through the high affinity IgE receptor of mast cells. Oncogene *13(12)*, 2595-2605.

Crespo P, Schuebel KE, Ostrom AA, Gutkind JS and Bustelo XR (1997). Phosphotyrosine-dependent activation of Rac-1 GDP/GTP exchange by the vav proto-oncogene product. Nature *385(6612)*, 169-172.

Cuevas BD, Lu Y, Mao M, Zhang J, LaPushin R, Siminovitch K and Mills GB (2001). Tyrosine phosphorylation of p85 relieves its inhibitory activity on phosphatidylinositol 3-kinase. J Biol Chem *276(29)*, 27455-27461.

Czupalla C, Nurnberg B and Krause E (2003). Analysis of class I phosphoinositide 3-kinase autophosphorylation sites by mass spectrometry. Rapid Commun Mass Spectrom *17(7)*, 690-696.

Davies SP, Reddy H, Caivano M and Cohen P (2000). Specificity and mechanism of action of some commonly used protein kinase inhibitors. Biochem J *351(Pt 1)*, 95-105.

Del Prete A, Vermi W, Dander E, Otero K, Barberis L, Luini W, Bernasconi S, Sironi M, Santoro A, Garlanda C, Facchetti F, Wymann MP, Vecchi A, Hirsch E, Mantovani A and Sozzani S (2004). Defective dendritic cell migration and activation of adaptive immunity in PI3Kgamma-deficient mice. EMBO J *23(17)*, 3505-3515.

Deng Z, Zink T, Chen HY, Walters D, Liu FT and Liu GY (2009). Impact of actin rearrangement and degranulation on the membrane structure of primary mast cells: a combined atomic force and laser scanning confocal microscopy investigation. Biophys J *96(4)*, 1629-1639.

Dhand R, Hiles I, Panayotou G, Roche S, Fry MJ, Gout I, Totty NF, Truong O, Vicendo P, Yonezawa K and et a (1994). PI 3-kinase is a dual specificity enzyme: autoregulation by an intrinsic protein-serine kinase activity. EMBO J *13(3)*, 522-533.

Di Virgilio F, Steinberg TH and Silverstein SC (1990). Inhibition of Fura-2 sequestration and secretion with organic anion transport blockers. Cell Calcium *11(2-3)*, 57-62.

Dombrosky-Ferlan PM and Corey SJ (1997). Yeast two-hybrid in vivo association of the Src kinase Lyn with the proto-oncogene product Cbl but not with the p85 subunit of PI 3-kinase. Oncogene *14(17)*, 2019-2024.

Domin J, Dhand R and Waterfield MD (1996). Binding to the platelet-derived growth factor receptor transiently activates the p85alpha-p110alpha phosphoinositide 3-kinase complex in vivo. J Biol Chem *271(35)*, 21614-21621.

Elstak ED, Neeft M, Nehme NT, Voortman J, Cheung M, Goodarzifard M, Gerritsen HC, van Bergen En Henegouwen PM, Callebaut I, de Saint Basile G and van der Sluijs P (2011). The munc13-4-rab27 complex is specifically required for tethering secretory lysosomes at the plasma membrane. Blood *118(6)*, 1570-1578.

Endo D, Gon Y, Nunomura S, Yamashita K, Hashimoto S and Ra C (2009). PI3Kgamma differentially regulates FcepsilonRI-mediated degranulation and migration of mast cells by and toward antigen. Int Arch Allergy Immunol *149 Suppl 1*, 66-72.

Engen JR (2009). Analysis of protein conformation and dynamics by hydrogen/deuterium exchange MS. Anal Chem *81(19)*, 7870-7875.

Falasca M and Maffucci T (2007). Role of class II phosphoinositide 3-kinase in cell signalling. Biochem Soc Trans *35(Pt 2)*, 211-214.

Fehrenbach K, Lessmann E, Zorn CN, Kuhny M, Grochowy G, Krystal G, Leitges M and Huber M (2009). Steel factor enhances supraoptimal antigen-induced IL-6 production from mast cells via activation of protein kinase C-beta. J Immunol *182(12)*, 7897-7905.

Forsythe P and Ennis M (1999). Adenosine, mast cells and asthma. Inflamm Res *48(6)*, 301-307.

Foster LJ, Yeung B, Mohtashami M, Ross K, Trimble WS and Klip A (1998). Binary interactions of the SNARE proteins syntaxin-4, SNAP23, and VAMP-2 and their regulation by phosphorylation. Biochemistry *37(31)*, 11089-11096.

Foukas LC, Berenjeno IM, Gray A, Khwaja A and Vanhaesebroeck B (2010). Activity of any class IA PI3K isoform can sustain cell proliferation and survival. Proc Natl Acad Sci U S A *107(25)*, 11381-11386.

Fujimoto M, Oka T, Murata T, Hori M and Ozaki H (2009). Fluvastatin inhibits mast cell degranulation without changing the cytoplasmic Ca2+ level. Eur J Pharmacol *602(2-3)*, 432-438.

Fukao T, Yamada T, Tanabe M, Terauchi Y, Ota T, Takayama T, Asano T, Takeuchi T, Kadowaki T, Hata Ji J and Koyasu S (2002). Selective loss of gastrointestinal mast cells and impaired immunity in PI3K-deficient mice. Nat Immunol *3(3)*, 295-304.

Gaidarov I, Smith ME, Domin J and Keen JH (2001). The class II phosphoinositide 3-kinase C2alpha is activated by clathrin and regulates clathrin-mediated membrane trafficking. Mol Cell *7(2)*, 443-449.

Galli SJ, Tsai M and Wershil BK (1993). The c-kit receptor, stem cell factor, and mast cells. What each is teaching us about the others. Am J Pathol *142(4)*, 965-974.

Gao Z, Li BS, Day YJ and Linden J (2001). A3 adenosine receptor activation triggers phosphorylation of protein kinase B and protects rat basophilic leukemia 2H3 mast cells from apoptosis. Mol Pharmacol *59(1)*, 76-82.

Gimborn K, Lessmann E, Kuppig S, Krystal G and Huber M (2005). SHIP down-regulates FcepsilonR1-induced degranulation at supraoptimal IgE or antigen levels. J Immunol *174(1)*, 507-516.

Gonzalez-Espinosa C, Odom S, Olivera A, Hobson JP, Martinez ME, Oliveira-Dos-Santos A, Barra L, Spiegel S, Penninger JM and Rivera J (2003). Preferential signaling and induction of allergy-promoting lymphokines upon weak stimulation of the high affinity IgE receptor on mast cells. J Exp Med *197(11)*, 1453-1465.

Gould HJ and Sutton BJ (2008). IgE in allergy and asthma today. Nat Rev Immunol *8(3)*, 205-217.

Graham TE, Pfeiffer JR, Lee RJ, Kusewitt DF, Martinez AM, Foutz T, Wilson BS and Oliver JM (1998). MEK and ERK activation in ras-disabled RBL-2H3 mast cells and novel roles for geranylgeranylated and farnesylated proteins in Fc epsilonRI-mediated signaling. J Immunol *161(12)*, 6733-6744.

Gschwendt M, Muller HJ, Kielbassa K, Zang R, Kittstein W, Rincke G and Marks F (1994). Rottlerin, a novel protein kinase inhibitor. Biochem Biophys Res Commun *199(1)*, 93-98.

Gu H, Pratt JC, Burakoff SJ and Neel BG (1998). Cloning of p97/Gab2, the major SHP2-binding protein in hematopoietic cells, reveals a novel pathway for cytokine-induced gene activation. Mol Cell *2(6)*, 729-740.

Gu H, Saito K, Klaman LD, Shen J, Fleming T, Wang Y, Pratt JC, Lin G, Lim B, Kinet JP and Neel BG (2001). Essential role for Gab2 in the allergic response. Nature *412(6843)*, 186-190.

Gupta S, Ramjaun AR, Haiko P, Wang Y, Warne PH, Nicke B, Nye E, Stamp G, Alitalo K and Downward J (2007). Binding of ras to phosphoinositide 3-kinase p110alpha is required for ras-driven tumorigenesis in mice. Cell *129(5)*, 957-968.

Gurish MF and Boyce JA (2006). Mast cells: ontogeny, homing, and recruitment of a unique innate effector cell. J Allergy Clin Immunol *117(6)*, 1285-1291.

Gymnopoulos M, Elsliger MA and Vogt PK (2007). Rare cancer-specific mutations in PIK3CA show gain of function. Proc Natl Acad Sci U S A *104(13)*, 5569-5574.

Hajkova Z, Bugajev V, Draberova E, Vinopal S, Draberova L, Janacek J, Draber P and Draber P (2011). STIM1-directed reorganization of microtubules in activated mast cells. J Immunol *186(2)*, 913-923.

Hale BG, Kerry PS, Jackson D, Precious BL, Gray A, Killip MJ, Randall RE and Russell RJ (2010). Structural insights into phosphoinositide 3-kinase activation by the influenza A virus NS1 protein. Proc Natl Acad Sci U S A *107(5)*, 1954-1959.

Harrison-Findik D, Susa M and Varticovski L (1995). Association of phosphatidylinositol 3-kinase with SHC in chronic myelogeneous leukemia cells. Oncogene *10(7)*, 1385-1391.

Hepp R, Puri N, Hohenstein AC, Crawford GL, Whiteheart SW and Roche PA (2005). Phosphorylation of SNAP-23 regulates exocytosis from mast cells. J Biol Chem *280(8)*, 6610-6620.

Hernandez-Hansen V, Smith AJ, Surviladze Z, Chigaev A, Mazel T, Kalesnikoff J, Lowell CA, Krystal G, Sklar LA, Wilson BS and Oliver JM (2004). Dysregulated FcepsilonRI signaling and altered Fyn and SHIP activities in Lyn-deficient mast cells. J Immunol *173(1)*, 100-112.

Hess D, Keusch JJ, Oberstein SA, Hennekam RC and Hofsteenge J (2008). Peters Plus syndrome is a new congenital disorder of glycosylation and involves defective Omicron-glycosylation of thrombospondin type 1 repeats. J Biol Chem *283(12)*, 7354-7360.

Hirsch E, Katanaev VL, Garlanda C, Azzolino O, Pirola L, Silengo L, Sozzani S, Mantovani A, Altruda F and Wymann MP (2000). Central role for G protein-coupled phosphoinositide 3-kinase gamma in inflammation. Science *287(5455)*, 1049-1053.

Ho SN, Hunt HD, Horton RM, Pullen JK and Pease LR (1989). Site-directed mutagenesis by overlap extension using the polymerase chain reaction. Gene *77(1)*, 51-59.

Holt KH, Olson L, Moye-Rowley WS and Pessin JE (1994). Phosphatidylinositol 3-kinase activation is mediated by high-affinity interactions between distinct domains within the p110 and p85 subunits. Mol Cell Biol *14(1)*, 42-49.

Hon WC, Berndt A and Williams RL (2012). Regulation of lipid binding underlies the activation of class IA PI3-kinases. Oncogene *31(32)*, 3655-3666.

Hsieh, S. N. Identification of PI3Kγ in Endothelial Cells and its Involvement in Sphingosine 1-Phosphate Mediated Endothelial Cell Migration. Friedrich Schiller University, Jena, Germany: 2003. p. Dissertation.

Huang CH, Mandelker D, Schmidt-Kittler O, Samuels Y, Velculescu VE, Kinzler KW, Vogelstein B, Gabelli SB and Amzel LM (2007). The structure of a human p110alpha/p85alpha complex elucidates the effects of oncogenic PI3Kalpha mutations. Science *318(5857)*, 1744-1748.

Huber M, Helgason CD, Damen JE, Liu L, Humphries RK and Krystal G (1998). The src homology 2-containing inositol phosphatase (SHIP) is the gatekeeper of mast cell degranulation. Proc Natl Acad Sci U S A *95(19)*, 11330-11335.

Hunter S, Koch BL and Anderson SM (1997). Phosphorylation of cbl after stimulation of Nb2 cells with prolactin and its association with phosphatidylinositol 3-kinase. Mol Endocrinol *11(9)*, 1213-1222.

Iacob RE, Pene-Dumitrescu T, Zhang J, Gray NS, Smithgall TE, Engen JR (2009). Conformational disturbance in Abl kinase upon mutation and deregulation. Proc Natl Acad Sci U S A *106(5)*, 1386-1391.

Ikenoue T, Kanai F, Hikiba Y, Obata T, Tanaka Y, Imamura J, Ohta M, Jazag A, Guleng B, Tateishi K, Asaoka Y, Matsumura M, Kawabe T and Omata M (2005). Functional analysis of PIK3CA gene mutations in human colorectal cancer. Cancer Res *65(11)*, 4562-4567.

Isakoff SJ, Engelman JA, Irie HY, Luo J, Brachmann SM, Pearline RV, Cantley LC and Brugge JS (2005). Breast cancer-associated PIK3CA mutations are oncogenic in mammary epithelial cells. Cancer Res *65(23)*, 10992-11000.

Iwaki S, Tkaczyk C, Satterthwaite AB, Halcomb K, Beaven MA, Metcalfe DD and Gilfillan AM (2005). Btk plays a crucial role in the amplification of Fc epsilonRI-mediated mast cell activation by kit. J Biol Chem *280(48)*, 40261-40270.

Jaiswal BS, Janakiraman V, Kljavin NM, Chaudhuri S, Stern HM, Wang W, Kan Z, Dbouk HA, Peters BA, Waring P, Dela Vega T, Kenski DM, Bowman KK, Lorenzo M, Li H, Wu J, Modrusan Z, Stinson J, Eby M, Yue P, Kaminker JS, de Sauvage FJ, Backer JM and Seshagiri S (2009). Somatic mutations in p85alpha promote tumorigenesis through class IA PI3K activation. Cancer Cell *16(6)*, 463-474.

Kambayashi T, Larosa DF, Silverman MA and Koretzky GA (2009). Cooperation of adapter molecules in proximal signaling cascades during allergic inflammation. Immunol Rev *232(1)*, 99-114.

Kambayashi T, Okumura M, Baker RG, Hsu CJ, Baumgart T, Zhang W and Koretzky GA (2010). Independent and cooperative roles of adaptor molecules in proximal signaling during FcepsilonRI-mediated mast cell activation. Mol Cell Biol *30(17)*, 4188-4196.

Kang S, Bader AG and Vogt PK (2005). Phosphatidylinositol 3-kinase mutations identified in human cancer are oncogenic. Proc Natl Acad Sci U S A *102(3)*, 802-807.

Kang S, Denley A, Vanhaesebroeck B and Vogt PK (2006). Oncogenic transformation induced by the p110beta, -gamma, and -delta isoforms of class I phosphoinositide 3-kinase. Proc Natl Acad Sci U S A *103(5)*, 1289-1294.

Kapeller R, Prasad KV, Janssen O, Hou W, Schaffhausen BS, Rudd CE and Cantley LC (1994). Identification of two SH3-binding motifs in the regulatory subunit of phosphatidylinositol 3-kinase. J Biol Chem *269(3)*, 1927-1933.

Karasarides M, Anand-Apte B and Wolfman A (2001). A direct interaction between oncogenic Ha-Ras and phosphatidylinositol 3-kinase is not required for Ha-Ras-dependent transformation of epithelial cells. J Biol Chem *276(43)*, 39755-39764.

Kavanaugh WM, Turck CW, Klippel A and Williams LT (1994). Tyrosine 508 of the 85-kilodalton subunit of phosphatidylinositol 3-kinase is phosphorylated by the platelet-derived growth factor receptor. Biochemistry *33(36)*, 11046-11050.

Kawakami Y, Kitaura J, Satterthwaite AB, Kato RM, Asai K, Hartman SE, Maeda-Yamamoto M, Lowell CA, Rawlings DJ, Witte ON and Kawakami T (2000). Redundant and opposing functions of two tyrosine kinases, Btk and Lyn, in mast cell activation. J Immunol *165(3)*, 1210-1219.

Kawakami Y, Nishimoto H, Kitaura J, Maeda-Yamamoto M, Kato RM, Littman DR, Leitges M, Rawlings DJ and Kawakami T (2004). Protein kinase C betaII regulates Akt phosphorylation on Ser-473 in a cell type- and stimulus-specific fashion. J Biol Chem *279(46)*, 47720-47725.

Kazanietz MG (2002). Novel "nonkinase" phorbol ester receptors: the C1 domain connection. Mol Pharmacol *61(4)*, 759-767.

Keranen LM and Newton AC (1997). Ca2+ differentially regulates conventional protein kinase Cs' membrane interaction and activation. J Biol Chem *272(41)*, 25959-25967.

Kerchner KR, Clay RL, McCleery G, Watson N, McIntire WE, Myung CS and Garrison JC (2004). Differential sensitivity of phosphatidylinositol 3-kinase p110gamma to isoforms of G protein betagamma dimers. J Biol Chem *279(43)*, 44554-44562.

Kettner A, Pivniouk V, Kumar L, Falet H, Lee JS, Mulligan R and Geha RS (2003). Structural requirements of SLP-76 in signaling via the high-affinity immunoglobulin E receptor (Fc epsilon RI) in mast cells. Mol Cell Biol *23(7)*, 2395-2406.

Kimura T, Kihara H, Bhattacharyya S, Sakamoto H, Appella E and Siraganian RP (1996). Downstream signaling molecules bind to different phosphorylated immunoreceptor tyrosine-based activation motif (ITAM) peptides of the high affinity IgE receptor. J Biol Chem *271(44)*, 27962-27968.

Kimura Y, Jones N, Kluppel M, Hirashima M, Tachibana K, Cohn JB, Wrana JL, Pawson T and Bernstein A (2004). Targeted mutations of the juxtamembrane tyrosines in the Kit receptor tyrosine kinase selectively affect multiple cell lineages. Proc Natl Acad Sci U S A *101(16)*, 6015-6020.

Kirshenbaum AS, Kessler SW, Goff JP and Metcalfe DD (1991). Demonstration of the origin of human mast cells from CD34+ bone marrow progenitor cells. J Immunol *146(5)*, 1410-1415.

Kissel H, Timokhina I, Hardy MP, Rothschild G, Tajima Y, Soares V, Angeles M, Whitlow SR, Manova K and Besmer P (2000). Point mutation in kit receptor tyrosine kinase reveals essential roles for kit signaling in spermatogenesis and oogenesis without affecting other kit responses. EMBO J *19(6)*, 1312-1326.

Kitaura J, Asai K, Maeda-Yamamoto M, Kawakami Y, Kikkawa U and Kawakami T (2000). Akt-dependent cytokine production in mast cells. J Exp Med *192(5)*, 729-740.

Klippel A, Escobedo JA, Fantl WJ and Williams LT (1992). The C-terminal SH2 domain of p85 accounts for the high affinity and specificity of the binding of phosphatidylinositol 3-kinase to phosphorylated platelet-derived growth factor beta receptor. Mol Cell Biol *12(4)*, 1451-1459.

Koyasu S (2004). Role of class IA phosphoinositide 3-kinase in B lymphocyte development and functions. Biochem Soc Trans *32(Pt 2)*, 320-325.

Koyasu S, Minowa A, Terauchi Y, Kadowaki T and Matsuda S (2005). The role of phosphoinositide-3-kinase in mast cell homing to the gastrointestinal tract. Novartis Found Symp *271*, 152-61; discussion 161-5, 198-9.

Krugmann S, Cooper MA, Williams DH, Hawkins PT and Stephens LR (2002). Mechanism of the regulation of type IB phosphoinositide 3OH-kinase byG-protein betagamma subunits. Biochem J *362(Pt 3)*, 725-731.

Krugmann S, Hawkins PT, Pryer N and Braselmann S (1999). Characterizing the interactions between the two subunits of the p101/p110gamma phosphoinositide 3-kinase and their role in the activation of this enzyme by G beta gamma subunits. J Biol Chem *274(24)*, 17152-17158.

Kurig B, Shymanets A, Bohnacker T, Prajwal Brock C, Ahmadian MR, Schaefer M, Gohla A, Harteneck C, Wymann MP, Jeanclos E and Nurnberg B (2009). Ras is an indispensable coregulator of the class IB phosphoinositide 3-kinase p87/p110gamma. Proc Natl Acad Sci U S A *106(48)*, 20312-20317.

Laffargue M, Calvez R, Finan P, Trifilieff A, Barbier M, Altruda F, Hirsch E and Wymann MP (2002). Phosphoinositide 3-kinase gamma is an essential amplifier of mast cell function. Immunity *16(3)*, 441-451.

Lam RS, Shumilina E, Matzner N, Zemtsova IM, Sobiesiak M, Lang C, Felder E, Dietl P, Huber SM and Lang F (2008). Phosphatidylinositol-3-kinase regulates mast cell ion channel activity. Cell Physiol Biochem *22(1-4)*, 169-176.

Leitges M, Gimborn K, Elis W, Kalesnikoff J, Hughes MR, Krystal G and Huber M (2002). Protein kinase C-delta is a negative regulator of antigen-induced mast cell degranulation. Mol Cell Biol *22(12)*, 3970-3980.

Leitges M, Schmedt C, Guinamard R, Davoust J, Schaal S, Stabel S and Tarakhovsky A (1996). Immunodeficiency in protein kinase cbeta-deficient mice. Science *273(5276)*, 788-791.

Leopoldt D, Hanck T, Exner T, Maier U, Wetzker R and Nurnberg B (1998). Gbetagamma stimulates phosphoinositide 3-kinase-gamma by direct interaction with two domains of the catalytic p110 subunit. J Biol Chem *273(12)*, 7024-7029.

Lessmann E, Leitges M and Huber M (2006). A redundant role for PKC-epsilon in mast cell signaling and effector function. Int Immunol *18(5)*, 767-773.

Li Z, Jiang H, Xie W, Zhang Z, Smrcka AV and Wu D (2000). Roles of PLC-beta2 and -beta3 and PI3Kgamma in chemoattractant-mediated signal transduction. Science *287(5455)*, 1046-1049.

Lin P and Gilfillan AM (1992). The role of calcium and protein kinase C in the IgE-dependent activation of phosphatidylcholine-specific phospholipase D in a rat mast (RBL 2H3) cell line. Eur J Biochem *207(1)*, 163-168.

Lu-Kuo JM, Fruman DA, Joyal DM, Cantley LC and Katz HR (2000). Impaired kit- but not FcepsilonRI-initiated mast cell activation in the absence of phosphoinositide 3-kinase p85alpha gene products. J Biol Chem *275(8)*, 6022-6029.

Ludowyke RI, Elgundi Z, Kranenburg T, Stehn JR, Schmitz-Peiffer C, Hughes WE and Biden TJ (2006). Phosphorylation of nonmuscle myosin heavy chain IIA on Ser1917 is mediated by protein kinase C beta II and coincides with the onset of stimulated degranulation of RBL-2H3 mast cells. J Immunol *177(3)*, 1492-1499.

Ludowyke RI, Peleg I, Beaven MA and Adelstein RS (1989). Antigen-induced secretion of histamine and the phosphorylation of myosin by protein kinase C in rat basophilic leukemia cells. J Biol Chem *264(21)*, 12492-12501.

Ludowyke RI, Scurr LL and McNally CM (1996). Calcium ionophore-induced secretion from mast cells correlates with myosin light chain phosphorylation by protein kinase C. J Immunol *157(11)*, 5130-5138.

Ma HT and Beaven MA (2009). Regulation of Ca2+ signaling with particular focus on mast cells. Crit Rev Immunol *29(2)*, 155-186.

MacDougall LK, Domin J and Waterfield MD (1995). A family of phosphoinositide 3-kinases in Drosophila identifies a new mediator of signal transduction. Curr Biol *5(12)*, 1404-1415.

Maier U, Babich A, Macrez N, Leopoldt D, Gierschik P, Illenberger D and Nurnberg B (2000). Gbeta 5gamma 2 is a highly selective activator of phospholipid-dependent enzymes. J Biol Chem *275(18)*, 13746-13754.

Maier U, Babich A and Nurnberg B (1999). Roles of non-catalytic subunits in gbetagamma-induced activation of class I phosphoinositide 3-kinase isoforms beta and gamma. J Biol Chem *274(41)*, 29311-29317.

Malbec O, Malissen M, Isnardi I, Lesourne R, Mura AM, Fridman WH, Malissen B and Daeron M (2004). Linker for activation of T cells integrates positive and negative signaling in mast cells. J Immunol *173(8)*, 5086-5094.

Mandelker D, Gabelli SB, Schmidt-Kittler O, Zhu J, Cheong I, Huang CH, Kinzler KW, Vogelstein B and Amzel LM (2009). A frequent kinase domain mutation that changes the interaction between PI3Kalpha and the membrane. Proc Natl Acad Sci U S A *106(40)*, 16996-17001.

Mangmool S and Kurose H (2011). G(i/o) Protein-Dependent and -Independent Actions of Pertussis Toxin (PTX). Toxins (Basel) *3(7)*, 884-899.

Marone R, Cmiljanovic V, Giese B and Wymann MP (2008). Targeting phosphoinositide 3-kinase: moving towards therapy. Biochim Biophys Acta *1784(1)*, 159-185.

Marquardt DL, Alongi JL and Walker LL (1996). The phosphatidylinositol 3-kinase inhibitor wortmannin blocks mast cell exocytosis but not IL-6 production. J Immunol *156(5)*, 1942-1945.

Marquardt DL, Gruber HE and Wasserman SI (1984). Adenosine release from stimulated mast cells. Proc Natl Acad Sci U S A *81(19)*, 6192-6196.

Maruotti N, Crivellato E, Cantatore FP, Vacca A and Ribatti D (2007). Mast cells in rheumatoid arthritis. Clin Rheumatol *26(1)*, 1-4.

Maurer M, Theoharides T, Granstein RD, Bischoff SC, Bienenstock J, Henz B, Kovanen P, Piliponsky AM, Kambe N, Vliagoftis H, Levi-Schaffer F, Metz M, Miyachi Y, Befus D, Forsythe P, Kitamura Y and Galli S (2003). What is the physiological function of mast cells? Exp Dermatol *12(6)*, 886-910.

Metcalfe DD, Baram D and Mekori YA (1997). Mast cells. Physiol Rev *77(4)*, 1033-1079.

Miled N, Yan Y, Hon WC, Perisic O, Zvelebil M, Inbar Y, Schneidman-Duhovny D, Wolfson HJ, Backer JM and Williams RL (2007). Mechanism of two classes of cancer mutations in the phosphoinositide 3-kinase catalytic subunit. Science *317(5835)*, 239-242.

Miller S, Tavshanjian B, Oleksy A, Perisic O, Houseman BT, Shokat KM and Williams RL (2010). Shaping development of autophagy inhibitors with the structure of the lipid kinase Vps34. Science *327(5973)*, 1638-1642.

Molz L, Chen YW, Hirano M and Williams LT (1996). Cpk is a novel class of Drosophila PtdIns 3-kinase containing a C2 domain. J Biol Chem *271(23)*, 13892-13899.

Mor A, Ben-Moshe O, Mekori YA and Kloog Y (2011). Inhibitory effect of farnesylthiosalicylic acid on mediators release by mast cells: preferential inhibition of prostaglandin D(2) and tumor necrosis factor-alpha release. Inflammation *34(5)*, 314-318.

Morgan A, Burgoyne RD, Barclay JW, Craig TJ, Prescott GR, Ciufo LF, Evans GJ and Graham ME (2005). Regulation of exocytosis by protein kinase C. Biochem Soc Trans *33(Pt 6)*, 1341-1344.

Mulero I, Sepulcre MP, Meseguer J, Garcia-Ayala A and Mulero V (2007). Histamine is stored in mast cells of most evolutionarily advanced fish and regulates the fish inflammatory response. Proc Natl Acad Sci U S A *104(49)*, 19434-19439.

Murphy TR, Legere HJr and Katz HR (2007). Activation of protein kinase D1 in mast cells in response to innate, adaptive, and growth factor signals. J Immunol *179(11)*, 7876-7882.

Nagai H, Sakurai T, Inagaki N and Mori H (1995). An immunopharmacological study of the biphasic allergic skin reaction in mice. Biol Pharm Bull *18(2)*, 239-245.

Nave BT, Siddle K and Shepherd PR (1996). Phorbol esters stimulate phosphatidylinositol 3,4,5-trisphosphate production in 3T3-L1 adipocytes: implications for stimulation of glucose transport. Biochem J *318 (Pt 1)*, 203-205.

Nechushtan H, Leitges M, Cohen C, Kay G and Razin E (2000). Inhibition of degranulation and interleukin-6 production in mast cells derived from mice deficient in protein kinase Cbeta. Blood *95(5)*, 1752-1757.

Nishida K, Wang L, Morii E, Park SJ, Narimatsu M, Itoh S, Yamasaki S, Fujishima M, Ishihara K, Hibi M, Kitamura Y and Hirano T (2002). Requirement of Gab2 for mast cell development and KitL/c-Kit signaling. Blood *99(5)*, 1866-1869.

Nishida K, Yoshida Y, Itoh M, Fukada T, Ohtani T, Shirogane T, Atsumi T, Takahashi-Tezuka M, Ishihara K, Hibi M and Hirano T (1999). Gab-family adapter proteins act downstream of cytokine and growth factor receptors and T- and B-cell antigen receptors. Blood *93(6)*, 1809-1816.

Nishikawa K, Toker A, Johannes FJ, Songyang Z and Cantley LC (1997). Determination of the specific substrate sequence motifs of protein kinase C isozymes. J Biol Chem *272(2)*, 952-960.

Nishizumi H and Yamamoto T (1997). Impaired tyrosine phosphorylation and Ca2+ mobilization, but not degranulation, in lyn-deficient bone marrow-derived mast cells. J Immunol *158(5)*, 2350-2355.

Odom S, Gomez G, Kovarova M, Furumoto Y, Ryan JJ, Wright HV, Gonzalez-Espinosa C, Hibbs ML, Harder KW and Rivera J (2004). Negative regulation of immunoglobulin E-dependent allergic responses by Lyn kinase. J Exp Med *199(11)*, 1491-1502.

Okkenhaug K, Bilancio A, Farjot G, Priddle H, Sancho S, Peskett E, Pearce W, Meek SE, Salpekar A, Waterfield MD, Smith AJ and Vanhaesebroeck B (2002). Impaired B and T cell antigen receptor signaling in p110delta PI 3-kinase mutant mice. Science *297(5583)*, 1031-1034.

Orme MH, Alrubaie S, Bradley GL, Walker CD and Leevers SJ (2006). Input from Ras is required for maximal PI(3)K signalling in Drosophila. Nat Cell Biol *8(11)*, 1298-1302.

Osborne MA, Zenner G, Lubinus M, Zhang X, Songyang Z, Cantley LC, Majerus P, Burn P and Kochan JP (1996). The inositol 5'-phosphatase SHIP binds to immunoreceptor signaling motifs and responds to high affinity IgE receptor aggregation. J Biol Chem *271(46)*, 29271-29278.

Ozawa K, Szallasi Z, Kazanietz MG, Blumberg PM, Mischak H, Mushinski JF and Beaven MA (1993). Ca(2+)-dependent and Ca(2+)-independent isozymes of protein kinase C mediate exocytosis in antigen-stimulated rat basophilic RBL-2H3 cells. Reconstitution of secretory responses with Ca2+ and purified isozymes in washed permeabilized cells. J Biol Chem *268(3)*, 1749-1756.

Pacold ME, Suire S, Perisic O, Lara-Gonzalez S, Davis CT, Walker EH, Hawkins PT, Stephens L, Eccleston JF and Williams RL (2000). Crystal structure and functional analysis of Ras binding to its effector phosphoinositide 3-kinase gamma. Cell *103(6)*, 931-943.

Pang H, Flinn R, Patsialou A, Wyckoff J, Roussos ET, Wu H, Pozzuto M, Goswami S, Condeelis JS, Bresnick AR, Segall JE and Backer JM (2009). Differential enhancement of breast cancer cell motility and metastasis by helical and kinase domain mutations of class IA phosphoinositide 3-kinase. Cancer Res *69(23)*, 8868-8876.

Parravicini V, Gadina M, Kovarova M, Odom S, Gonzalez-Espinosa C, Furumoto Y, Saitoh S, Samelson LE, O'Shea JJ and Rivera J (2002). Fyn kinase initiates complementary signals required for IgE-dependent mast cell degranulation. Nat Immunol *3(8)*, 741-748.

Pendl GG, Prieschl EE, Thumb W, Harrer NE, Auer M and Baumruker T (1997). Effects of phosphatidylinositol-3-kinase inhibitors on degranulation and gene induction in allergically triggered mouse mast cells. Int Arch Allergy Immunol *112(4)*, 392-399.

Peres C, Yart A, Perret B, Salles JP and Raynal P (2003). Modulation of phosphoinositide 3-kinase activation by cholesterol level suggests a novel positive role for lipid rafts in lysophosphatidic acid signalling. FEBS Lett *534(1-3)*, 164-168.

Perkins DN, Pappin DJ, Creasy DM and Cottrell JS (1999). Probability-based protein identification by searching sequence databases using mass spectrometry data. Electrophoresis *20(18)*, 3551-3567.

Pfeiffer JR, Seagrave JC, Davis BH, Deanin GG and Oliver JM (1985). Membrane and cytoskeletal changes associated with IgE-mediated serotonin release from rat basophilic leukemia cells. J Cell Biol *101(6)*, 2145-2155.

Pierce KL, Premont RT and Lefkowitz RJ (2002). Seven-transmembrane receptors. Nat Rev Mol Cell Biol *3(9)*, 639-650.

Pirola L, Zvelebil MJ, Bulgarelli-Leva G, Van Obberghen E, Waterfield MD and Wymann MP (2001). Activation loop sequences confer substrate specificity to phosphoinositide 3-kinase alpha (PI3Kalpha). Functions of lipid kinase-deficient PI3Kalpha in signaling. J Biol Chem *276(24)*, 21544-21554.

Pivniouk VI, Martin TR, Lu-Kuo JM, Katz HR, Oettgen HC and Geha RS (1999). SLP-76 deficiency impairs signaling via the high-affinity IgE receptor in mast cells. J Clin Invest *103(12)*, 1737-1743.

Ponzetto C, Bardelli A, Maina F, Longati P, Panayotou G, Dhand R, Waterfield MD and Comoglio PM (1993). A novel recognition motif for phosphatidylinositol 3-kinase binding mediates its association with the hepatocyte growth factor/scatter factor receptor. Mol Cell Biol *13(8)*, 4600-4608.

Ramkumar V, Stiles GL, Beaven MA and Ali H (1993). The A3 adenosine receptor is the unique adenosine receptor which facilitates release of allergic mediators in mast cells. J Biol Chem *268(23)*, 16887-16890.

Ravetch JV and Kinet JP (1991). Fc receptors. Annu Rev Immunol *9*, 457-492.

Reif K, Gout I, Waterfield MD and Cantrell DA (1993). Divergent regulation of phosphatidylinositol 3-kinase P85 alpha and P85 beta isoforms upon T cell activation. J Biol Chem *268(15)*, 10780-10788.

Resnick AC, Snowman AM, Kang BN, Hurt KJ, Snyder SH and Saiardi A (2005). Inositol polyphosphate multikinase is a nuclear PI3-kinase with transcriptional regulatory activity. Proc Natl Acad Sci U S A *102(36)*, 12783-12788.

Rodriguez-Viciana P, Warne PH, Dhand R, Vanhaesebroeck B, Gout I, Fry MJ, Waterfield MD and Downward J (1994). Phosphatidylinositol-3-OH kinase as a direct target of Ras. Nature *370(6490)*, 527-532.

Rodriguez-Viciana P, Warne PH, Vanhaesebroeck B, Waterfield MD and Downward J (1996). Activation of phosphoinositide 3-kinase by interaction with Ras and by point mutation. EMBO J *15(10)*, 2442-2451.

Roget K, Malissen M, Malbec O, Malissen B and Daeron M (2008). Non-T cell activation linker promotes mast cell survival by dampening the recruitment of SHIP1 by linker for activation of T cells. J Immunol *180(6)*, 3689-3698.

Rommel C, Camps M and Ji H (2007). PI3K delta and PI3K gamma: partners in crime in inflammation in rheumatoid arthritis and beyond? Nat Rev Immunol *7(3)*, 191-201.

Rubio I, Rodriguez-Viciana P, Downward J and Wetzker R (1997). Interaction of Ras with phosphoinositide 3-kinase gamma. Biochem J *326 (Pt 3)*, 891-895.

Rubio I, Wittig U, Meyer C, Heinze R, Kadereit D, Waldmann H, Downward J and Wetzker R (1999). Farnesylation of Ras is important for the interaction with phosphoinositide 3-kinase gamma. Eur J Biochem *266(1)*, 70-82.

Rudd ML, Price JC, Fogoros S, Godwin AK, Sgroi DC, Merino MJ and Bell DW (2011). A unique spectrum of somatic PIK3CA (p110alpha) mutations within primary endometrial carcinomas. Clin Cancer Res *17(6)*, 1331-1340.

Ruitenberg EJ and Elgersma A (1976). Absence of intestinal mast cell response in congenitally athymic mice during Trichinella spiralis infection. Nature *264(5583)*, 258-260.

Saito H, Okajima F, Molski TF, Sha'afi RI, Ui M and Ishizaka T (1987). Effects of ADP-ribosylation of GTP-binding protein by pertussis toxin on immunoglobulin E-dependent and -independent histamine release from mast cells and basophils. J Immunol *138(11)*, 3927-3934.

Saitoh S, Arudchandran R, Manetz TS, Zhang W, Sommers CL, Love PE, Rivera J and Samelson LE (2000). LAT is essential for Fc(epsilon)RI-mediated mast cell activation. Immunity *12(5)*, 525-535.

Saitoh S, Odom S, Gomez G, Sommers CL, Young HA, Rivera J and Samelson LE (2003). The four distal tyrosines are required for LAT-dependent signaling in FcepsilonRI-mediated mast cell activation. J Exp Med *198(5)*, 831-843.

Samuels Y and Velculescu VE (2004). Oncogenic mutations of PIK3CA in human cancers. Cell Cycle *3(10)*, 1221-1224.

Samuels Y, Wang Z, Bardelli A, Silliman N, Ptak J, Szabo S, Yan H, Gazdar A, Powell SM, Riggins GJ, Willson JK, Markowitz S, Kinzler KW, Vogelstein B and Velculescu VE (2004). High frequency of mutations of the PIK3CA gene in human cancers. Science *304(5670)*, 554.

Sanchez-Miranda E, Ibarra-Sanchez A and Gonzalez-Espinosa C (2010). Fyn kinase controls FcepsilonRI receptor-operated calcium entry necessary for full degranulation in mast cells. Biochem Biophys Res Commun *391(4)*, 1714-1720.

Sasaki AT, Chun C, Takeda K and Firtel RA (2004). Localized Ras signaling at the leading edge regulates PI3K, cell polarity, and directional cell movement. J Cell Biol *167(3)*, 505-518.

Sasaki J, Sasaki T, Yamazaki M, Matsuoka K, Taya C, Shitara H, Takasuga S, Nishio M, Mizuno K, Wada T, Miyazaki H, Watanabe H, Iizuka R, Kubo S, Murata S, Chiba T, Maehama T, Hamada K, Kishimoto H, Frohman MA, Tanaka K, Penninger JM, Yonekawa H, Suzuki A and Kanaho Y (2005). Regulation of anaphylactic responses by phosphatidylinositol phosphate kinase type I {alpha}. J Exp Med *201(6)*, 859-870.

Sasaki T, Irie-Sasaki J, Jones RG, Oliveira-dos-Santos AJ, Stanford WL, Bolon B, Wakeham A, Itie A, Bouchard D, Kozieradzki I, Joza N, Mak TW, Ohashi PS, Suzuki A and Penninger JM (2000). Function of PI3Kgamma in thymocyte development, T cell activation, and neutrophil migration. Science *287(5455)*, 1040-1046.

Scharenberg AM and Kinet JP (1994). Initial events in Fc epsilon RI signal transduction. J Allergy Clin Immunol *94(6 Pt 2)*, 1142-1146.

Schwartz LB, Austen KF and Wasserman SI (1979). Immunologic release of beta-hexosaminidase and beta-glucuronidase from purified rat serosal mast cells. J Immunol *123(4)*, 1445-1450.

Serve H, Yee NS, Stella G, Sepp-Lorenzino L, Tan JC and Besmer P (1995). Differential roles of PI3-kinase and Kit tyrosine 821 in Kit receptor-mediated proliferation, survival and cell adhesion in mast cells. EMBO J *14(3)*, 473-483.

Shevchenko A, Wilm M, Vorm O and Mann M (1996). Mass spectrometric sequencing of proteins silver-stained polyacrylamide gels. Anal Chem *68(5)*, 850-858.

Snyder DA, Kelly ML and Woodbury DJ (2006). SNARE complex regulation by phosphorylation. Cell Biochem Biophys *45(1)*, 111-123.

Soltoff SP (2007). Rottlerin: an inappropriate and ineffective inhibitor of PKCdelta. Trends Pharmacol Sci *28(9)*, 453-458.

Soltoff SP and Cantley LC (1996). p120cbl is a cytosolic adapter protein that associates with phosphoinositide 3-kinase in response to epidermal growth factor in PC12 and other cells. J Biol Chem *271(1)*, 563-567.

Songyang Z, Shoelson SE, Chaudhuri M, Gish G, Pawson T, Haser WG, King F, Roberts T, Ratnofsky S, Lechleider RJ and et a (1993). SH2 domains recognize specific phosphopeptide sequences. Cell *72(5)*, 767-778.

Sparmann A and Bar-Sagi D (2004). Ras-induced interleukin-8 expression plays a critical role in tumor growth and angiogenesis. Cancer Cell *6(5)*, 447-458.

Standaert ML, Bandyopadhyay G, Galloway L, Soto J, Ono Y, Kikkawa U, Farese RV and Leitges M (1999). Effects of knockout of the protein kinase C beta gene on glucose transport and glucose homeostasis. Endocrinology *140(10)*, 4470-4477.

Stephens L, Jackson T and Hawkins PT (1993). Synthesis of phosphatidylinositol 3,4,5-trisphosphate in permeabilized neutrophils regulated by receptors and G-proteins. J Biol Chem *268(23)*, 17162-17172.

Stephens L, Smrcka A, Cooke FT, Jackson TR, Sternweis PC and Hawkins PT (1994). A novel phosphoinositide 3 kinase activity in myeloid-derived cells is activated by G protein beta gamma subunits. Cell *77(1)*, 83-93.

Stephens LR, Eguinoa A, Erdjument-Bromage H, Lui M, Cooke F, Coadwell J, Smrcka AS, Thelen M, Cadwallader K, Tempst P and Hawkins PT (1997). The G beta gamma sensitivity of a PI3K is dependent upon a tightly associated adaptor, p101. Cell *89(1)*, 105-114.

Stoyanov B, Volinia S, Hanck T, Rubio I, Loubtchenkov M, Malek D, Stoyanova S, Vanhaesebroeck B, Dhand R, Nurnberg B, Gierschik P, Seedorf K, JJ H, Waterfield MD and Wetzker R (1995). Cloning and characterization of a G protein-activated human phosphoinositide-3 kinase. Science *269(5224)*, 690-693.

Stoyanova S, Bulgarelli-Leva G, Kirsch C, Hanck T, Klinger R, Wetzker R and Wymann MP (1997). Lipid kinase and protein kinase activities of G-protein-coupled phosphoinositide 3-kinase gamma: structure-activity analysis and interactions with wortmannin. Biochem J *324 (Pt 2)*, 489-495.

Sugimoto Y, Whitman M, Cantley LC and Erikson RL (1984). Evidence that the Rous sarcoma virus transforming gene product phosphorylates phosphatidylinositol and diacylglycerol. Proc Natl Acad Sci U S A *81(7)*, 2117-2121.

Suire S, Coadwell J, Ferguson GJ, Davidson K, Hawkins P and Stephens L (2005). p84, a new Gbetagamma-activated regulatory subunit of the type IB phosphoinositide 3-kinase p110gamma. Curr Biol *15(6)*, 566-570.

Suire S, Condliffe AM, Ferguson GJ, Ellson CD, Guillou H, Davidson K, Welch H, Coadwell J, Turner M, Chilvers ER, Hawkins PT and Stephens L (2006). Gbetagammas and the Ras binding domain of p110gamma are both important regulators of PI3Kgamma signalling in neutrophils. Nat Cell Biol *8(11)*, 1303-1309.

Suire S, Hawkins P and Stephens L (2002). Activation of phosphoinositide 3-kinase gamma by Ras. Curr Biol *12(13)*, 1068-1075.

Suzuki K and Verma IM (2008). Phosphorylation of SNAP-23 by IkappaB kinase 2 regulates mast cell degranulation. Cell *134(3)*, 485-495.

Tan BL, Yazicioglu MN, Ingram D, McCarthy J, Borneo J, Williams DA and Kapur R (2003). Genetic evidence for convergence of c-Kit- and alpha4 integrin-mediated signals on class IA PI-3kinase and the Rac pathway in regulating integrin-directed migration in mast cells. Blood *101(12)*, 4725-4732.

Tang X and Downes CP (1997). Purification and characterization of Gbetagamma-responsive phosphoinositide 3-kinases from pig platelet cytosol. J Biol Chem *272(22)*, 14193-14199.

Thastrup O, Cullen PJ, Drobak BK, Hanley MR and Dawson AP (1990). Thapsigargin, a tumor promoter, discharges intracellular Ca2+ stores by specific inhibition of the endoplasmic reticulum Ca2(+)-ATPase. Proc Natl Acad Sci U S A *87(7)*, 2466-2470.

Tilley SL, Wagoner VA, Salvatore CA, Jacobson MA and Koller BH (2000). Adenosine and inosine increase cutaneous vasopermeability by activating A(3) receptors on mast cells. J Clin Invest *105(3)*, 361-367.

Timokhina I, Kissel H, Stella G and Besmer P (1998). Kit signaling through PI 3-kinase and Src kinase pathways: an essential role for Rac1 and JNK activation in mast cell proliferation. EMBO J *17(21)*, 6250-6262.

Tkaczyk C, Beaven MA, Brachman SM, Metcalfe DD and Gilfillan AM (2003). The phospholipase C gamma 1-dependent pathway of Fc epsilon RI-mediated mast cell activation is regulated independently of phosphatidylinositol 3-kinase. J Biol Chem *278(48)*, 48474-48484.

Tolias KF, Cantley LC and Carpenter CL (1995). Rho family GTPases bind to phosphoinositide kinases. J Biol Chem *270(30)*, 17656-17659.

Urata C and Siraganian RP (1985). Pharmacologic modulation of the IgE or Ca2+ ionophore A23187 mediated Ca2+ influx, phospholipase activation, and histamine release in rat basophilic leukemia cells. Int Arch Allergy Appl Immunol *78(1)*, 92-100.

Vanhaesebroeck B, Leevers SJ, Ahmadi K, Timms J, Katso R, Driscoll PC, Woscholski R, Parker PJ and Waterfield MD (2001). Synthesis and function of 3-phosphorylated inositol lipids. Annu Rev Biochem *70*, 535-602.

Vanhaesebroeck B, Welham MJ, Kotani K, Stein R, Warne PH, Zvelebil MJ, Higashi K, Volinia S, Downward J and Waterfield MD (1997). P110delta, a novel phosphoinositide 3-kinase in leukocytes. Proc Natl Acad Sci U S A *94(9)*, 4330-4335.

Vichalkovski A, Gresko E, Hess D, Restuccia DF and Hemmings BA (2010). PKB/AKT phosphorylation of the transcription factor Twist-1 at Ser42 inhibits p53 activity in response to DNA damage. Oncogene *29(24)*, 3554-3565.

Vig M, DeHaven WI, Bird GS, Billingsley JM, Wang H, Rao PE, Hutchings AB, Jouvin MH, Putney JW and Kinet JP (2008). Defective mast cell effector functions in mice lacking the CRACM1 pore subunit of store-operated calcium release-activated calcium channels. Nat Immunol *9(1)*, 89-96.

Voigt P, Brock C, Nurnberg B and Schaefer M (2005). Assigning functional domains within the p101 regulatory subunit of phosphoinositide 3-kinase gamma. J Biol Chem *280(6)*, 5121-5127.

Voigt P, Dorner MB and Schaefer M (2006). Characterization of p87PIKAP, a novel regulatory subunit of phosphoinositide 3-kinase gamma that is highly expressed in heart and interacts with PDE3B. J Biol Chem *281(15)*, 9977-9986.

von Willebrand M, Williams S, Saxena M, Gilman J, Tailor P, Jascur T, Amarante-Mendes GP, Green DR and Mustelin T (1998). Modification of phosphatidylinositol 3-kinase SH2 domain binding properties by Abl- or Lck-mediated tyrosine phosphorylation at Tyr-688. J Biol Chem *273(7)*, 3994-4000.

Vorndran C, Minta A and Poenie M (1995). New fluorescent calcium indicators designed for cytosolic retention or measuring calcium near membranes. Biophys J *69(5)*, 2112-2124.

Walker EH, Perisic O, Ried C, Stephens L and Williams RL (1999). Structural insights into phosphoinositide 3-kinase catalysis and signalling. Nature *402(6759)*, 313-320.

Wang D, Feng J, Wen R, Marine JC, Sangster MY, Parganas E, Hoffmeyer A, Jackson CW, Cleveland JL, Murray PJ and Ihle JN (2000). Phospholipase Cgamma2 is essential in the functions of B cell and several Fc receptors. Immunity *13(1)*, 25-35.

Wen R, Jou ST, Chen Y, Hoffmeyer A and Wang D (2002). Phospholipase C gamma 2 is essential for specific functions of Fc epsilon R and Fc gamma R. J Immunol *169(12)*, 6743-6752.

Wymann MP, Bjorklof K, Calvez R, Finan P, Thomast M, Trifilieff A, Barbier M, Altruda F, Hirsch E and Laffargue M (2003). Phosphoinositide 3-kinase gamma: a key modulator in inflammation and allergy. Biochem Soc Trans *31(Pt 1)*, 275-280.

Xiao W, Nishimoto H, Hong H, Kitaura J, Nunomura S, Maeda-Yamamoto M, Kawakami Y, Lowell CA, Ra C and Kawakami T (2005). Positive and negative regulation of mast cell activation by Lyn via the FcepsilonRI. J Immunol *175(10)*, 6885-6892.

Yee NS, Hsiau CW, Serve H, Vosseller K and Besmer P (1994). Mechanism of down-regulation of c-kit receptor. Roles of receptor tyrosine kinase, phosphatidylinositol 3'-kinase, and protein kinase C. J Biol Chem *269(50)*, 31991-31998.

Yu M, Lowell CA, Neel BG and Gu H (2006). Scaffolding adapter Grb2-associated binder 2 requires Syk to transmit signals from FcepsilonRI. J Immunol *176(4)*, 2421-2429.

Yu M, Luo J, Yang W, Wang Y, Mizuki M, Kanakura Y, Besmer P, Neel BG and Gu H (2006). The scaffolding adapter Gab2, via Shp-2, regulates kit-evoked mast cell proliferation by activating the Rac/JNK pathway. J Biol Chem *281(39)*, 28615-28626.

Zhang X, Vadas O, Perisic O, Anderson KE, Clark J, Hawkins PT, Stephens LR and Williams RL (2011). Structure of Lipid Kinase p110beta/p85beta Elucidates an Unusual SH2-Domain-Mediated Inhibitory Mechanism. Mol Cell *41(5)*, 567-578.

Zhao JJ, Gjoerup OV, Subramanian RR, Cheng Y, Chen W, Roberts TM and Hahn WC (2003). Human mammary epithelial cell transformation through the activation of phosphatidylinositol 3-kinase. Cancer Cell *3(5)*, 483-495.

Zhao JJ, Liu Z, Wang L, Shin E, Loda MF and Roberts TM (2005). The oncogenic properties of mutant p110alpha and p110beta phosphatidylinositol 3-kinases in human mammary epithelial cells. Proc Natl Acad Sci U S A *102(51)*, 18443-18448.

Zhao L and Vogt PK (2008). Helical domain and kinase domain mutations in p110alpha of phosphatidylinositol 3-kinase induce gain of function by different mechanisms. Proc Natl Acad Sci U S A *105(7)*, 2652-2657.

Zhao L and Vogt PK (2010). Hot-spot mutations in p110alpha of phosphatidylinositol 3-kinase (pI3K): differential interactions with the regulatory subunit p85 and with RAS. Cell Cycle *9(3)*, 596-600.

Zheng Y, Bagrodia S and Cerione RA (1994). Activation of phosphoinositide 3-kinase activity by Cdc42Hs binding to p85. J Biol Chem *269(29)*, 18727-18730.

Zhu M, Liu Y, Koonpaew S, Granillo O and Zhang W (2004). Positive and negative regulation of FcepsilonRI-mediated signaling by the adaptor protein LAB/NTAL. J Exp Med *200(8)*, 991-1000.

9. Appendix

Publications

PKCβ phosphorylates PI3Kγ to activate it and release it from GPCR control
Walser R, Burke JE, Gogvadze E, Bohnacker T, Zhang X, Hess D, Küenzi P[1], Laffargue M, Leitges M, Hirsch E, Williams RL, Wymann MP.
PloS Biol. 2013; 11(6): e1001587. doi: 10.1371/journal.pbio.1001587.

Integrating cardiac PIP3 and cAMP signaling through a PKA anchoring function of p110γ.
Perino A, Ghigo A, Ferrero E, Morello F, Santulli G, Baillie GS, Damilano F, Dunlop AJ, Pawson C, Walser R, Levi R, Altruda F, Silengo L, Langeberg LK, Neubauer G, Heymans S, Lembo G, Wymann MP, Wetzker R, Houslay MD, Iaccarino G, Scott JD, Hirsch E.
Mol Cell. 2011 Apr 8; 42(1): 84-95. doi: 10.1016/j.molcel.2011.01.030.

Reviews in preparation:

Regulation of class I phosphoinositide 3-kinases. Walser R.

Mast cells in allergy – signal transduction and mechanisms of activation. Walser R.

Protein kinase C (PKC) regulation by its domains and phosphorylation sites. Walser R.

OPEN ACCESS Freely available online

PLOS | BIOLOGY

PKCβ Phosphorylates PI3Kγ to Activate It and Release It from GPCR Control

Romy Walser[1], John E. Burke[2], Elena Gogvadze[1], Thomas Bohnacker[1], Xuxiao Zhang[2], Daniel Hess[3], Peter Küenzi[1], Michael Leitges[4], Emilio Hirsch[5], Roger L. Williams[2], Muriel Laffargue[6], Matthias P. Wymann[1]*

1 Department of Biomedicine, University of Basel, Basel, Switzerland, **2** Medical Research Council, Laboratory of Molecular Biology, Cambridge, United Kingdom, **3** Friedrich Miescher Institute for Biomedical Research, Basel, Switzerland, **4** Biotechnology Centre, University of Oslo, Oslo, Norway, **5** Department of Genetics, Biology and Biochemistry, University of Torino, Torino, Italy, **6** INSERM, UMR1048, Institut des Maladies Métaboliques et Cardiovasculaires, Toulouse, France

Abstract

All class I phosphoinositide 3-kinases (PI3Ks) associate tightly with regulatory subunits through interactions that have been thought to be constitutive. PI3Kγ is key to the regulation of immune cell responses activated by G protein-coupled receptors (GPCRs). Remarkably we find that PKCβ phosphorylates Ser582 in the helical domain of the PI3Kγ catalytic subunit p110γ in response to clustering of the high-affinity IgE receptor (FcεRI) and/or store-operated Ca^{2+}- influx in mast cells. Phosphorylation of p110γ correlates with the release of the p84 PI3Kγ adapter subunit from the p84-p110γ complex. Ser582 phospho-mimicking mutants show increased p110γ activity and a reduced binding to the p84 adapter subunit. As functional p84-p110γ is key to GPCR-mediated p110γ signaling, this suggests that PKCβ-mediated p110γ phosphorylation disconnects PI3Kγ from its canonical inputs from trimeric G proteins, and enables p110γ to operate downstream of Ca^{2+} and PKCβ. Hydrogen deuterium exchange mass spectrometry shows that the p84 adaptor subunit interacts with the p110γ helical domain, and reveals an unexpected mechanism of PI3Kγ regulation. Our data show that the interaction of p110γ with its adapter subunit is vulnerable to phosphorylation, and outline a novel level of PI3K control.

Citation: Walser R, Burke JE, Gogvadze E, Bohnacker T, Zhang X, et al. (2013) PKCβ Phosphorylates PI3Kγ to Activate It and Release It from GPCR Control. PLoS Biol 11(6): e1001587. doi:10.1371/journal.pbio.1001587

Academic Editor: Len Stephens, The Babraham Institute, United Kingdom

Received November 14, 2012; **Accepted** May 8, 2013; **Published** June 25, 2013

Funding: This work was supported by the Swiss National Science Foundation (310030_127574 & 31EM30-126143; www.snf.ch), the ESF EuroMEMBRANE programme grant FP-018 (www.esf.org), and the Medical Research Council (file reference number U105184308). JEB was supported by an EMBO long-term fellowship (ALTF268-2009; www.embo.org) and the British Heart Foundation (PG11/109/29247; www.bhf.org.uk). The funders had no role in study design, data collection and analysis, decision to publish, or preparation of the manuscript.

Competing Interests: The authors have declared that no competing interests exist.

Abbreviations: A3AR, A3 adenosine receptor; ADA, adenosine deaminase; BAPTA-AM, 1,2-Bis(2-aminophenoxy)ethane-N,N,N′,N′-tetraacetic acid tetrakis(acetoxymethyl ester); BMMC, bone marrow-derived mast cell; CAMK, calmodulin-dependent kinase; FcεRI, high-affinity IgE receptor; GPCR, G protein-coupled receptor; GST, glutathione S-transferase; HDX-MS, hydrogen deuterium exchange mass spectrometry; MRM, multiple reaction monitoring; PAF, platelet activating factor; PI3K, phosphoinositide 3-kinase; PKC, protein kinase C; PMA, phorbol 12-myristate 13-acetate; PtdIns, phosphatidylinositol; PKB/Akt, protein kinase B; PTx, *B. pertussis* toxin; SCF, stem cell factor, c-kit ligand; SOCE, store-operated Ca2+ entry.

* E-mail: Matthias.Wymann@UniBas.CH

Introduction

Class I phosphoinositide 3-kinases (PI3Ks) produce the lipid second messenger phosphatidylinositol(3,4,5)-trisphosphate [PtdIns(3,4,5)P_3] and consist of a p110 catalytic and a regulatory subunit. The class IA catalytic subunits, p110α, β, and δ, are constitutively bound to p85-related regulatory proteins that link them to the activation by protein tyrosine kinase receptors. The only class IB PI3K member, p110γ, is activated downstream of G protein-coupled receptors (GPCRs), and interacts with p101 or p84 (also known as $p87^{PIKAP}$) adaptor subunits [1–3]. A tight complex of the p110γ catalytic subunit (PK3CG) with p101 was first discovered in neutrophils [1]. The p101 subunit (PI3R5) sensitizes PI3Kγ for activation by Gβγ subunits of trimeric G proteins, and is essential for chemotaxis of neutrophils towards GPCR-ligands [1,4,5].

Mast cells do not express p101; however, they do express the homologous adaptor protein p84 ([PI3R6]) [6], which shares 30% sequence identity with p101. Both p101 and p84 potentiate the activation of p110γ by Gβγ, but the p110γ-p101 complex is significantly more sensitive towards Gβγ, and displays an enhanced translocation to the plasma membrane as compared with p110γ-p84 [7]. Although p84 is absolutely required to relay GPCR signals to protein kinase B (PKB/Akt) phosphorylation and degranulation [6], its role is not completely understood: contrary to p110γ-p101, p110γ-p84 requires additionally the presence of the small G protein Ras, and might operate in distinct membrane micro-domains [6,7].

Interestingly, genetic ablation of p110γ blocks high-affinity IgE receptor (FcεRI)-dependent mast cell degranulation in vitro and in vivo [8]. In part this is due to the fact that initial IgE/antigen-mediated mast cell stimulation triggers the release of adenosine and other GPCR ligands to feed an autocrine/paracrine activation of PI3Kγ, which then functions as an amplifier of mast cell degranulation. Interestingly, a substantial part of the observed PI3Kγ-dependent histamine-containing granule release (ca. 40%) was found to be resistant to *Bordetella pertussis* toxin (*P*Tx) pretreatment [9,10]. Furthermore, although adenosine activates PI3Kγ via the A3 adenosine receptor (A_3AR; [ADORA3]), A_3AR

Author Summary

Phosphoinositide 3-kinases (PI3Ks) are involved in most essential cellular processes. Class I PI3Ks are heterodimers: class IA PI3Ks are made up of one of a group of regulatory p85-like subunits and one p110α, p110β, or p110δ catalytic p110 subunit, and are activated via binding of their p85 subunit to phosphorylated tyrosine receptors or their substrates. The only, class IB PI3K member, PI3Kγ, operates downstream of G protein-coupled receptors (GPCRs). Recent work suggested that PI3Kγ also operates downstream of IgE-antigen complexes in mast cell activation, but no mechanism was provided. We show that clustering of the high-affinity IgE receptor FcεRI triggers a massive calcium ion influx, which leads to PKCβ activation. In turn, PKCβ phosphorylates Ser582 of the PI3Kγ catalytic p110γ subunit's helical domain. Downstream of GPCRs, p110γ requires a p84 adapter to be functional. Phosphomimicking mutations at Ser582 disrupt the p84-p110γ interaction, and cellular Ser582 phosphorylation correlates with the loss of p84 from p110γ. Thus our data suggest that PKCβ phosphorylates and activates p110γ downstream of calcium ion influx, while simultaneously disconnecting the phosphorylated p110γ from GPCR signaling. Exploration of the p84-p110γ interaction surface by hydrogen- deuterium exchange mass spectrometry confirmed that the p110γ helical domain forms the main p84-p110γ contact surface. Taken together, the results suggest an unprecedented mechanism of PI3Kγ regulation.

null mice are still sensitive to passive systemic anaphylaxis, and degranulation in $A_3AR^{-/-}$ bone marrow-derived mast cells (BMMCs) upon antigen stimulation remains functional [11,12]. This and the strong degranulation phenotype of PI3Kγ$^{-/-}$ BMMCs suggest that GPCR signaling does not generate the full input to PI3Kγ-dependent degranulation, but a GPCR-independent activation mechanism for PI3Kγ has yet to be defined.

Here we identify a mechanism that activates PI3Kγ independently of GPCRs: we demonstrate that (i) IgE/antigen complexes and extracellular Ca^{2+} influx activate PI3Kγ, (ii) PI3Kγ is operationally linked to the FcεRI specifically by PKCβ (PRKCB), (iii) and that the phosphorylation of Ser582 located in the helical domain of p110γ by PKCβ leads to the dissociation of the p84 adapter to decouple phosphorylated p110γ from GPCR inputs. Further we characterize the p110γ-p84 interface, and delineate an activation process that seems to be conserved among class I PI3Ks.

Results

Thapsigargin-Induced Mast Cell Activation Needs PI3Kγ

A committed step in mast cell activation is the influx of extracellular Ca^{2+} by store-operated Ca^{2+} entry (SOCE) [13]. Thapsigargin, which inhibits the sarco/endoplasmic reticulum Ca^{2+} reuptake ATPase (SERCA), causes depletion of Ca^{2+} stores, triggering SOCE. The latter achieves full-scale degranulation of BMMCs [14]. Surprisingly, BMMCs devoid of the p110γ catalytic subunit of PI3Kγ lost their responsiveness to thapsigargin and matched degranulation responses attained by wortmannin-pretreated cells (Figure 1A). To investigate if thapsigargin-triggered, p110γ-dependent degranulation involved release of adenosine, BMMCs were preincubated with adenosine deaminase (ADA) (Figure 1B) to convert adenosine to inosine, which has a very low affinity for adenosine receptors. ADA attenuated degranulation induced by IgE/antigen but did not affect thapsigargin-stimulated degranulation in wild type cells and did not further attenuate

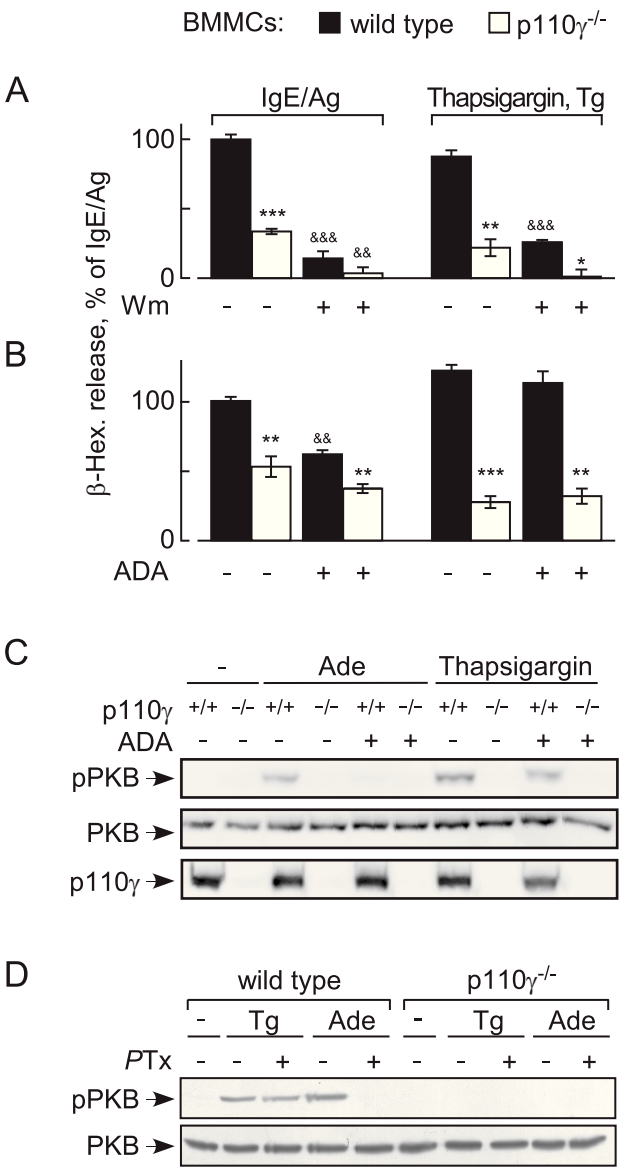

Figure 1. Thapsigargin-induced mast cell degranulation requires PI3Kγ, but not GPCR signaling. (A) Granule release of wild type and p110γ$^{-/-}$ BMMCs was determined detecting β-hexosaminidase (β-Hex) release into extracellular media. BMMC stimulation with IgE/antigen was initiated with the antigen (Ag, DNP-HSA at 10 ng/ml; 100 ng/ml IgE overnight). Alternatively, BMMCs were stimulated by the addition of thapsigargin (1 μM). Where indicated, BMMCs were preincubated for 15 min with 100 nM wortmannin. Released β-Hex was quantified 20 min after stimulation, and is expressed as mean ± standard error of the mean (SEM) ($n = 3$; p-values in all figures are * or &: $p<0.05$, **: $p<0.005$; ***: $p<0.0005$; * depict here comparison with respective wild type control; & refer to comparison of untreated versus treated samples). (B) Granule release was assessed as above, but ADA (10 units/ml) was added to BMMC suspensions 1 min before stimulation where depicted. (C) Wild type or p110γ$^{-/-}$ BMMCs were stimulated with adenosine (Ade; 1 μM) or thapsigargin (1 μM) for 2 min, and phosphorylation of PKB/Akt on Thr308 (pPKB), total PKB and p110γ was analyzed by Western blotting. BMMCs were incubated in starving medium (2% FCS, without IL-3) for 3 h before stimulation, and pretreated with ADA where indicated. (D) Heterotrimeric $G\alpha_i$ proteins were inactivated by preincubation of wild type and p110γ$^{-/-}$ BMMCs with 100 ng/ml *P*Tx for 4 h, before thapsigargin (Tg) or adenosine was added as in (C).
doi:10.1371/journal.pbio.1001587.g001

residual degranulation in p110γ null BMMCs. Likewise, presence of ADA did not reduce the phosphorylation of PKB/Akt in response to thapsigargin via the p110γ-dependent pathway (Figure 1C) but did reduce phosphorylation of PKB/Akt in response to adenosine—illustrating that the added ADA removes adenosine quantitatively. *P*Tx treatment of BMMCs (Figure 1D) blocked adenosine—but not thapsigargin-stimulated PKB/Akt phosphorylation.

To exclude that autocrine/paracrine signaling to p110γ occurred through *P*Tx-insensitive Gαq subunits to phospholipase β (PLCβ [PLCB2, PLCB3]), and a subsequent Ras activation by the Ras guanine nucleotide exchange factor RasGRP4 as described earlier in neutrophils [15], we used platelet activating factor (PAF) to trigger cyclic AMP-responsive element-binding protein (CREB) phosphorylation. PAF was reported earlier to trigger a *P*Tx-insensitive Ca^{2+} release from mast cells [9], and induced here a robust CREB phosphorylation comparable to adenosine and IgE/antigen. In contrast, PAF failed to trigger phosphorylation of PKB/Akt by itself, and did not enhance signaling of IgE/antigen to PKB/Akt (Figure S1).

Altogether, these results clearly illustrate that thapsigargin stimulates BMMCs via a PI3Kγ-dependent activation pathway, which operates separately from adenosine-induced activation of Gαi/o trimeric G proteins.

Thapsigargin-Induced PI3Kγ Is Downstream of Extracellular Ca^{2+} Influx

PI3Kγ activation has been linked to ligation of GPCRs [1,16], but not to elevated intracellular Ca^{2+} concentration ($[Ca^{2+}]_i$). We therefore chelated extracellular Ca^{2+} using EDTA, and buffered intracellular Ca^{2+} with the cell permeable Ca^{2+} chelator 1,2-Bis(2-aminophenoxy)ethane-N,N,N′,N′-tetraacetic acid tetrakis(acetoxymethyl ester) (BAPTA-AM). Extracellular and intracellular Ca^{2+} chelation prevented phosphorylation of PKB/Akt induced by thapsigargin or the Ca^{2+} ionophore ionomycin, while IL-3 and adenosine signaling to PKB/Akt remained unperturbed (Figure 2A and 2B).

Interestingly, the concentration of Ca^{2+} required to trigger PI3Kγ-dependent phosphorylation of PKB/Akt exceeded peak concentrations that are reached by GPCR stimulation: GPCR agonists release Ca^{2+} only from internal stores (maximum $[Ca^{2+}]_i$<300 nM), while thapsigargin (Figure 2C–2F) and IgE/antigen trigger SOCE and elevate $[Ca^{2+}]_i$ to μM concentrations [9,14,17]. Moreover, the correlation of maximally achieved $[Ca^{2+}]_i$ after thapsigargin revealed a steep, switch-like activation of PKB/Akt. While Ca^{2+} release from internal stores triggered by Gαi-coupled GPCRs (such as the A_3AR stimulated by N^6-(3-iodobenzyl)-adenosine-5′-*N*-methylcarbox-amide [IB-MECA]) is sensitive to *P*Tx, thapsigargin-induced SOCE is not. Ca^{2+}-induced activation of PI3Kγ only occurs after SOCE, and is therefore clearly separated from the GPCR/trimeric G protein/PI3Kγ axis.

PKCβ Links Ca^{2+} Mobilization to PI3Kγ Activation

Protein kinase C (PKC) inhibitors (Ro318425, Gö6983, Gö6976) targeting classical and atypical PKCs, and the inhibitor PKC412, which mainly inhibits classical PKCs, all substantially blocked PKB/Akt phosphorylation in response to thapsigargin and phorbol 12-myristate 13-acetate (PMA) (Figures 3A and S2A). Rottlerin, with a limited selectivity for PKCδ, had no effect on PKB/Akt activation. GPCR-dependent PI3Kγ activation by adenosine was resistant to all tested PKC inhibitors (Figure S2B). The inhibitor profile suggested that a classical PKC activates PI3Kγ. While PKB/Akt activation by PMA and thapsigargin was blocked in PKCβ$^{-/-}$ BMMCs (Figure 3B), signaling in PKCα$^{-/-}$ and PKCγ$^{-/-}$ BMMCs remained intact (Figure S2C). Deletion of PKCβ eliminated phosphorylation of PKB/Akt on Thr308 and Ser473 completely, whereas a residual signal on Ser473 was observed after PI3K-inhibition by wortmannin. This may be explained by the observation that PKCβ2 can function as a Ser473 kinase [18]. Adenosine, IL-3, and stem cell factor (SCF)-induced PKB/Akt activation was not affected by elimination of PKCβ (Figure 3C), demonstrating that PKCβ does not relay adenosine signals to PI3Kγ, and is not required in cytokine and growth factor receptor-dependent activation of class IA PI3Ks in mast cells.

The direct measurement of phosphoinositides in BMMCs confirmed that ablation of PKCβ or its inhibition eliminated production of PtdIns(3,4,5)P_3 triggered by thapsigargin and PMA, but not adenosine (Figure 3D–3F). Interestingly, the link between PKCβ and PI3Kγ seems to be transient in nature, as PMA stimulation triggers short lived PtdIns(3,4,5)P_3 peaks (Figure 3F). Impaired FcεRI-triggered degranulation has been reported in both p110γ$^{-/-}$ [9] and PKCβ$^{-/-}$ BMMCs [19], and the sensitivity of degranulation to PKC inhibition fits the phospho-PKB/Akt output (Figure 3G). This, combined with the similarity of p110γ and PKCβ null phenotypes in IgE/antigen-induced degranulation (Figure 3H), suggests a direct link of PKCβ and PI3Kγ downstream of FcεRI.

PKCβ Binds and Phosphorylates PI3Kγ

Co-expression of p110γ with tagged full length or truncated PKCβ2 (Figure 4A) revealed that only the catalytic domain fragment and a pseudo-substrate deletion mutant of PKCβ2 formed complexes with p110γ (Figure 4B), suggesting that the presence of the pseudo-substrate in PKCβ results in a closed conformation that is unable to interact with p110γ. An in vitro protein kinase assay with recombinant PKCβ2 and glutathione S-transferase (GST)-tagged wild type p110γ or catalytically inactive p110γ (KR; Lys833Arg mutant) as substrate, showed that PKCβ robustly phosphorylated p110γ (Figure 4C). The capability of p110γ to auto-phosphorylate [20] was not required in the process.

Analysis of phosphorylated, catalytically inactive p110γ by liquid chromatography tandem mass spectrometry (LC-MS/MS) identified Ser582 as a target residue of PKCβ (YES^{P}[582]LKHPK; spectra in Figure S3). Mass spectrometric multiple reaction monitoring (MRM) (Figure S3C) showed that Ser582 phosphorylation was absent in assays lacking PKCβ, or when PKC-inhibitor was added (Figure 4D). Ser582 phosphorylation was also detected by MRM in PMA and IgE/antigen stimulated BMMCs (Figure 4D, lower panel).

Phospho-Ser582 site-specific antibodies (see Figure S4) revealed p110γ Ser852 phosphorylation in PMA-, thapsigargin-, and IgE/antigen-stimulated BMMCs, but not in mast cells exposed to adenosine or IgE alone (Figure 5A). Consistent with the requirement of Ca^{2+} mobilization, IgE/DNP-induced phosphorylation of p110γ on Ser582 was blocked by extracellular (EDTA, EGTA) and intracellular (BAPTA/AM) Ca^{2+} chelation (Figure 5B).

Although the extended peptide around Ser582 scores as a PKC substrate site, the core Arg-X-X-Ser582 sequence is a putative recognition site for several protein kinases (scores are PKC>protein kinase A>calcium/calmodulin-dependent kinases [CAMK]). As mast cell activation is accompanied by a massive influx of extracellular Ca^{2+}, we assessed if CAMK could phosphorylate p110γ directly. In the presence of ^{32}P-γ-ATP, recombinant CAMKII (CAMK2) incorporated equal amounts of phosphate into free and p84-bound p110γ. In the same experiment, PKCβ preferentially phosphorylated free p110γ, illustrating a preference

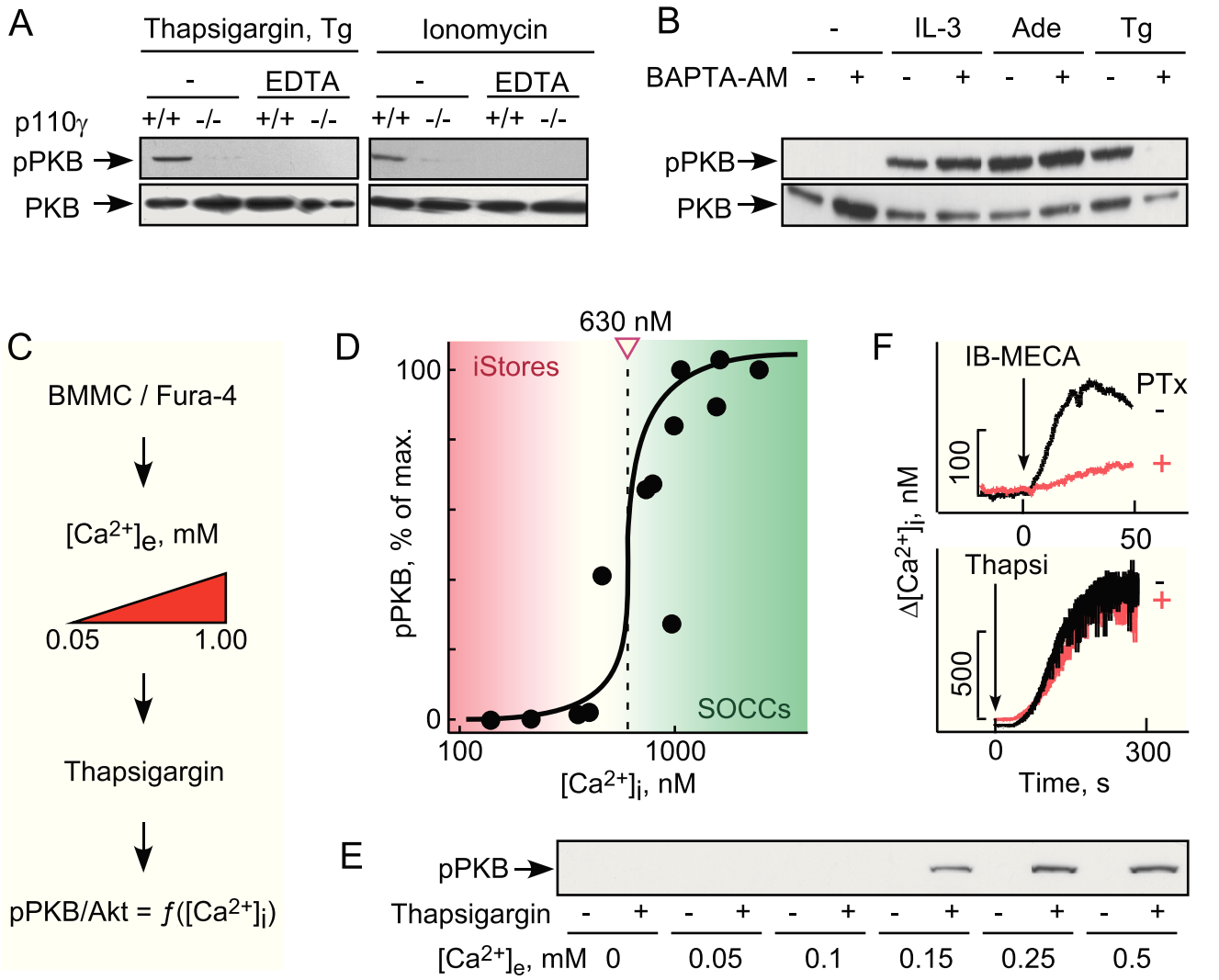

Figure 2. Thapsigargin-triggered PI3Kγ activation requires influx of extracellular Ca^{2+}. (A) Where indicated, IL-3 starved BMMCs were incubated with EDTA (5 mM) for 5 min, before cells were stimulated with thapsigargin (1 μM) or ionomycin (1 μM). Cells were lysed 5 min after stimulation, and phosphorylation of PKB/Akt on Ser473 was analyzed. (B) BMMCs as in (A) were pretreated for 10 min with the cell-permeable Ca^{2+}-chelator BAPTA/AM (10 μM) and stimulated either with IL-3 (10 ng/ml), adenosine (1 μM), or thapsigargin (1 μM). (C, D) BMMCs were loaded with the ratiometric low affinity Ca^{2+} probe Fura-4F/AM for 10 min in physiologic HEPES buffer at 1 mM Ca^{2+} (for details see Text S1). After the loading, washed cells were resuspended in the presence of increasing Ca^{2+} concentrations (extracellular Ca^{2+}, $[Ca^{2+}]_e$) to modulate maximal stimulation-induced intracellular Ca^{2+} levels ($[Ca^{2+}]_i$). Cells were then stimulated with 0.5 μM thapsigargin, and maximal $[Ca^{2+}]_i$ increase and phosphorylation of PKB/Akt were measured. pPKB S473 levels are displayed as a function of the individually determined $[Ca^{2+}]_i$. Data points come from two independently performed experiments. (E) Representative anti-phospho-PKB/Akt immunoblot as used to determine pPKB/Akt levels in (D). (F) Intracellular Ca^{2+} concentrations were measured in wild type BMMCs following stimulation with the adenosine 3A receptor-selective agonist N^6-(3-iodobenzyl)-adenosine-5′-*N*-methylcarbox-amide (IB-MECA) (10 nM) or thapsigargin (1 μM). *B. Pertussis* toxin (100 ng/ml) was added 4 h before stimulation where marked.
doi:10.1371/journal.pbio.1001587.g002

of PKCβ for p110γ surfaces obscured in the p84-p110γ complex. CAMK also substantially phosphorylated p84, which was borderline in in vitro assays with PKC (12 versus 3 mol %) (Figure S5A). Probing the phosphorylation of Ser582 in vitro demonstrated that access to this site is blocked when p84 is bound to p110γ (Figure S5B).

In cellular assays stimulating BMMCs with thapsigargin, CAMK activation could be monitored using anti-phospho-CAMKII antibodies. While PKC inhibitors left CAMKII phosphorylation >50% intact, Ser582 and PKB/Akt phosphorylation were both reduced to background levels (Figure S6), even in a context favoring Ca^{2+}-triggered responses. The above, and the fact that PKCβ$^{-/-}$ BMMCs showed a major reduction in phospho-Ser582 after PMA or IgE/antigen stimulation (Figure 5C and 5D), illustrate that phosphorylation of p110γ is mainly mediated by PKCβ, and that other PKC isoforms (see also Figure S2) and Ca^{2+}-dependent kinases attribute to less than 18% of the observed overall signal.

Phosphorylation of Ser582 Positively Regulates p110γ's Activity and Displaces p84

To evaluate if the Ser582 phosphorylation affected the intrinsic activity of p110γ, a phosphorylation-mimicking mutant (Ser582-Glu) was produced. The activity of the p110γ Ser582Glu mutant

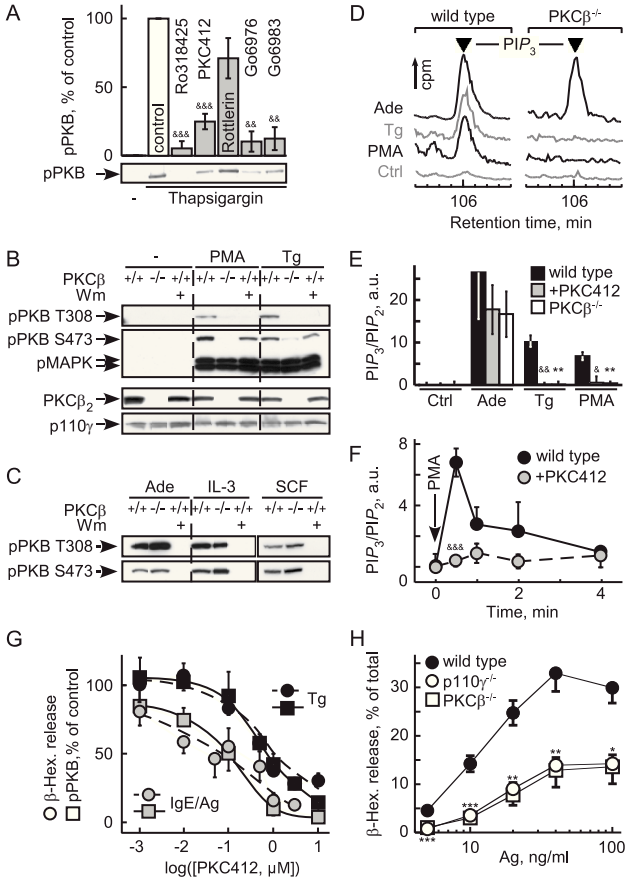

Figure 3. PKCβ relays thapsigargin-induced PI3Kγ activation. (A) Effect of PKC inhibitors on thapsigargin-induced PKB phosphorylation on Ser473 (S473). IL-3 starved BMMCs were preincubated with the indicated compounds for 20 min before stimulation (pan-PKC: Ro318425, Gö6983; classical PKC: PKC412 (CPG41251); classical and atypical PKC: Gö6976; Rotterlin: broad band inhibitor; see Text S1; & refers to comparison with untreated control; *p*-values see Figure 1). (B) PKB/Akt activation in response to 100 nM PMA or 1 μM thapsigargin was analyzed in wild type and PKCβ$^{-/-}$ BMMCs. Cells were IL-3 deprived as in (A), and were pretreated with wortmannin (Wm, 100 nM) for 15 min before stimulation where indicated. Cells were lysed 2 min after stimulation, and analyzed for phosphorylation of PKB/Akt (T308 and S473) and MAPK (T183/Y185). (C) Wild type and PKCβ$^{-/-}$ BMMCs were stimulated with 1 μM adenosine, 10 ng/ml IL3, or 10 ng/ml SCF, and processed as in (B). (D–F) PtdIns(3,4,5)P_3 (PIP_3) levels were determined in untreated (Ctrl) and classical PKC-inhibitor (PKC412)-treated wild type BMMCs and PKCβ$^{-/-}$ BMMCs after stimulation with 0.5 μM thapsigargin, 200 ng/ml PMA, or 5 μM adenosine (30 s). BMMCs were metabolically labeled with [^{32}P]-orthophosphate, lipids were extracted, deacylated, and applied to high-pressure liquid chromatography (HPLC). (D) shows representative elution peaks of PIP_3 of the HPLC chromatograms. (E) Levels of PIP_3 in relation to PtdIns(4,5)P_2 (PIP_2) were quantified by integration of the peak areas of PIP_3 and PIP_2 and expressed as ratio of PIP_3/PIP_2 (data shown as mean ± standard error of the mean [SEM], $n \geq 4$–6). (F) Cellular PIP_3 production was measured over time in wild type BMMCs in response to PMA (200 nM) stimulation in the presence or absence of the classical PKC inhibitor PKC412 (mean ± SEM, $n = 3$). (G) Granule release and PKB activation (S473) in response to thapsigargin (1 μM) or IgE/antigen (100 ng/ml IgE overnight, 10 ng/ml DNP) was measured in the presence of increasing concentrations of the classical PKC inhibitor PKC412. Cells starved as in (A) were stimulated with IgE/antigen (IgE/Ag) or thapsigargin (Tg), and PKB phosphorylation and β-hexosaminidase release assays were performed in parallel (mean ± SEM, $n = 3$). (H) β-hexosaminidase release determined in wild type, PKCβ$^{-/-}$, and p110γ$^{-/-}$ BMMCs incubated with IgE, and stimulated with the indicated antigen (Ag) concentrations (mean ± SEM, $n = 5$; * refer to comparison with wild type control. Only the higher *p*-values of the overlapping data points are indicated).
doi:10.1371/journal.pbio.1001587.g003

was enhanced approximately 2-fold independently of the substrate used (PtdIns(4,5)P_2, PtdIns, or auto-phosphorylation) (Figure 6A–6C). Ser582 is localized in the helical domain of p110γ, and it is interesting to note that helical domain mutants of p110α found in tumors display a similar increase in enzyme activity [21–25].

As mutations in the helical domain of p110α attenuate contacts with the p85 regulatory subunit [21], we examined binding of p110γ mutants to the PI3Kγ adaptor subunit p84: the substitution of Ser582 with Glu and Asp, abrogated p110γ-p84 interactions in HEK293 cells and BMMCs, while the Ser582Ala replacement favored p110γ-p84 complex formation (Figure 6D–6F). In line with this, PMA-induced phosphorylation of Ser582 in BMMCs was suppressed by the overexpression of p84 (Figure 6G), which fits the very limited access of PKCβII to in vitro phosphorylate Ser582 in the p110γ-p84 complex (reduced to 20% of phosphorylation of free p110γ) (Figure S5B).

Most importantly, the correlation of phosphorylation of Ser582 on p110γ and the release of p84 could also be established in wild type BMMCs: when stimulated with PMA, the amount of p84 that could be co-precipitated with p110γ was reduced significantly, and was linked to Ser582 phosphorylation of p110γ. In the inverse co-immunoprecipitation, anti-p84-associated p110γ was reduced, and phosphorylation was below detection levels in the remaining p84-associated p110γ (Figure S7). The collected results are in agreement with a mechanism in which PKCβII-mediated phosphorylation of Ser582 and the interaction of p84 and p110γ are exclusive events, and in which PKCβ action displaces p84 from p110γ.

The Helical Domain of p110γ Binds and Is Stabilized by p84

In order to understand how p84 could mask Ser582 phosphorylation, and to map the p110γ-p84 contact interface, hydrogen deuterium exchange mass spectrometry (HDX-MS) was used. HDX-MS elucidated contacts of class IA p110δ with its p85 regulatory subunit, and the mechanism of action of cancer-linked mutations in p110α [25,26]. HDX-MS relies on amide hydrogen exchange with solvent at a rate dependent on their involvement in secondary structure and solvent accessibility. Following proteolysis, location and extent of deuterium uptake are analyzed by peptide mass determination. The primary sequence of p110γ was covered >90% by 202 peptide fragments (Figure S8; Table S1).

Deuterium (^{2}H) incorporation into free and p84-complexed p110γ was analyzed at seven time points (3 to 3,000 s). Differences in ^{2}H-exchange of free and complexed p110γ were mapped onto the crystal structure of p110γ lacking the N-terminal domain (PDB ID:2CHX, residues 144–1,093), to visualize conformational changes induced by p84 (Figures 7A, S9, and S10). Peptides with highest decrease in ^{2}H incorporation (>1.0 Da) clustered to the RBD-C2 linker, the C2-helical domain linker, and the helical domain. The ^{2}H-incorporation in the presence of p84 is visualized as integrated average difference in exchange at all seven time points in Figure 7B, illustrating that the helical domain provides the dominant interface with p84. Due to difficulties in producing free p84, the contacts on p84 with p110γ could not be mapped. Interestingly, in the absence of the p84 subunit, the majority of peptides in the helical domain exhibited broad isotopic profiles (HDX of peptide 623–630, which is representative of peptides in the helical domain, is shown in Figures 7C and S11). This type of profile known as type 1 exchange (EX1) kinetics is indicative of

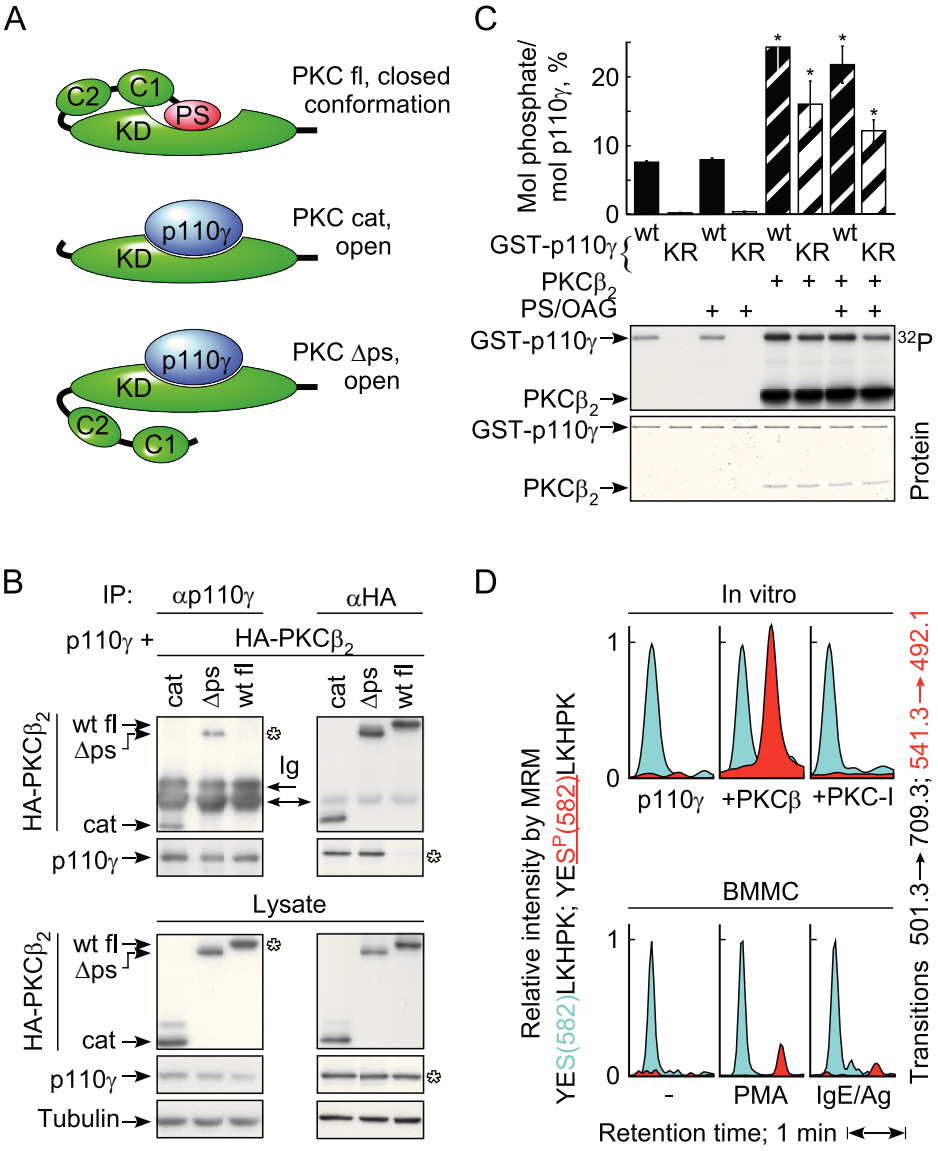

Figure 4. PKCβ interacts with and phosphorylates the catalytic subunit of PI3Kγ. (A) Schematic representation of the PKCβ-p110γ interaction: full-length (fl) PKCβ is in a closed conformation due to the interaction of the pseudo-substrate domain with the catalytic pocket of PKCβ, while the truncated catalytic domain (cat; amino acids 302–673) and pseudo-substrate deletion mutant (Δps; deletion of aa 19–31) give access to p110γ. (B) HEK293 cells were co-transfected with p110γ and HA-tagged PKCβ2 constructs. Protein complexes were immunoprecipitated with anti-p110γ or anti-HA antibodies, before HA-PKCβ2 and p110γ was detected by immunoblotting. Ig: immunoglobulin heavy chain signals of mouse anti-p110γ and anti-HA antibodies. (C) Recombinant GST-p110γ wild type (wt) or a catalytically inactive p110γ mutant (KR, Lys833Arg mutant) were incubated with recombinant PKCβ2 and [γ^{32}P]-ATP in kinase buffer for 30 min, before proteins were denatured and separated by SDS-PAGE. Phosphatidylserine (PS) lipid vesicles containing 1-oleoyl-2-acetyl-sn-glycerol (OAG) were present during the reaction where marked. Protein-bound ^{32}P was determined by radioisotope imaging, and recombinant proteins were stained with Coomassie blue (mean ± standard error of the mean [SEM], $n = 3$; * point to comparison with respective sample without PKC). (D) In vitro and in vivo phosphorylation of PI3Kγ on S582, analyzed by LC-MRM. S582 non-phospho- and phospho-peptides were detected in the MRM mode, quantifying the transition 501.1 to 709.3 for the non-modified peptide (blue) and 541.3 to 492.1 for the phospho-peptide (red). Data were normalized to the transition of the non-modified peptide, which was set to 1. Upper part: recombinant catalytically inactive human GST-PI3Kγ (2 μg) was incubated alone, together with PKCβ2 or with PKCβ2 and PKC-inhibitor (Ro318425, 2 μM) as in (C). After SDS-PAGE and Coomassie staining, PI3Kγ was excised from the gel and prepared for LC-MRM. Lower part: wild type BMMCs (300 M cells/stimulation) were starved for 4 h in IL-3 free medium/2% FCS, and were left unstimulated or were treated for 2 min with 50 nM PMA or for 4 min with 10 ng/ml antigen (cells preloaded with 100 ng/ml IgE overnight). Endogenous PI3Kγ was immunoprecipitated from cell lysates, resolved by SDS-PAGE and analyzed with LC-MRM.
doi:10.1371/journal.pbio.1001587.g004

concerted dynamic motions of a substructure in a protein, rather than the local fluctuations characteristic of EX2 kinetics [27].

The N-terminus of p110γ was shown to stabilize the p110γ-p101 heterodimer [28]. Expression of p110γ mutants lacking the first 130 amino acids (Δ130–p110γ) seemed to support this view, as association with p84 was lost (Figure 7D). However, when truncated p110γ was N-terminally tagged with GST (GST-Δ130-p110γ), binding of p84 was restored. Although we detected a small decrease in the ^{2}H-incorporation in two N-terminal p110γ peptides (59–70 and 107–113) in the presence of p84, this

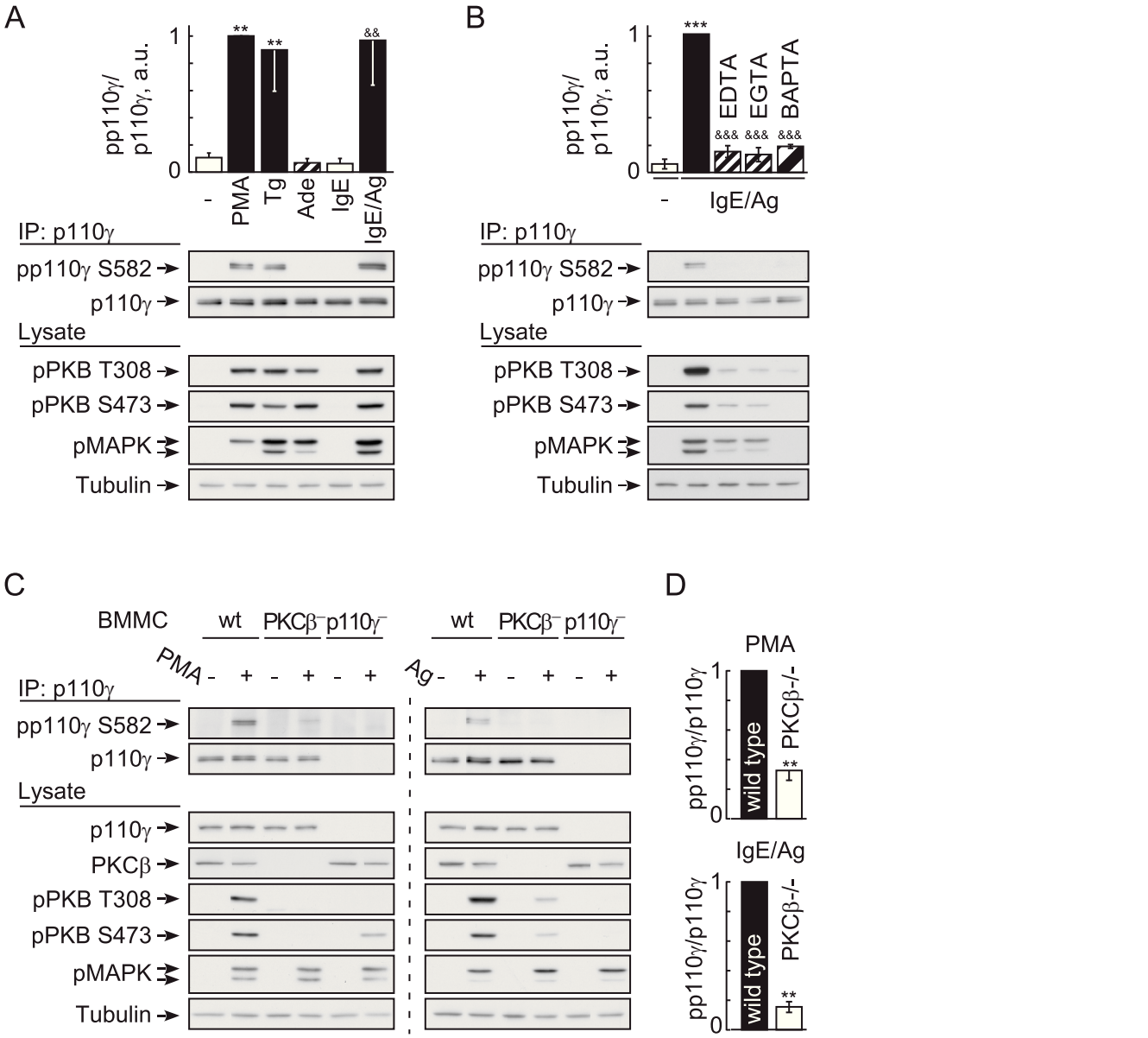

Figure 5. Phosphorylation of PI3Kγ requires Ca^{2+} and is PKCβ-dependent. (A) Stimulus-induced phosphorylation of endogenous p110γ on Ser582 in wild type BMMCs. IL-3 deprived cells were stimulated with 100 nM PMA, 1 μM thapsigargin, 1 μM adenosine, or 20 ng/ml DNP for 2 min. Where indicated (IgE), BMMCs were loaded with IgE (100 ng/ml) overnight. PI3Kγ was immunoprecipitated from cell lysates with an anti-PI3Kγ antibody, before precipitated protein was probed for phosphorylated p110γ (pp110γ) with a phospho-specific anti-pSer582 antibody (validation of antibody see Figure S4). PI3Kγ phosphorylation is shown normalized to total PI3Kγ levels (mean ± standard error of the mean [SEM], $n = 3$; * depict analysis using unstimulated control. & reference point is IgE only). (B) IgE/antigen-induced Ser582 phosphorylation of p110γ requires Ca^{2+} influx. Cells were stimulated as in (A), but exposed to EDTA, EGTA, or loaded with BAPTA/AM where indicated (see Figure 2). Phosphorylated p110γ was detected as in (A); mean ± SEM, $n = 3$; * comparison with unstimulated control; $^{\&}$analysis of stimulated versus chelator treated). (C) Phosphorylation of p110γ in wild type and PKCβ$^{-/-}$ BMMCs. Experimental settings were as in (A), and (D) depicts quantification of pp110γ in relation to total p110γ protein (mean ± SEM; PMA $n = 4$, antigen $n = 3$). Cells devoid of p110γ were included as negative control.
doi:10.1371/journal.pbio.1001587.g005

interaction seems to be dispensable. The N-terminus of p110γ instead has a role in stabilizing the intact catalytic subunit. The helical domain is the main location of interaction with p84; however, it appears that this interaction is vulnerable and easily broken, as a single phosphorylation at Ser582 is able to disrupt the contact.

Discussion

The activation of PI3Kγ has been tightly linked to GPCRs-triggered dissociation of trimeric Gαi proteins, and has been shown to require the interaction of Gβγ subunits with p110γ and the PI3Kγ adaptor subunits p101 and p84 [1,2,4,16,29,30]. Moreover, GPCRs generate PI3K signals typically through PI3Kγ, thereby controlling extravasation of hematopoietic cells [31,32], cardiovascular parameters [33,34], and metabolic output [35,36].

Non-GPCR-mediated activation of PI3Kγ has not been reported so far, but it has been shown that phorbol esters and Ca^{2+} ionophores can modulate phosphoinositide levels in a variety of cells, including platelets [37], adipocites [38], fibroblasts [39], and hematopoietic cells [40]. The proposed mechanisms have

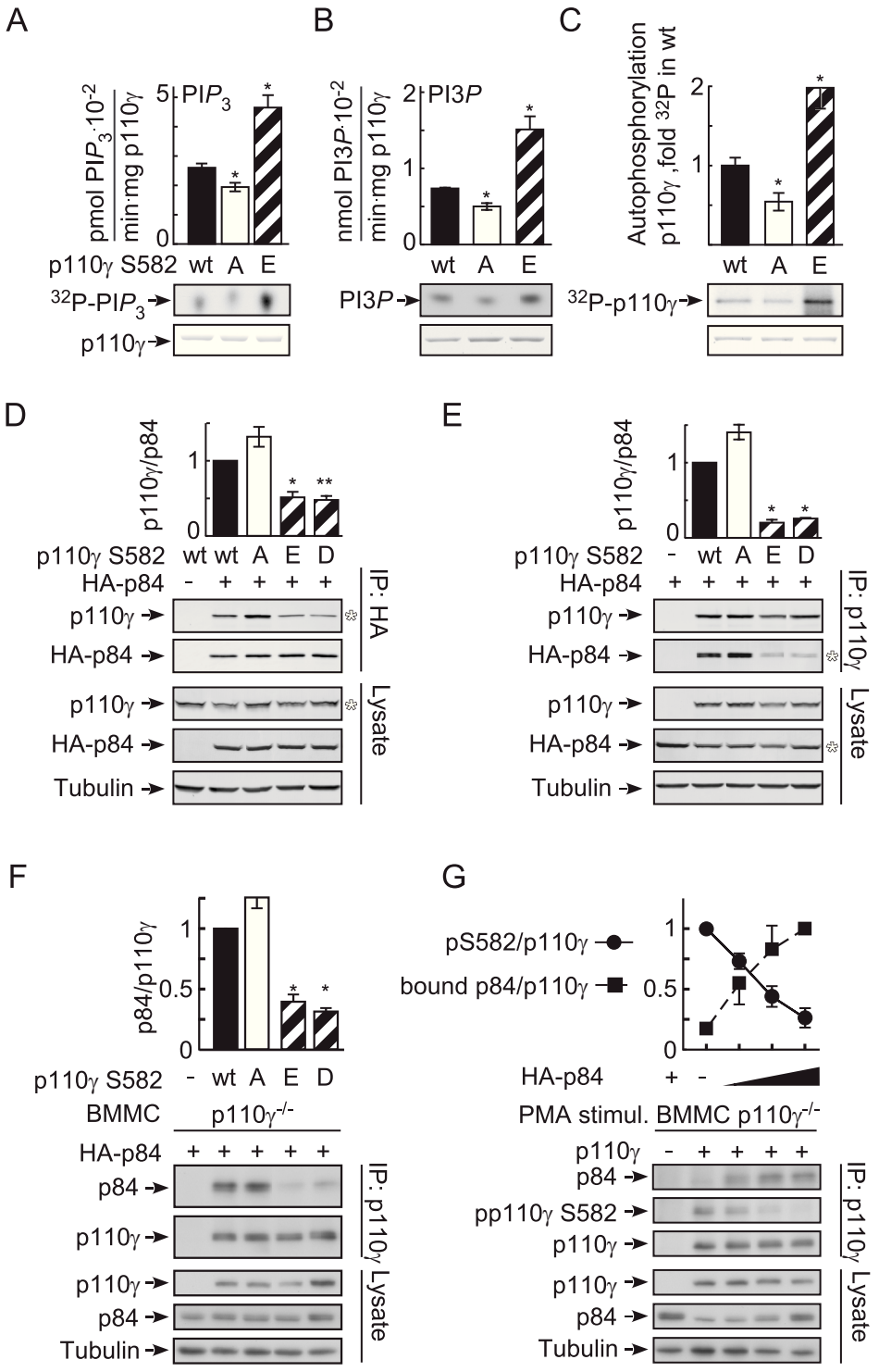

Figure 6. Ser582 phosphorylation increases p110γ activity and displaces p84. (A–C) Lipid and protein kinase activities of recombinant p110γ wild type (wt) and phosphorylation site mutants (Ser582Ala, [A]; Ser582Glu, [E]). (A) Mixed phospholipid vesicles containing PtdIns(4,5)P_2 were used to measure PtdIns(3,4,5)P_3 (PIP_3) production, while in (B) PtdIns was used as a substrate. Protein kinase activity of p110γ was determined by auto-phosphorylation in (C). Bars display quantifications of incorporated ^{32}P as mean ± standard error of the mean [SEM] ($n = 3$; * comparison with wt protein), and representative thin layer chromatograms [^{32}P] and loaded p110γ protein (Coomassie blue) are shown below. (D, E) Wild type p110γ and Ser582 mutants (Ser582Asp, [D]) were expressed together with HA-tagged p84 in HEK293 cells. In (D), the PI3Kγ complex was immunoprecipitated with anti-HA antibodies directed against HA-p84 ($n = 4$). In (E) PI3Kγ was immunoprecipitated using anti-p110γ antibodies ($n = 2$). (F) Wild type p110γ and Ser582 mutants were co-expressed with p84 in p110$\gamma^{-/-}$ BMMCs. PI3Kγ was immunoprecipitated from cell lysates as in E (mean ± SEM, $n = 3$). (G) The p84 adapter competes with PKCβ for access to p110γ. Increasing amounts of HA-p84 expression plasmid were transfected into p110$\gamma^{-/-}$ BMMCs, before the cells were stimulated with PMA for 30 s. PI3Kγ was subsequently immunoprecipitated with an anti-p110γ antibody, and bound p84 and Ser582 phosphorylation were quantified. The values are normalized to total p110γ protein (mean ± SEM, $n = 2$).
doi:10.1371/journal.pbio.1001587.g006

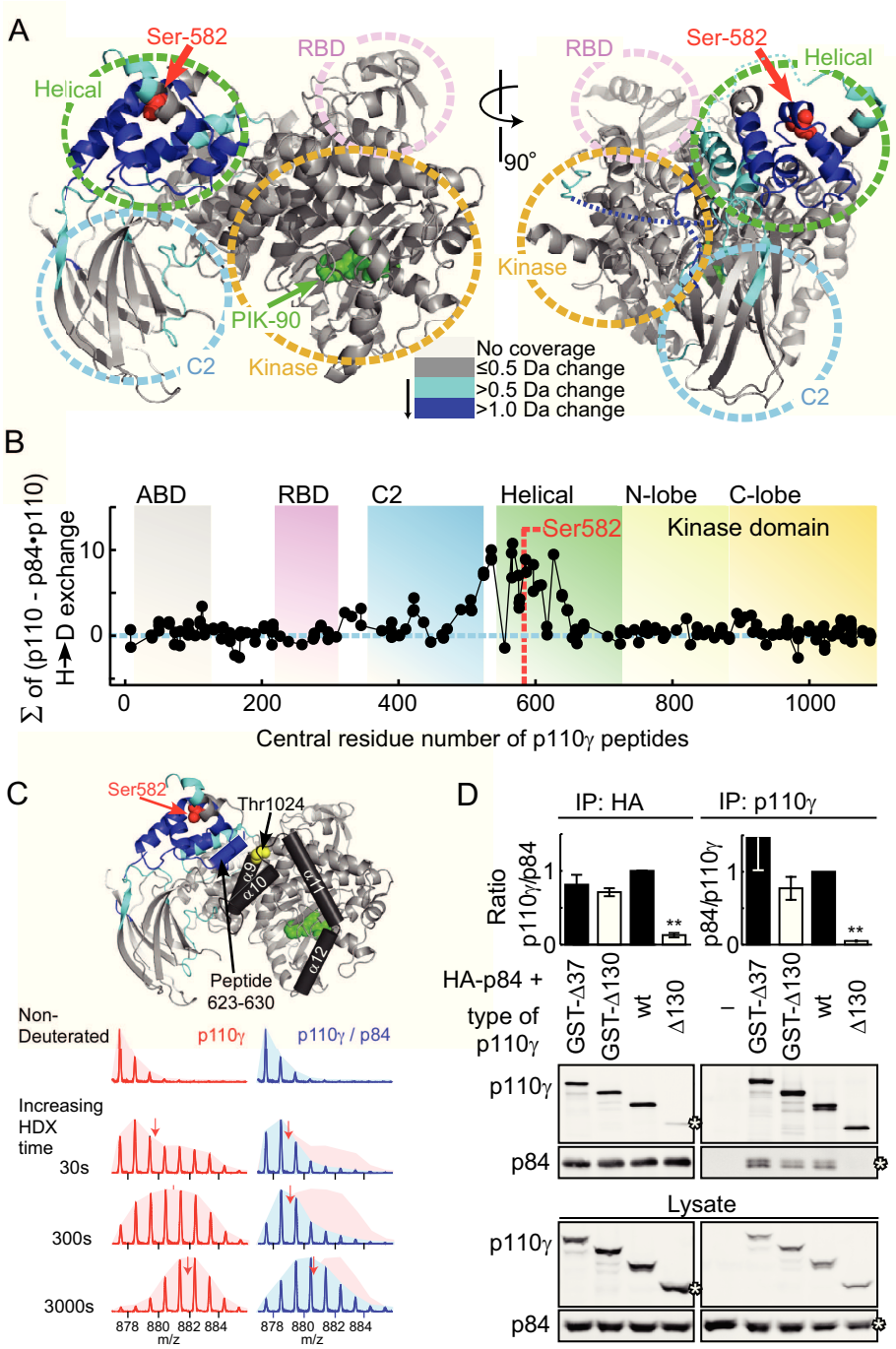

Figure 7. p84 Interacts with the helical domain of p110γ. (A) Changes in deuteration levels between free and p84-bound PI3Kγ are mapped onto the crystal structure of PI3Kγ (PDB ID: 2CHX). Regions that are covered by peptides of PI3Kγ (labeled A–R) that showed greater than 0.5 or 1.0 Da changes in deuteration are colored light or dark blue, respectively. The greatest difference in exchange observed at any time was used for the mapping. S582 is labeled red. The ATP competitive inhibitor PIK-90 in the crystal structure is shown in green as a reference point for the kinase domain. The linker regions between the RBD and the C2 domain and the C2 and the helical domain are shown as dotted lines (right part). (B) The percent deuterium exchange differences between free and p84-bound PI3Kγ were summed up over all seven time points for every identified peptide (*y*-axis), which were graphed according to their central residue number (*x*-axis). (C) A selected peptide (623–630) from the helical domain is shown at four time points of H/D on-exchange +/− the p84 subunit. In the absence of the p84 adaptor the majority of peptides in the helical domain showed broadening of the isotopic profiles indicative of EX1 kinetics (see 30, or 300 s in free p110γ). The helix A3 (624–631) selected is located at the interface of the helical domain with the C-lobe. Ser582 and Thr1024 have been highlighted as a reference. (D) p84 was coexpressed with GST-tagged or untagged PI3Kγ constructs in HEK293 cells. N-terminal deletions of 37 or 130 amino acids are denoted Δ37 or Δ130, respectively. HA-p84 (left) or PI3Kγ (right) was immunoprecipitated from cell lysates with anti-HA or anti-PI3Kγ antibodies and protein G beads. PI3Kγ-p84 interactions were analyzed by Western blotting, quantified with Odyssey Imager software and expressed as fold of untagged, full-length p110γ-p84 association (mean ± standard error of the mean [SEM], left: $n = 4, 6, 6, 6$; right: $n = 2, 4, 4, 4$).
doi:10.1371/journal.pbio.1001587.g007

been diverse and involved protein tyrosine kinases and GPCR signaling. A recent finding that protein kinase D (PKD) can phosphorylate two distinct sites on the p85 regulatory subunit to control class IA PI3K activity [41] is an indication that PI3K control is more complex than anticipated.

PI3Kγ has been shown to be a key element in enhancing IgE/antigen output by the release of adenosine. This process involves signaling downstream of Gαi-coupled A_3AR, and is sensitive to *P*Tx and ADA [9]. The resistance of thapsigargin-induced degranulation to ADA shown here, and the fact that *P*Tx did not diminish the PI3Kγ-dependent, thapsigargin-induced phosphorylation of PKB/Akt, points to a novel mechanism of PI3Kγ activation, which is clearly distinct from GPCR action. This Ca^{2+}-mediated PI3Kγ activation requires SOCE and $[Ca^{2+}]_i$ >600 nM. In contrast, GPCRs yield phosphorylation of PKB/Akt in mast cells even in the absence of a change in $[Ca^{2+}]_i$. Furthermore, increases in $[Ca^{2+}]_i$ triggered via GPCRs remain at levels incapable of engaging a Ca^{2+}-dependent activation of PI3Kγ.

Thapsigargin bypasses the signaling chain from IgE/antigen-clustered FcεRI to the activation of phospholipase Cγ (PLCγ) and inositol(1,4,5)-trisphosphate (Ins(1,4,5)P_3) production, and triggers SOCE by the depletion of Ca^{2+} stores. That thapsigargin requires functional PI3K activity to induce mast cell degranulation was first demonstrated using the PI3K inhibitors wortmannin and LY294002 [14], but no link between $[Ca^{2+}]_i$ rise and PI3Kγ activity was established previously. The fact that inhibitors for classical PKCs only prevented the thapsigargin- and PMA-induced phosphorylation of PKB/Akt, while the GPCR-mediated phosphorylation of PKB/Akt remained intact, points to a link between classical PKCs and PI3Kγ. Experiments on BMMCs lacking PKCα, PKCβ, and PKCγ, showed that only the PKCβ null cells lost the ability to activate PKB/Akt in response to thapsigargin or PMA stimulation. As the PMA- and thapsigargin-induced phosphorylation of PKB/Akt on Ser473 showed a partial resistance to wortmannin, and as it has been reported that PKCβ can directly phosphorylate Ser473 in the hydrophobic motif of PKB/Akt [18], the effect of genetic and pharmacological targeting of PKCβ was also validated measuring PtdIns(3,4,5)P_3 production directly. The lack of PtdIns(3,4,5)P_3 production in thapsigargin or PMA-stimulated BMMCs treated with the PKC inhibitor PKC412, and in cells devoid of PKCβ, is in agreement with a requirement of PKCβ upstream of PI3Kγ. That signaling from PKC to PI3K plays a role in mast cell degranulation is further supported by the close correlation of PKC inhibitor sensitivity of phosphorylated PKB/Akt and degranulation responses. Moreover, the loss of PKCβ or PI3Kγ results in a similar reduction of degranulation over a wide range of IgE/antigen concentrations. The results obtained here are in agreement with previous findings that mast cells and mice devoid of p85α/p55α/p50α [42,43] and p85β [44] remain fully responsive to IgE/antigen complexes. A previous report showed a biphasic activation of PI3K with PI3Kγ having an early role and PI3Kδ a later role downstream of FcεRI in murine mast cells [45,46].

A mechanistic link between PKCβ and the catalytic subunit of PI3Kγ was initially difficult to establish, as the direct PtdIns(3,4,5)P_3 response to PMA-stimulation was transient (main peak half life <1 min), and the two full-length enzymes interacted only weakly. The observation that truncated, activated forms of PKCβ formed stable complexes with p110γ, suggested that PKCβ must attain an open conformation to interact with p110γ, and that PKCβ binds to p110γ via its catalytic domain. This contact resulted in phosphorylation of Ser582 on p110γ, which could be detected both in vitro and in PMA or IgE/antigen-stimulated BMMCs by mass spectrometry. The PKCβ-mediated phosphorylation of p110γ was confirmed using site-specific anti-phospho-Ser582 antibodies. Stimuli like PMA, thapsigargin, and IgE/antigen complexes all required PKC to signal to PKB/Akt, which correlated with the phosphorylation of Ser582 on p110γ. Moreover, the phosphorylation of Ser582 on p110γ was sensitive to removal of extracellular Ca^{2+}, buffering of $[Ca^{2+}]_i$, and the genetic deletion of PKCβ. Adenosine stimulates PI3Kγ via GPCRs and *P*Tx-sensitive trimeric G proteins [9] in a Ca^{2+}-independent process, and did not yield a detectable phosphorylation of Ser582.

The increased turnover of PtdIns and PtdIns(4,5)P_2, and the increased rate of auto-phosphorylation displayed by p110γ with a phosphate-mimicking mutation (Ser582Glu), suggests that a structural change in the helical domain of p110γ is sufficient to increase the catalytic activity independent of the presence of the p84 subunit. Previous work examining the activation of the class IA p110α, p110β, and p110δ catalytic subunits has shown that part of the activation mechanism occurs through a conformational change from a closed cytosolic form to an open form on membranes [25,26]. The helical domain of p110γ is exquisitely well placed to propagate conformational changes due to the fact that it is in contact with every other domain in p110γ. In the crystal structure of N-terminally truncated (Δ144) p110γ, the side chain of Ser582 points inward [47,48], and has to rotate to accommodate a phosphate. Our HDX-MS results showed a dynamic "breathing" motion in the helical domain in the free p110γ catalytic subunit that may allow for temporary exposure of Ser582, enabling modification by PKC. HDX results showed that the p84 subunit slowed or prevented this dynamic motion, and this correlated with a decreased efficiency of phosphorylation by PKC in cells in the presence of p84.

Although Ser582 is not in a direct contact with the kinase domain, it is structurally linked to it: the heat repeat HA1/HB1 housing Ser582, and the connecting intra-helical loop (residues 560 to 570), along with helix A3 (624–631) are in contact with helices kα9 and kα10 in the C-lobe of the kinase domain (known as the regulatory arch [49,50]) and could transduce a conformational change to the catalytic center of p110γ (Figure 7C). The phosphorylated Ser582 and phosphorylation-mimicking mutants may activate lipid kinase activity by causing a conformational shift at this interface. It has been shown recently that this region of the p110γ kinase domain is critical in regulating lipid kinase activity, as phosphorylation of Thr1024 in the kα9 by protein kinase A (PKA) negatively regulates p110γ activity in vitro and in cardiomyocytes (Figure 7C) [51].

In contrast to the p110α-p85 heterodimer, stabilized by the N-terminal adaptor-binding domain (ABD)/inter SH2 domain interaction, the association of the p110γ subunit with its adaptor subunit is quite vulnerable, and the Ser582Glu mutant, but not Ser582Ala, abrogated the formation of a p110γ-p84 complex. HDX-MS revealed that the helical domain of p110γ was stabilized by p84. Ser582 is located in the center of the p110γ-p84 contact surface, which explains how a change in charge (Ser582Glu) breaks the interaction with p84, either by direct contact or by destabilization of the helical domain. Overexpression of p84 shields p110γ from a PMA-induced phosphorylation, and suggests that binding of p84 to p110γ, and Ser582 phosphorylation by PKCβ are mutually exclusive. This implies that the two activation modes of PI3Kγ—by GPCRs or PKCβ—are completely separated. At low $[Ca^{2+}]_i$, PI3Kγ is exclusively activated by Gβγ subunits. It has been demonstrated that a PI3Kγ adapter protein is absolutely needed for functional GPCR inputs to p110γ [6]. If the interaction of p84 with p110γ is blocked by the phosphorylation of

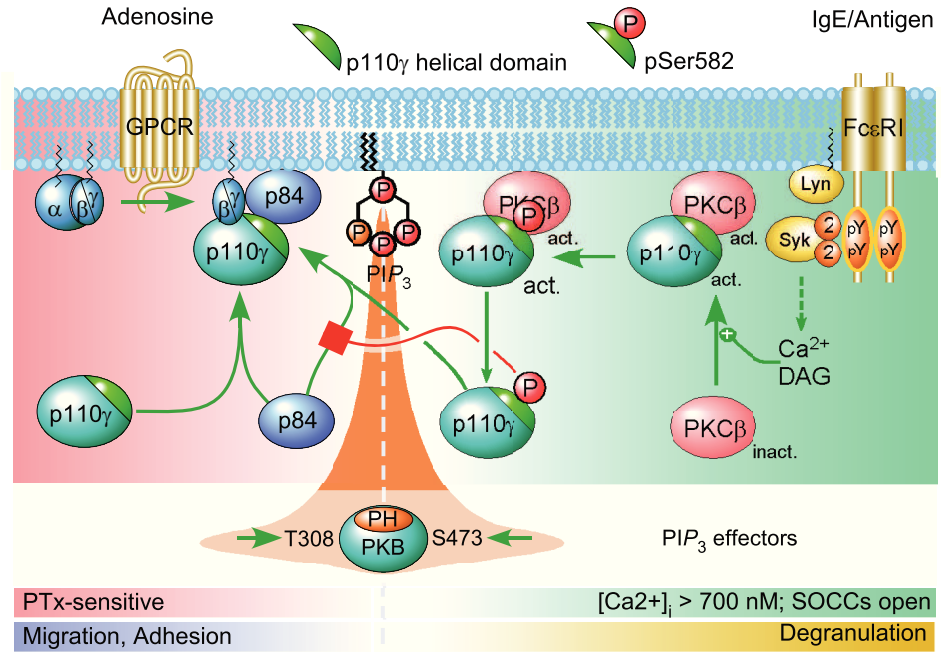

Figure 8. Phosphorylation of Ser582—loss of GPCR coupling of p110γ. In a resting mast cell, the PI3Kγ complex is responsive to GPCR-mediated dissociation of trimeric G proteins. An adapter protein (here p84) is required for a productive relay of the GPCR signal to PI3Kγ. When FcεRI receptors are clustered via IgE/antigen complexes, a signaling cascade is initiated, which triggers the depletion of intracellular Ca^{2+} stores and the opening of store-operated Ca^{2+} channels. The resulting increase in $[Ca^{2+}]_i$ and PLCγ-derived diacylglycerol activate PKCβ, which binds to p110γ and subsequently phosphorylates Ser582 (→pp110γ). Phosphorylated p110γ cannot interact with p84, and is therefore unresponsive to GPCR inputs. GPCR input to PI3Kγ coincides with migration and adhesion, while Ca^{2+}/PKCβ activation of p110γ occurs when mast cells degranulate. The phosphorylation of PKB/Akt occurs downstream of PtdIns(3,4,5)P_3, which originates from G protein-activated p84-p110γ complex or PKCβ-activated pp110γ. The phosphorylated residues Thr308 and Ser473 of PKB/Akt are used to monitor PI3K activation. More detailed effector signaling event schemes can be found in [52].
doi:10.1371/journal.pbio.1001587.g008

Ser582, p110γ is decoupled from its GPCR input (for a schematic view of the process see Figure 8). The PKCβ-mediated activation and phosphorylation of p110γ constitutes therefore an unprecedented PI3K molecular switch, which enables the operation of p110γ downstream of FcεRI signaling, and will elucidate cell type-specific activation processes in allergy and chronic inflammation.

Materials and Methods

Cells and Mice

BMMCs were derived from bone marrow of 8–12-wk-old C57BL/6J wild type, p110γ$^{-/-}$, PKCα$^{-/-}$, PKCβ$^{-/-}$, and PKCγ$^{-/-}$ mice, and cultured and characterized as described in [9]. Animal experiments were carried out in accordance with institutional guidelines and national legislation. Human embryonic kidney 293 (*HEK293*) cells were grown in DMEM supplemented with 10% HI-FCS, 2 mM L-glutamine, 100 units/ml penicillin, 100 µg/ml streptomycin. *Sf9* cells were cultivated in IPL-41 medium (Genaxxon Bioscience) supplemented with 10% HI-FCS, 2% yeastolate, 1% lipid concentrate, 50 µg/ml gentamicin (Invitrogen), and 2.5 µg/ml amphotericin B (Genaxxon Bioscience). Detailed descriptions and references are available in Text S1.

Cellular PdtIns(3,4,5)P_3 Measurements

PtdIns(3,4,5)P_3 levels have been measured as described in [9] with some modifications. BMMCs were cultured for 2 h in phosphate-free RPMI medium/2% FCS at 37°C and 5% CO_2, followed by labelling with 1 mCi/ml [^{32}P]-orthophosphate for 4 h. Cells were washed, stimulated, and lysed by the addition of chloroform/methanol (1:2, v/v, with butylated hydroxytoluene and carrier phosphoinositides). Lipids were extracted, deacylated, and separated by high-pressure liquid chromatography (HPLC).

In Vitro Lipid Kinase Assay

PI3Kγ-His_6 was incubated with PtdIns(4,5)P_2-containing lipid vesicles (PE/PS/PC/SM/PIP_2 = 30/20/10/4.5/1.2; PIP_2 final 5 µM), 10 µM ATP, and 4 µCi of [γ^{32}P]-ATP in lipid kinase buffer (40 mM HEPES [pH 7.4], 150 mM NaCl, 4 mM $MgCl_2$, 1 mM DTT [1,4-Dithio-DL-threitol], 0.1 mg/ml fatty-acid free BSA) for 10 min at 30°C. Alternatively, PtdIns/PS vesicles (~200 µM each) were used. Reactions were terminated by addition of 1 M HCl and $CHCl_3$/MeOH. Lipids were isolated by chloroform extraction, separated by TLC and quantified on a Typhoon 9400.

Statistical Analysis

Numeric results were tested for significance using a two-tailed Student's *t* test, (paired or unpaired, as imposed by datasets). * or $^{\&}$, ** or $^{\&\&}$, and *** or $^{\&\&\&}$ refer to *p*-values $p<0.05$, $p<0.005$, and $p<0.0005$. * and $^{\&}$ were used for comparison of different genotypes, stimuli an conditions as indicated. Calculations were carried out using Graph Pad Prism, Microsoft Excel, or Kaleidagraph software.

Deuterium Exchange Reactions

Protein stock solutions (5 µl; Hsp110γ-C-His_6: 30 µM; Hsp110γ-C-His_6/Mmp84-C-His_6: 35 µM) were prepared in 20 mM Tris [pH 7.5], 100 mM NaCl, 1 mM ammonium sulfate,

and 5 mM DTT. Exchange reactions were initiated by addition of 25 µl of a 98% D_2O solution containing 10 mM HEPES (pH 7.2), 50 mM NaCl, and 2 mM DTT, giving a final concentration of 82% D_2O. Deuterium exchange reactions were allowed to carry on for seven time periods, 3, 10, 30, 100, 300, 1,000, and 3,000 s of on-exchange at 23°C, before addition of quench buffer. On-exchange was stopped by the addition of 40 µl of a quench buffer containing 1.2% formic acid and 0.833 M guanidine-HCl, which lowered the pH to 2.6. Samples were then immediately frozen in liquid nitrogen until mass analysis. The full HDX-MS protocol can be found in Text S1.

Supporting Information

Figure S1 PAF-mediated signaling does not activate PI3K, and does not synergize with FcεRI co-stimulation (related to Figure 1). IgE-sensitized (100 ng/ml IgE, overnight) or non-sensitized wild type BMMCs were IL-3 depleted for 3 h and stimulated with either 1 µM adenosine (Ade), 1 µM PAF, or 5 ng/ml antigen (post IgE-sensitization) ± PAF for 2 min. Subsequently, cell lysates were subjected to SDS-PAGE. Phosphorylation of Ser473 in PKB/Akt (A), (B) Ser133 in cyclic AMP-responsive element-binding protein (CREB) and Ser660 in PKCβII was monitored by immunodetection with phosphosite-specific antibodies ($n = 3$, *: $p<0.05$; * refers to unstimulated control).
(EPS)

Figure S2 Effect of PKC-inhibitors on PMA- or adenosine-induced PKB phosphorylation (S473) (related to Figure 3). (A/B) Wild type BMMCs were starved for 3 h in IL-3 free medium supplemented with 2% FCS, and preincubated with the inhibitors for 20 min before stimulation (pan-PKC: Ro318425, Gö6983; classical PKC: PKC412 [CPG41251]; classical and atypical PKC: Gö6976; Rotterlin: broad band inhibitor; all 1 µM; & refers to comparison with untreated, stimulated control). (C) PKB activation in response to 100 nM PMA or 1 µM Thapsigargin (2 min) was analyzed in wild type, PKCα$^{-/-}$ and PKCγ$^{-/-}$ BMMCs. Cells were deprived of IL-3 as in (A/B). PKB (S473) and MAPK (T183/Y185) phosphorylation was determined by Western blotting. (D) Wild type, PKCβ$^{-/-}$ and PI3Kγ$^{-/-}$ BMMCs were stimulated with different concentrations of thapsigargin, before degranulation was quantified by the measurement of β-hexosaminidase release into cell supernatants (data are the average of three independent experiments ± standard error of the mean [SEM]; * comparison to wild type (both genotypes); & only the p110γ$^{-/-}$ dataset reached significance).
(EPS)

Figure S3 Identification of PI3Kγ phosphorylation sites by MS (related to Figure 4). (A/B) Recombinant, catalytically inactive GST-PI3Kγ (K833R mutant; GST fused to p110γ amino acids 38–1,102) was phosphorylated in vitro by recombinant PKCβ in the presence of 100 µM ATP/[γ^{32}P]-ATP. Proteins were separated by SDS-PAGE and trypsin-digested PI3Kγ was analyzed by LC-MSMS. (A) Enhanced product ion spectra of the tryptic phospho-S582-peptide of PI3Kγ. The y- and b-fragments detected are indicated in the sequence. Fragments showing a H_3PO_4 loss are marked with an asterisk. The b_2, y_6, and y_7 fragments allow assignment of the phosphorylation to serine 3 in the peptide. (B) Enhanced product ion spectra of the non-phosphorylated form of this peptide. (C) Relevant information for the MRM analysis of the peptides containing Ser582. The amino acid numbering is as in Swiss-Prot entry P48736. (D) Sequence alignment of the beginning of the helical domain of class I PI3Ks. Alignments were done by inspection of the crystal structures of PI3Kγ (1E8Y), PI3Kα (3HHM), PI3Kβ (2Y3A), and PI3Kδ (2WXR). Secondary structure elements are labeled as indicated in the legend. S582 is colored red, while cancer-associated PI3Kα mutations are marked as blue.
(TIF)

Figure S4 Anti-phospho-Ser582 antibody validation (related to Figure 5). (A) Wild type BMMCs were transfected with empty vector, expression plasmid for GFP-PI3Kγ wild type or the GFP-PI3Kγ S582A mutant. On the next day, cells were stimulated with 200 nM PMA for 45 s, and PI3Kγ was immunoprecipitated from cell lysates. Specificity of the anti-S582 antibodies was validated by Western blotting.
(EPS)

Figure S5 Global and site-specific in vitro phosphorylation of monomeric p110γ and p110γ-p84 complexes by PKCβ and CamKII (related to Figure 5). (A) Equal amounts of purified recombinant p110γ-His_6 (2.5 pmole) or p110γ-His_6/EE-p84 complexes were incubated with 20 pmole wortmannin to eliminate auto-phosphorylation signals. Free or complexed p110γ (with p84 protein) was incubated with 10 µM ATP and 5 µCi of [^{32}P]-γ-ATP, and equal specific activity of recombinant PKCβII and CamKII (Life Technologies assays: 30 pmol phosphate incorporation/min.) for 30 min at 30°C. Subsequently, proteins were denatured and separated by SDS-PAGE followed by Coomassie staining (lower panel). ^{32}P-incorporation was visualized by autoradiography and quantified on a phospho-imager (Typhoon 9400, middle panel). Band intensities were quantified with ImageQuant TL Software (Amersham Biosciences, top panel; $n = 4$, * $p<0.05$). Insert: quantification of p84 phosphorylation from the reactions shown in (A), (open bars, $n = 4$, * $p<0.05$). Phospho-PKCβII levels were subtracted from phospho-p84 signals (due to identical apparent Mr on SDS-PAGE). The filled bar represents phosphorylated p84-His_6 after Ni^{2+}-NTA pull-down to minimize contaminating PKCβII autophosphorylation signals ($n = 3$). (B) Equal amounts of purified recombinant p110γ-His_6 (2.5 pmole) or p110γ-His_6/EE-p84 complexes were incubated as indicated with ATP (100 µM), recombinant PKCβII and CamKII for 30 min at 30°C. Proteins were denatured, separated by SDS-PAGE followed by immunological detection of p110γ and p84 protein, as well as site-specific phosphorylation of residue Ser582 (pp110γ S582) in p110γ. PKCβII and CamKII input was adjusted to equal protein kinase activity (30 pmol of transferred phosphate/min). For quantification, Ser582 phosphorylation levels were normalized ($n = 4$, *: $p<0.05$, ***: $p<0.0005$).
(EPS)

Figure S6 Phosphorylation of p110γ requires active PKCβ (related to Figure 5). (A) Effect of PKC inhibitors on thapsigargin induced p110γ Ser582 phosphorylation. IL-3 deprived BMMCs were preincubated with PKC inhibitors (1 µM Ro318425 or 1 µM AEB071) for 20 min before stimulation with 1 µM thapsigargin for 2 min. PI3Kγ was immunoprecipitated from cell lysates with anti-p110γ antibody (see Methods). Precipitated protein was then probed for phosphorylated p110γ (pp110γ) using phospho-specific anti-pSer582 antibodies. PI3Kγ phosphorylation is shown normalized to total p110γ levels (mean ± standard error of the mean [SEM], $n = 3$; * depict comparison with stimulated control). (B) Cells were stimulated as in (A). PKB (T308) and CamKII (T286) phosphorylation was determined by Western blotting. Data are the average of three independent experiments ± SEM.
(EPS)

Figure S7 Ser582 phosphorylation releases p84 from p110γ (related to Figure 6). IL-3 deprived BMMCs were stimulated with 100 nM PMA for 2 min. PI3Kγ complex was co-immunoprecipitated from cell lysates using either (A) anti-p110γ or (B) anti-p84 antibodies. The amount of p84 co-immunoprecipitated with p110γ (A) or p110γ co-immunoprecipitated with p84 (B) was normalized to the total amount of p110γ or p84, respectively. Data are the average of five independent experiments ± standard error of the mean [SEM].
(EPS)

Figure S8 PI3Kγ domain order and peptide coverage after pepsin digestion (related to Figure 7). Identified and analyzed peptides are shown under the primary sequence of PI3Kγ, which has been colored according to the domain boundaries shown above.
(EPS)

Figure S9 Changes in deuteration levels of PI3Kγ in the presence of p84 (related to Figure 7). Peptides spanning PI3Kγ (labeled A–Q) that showed greater than 0.5 Da changes in deuteration in the presence and absence of p84 were mapped onto the PI3Kγ structure (PDB ID: 2CHX, residues 144–1,093). The greatest difference in exchange observed at any time was used for the mapping. S582 is shown as red balls. The ATP competitive inhibitor PIK-90 is shown in green as a reference point for the kinase domain. The linker regions between the RBD and the C2 domain and the C2 and helical domain are shown as dotted lines.
(EPS)

Figure S10 Changes in deuteration levels of PI3Kγ peptides in the presence of p84 (related to Figure 7). The graphs showing the number of incorporated deuterium atoms in the presence (o) and absence (•) of p84 at seven time points in peptides that showed a greater than 0.5 Da H/D exchange difference. Data represent mean ± standard deviation (SD) of two independent experiments.
(EPS)

Figure S11 Deuteration levels in free and p84-bound p110γ (related to Figure 7). Changes in deuteration levels were mapped onto the crystal structure of PI3Kγ (PDB ID: 2CHX) as in Figure 7.The isotopic profiles of two selected peptides (579–592, 623–630) from the helical domain are shown at three or four time points of H/D on exchange +/− the p84 subunit. In the absence of the p84 adaptor the majority of peptides in the helical domain showed broadening of the isotopic profiles indicative of EX1 kinetics (see 30 s of HDX in free p110γ). The helices HB1, HA2 (579–592), and HA3 (624–631) selected are all structurally linked, with HA3 located at the interface of the helical domain with the C-lobe. Ser582 (red) and Thr1024 (yellow) have been highlighted as a reference.
(TIF)

Table S1 Deuterium exchange data of all analyzed peptides of PI3Kγ in the absence or presence of p84 are summarized in tabular form (related to Figure 7). Percent hydrogen deuterium exchange was calculated for each of the seven time points and colored according to the legend. Data show the mean of two independent experiments. The charge state (Z), maximal number of exchangeable amides (#D), starting residue number (S), and ending residue number (E) are displayed for every peptide.
(XLSX)

Text S1 Extended experimental procedures, reference to animals and plasmids. Detailed description of experimental procedures, materials, and further reference to the origin of genetically modified mice used here, and a primer to the determination of deuterium incorporation (HDX_MS).
(DOCX)

Acknowledgments

We would like to thank Priska Reinhard and Jan Völzmann for valuable technical help, Sophie Tornay and Katja Björklöf for the help with initial experiments, and Olga Perisic for critical comments and discussions. We would like to thank Mark Skehel, Elaine Stephens, Sew Yeu Peak-Chew, and Farida Bergum for help with the HDX-MS setup.

Author Contributions

The author(s) have made the following declarations about their contributions: Conceived and designed the experiments: RW JEB EG TB RLW MPW. Performed the experiments: RW JEB EG TB XZ DH PK MuL MPW. Analyzed the data: RW JEB EG TB DH RLW MPW. Contributed reagents/materials/analysis tools: MiL EH. Wrote the paper: RW JEB EG TB RLW MPW.

References

1. Stephens LR, Eguinoa A, Erdjument-Bromage H, Lui M, Cooke F, et al. (1997) The G beta gamma sensitivity of a PI3K is dependent upon a tightly associated adaptor, p101. Cell 89: 105–114.
2. Suire S, Coadwell J, Ferguson GJ, Davidson K, Hawkins P, et al. (2005) p84, a new Gbetagamma-activated regulatory subunit of the type IB phosphoinositide 3-kinase p110gamma. Curr Biol 15: 566–570.
3. Voigt P, Dorner MB, Schaefer M (2006) Characterization of p87PIKAP, a novel regulatory subunit of phosphoinositide 3-kinase gamma that is highly expressed in heart and interacts with PDE3B. J Biol Chem 281: 9977–9986.
4. Brock C, Schaefer M, Reusch HP, Czupalla C, Michalke M, et al. (2003) Roles of G beta gamma in membrane recruitment and activation of p110 gamma/p101 phosphoinositide 3-kinase gamma. J Cell Biol 160: 89–99.
5. Suire S, Condliffe AM, Ferguson GJ, Ellson CD, Guillou H, et al. (2006) Gbetagammas and the Ras binding domain of p110gamma are both important regulators of PI3Kgamma signalling in neutrophils. Nat Cell Biol 8: 1303–1309.
6. Bohnacker T, Marone R, Collmann E, Calvez R, Hirsch E, et al. (2009) PI3Kgamma adaptor subunits define coupling to degranulation and cell motility by distinct PtdIns(3,4,5)P3 pools in mast cells. Sci Signal 2: ra27.
7. Kurig B, Shymanets A, Bohnacker T, Prajwal Brock C, et al. (2009) Ras is an indispensable coregulator of the class IB phosphoinositide 3-kinase p87/p110gamma. Proc Natl Acad Sci U S A 106: 20312–20317.
8. Collmann E, Bohnacker T, Marone R, Dawson J, Rehberg M, et al. (2013) Transient targeting of PI3K acts as a roadblock in mast cells' route to allergy. J Allergy Clin Immunol. doi:pii: S0091-6749(13)00428-4.10.1016/j.jaci.2013.03.008. [Epub ahead of print].
9. Laffargue M, Calvez R, Finan P, Trifilieff A, Barbier M, et al. (2002) Phosphoinositide 3-kinase gamma is an essential amplifier of mast cell function. Immunity 16: 441–451.
10. Endo D, Gon Y, Nunomura S, Yamashita K, Hashimoto S, et al. (2009) PI3Kgamma differentially regulates FcepsilonRI-mediated degranulation and migration of mast cells by and toward antigen. Int Arch Allergy Immunol 149 Suppl 1: 66–72.
11. Tilley SL, Wagoner VA, Salvatore CA, Jacobson MA, Koller BH (2000) Adenosine and inosine increase cutaneous vasopermeability by activating A(3) receptors on mast cells. J Clin Invest 105: 361–367.
12. Gao Z, Li BS, Day YJ, Linden J (2001) A3 adenosine receptor activation triggers phosphorylation of protein kinase B and protects rat basophilic leukemia 2H3 mast cells from apoptosis. Mol Pharmacol 59: 76–82.
13. Ma HT, Beaven MA (2009) Regulation of Ca2+ signaling with particular focus on mast cells. Crit Rev Immunol 29: 155–186.
14. Huber M, Hughes MR, Krystal G (2000) Thapsigargin-induced degranulation of mast cells is dependent on transient activation of phosphatidylinositol-3 kinase. J Immunol 165: 124–133.
15. Suire S, Lecureuil C, Anderson KE, Damoulakis G, Niewczas I, et al. (2012) GPCR activation of Ras and PI3Kc in neutrophils depends on PLCb2/b3 and the RasGEF RasGRP4. EMBO J 31: 3118–3129.
16. Stoyanov B, Volinia S, Hanck T, Rubio I, Loubtchenkov M, et al. (1995) Cloning and characterization of a G protein-activated human phosphoinositide-3 kinase. Science 269: 690–693.

17. Baba Y, Nishida K, Fujii Y, Hirano T, Hikida M, et al. (2008) Essential function for the calcium sensor STIM1 in mast cell activation and anaphylactic responses. Nat Immunol 9: 81–88.
18. Kawakami Y, Nishimoto H, Kitaura J, Maeda-Yamamoto M, Kato RM, et al. (2004) Protein kinase C betaII regulates Akt phosphorylation on Ser-473 in a cell type- and stimulus-specific fashion. J Biol Chem 279: 47720–47725.
19. Nechushtan H, Leitges M, Cohen C, Kay G, Razin E (2000) Inhibition of degranulation and interleukin-6 production in mast cells derived from mice deficient in protein kinase Cbeta. Blood 95: 1752–1757.
20. Stoyanova S, Bulgarelli-Leva G, Kirsch C, Hanck T, Klinger R, et al. (1997) Lipid kinase and protein kinase activities of G-protein-coupled phosphoinositide 3-kinase gamma: structure-activity analysis and interactions with wortmannin. Biochem J 324: 489–495.
21. Miled N, Yan Y, Hon WC, Perisic O, Zvelebil M, et al. (2007) Mechanism of two classes of cancer mutations in the phosphoinositide 3-kinase catalytic subunit. Science 317: 239–242.
22. Carson JD, Van Aller G, Lehr R, Sinnamon RH, Kirkpatrick RB, et al. (2008) Effects of oncogenic p110alpha subunit mutations on the lipid kinase activity of phosphoinositide 3-kinase. Biochem J 409: 519–524.
23. Gymnopoulos M, Elsliger MA, Vogt PK (2007) Rare cancer-specific mutations in PIK3CA show gain of function. Proc Natl Acad Sci U S A 104: 5569–5574.
24. Hon WC, Berndt A, Williams RL (2012) Regulation of lipid binding underlies the activation mechanism of class IA PI3-kinases. Oncogene 31: 3655–3666.
25. Burke JE, Perisic O, Masson GR, Vadas O, Williams RL (2012) Oncogenic mutations mimic and enhance dynamic events in the natural activation of phosphoinositide 3-kinase p110alpha (PIK3CA). Proc Natl Acad Sci U S A 109: 15259–15264
26. Burke JE, Vadas O, Berndt A, Finegan T, Perisic O, et al. (2011) Dynamics of the phosphoinositide 3-kinase p110delta interaction with p85alpha and membranes reveals aspects of regulation distinct from p110alpha. Structure 19: 1127–1137.
27. Weis DD, Wales TE, Engen JR, Hotchko M, Ten Eyck LF (2006) Identification and characterization of EX1 kinetics in H/D exchange mass spectrometry by peak width analysis. J Am Soc Mass Spectrom 17: 1498–1509.
28. Krugmann S, Hawkins PT, Pryer N, Braselmann S (1999) Characterizing the interactions between the two subunits of the p101/p110gamma phosphoinositide 3-kinase and their role in the activation of this enzyme by G beta gamma subunits. J Biol Chem 274: 17152–17158.
29. Maier U, Babich A, Nurnberg B (1999) Roles of non-catalytic subunits in gbetagamma-induced activation of class I phosphoinositide 3-kinase isoforms beta and gamma. J Biol Chem 274: 29311–29317.
30. Shymanets A, Ahmadian MR, Kossmeier KT, Wetzker R, Harteneck C, et al. (2012) The p101 subunit of PI3Kgamma restores activation by Gbeta mutants deficient in stimulating p110gamma. Biochem J 441: 851–858.
31. Hirsch E, Katanaev VL, Garlanda C, Azzolino O, Pirola L, et al. (2000) Central role for G protein-coupled phosphoinositide 3-kinase gamma in inflammation. Science 287: 1049–1053.
32. Del Prete A, Vermi W, Dander E, Otero K, Barberis L, et al. (2004) Defective dendritic cell migration and activation of adaptive immunity in PI3Kgamma-deficient mice. EMBO J 23: 3505–3515.
33. Patrucco E, Notte A, Barberis L, Selvetella G, Maffei A, et al. (2004) PI3Kgamma modulates the cardiac response to chronic pressure overload by distinct kinase-dependent and -independent effects. Cell 118: 375–387.
34. Vecchione C, Patrucco E, Marino G, Barberis L, Poulet R, et al. (2005) Protection from angiotensin II-mediated vasculotoxic and hypertensive response in mice lacking PI3Kgamma. J Exp Med 201: 1217–1228.
35. Kobayashi N, Ueki K, Okazaki Y, Iwane A, Kubota N, et al. (2011) Blockade of class IB phosphoinositide-3 kinase ameliorates obesity-induced inflammation and insulin resistance. Proc Natl Acad Sci U S A 108: 5753–5758.
36. Becattini B, Marone R, Zani F, Arsenijevic D, Seydoux J, et al. (2011) PI3Kgamma within a nonhematopoietic cell type negatively regulates diet-induced thermogenesis and promotes obesity and insulin resistance. Proc Natl Acad Sci U S A 108: E854–E863.
37. Yamamoto K, Lapetina EG (1990) Protein kinase C-mediated formation of phosphatidylinositol 3,4-bisphosphate in human platelets. Biochem Biophys Res Commun 168: 466–472.
38. Nave BT, Siddle K, Shepherd PR (1996) Phorbol esters stimulate phosphatidylinositol 3,4,5-trisphosphate production in 3T3-L1 adipocytes: implications for stimulation of glucose transport. Biochem J 318: 203–205.
39. Petritsch C, Woscholski R, Edelmann HM, Parker PJ, Ballou LM (1995) Selective inhibition of p70 S6 kinase activation by phosphatidylinositol 3-kinase inhibitors. Eur J Biochem 230: 431–438.
40. Stephens L, Eguinoa A, Corey S, Jackson T, Hawkins PT (1993) Receptor stimulated accumulation of phosphatidylinositol (3,4,5)-trisphosphate by G-protein mediated pathways in human myeloid derived cells. EMBO J 12: 2265–2273.
41. Lee JY, Chiu YH, Asara J, Cantley LC (2011) Inhibition of PI3K binding to activators by serine phosphorylation of PI3K regulatory subunit p85alpha Src homology-2 domains. Proc Natl Acad Sci U S A 108: 14157–14162.
42. Lu-Kuo JM, Fruman DA, Joyal DM, Cantley LC, Katz HR (2000) Impaired kit-but not FcepsilonRI-initiated mast cell activation in the absence of phosphoinositide 3-kinase p85alpha gene products. J Biol Chem 275: 6022–6029.
43. Fukao T, Yamada T, Tanabe M, Terauchi Y, Ota T, et al. (2002) Selective loss of gastrointestinal mast cells and impaired immunity in PI3K-deficient mice. Nat Immunol 3: 295–304.
44. Krishnan S, Mali RS, Ramdas B, Sims E, Ma P, et al. (2012) p85beta regulatory subunit of class IA PI3 kinase negatively regulates mast cell growth, maturation, and leukemogenesis. Blood 119: 3951–3961.
45. Ali K, Bilancio A, Thomas M, Pearce W, Gilfillan AM, et al. (2004) Essential role for the p110delta phosphoinositide 3-kinase in the allergic response. Nature 431: 1007–1011.
46. Ali K, Camps M, Pearce WP, Ji H, Ruckle T, et al. (2008) Isoform-specific functions of phosphoinositide 3-kinases: p110 delta but not p110 gamma promotes optimal allergic responses in vivo. J Immunol 180: 2538–2544.
47. Walker EH, Perisic O, Ried C, Stephens L, Williams RL (1999) Structural insights into phosphoinositide 3-kinase catalysis and signalling. Nature 402: 313–320.
48. Pacold ME, Suire S, Perisic O, Lara-Gonzalez S, Davis CT, et al. (2000) Crystal structure and functional analysis of Ras binding to its effector phosphoinositide 3-kinase gamma. Cell 103: 931–943.
49. Zhang X, Vadas O, Perisic O, Anderson KE, Clark J, et al. (2011) Structure of lipid kinase p110beta/p85beta elucidates an unusual SH2-domain-mediated inhibitory mechanism. Mol Cell 41: 567–578.
50. Vadas O, Burke JE, Zhang X, Berndt A, Williams RL (2011) Structural basis for activation and inhibition of class I phosphoinositide 3-kinases. Sci Signal 4: re2.
51. Perino A, Ghigo A, Ferrero E, Morello F, Santulli G, et al. (2011) Integrating cardiac PIP(3) and cAMP signaling through a PKA anchoring function of p110gamma. Mol Cell 42: 84–95.
52. Wymann MP, Marone R (2005) Phosphoinositide 3-kinase in disease: timing, location, and scaffolding. Curr Opin Cell Biol 17: 141–149.

Supporting information

Figure S1

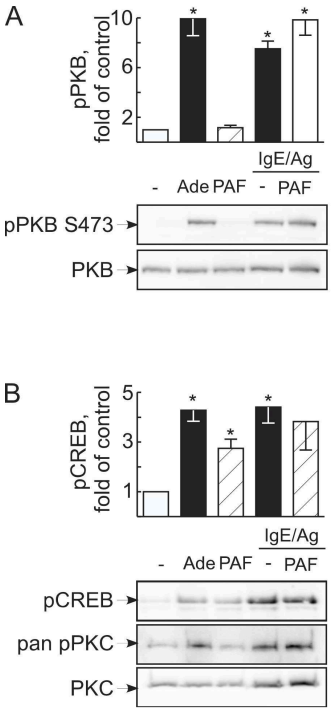

Figure S2

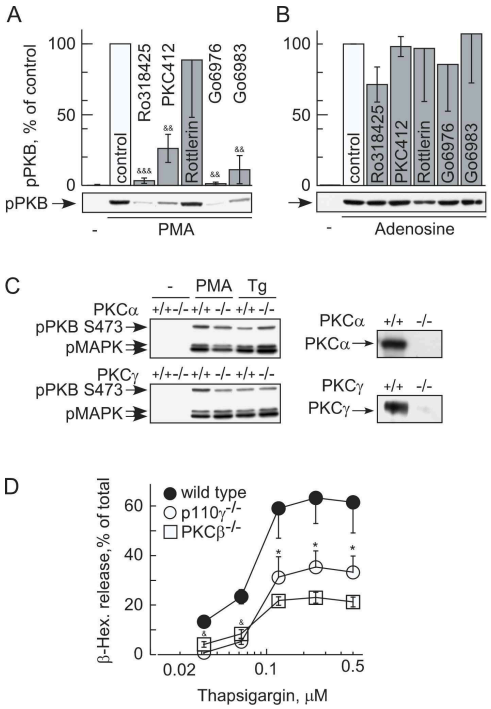

Figure S3

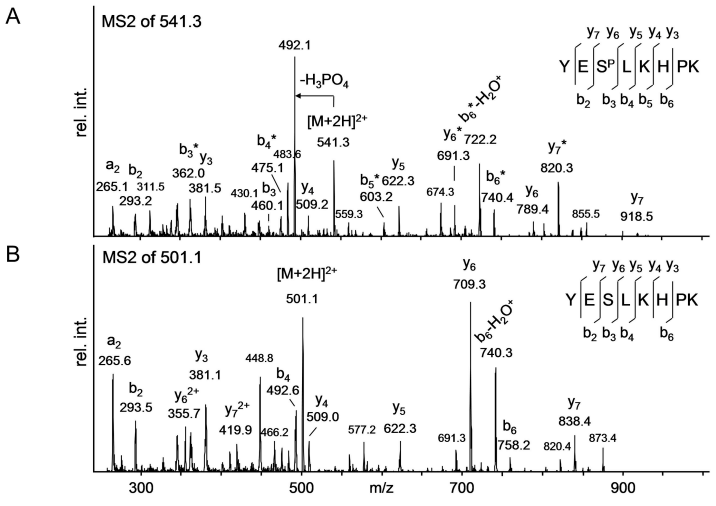

C

Peptide	Precursor m/z	Fragment m/z	Time min	Dwell time ms	Collision energy
$Y_{580}ES^{P}LKHPK$	541.3	492.1	16.8	200	40
$Y_{580}ESLKHPK$	501.1	709.3	16.0	100	30

D

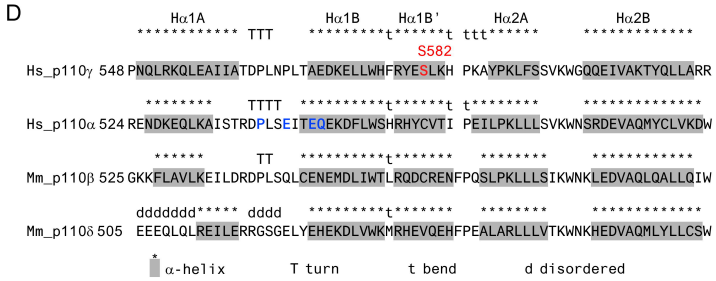

Figure S4

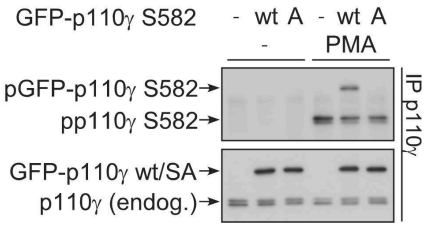

Figure S5

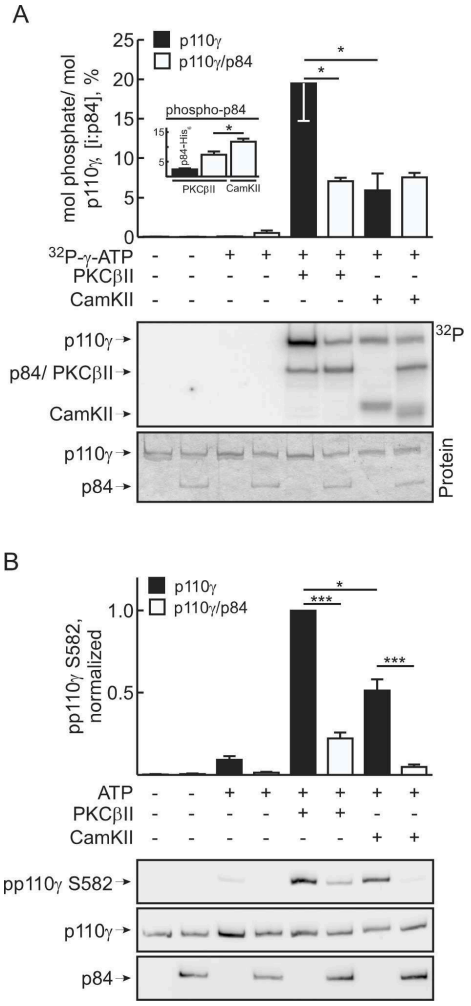

Figure S6

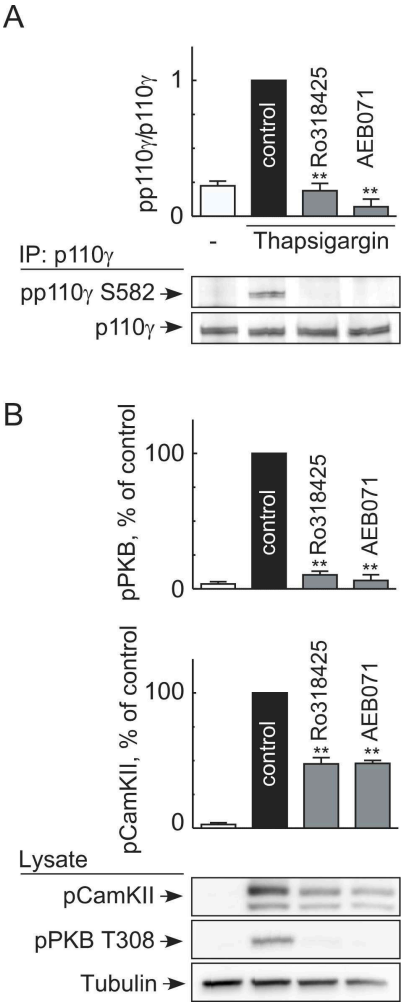

Figure S7

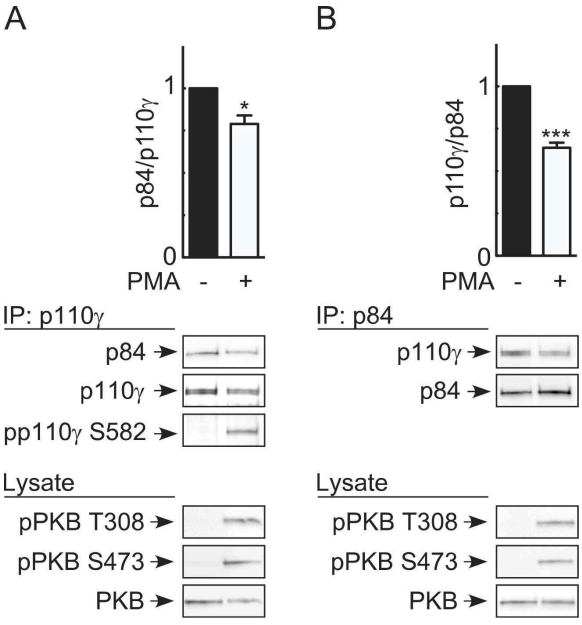

Figure S8

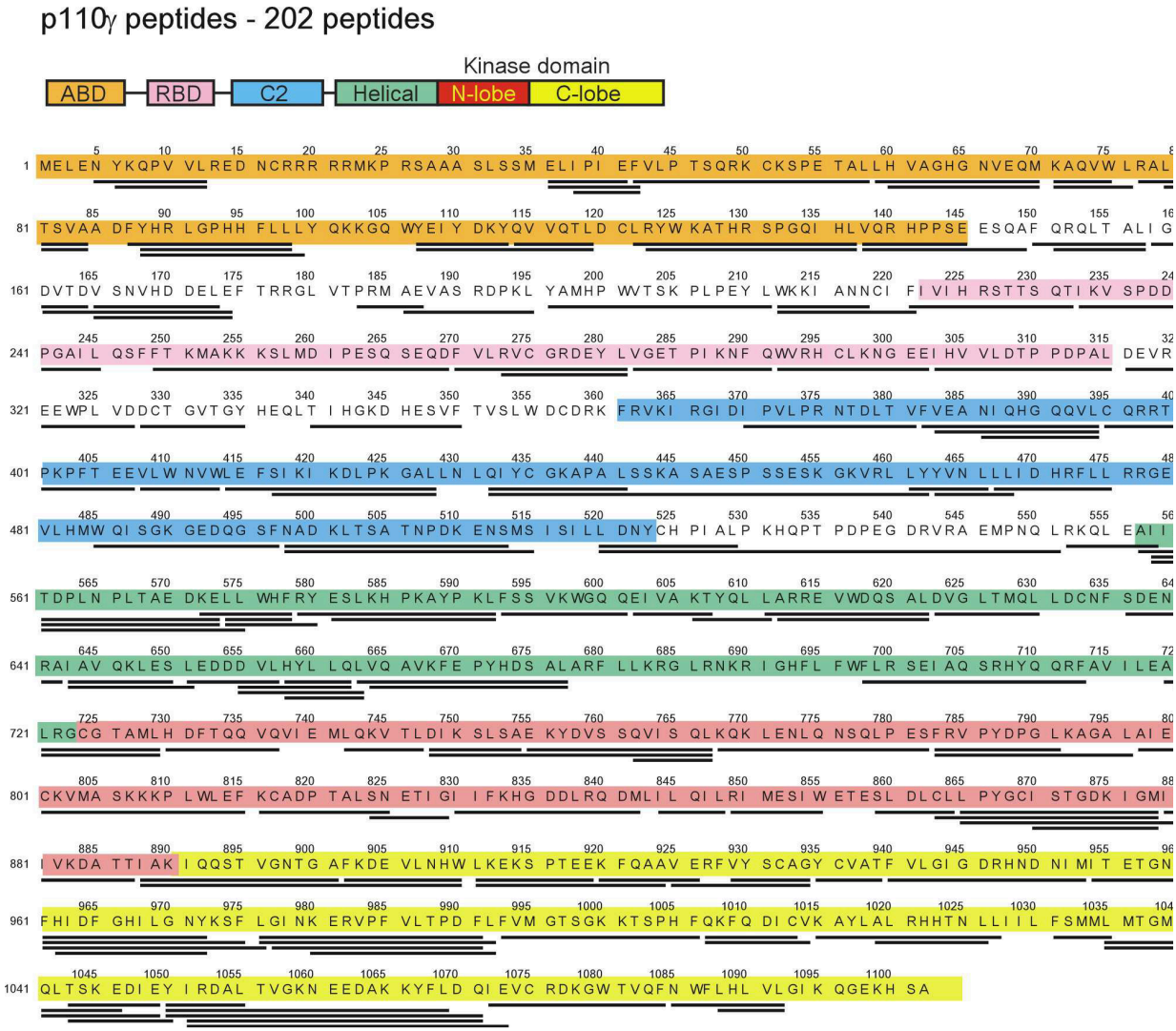
p110γ peptides - 202 peptides
Kinase domain
ABD
RBD
C2
Helical
N-lobe
C-lobe

Figure S9

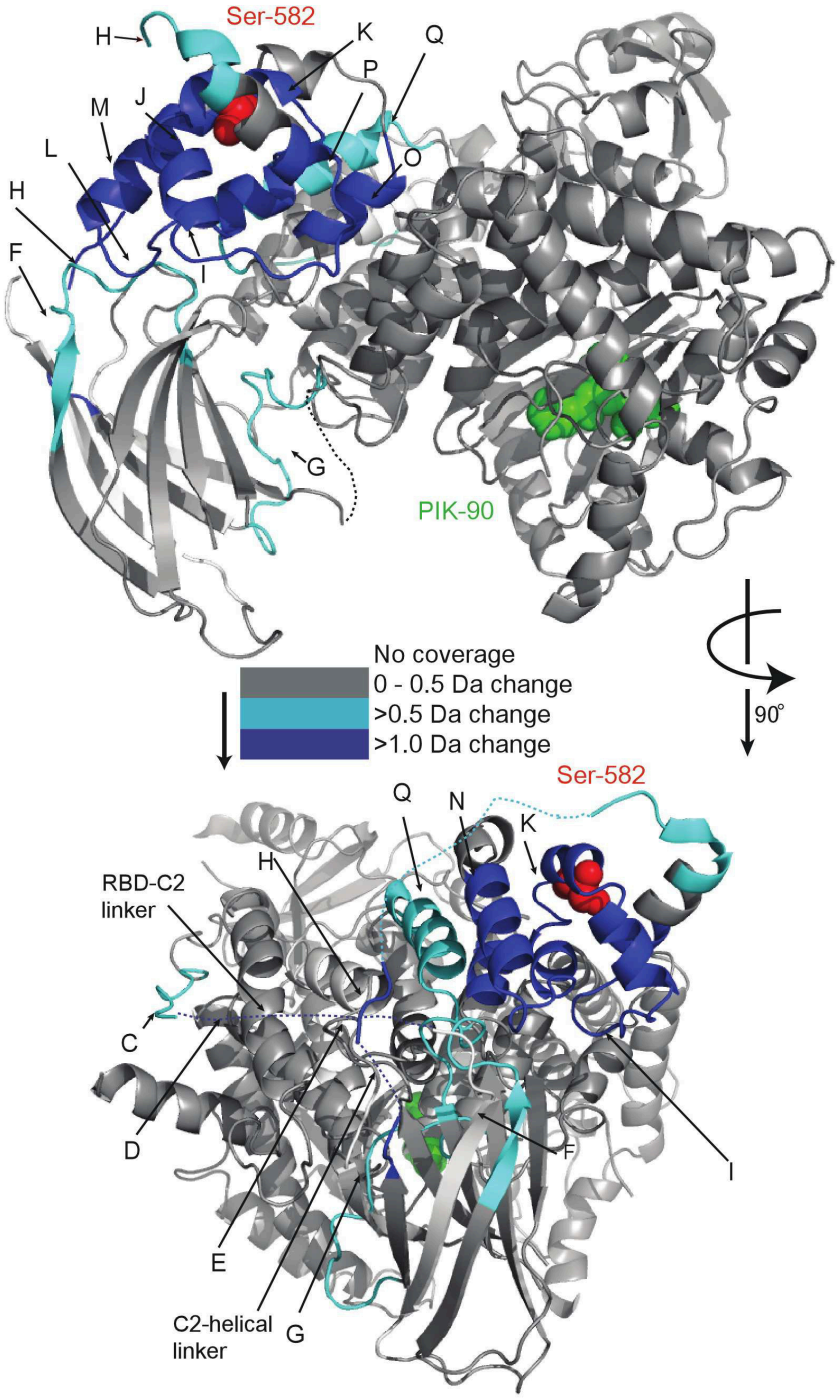
Ser-582
H
K
Q
P
M
J
L
O
H
F
I
G
PIK-90
No coverage
0 - 0.5 Da change
>0.5 Da change
>1.0 Da change
90°
Ser-582
Q
N
K
H
RBD-C2
linker
C
D
E
F
I
C2-helical
linker
G

Figure S10

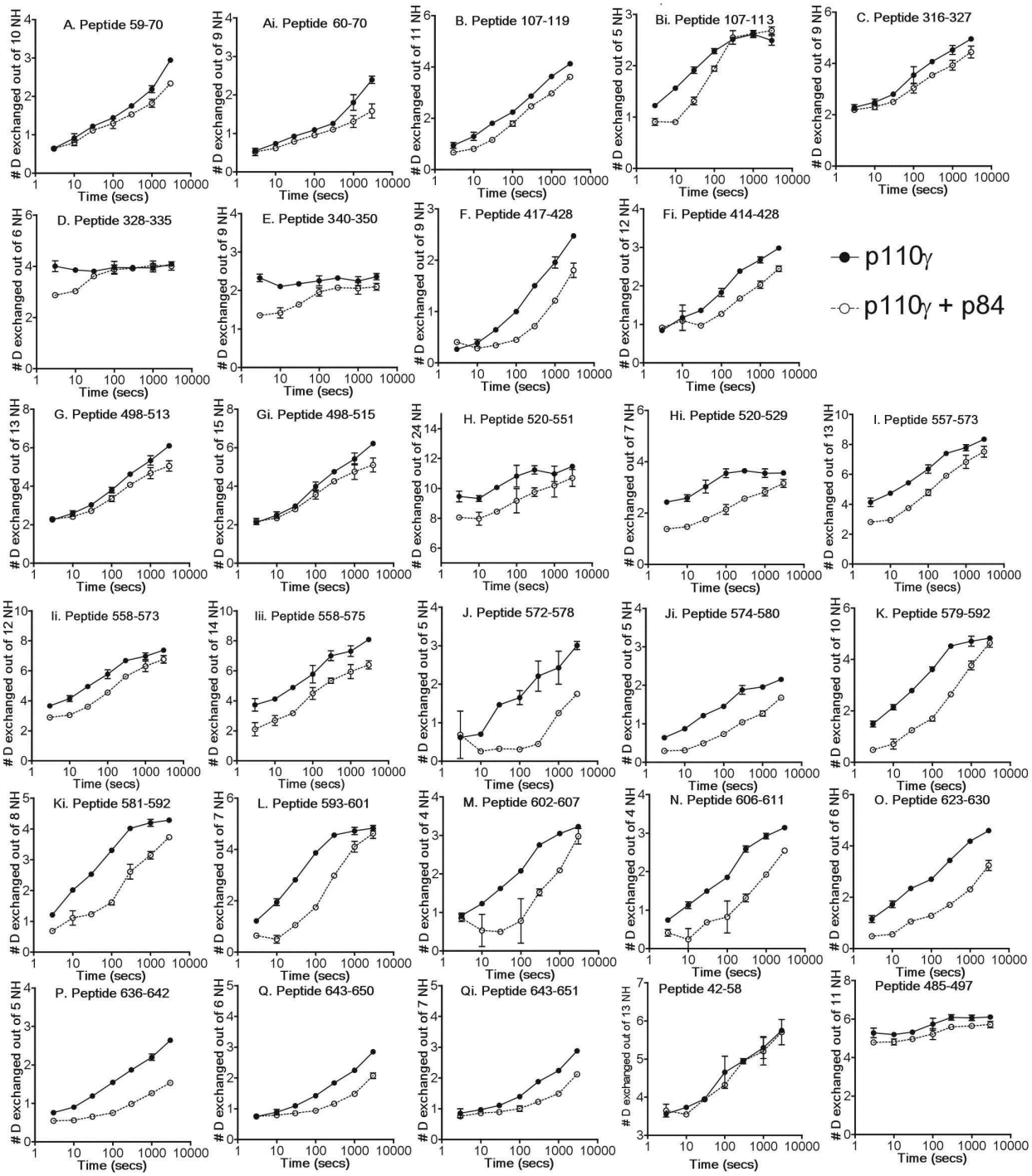
A. Peptide 59-70
Ai. Peptide 60-70
B. Peptide 107-119
Bi. Peptide 107-113
C. Peptide 316-327
D. Peptide 328-335
E. Peptide 340-350
F. Peptide 417-428
Fi. Peptide 414-428
p110γ
p110γ + p84
G. Peptide 498-513
Gi. Peptide 498-515
H. Peptide 520-551
Hi. Peptide 520-529
I. Peptide 557-573
Ii. Peptide 558-573
Iii. Peptide 558-575
J. Peptide 572-578
Ji. Peptide 574-580
K. Peptide 579-592
Ki. Peptide 581-592
L. Peptide 593-601
M. Peptide 602-607
N. Peptide 606-611
O. Peptide 623-630
P. Peptide 636-642
Q. Peptide 643-650
Qi. Peptide 643-651
Peptide 42-58
Peptide 485-497
D exchanged out of
Time (secs)

Figure S11

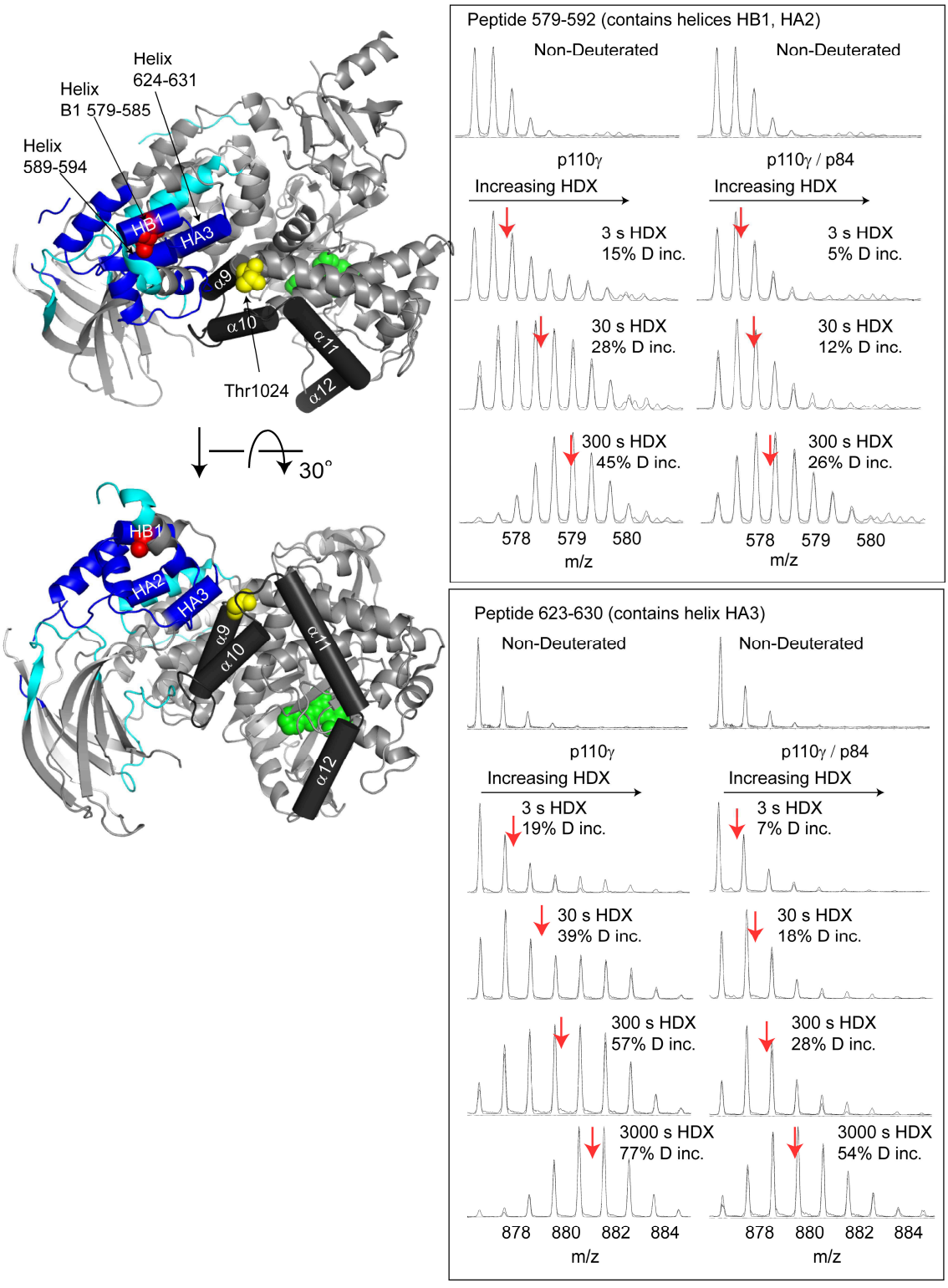
Helix
624-631
Helix
B1 579-585
Helix
589-594
HB1
HA3
α9
α10
α11
α12
Thr1024
30°
HB1
HA2
HA3
α9
α10
α11
α12
Peptide 579-592 (contains helices HB1, HA2)
Non-Deuterated
Non-Deuterated
p110γ
Increasing HDX
p110γ / p84
Increasing HDX
3 s HDX
15% D inc.
3 s HDX
5% D inc.
30 s HDX
28% D inc.
30 s HDX
12% D inc.
300 s HDX
45% D inc.
300 s HDX
26% D inc.
578 579 580
m/z
578 579 580
m/z
Peptide 623-630 (contains helix HA3)
Non-Deuterated
Non-Deuterated
p110γ
Increasing HDX
p110γ / p84
Increasing HDX
3 s HDX
19% D inc.
3 s HDX
7% D inc.
30 s HDX
39% D inc.
30 s HDX
18% D inc.
300 s HDX
57% D inc.
300 s HDX
28% D inc.
3000 s HDX
77% D inc.
3000 s HDX
54% D inc.
878 880 882 884
m/z
878 880 882 884
m/z

Table S1

Supplemental Table S1

				p110 γ							p110 γ+p84						
				Time													
Z	#D	S	E	3	10	30	100	300	1000	3000	3	10	30	100	300	1000	3000
1	5	5	12	85%	86%	86%	89%	90%	94%	86%	86%	84%	85%	85%	87%	89%	85%
1	4	6	12	76%	74%	75%	77%	75%	74%	75%	81%	78%	80%	79%	80%	80%	80%
1	3	36	41	3%	4%	5%	7%	11%	16%	19%	4%	4%	5%	6%	11%	14%	17%
1	3	38	42	2%	4%	6%	6%	5%	7%	6%	9%	4%	3%	3%	4%	12%	9%
2	13	42	58	28%	30%	31%	37%	39%	41%	45%	28%	27%	30%	33%	38%	41%	44%
3	13	42	58	27%	29%	31%	36%	39%	41%	44%	27%	26%	30%	33%	37%	40%	42%
4	13	42	58	27%	29%	30%	36%	38%	41%	44%	28%	27%	30%	33%	38%	40%	44%
2	10	59	70	6%	9%	12%	14%	18%	22%	29%	6%	8%	11%	13%	15%	18%	23%
1	9	60	70	6%	7%	10%	12%	14%	19%	26%	6%	7%	9%	12%	13%	15%	18%
2	9	60	70	5%	7%	9%	12%	14%	19%	25%	5%	6%	8%	10%	12%	15%	18%
1	3	71	75	2%	3%	2%	3%	2%	3%	5%	6%	7%	4%	7%	8%	12%	11%
1	4	71	76	3%	2%	3%	4%	6%	8%	9%	3%	2%	3%	4%	4%	5%	6%
1	6	77	84	51%	50%	51%	51%	50%	50%	50%	54%	52%	54%	53%	53%	54%	54%
1	4	79	84	48%	61%	65%	74%	76%	76%	78%	47%	55%	62%	72%	76%	76%	76%
3	9	87	98	4%	5%	3%	7%	8%	8%	11%	5%	4%	7%	5%	8%	6%	9%
2	8	88	98	6%	8%	9%	11%	12%	14%	17%	5%	6%	7%	8%	10%	10%	12%
3	9	88	99	4%	5%	6%	7%	8%	8%	11%	4%	4%	5%	6%	7%	7%	9%
1	5	100	106	32%	40%	52%	57%	56%	57%	59%	32%	37%	48%	56%	58%	60%	61%
1	5	107	113	25%	31%	38%	46%	50%	52%	50%	18%	18%	26%	39%	51%	53%	54%
2	5	107	113	25%	29%	37%	45%	51%	52%	54%	18%	21%	29%	40%	50%	54%	55%
2	11	107	119	9%	12%	16%	20%	26%	33%	37%	6%	7%	11%	16%	22%	27%	33%
1	4	114	119	0%	-1%	-1%	-1%	0%	2%	7%	0%	-2%	-2%	-2%	-2%	6%	3%
1	6	114	121	19%	19%	19%	20%	21%	25%	30%	14%	16%	20%	20%	22%	23%	26%
2	13	122	137	4%	5%	8%	13%	17%	19%	21%	4%	4%	6%	10%	16%	20%	21%
3	12	123	137	7%	8%	9%	13%	18%	21%	25%	6%	7%	9%	12%	17%	20%	26%
1	4	138	145	4%	4%	4%	8%	13%	21%	24%	6%	7%	6%	9%	14%	21%	25%
2	4	138	145	6%	6%	10%	10%	18%	23%	47%	6%	6%	6%	8%	12%	18%	43%
2	8	138	149	33%	37%	39%	50%	52%	54%	56%	33%	33%	39%	46%	51%	53%	52%
1	6	150	157	-1%	-1%	0%	4%	11%	17%	24%	-1%	-1%	0%	6%	13%	17%	23%
2	6	150	157	3%	4%	5%	8%	14%	25%	28%	3%	4%	6%	9%	14%	20%	25%
1	5	151	157	5%	3%	5%	10%	18%	22%	28%	4%	3%	5%	9%	17%	24%	27%
2	5	151	157	4%	4%	5%	9%	17%	30%	34%	6%	5%	6%	11%	23%	31%	35%
1	5	158	164	11%	13%	15%	24%	36%	45%	53%	21%	16%	22%	31%	44%	51%	59%
2	12	161	174	20%	26%	28%	33%	37%	41%	46%	25%	28%	32%	35%	41%	45%	47%
1	7	165	173	13%	22%	26%	32%	33%	32%	34%	18%	21%	27%	30%	32%	32%	32%
1	7	165	173	15%	24%	27%	32%	37%	36%	36%	19%	22%	28%	30%	37%	34%	33%
1	8	165	174	17%	24%	26%	31%	33%	35%	38%	18%	22%	26%	28%	32%	36%	36%
1	7	174	182	2%	2%	3%	4%	8%	13%	16%	2%	3%	2%	3%	5%	11%	14%
1	7	186	195	11%	19%	19%	25%	32%	40%	47%	15%	19%	21%	25%	34%	43%	47%
2	7	186	195	11%	17%	20%	25%	32%	40%	48%	13%	15%	19%	24%	32%	41%	47%
2	11	196	211	22%	25%	29%	35%	39%	42%	47%	23%	23%	29%	32%	37%	42%	45%
3	11	196	211	22%	25%	28%	35%	38%	42%	46%	22%	23%	28%	31%	36%	41%	44%
1	5	212	218	39%	45%	51%	60%	67%	69%	71%	47%	48%	55%	61%	69%	72%	72%
2	5	212	218	43%	50%	55%	66%	72%	74%	76%	45%	46%	55%	63%	70%	73%	75%
1	8	212	221	20%	26%	30%	41%	49%	53%	57%	19%	21%	27%	35%	48%	52%	56%
2	8	212	221	25%	31%	28%	43%	52%	55%	56%	24%	29%	26%	42%	50%	54%	54%
1	9	222	232	28%	27%	27%	29%	30%	33%	36%	28%	27%	28%	29%	30%	33%	35%
2	9	233	245	8%	9%	10%	14%	18%	21%	25%	10%	10%	10%	14%	19%	22%	27%
4	18	249	269	48%	48%	48%	51%	50%	50%	52%	49%	47%	50%	49%	52%	52%	53%
2	10	270	281	-11%	-12%	-10%	-10%	-8%	-8%	-6%	-9%	-9%	-11%	-10%	-9%	-7%	-7%
1	7	273	281	1%	2%	3%	4%	6%	5%	7%	3%	1%	4%	6%	2%	3%	5%
2	7	273	281	2%	2%	2%	2%	3%	4%	5%	3%	3%	3%	4%	3%	3%	4%
1	7	282	291	10%	9%	9%	10%	10%	11%	15%	8%	7%	7%	6%	9%	9%	13%
2	7	282	291	6%	8%	9%	10%	10%	11%	14%	7%	6%	6%	7%	8%	8%	11%
2	9	292	302	5%	11%	15%	21%	21%	21%	23%	6%	8%	16%	19%	21%	21%	22%
3	9	292	302	5%	11%	15%	21%	21%	21%	23%	7%	10%	17%	21%	23%	22%	22%
2	8	303	315	12%	9%	13%	17%	20%	23%	22%	12%	9%	16%	16%	20%	22%	24%
2	9	316	327	25%	28%	31%	39%	45%	50%	55%	24%	26%	28%	34%	39%	44%	49%
1	6	328	335	67%	64%	64%	66%	66%	66%	68%	48%	51%	60%	65%	65%	67%	67%
2	9	340	350	26%	23%	24%	25%	26%	25%	26%	15%	16%	18%	22%	23%	23%	23%
3	9	340	350	25%	23%	23%	24%	24%	24%	25%	17%	17%	20%	23%	25%	24%	27%
2	9	370	381	31%	35%	39%	47%	55%	56%	58%	33%	33%	38%	46%	53%	56%	57%
2	11	382	394	9%	13%	15%	17%	19%	21%	25%	10%	11%	14%	15%	18%	20%	23%
2	10	383	394	8%	13%	14%	16%	18%	21%	25%	9%	11%	14%	15%	18%	20%	22%
1	7	386	394	15%	21%	23%	26%	30%	35%	41%	15%	17%	21%	23%	26%	32%	37%
2	7	386	394	16%	24%	25%	28%	31%	34%	41%	21%	24%	24%	25%	30%	34%	42%
2	9	395	407	11%	13%	16%	22%	25%	28%	32%	13%	13%	17%	20%	25%	29%	31%
3	9	395	407	11%	13%	15%	22%	26%	28%	32%	12%	13%	17%	20%	25%	29%	32%
1	4	408	413	15%	27%	32%	37%	42%	52%	62%	13%	19%	29%	35%	42%	51%	57%
2	12	414	428	7%	10%	11%	15%	20%	22%	25%	8%	9%	8%	11%	14%	17%	20%
2	9	417	428	3%	5%	8%	13%	19%	23%	30%	3%	2%	4%	5%	6%	11%	21%
3	9	417	428	3%	4%	7%	11%	17%	22%	27%	4%	3%	4%	5%	8%	13%	20%
2	7	432	441	45%	43%	45%	50%	54%	55%	54%	42%	40%	43%	45%	48%	53%	53%
4	27	432	462	31%	30%	32%	34%	35%	35%	36%	30%	31%	32%	35%	35%	37%	35%
1	4	461	466	0%	0%	0%	0%	0%	1%	0%	-1%	-1%	0%	0%	0%	1%	-1%
1	4	463	468	0%	1%	1%	5%	14%	20%	21%	5%	4%	2%	5%	11%	15%	25%
2	7	467	475	1%	1%	7%	7%	13%	14%	14%	2%	1%	2%	8%	11%	11%	11%
2	11	485	497	48%	47%	48%	52%	55%	55%	56%	44%	44%	45%	47%	51%	51%	52%
2	13	498	513	17%	20%	23%	29%	35%	41%	47%	17%	18%	21%	25%	31%	36%	38%
3	13	498	513	18%	21%	24%	30%	36%	42%	47%	18%	18%	21%	25%	31%	34%	38%
2	15	498	515	14%	17%	20%	26%	31%	35%	41%	14%	15%	18%	23%	28%	32%	34%
3	15	498	515	14%	16%	19%	26%	31%	36%	41%	14%	15%	18%	23%	28%	31%	34%
1	7	520	529	33%	35%	41%	51%	52%	50%	51%	19%	21%	25%	31%	36%	37%	40%
2	7	520	529	35%	37%	43%	51%	52%	51%	51%	20%	21%	25%	31%	37%	40%	45%
3	24	520	551	39%	39%	42%	45%	47%	46%	48%	34%	34%	36%	39%	41%	43%	45%
4	24	520	551	39%	39%	42%	45%	47%	46%	48%	34%	33%	35%	38%	41%	42%	45%
5	24	520	551	35%	36%	39%	42%	43%	42%	45%	29%	30%	32%	35%	38%	37%	42%
2	5	552	558	15%	15%	19%	18%	18%	24%	26%	19%	18%	17%	25%	36%	23%	25%
2	13	557	573	32%	36%	42%	49%	57%	60%	64%	22%	23%	29%	37%	45%	53%	58%
2	12	558	573	31%	35%	41%	48%	56%	58%	61%	24%	25%	30%	38%	47%	53%	56%
2	14	558	575	27%	29%	35%	41%	50%	52%	58%	15%	19%	23%	32%	38%	42%	46%
2	5	572	578	12%	14%	29%	33%	44%	49%	60%	14%	5%	6%	6%	9%	25%	35%
1	3	574	578	9%	11%	15%	19%	27%	32%	37%	-1%	0%	1%	2%	5%	13%	22%
2	3	574	578	17%	21%	25%	29%	37%	43%	48%	5%	5%	8%	9%	13%	21%	31%
2	5	574	580	13%	17%	24%	29%	38%	39%	43%	6%	6%	10%	15%	21%	25%	34%
2	10	579	592	15%	21%	28%	36%	45%	47%	48%	5%	7%	12%	17%	26%	38%	47%
3	8	581	592	15%	25%	32%	41%	50%	52%	54%	9%	14%	15%	20%	33%	39%	47%
1	7	593	601	17%	28%	40%	55%	65%	67%	69%	9%	7%	15%	25%	43%	59%	66%
2	7	593	601	18%	22%	39%	53%	64%	65%	66%	6%	13%	25%	27%	56%	60%	64%
1	4	602	607	23%	31%	41%	52%	69%	76%	81%	21%	8%	12%	20%	38%	52%	75%
1	4	606	611	19%	28%	37%	46%	65%	73%	79%	10%	6%	17%	21%	33%	48%	64%

				p110 γ							p110 γ+p84						
				Time													
Z	#D	S	E	3	10	30	100	300	1000	3000	3	10	30	100	300	1000	3000
2	10	611	622	50%	54%	54%	56%	57%	57%	59%	52%	51%	53%	53%	56%	56%	56%
2	9	612	622	51%	53%	52%	55%	54%	54%	55%	53%	51%	53%	52%	55%	54%	54%
1	6	623	630	19%	29%	39%	45%	57%	70%	77%	8%	9%	18%	21%	28%	38%	54%
1	5	636	642	15%	19%	25%	32%	38%	45%	53%	12%	12%	14%	16%	22%	28%	32%
2	5	636	642	15%	18%	24%	31%	37%	44%	53%	11%	11%	13%	15%	20%	25%	31%
1	6	643	650	13%	14%	19%	23%	30%	35%	45%	12%	13%	15%	15%	18%	24%	34%
2	6	643	650	12%	15%	18%	24%	31%	37%	48%	13%	13%	14%	16%	19%	25%	35%
2	7	643	651	12%	14%	16%	20%	27%	32%	41%	11%	12%	13%	14%	18%	21%	30%
1	5	651	657	3%	3%	4%	6%	9%	13%	18%	3%	2%	3%	4%	9%	19%	20%
1	6	655	662	12%	11%	8%	14%	24%	31%	39%	11%	11%	7%	11%	20%	32%	38%
2	6	655	662	1%	3%	5%	10%	20%	30%	36%	3%	3%	4%	9%	20%	29%	37%
1	7	655	663	2%	2%	3%	8%	20%	25%	31%	1%	2%	1%	7%	15%	25%	31%
2	7	655	663	1%	2%	4%	9%	18%	27%	32%	1%	1%	3%	7%	16%	26%	32%
1	3	658	662	4%	6%	8%	13%	24%	31%	33%	4%	4%	6%	10%	19%	29%	32%
1	4	658	663	0%	1%	1%	4%	17%	25%	25%	1%	1%	1%	4%	17%	25%	21%
2	4	658	663	-3%	-2%	0%	7%	15%	20%	22%	4%	4%	4%	7%	16%	21%	26%
3	12	663	677	3%	4%	5%	6%	7%	7%	9%	3%	3%	4%	5%	6%	6%	7%
2	11	664	677	3%	4%	6%	7%	8%	9%	10%	2%	2%	5%	6%	7%	7%	8%
3	11	664	677	4%	5%	6%	8%	8%	9%	10%	2%	3%	4%	5%	8%	7%	8%
4	14	698	713	4%	5%	6%	9%	12%	17%	20%	4%	4%	5%	8%	13%	17%	21%
1	9	719	729	0%	1%	3%	7%	10%	16%	25%	-1%	0%	4%	8%	12%	21%	29%
1	8	720	729	2%	6%	9%	12%	14%	19%	27%	3%	3%	6%	9%	12%	19%	28%
2	8	720	729	3%	5%	9%	13%	16%	24%	31%	4%	4%	7%	10%	15%	22%	33%
1	6	730	737	1%	1%	1%	1%	1%	1%	1%	1%	0%	0%	0%	0%	1%	1%
1	4	742	747	9%	17%	28%	40%	51%	61%	69%	7%	12%	23%	38%	48%	60%	68%
1	5	748	754	69%	69%	71%	75%	76%	77%	81%	77%	74%	75%	75%	77%	77%	78%
2	18	748	767	64%	62%	63%	64%	66%	64%	66%	64%	62%	63%	64%	64%	64%	65%
2	11	755	767	64%	68%	69%	66%	70%	73%	74%	61%	65%	68%	68%	69%	70%	72%
1	4	762	767	3%	4%	4%	6%	8%	11%	24%	9%	2%	2%	4%	7%	12%	17%
2	12	768	782	30%	37%	46%	62%	67%	67%	69%	31%	35%	46%	58%	66%	67%	66%
3	12	768	782	30%	39%	45%	59%	64%	64%	66%	31%	34%	45%	56%	64%	65%	65%
1	5	783	791	2%	1%	2%	3%	7%	11%	13%	0%	1%	1%	2%	5%	10%	11%
2	5	783	791	-3%	-1%	1%	3%	5%	6%	10%	0%	1%	5%	2%	5%	7%	8%
2	10	783	796	3%	3%	3%	6%	12%	18%	22%	3%	3%	3%	7%	12%	18%	22%
3	10	783	796	3%	3%	5%	7%	12%	18%	21%	4%	3%	3%	6%	12%	18%	21%
4	16	797	815	7%	7%	10%	13%	15%	16%	18%	6%	7%	8%	11%	15%	17%	17%
1	7	816	825	36%	41%	49%	60%	65%	67%	69%	34%	36%	45%	55%	61%	63%	65%
1	4	824	829	30%	38%	43%	52%	55%	56%	60%	38%	40%	51%	56%	55%	56%	63%
2	11	830	842	4%	6%	10%	15%	18%	19%	21%	3%	3%	8%	13%	16%	19%	21%
3	11	830	842	2%	5%	8%	13%	16%	20%	21%	2%	3%	7%	13%	19%	19%	20%
1	3	844	848	4%	3%	6%	7%	16%	5%	4%	1%	6%	6%	7%	9%	6%	5%
1	5	849	855	1%	1%	0%	0%	5%	6%	3%	0%	0%	0%	-1%	6%	-1%	1%
1	4	859	864	0%	0%	1%	4%	1%	1%	1%	7%	0%	1%	1%	1%	2%	1%
2	13	863	878	4%	4%	4%	8%	13%	17%	21%	4%	4%	4%	6%	12%	16%	21%
2	12	865	878	4%	5%	5%	8%	11%	14%	17%	4%	4%	4%	6%	9%	12%	16%
2	14	865	880	3%	6%	6%	8%	8%	11%	12%	3%	3%	3%	7%	8%	11%	12%
1	7	870	878	5%	6%	6%	10%	15%	18%	22%	6%	5%	6%	8%	14%	18%	21%
1	7	879	887	22%	31%	37%	45%	50%	53%	55%	26%	31%	36%	45%	51%	54%	56%
2	7	879	887	26%	34%	39%	44%	53%	52%	54%	28%	41%	40%	41%	48%	52%	54%
2	12	888	901	46%	45%	47%	51%	54%	58%	63%	43%	43%	45%	48%	50%	55%	59%
4	21	888	910	23%	25%	28%	29%	32%	34%	38%	23%	24%	27%	28%	31%	34%	36%
1	5	902	910	7%	9%	9%	11%	17%	21%	23%	5%	5%	6%	7%	11%	14%	17%
3	6	911	919	9%	9%	8%	11%	15%	19%	22%	6%	4%	5%	6%	8%	11%	16%
3	11	911	924	14%	16%	19%	23%	27%	32%	41%	15%	13%	18%	22%	27%	33%	40%
1	5	920	926	4%	11%	12%	13%	12%	16%	20%	4%	4%	4%	7%	8%	14%	21%
1	8	925	934	3%	2%	1%	1%	2%	1%	3%	3%	1%	0%	2%	1%	0%	2%
1	4	929	934	1%	1%	1%	2%	2%	2%	2%	1%	2%	1%	2%	2%	-1%	1%
1	3	935	939	-4%	-4%	-4%	-4%	-4%	-4%	-4%	0%	1%	2%	2%	2%	1%	-1%
2	12	940	953	2%	1%	2%	3%	5%	7%	9%	2%	1%	2%	3%	5%	7%	8%
3	12	940	953	1%	1%	2%	2%	4%	7%	9%	1%	1%	2%	2%	4%	7%	8%
1	5	954	960	4%	7%	10%	18%	22%	25%	28%	4%	5%	10%	17%	22%	25%	28%
2	10	961	972	29%	30%	31%	34%	36%	35%	38%	29%	28%	31%	31%	34%	34%	36%
3	10	961	972	27%	29%	30%	33%	35%	34%	37%	28%	27%	30%	31%	33%	34%	36%
3	13	961	975	32%	33%	33%	36%	38%	37%	40%	33%	33%	36%	35%	37%	37%	37%
2	14	961	976	35%	34%	34%	37%	37%	37%	40%	34%	32%	33%	33%	36%	36%	38%
3	14	961	976	38%	39%	40%	42%	44%	43%	46%	38%	37%	39%	39%	41%	42%	43%
2	9	962	972	38%	39%	40%	41%	43%	44%	44%	38%	37%	40%	39%	41%	42%	43%
3	12	976	991	34%	36%	38%	41%	42%	43%	45%	35%	35%	37%	40%	40%	42%	44%
3	13	976	992	8%	8%	9%	13%	16%	15%	18%	10%	10%	17%	15%	19%	18%	20%
2	11	977	991	12%	11%	12%	16%	19%	18%	21%	13%	11%	14%	16%	19%	19%	21%
3	11	977	991	12%	11%	14%	17%	20%	20%	21%	12%	11%	13%	16%	20%	20%	21%
2	9	980	992	13%	13%	14%	18%	20%	22%	24%	14%	13%	13%	17%	20%	23%	22%
2	11	993	1006	3%	4%	6%	8%	11%	12%	12%	3%	2%	4%	8%	12%	10%	14%
3	11	993	1006	16%	15%	16%	20%	22%	23%	27%	16%	15%	16%	20%	21%	23%	22%
1	5	1007	1013	21%	20%	19%	22%	26%	28%	31%	18%	19%	18%	22%	26%	25%	29%
1	6	1007	1014	3%	3%	2%	3%	4%	3%	5%	7%	4%	6%	0%	5%	3%	6%
2	6	1007	1014	2%	3%	3%	3%	4%	4%	5%	2%	2%	1%	1%	4%	2%	4%
2	6	1007	1014	0%	0%	-2%	-1%	0%	4%	1%	3%	2%	-1%	-1%	2%	1%	1%
2	11	1015	1027	1%	2%	2%	3%	6%	8%	9%	1%	1%	1%	2%	5%	8%	9%
3	11	1015	1027	3%	3%	4%	5%	8%	10%	13%	2%	2%	2%	3%	6%	9%	10%
1	6	1019	1026	8%	10%	11%	13%	17%	24%	24%	13%	16%	13%	17%	25%	20%	21%
2	6	1019	1026	7%	7%	7%	10%	15%	17%	19%	11%	11%	10%	15%	20%	23%	19%
1	3	1031	1035	-3%	-2%	-2%	-2%	-1%	1%	2%	-2%	-1%	-1%	-1%	-1%	0%	-1%
2	9	1035	1046	7%	12%	13%	16%	17%	20%	25%	7%	9%	12%	14%	17%	20%	24%
2	12	1035	1049	30%	34%	37%	44%	50%	52%	56%	31%	31%	36%	43%	49%	54%	56%
1	5	1043	1049	27%	33%	36%	45%	54%	61%	64%	30%	29%	32%	37%	51%	58%	62%
1	6	1043	1050	21%	23%	31%	39%	49%	57%	62%	20%	18%	25%	33%	44%	54%	59%
2	6	1043	1050	22%	23%	28%	38%	47%	52%	56%	22%	20%	23%	31%	41%	49%	52%
1	4	1050	1055	1%	2%	1%	0%	-1%	-1%	-1%	9%	1%	1%	0%	0%	-1%	0%
3	18	1050	1069	11%	10%	10%	12%	12%	14%	18%	11%	10%	9%	9%	10%	12%	17%
3	20	1050	1071	9%	10%	10%	11%	12%	14%	16%	9%	9%	10%	9%	11%	12%	14%
4	20	1050	1071	10%	11%	11%	13%	14%	15%	17%	10%	10%	11%	12%	14%	15%	18%
2	19	1051	1071	11%	11%	11%	13%	13%	14%	17%	11%	11%	10%	11%	12%	13%	15%
3	19	1051	1071	10%	11%	10%	12%	12%	13%	16%	11%	10%	10%	11%	12%	12%	15%
4	19	1051	1071	10%	10%	11%	12%	13%	13%	16%	11%	10%	10%	11%	11%	14%	15%
4	21	1051	1073	9%	9%	10%	11%	12%	12%	14%	11%	10%	10%	11%	12%	12%	13%
2	11	1072	1084	12%	17%	23%	34%	41%	41%	42%	13%	15%	23%	33%	40%	41%	42%
3	11	1072	1084	12%	16%	21%	32%	39%	41%	44%	11%	13%	22%	32%	38%	41%	42%
1	6	1085	1092	31%	38%	49%	58%	57%	59%	58%	31%	34%	44%	55%	61%	59%	62%
2	6	1085	1092	22%	39%	57%	66%	69%	68%	66%	23%	34%	55%	69%	72%	72%	71%
1	3	1088	1092	37%	63%	69%	74%	74%	73%	75%	43%	53%	68%	73%	75%	76%	77%

Text S1

SUPPLEMENTAL INFORMATION

PKCβ Phosphorylates PI3Kγ to Activate it and Release it from GPCR Control

Romy Walser[1], John E. Burke[2], Elena Gogvadze[1], Thomas Bohnacker[1], Xuxiao Zhang[2], Daniel Hess[3], Peter Küenzi[1], Michael Leitges[4], Emilio Hirsch[5], Roger L. Williams[2], Muriel Laffargue[6], Matthias P. Wymann[1,*]

[1]Department of Biomedicine, University of Basel, 4058 Basel, Switzerland;
[2]Medical Research Council, Laboratory of Molecular Biology, Cambridge CB2 0QH, UK;
[3]Friedrich Miescher Institute for Biomedical Research, Basel 4058, Switzerland;
[4]Biotechnology Centre, University of Oslo, 0349 Oslo, Norway.
[5]Department of Genetics, Biology and Biochemistry, University of Torino, Torino 10126, Italy;
[6]INSERM U563, Département Lipoprotéines et Médiateurs Lipidiques, Toulouse 31300, France

*_Correspondence_: Matthias.Wymann@UniBas.CH
Matthias P. Wymann
Inst. Biochemistry & Genetics
Dept. Biomedicine
University of Basel
Mattenstrasse 28
4058 Basel, Switzerland

EXTENDED EXPERIMENTAL PROCEDURES

Materials

Where not indicated otherwise, materials and chemicals were purchased from Sigma-Aldrich.

Mice

C57BL6/J wild type (Jackson Laboratories), p110$\gamma^{-/-}$ [1], PKC$\alpha^{-/-}$ [2,3], PKC$\beta^{-/-}$ [4], and PKC$\gamma^{-/-}$ [5] mice were used for the preparation of BMMCs.

Cell Culture

Mouse bone marrow-derived mast cells (BMMCs) were developed from progenitor cells of femurs of 8-12 week old mice on a pure C57BL/6J genetic background [6]. Femurs were cut off at both ends and the marrow collected by centrifugation. Cells were resuspended in complete growth medium: Iscove's modified Dulbecco's medium (IMDM) supplemented with 10% heat-inactivated fetal calf serum (HI-FCS), 2 mM L-glutamine, 100 units/ml penicillin, 100 µg/ml streptomycin, 50 µM β-mercaptoethanol, 2 ng/ml recombinant murine IL-3 (Peprotech) and initially 1x 5 ng/ml SCF, and cultured at 37°C, 5% CO_2. IL-3 was re-added every third day. Non-adherent cells were transferred to new flasks and diluted weekly to 0.5 M cells/ml using 80% of fresh and 20% of conditioned medium. Differentiation of BMMCs was confirmed by measuring expressing of c-Kit and IgE receptors by flow cytometry. All mast cell experiments were carried out with BMMCs cultured for 4 to max. 16 weeks.

The human embryonic kidney 293 (*HEK293*) cell line was grown in Dulbecco's modified essential medium (DMEM) supplemented with 10% HI-FCS, 2 mM L-glutamine , 100 units/ml penicillin, 100 µg/ml streptomycin at 37°C, 5% CO2.

Spodoptera frugiperda *(Sf9*) cells were grown in IPL-41 medium (Genaxxon Bioscience) supplemented with 10% HI-FCS (Sigma-Aldrich), 2% yeastolate, 1% lipid concentrate, 50 µg/ml gentamicin (all Invitrogen) and 2.5 µg/ml amphotericin B (Genaxxon Bioscience). Sf9 cells were cultured as adherent or suspension culture at 27°C. Suspension cells were grown in Erlenmeyer flasks in a shaking incubator at 75-90 rpm.

Plasmids

Full-length, untagged human PI3Kγ was expressed from pcDNA3 (Invitrogen) [7]. Point mutations were introduced by polymerase chain reaction (PCR) using the overlap extension technique [8]. The mouse PKCβ2 cDNA was kindly obtained from Jae-Won Soh (PKClab.org) and inserted BamHI-BstEII-XhoI into pcDNA3 containing a Kozak translation initiation sequence and the human influenza hemagglutinin (HA)-tag between HindIII and BamHI (pcDNA3-kzHA). The catalytic part of PKCβ2 (PKCβ2-CAT) including amino acids 302-673, was amplified from full-length PKCβ2 with the forward primer 5'-ccgcaGGATCCcagaagtttgagagagccaagattg and the reverse primer 5'-ggcgTCTAGAttagctcttgacttcaggttttaaaaattc and inserted BamHI-XbaI into pcDNA3-kzHA. The pseudosubstrate deletion mutant of PKCβ2 was produced by the overlap extension technique with primers lacking the coding sequence for amino acids 19-31 of PKCβ2 (forward: 5'-gagcacagtgcacgaggtgaagaaccacaaattcac, reverse: 5'-cacctcgtgcactgtgctctcctcgccc) and two helper primers. The baculovirus transfer plasmid encoding GST-PI3Kγ (pAcG2T-PI3Kγ, codons 38-1102) has been described [9]. The transfer plasmid for baculovirus-mediated expression of C-terminal His-tagged full-length human PI3Kγ has been derived from pVL1393 (Invitrogen) containing codons 144-1102 of human PI3Kγ [10]) by inclusion of codons 1-143 by PCR. Serine 582 mutations were introduced into this construct by insertion of a PciI-EcoRI or BstEII-EcoRI fragment from mutant PI3Kγ in pcDNA3, respectively. All constructs were confirmed by sequencing.

Transfections

HEK293 cells were seeded into 6 cm dishes and were transfected with JetPEI™ (Polyplus-transfection) using 2.5 μg of total plasmid DNA. BMMCs were transfected by nucleofection (Amaxa) using solution T, 1-3 μg of PI3Kγ and, if indicated, 0.2-2 μg of p84 expression plasmid. Total DNA concentration was adjusted to 10 μg with pcDNA3 vector.

Stimulation of BMMCs

BMMCs were incubated overnight with 100 ng/ml anti-dinitrophenyl (DNP)-specific immunoglobulin E (clone SPE-7) in complete growth medium (see cell culture, above). Next day, cells were centrifuged for 5 min at 146 g and resuspended in IL-3 free growth medium containing 2% (signaling experiments) or 10% FCS (degranulation assay). Degranulation was induced by the addition of DNP coupled to human serum albumin (DNP-HSA) at the indicated concentrations. Other stimuli used to trigger BMMC activation were thapsigargin, phorbol 12-myristate 13-actetate (PMA; 100nM, Alexis), adenosine (1 μM), N^6-(3-iodobenzyl)-adenosine-5'-*N*-methylcarbox-amide (IB-MECA; 10 nM), stem cell factor (SCF; 10 ng/ml, Peprotech), interleukin-3 (IL-3; 10 ng/ml, Peprotech), and platelet activating factor (PAF [1 uM], β-Acetyl-γ-O-alkyl-L-α-phosphatidylcholine). Stimulations were done at 37°C. Preincubation with *B. Pertussis Toxin* (*P*Tx; 100 ng/ml) was done for 4 hours, and adenosine deaminase (ADA; 10 units/ml) was added 1 min before stimulation. Inhibitor pretreatment time was 15 min for wortmannin (100 nM), and 20 min for the PKC inhibitors (Ro318425 (1 μM), Gö9683 (0.5 μM), Gö6976 (0.5 μM), and Rottlerin (10 μM), a brad-band kinase inhibitor [11] [all from Calbiochem]; PKC412/CPG41251 (1 μM, LC Laboratories), Sotrastaurin (AEB071; 1μM, Selleckchem). For Western blot analysis of PKB and MAPK phosphorylation, stimulations were stopped on ice, and cells were collected by centrifugation for 1 min at 2000 g (4°C) and immediately lysed in 1x Laemmli sample buffer [62.5 mM Tris/HCl pH 6.8, 2% SDS, 10% glycerol, 5% β-mercaptoethanol, bromophenolblue].

(Co-)Immunoprecipitation

Transfected HEK293 cells were washed with phosphate buffered saline (PBS) and lysed with NP-40 lysis buffer [50 mM Tris/HCl pH 7.4, 138 mM NaCl, 2.7 mM KCl, 5% glycerol, 1% NP-40] supplemented with protease inhibitors [20 μM leupeptin, 18 μM pepstatin, 5 μg/ml aprotinin, phenylmethylsulfonylfluorid (PMSF)], phosphatase inhibitors [40 mM NaF, 2 mM Na_3VO_4], 0.5 mM EDTA and 0.5 mM EGTA for 15 min on ice. Insoluble material was pelleted by centrifugation and one-tenth of clarified lysate was mixed with Laemmli sample buffer to examine overall protein expression. The remainder of lysate was incubated with anti-p110γ (ascites fluid, 641, corresponds to Jena Bioscience ABD-027) or anti-HA.11 (Covance) antibodies for 1 hour at 4°C on a rotating wheel, followed by incubation with 25 μl of a 50% slurry of GammaBind Plus Sepharose (Amersham Biosciences) or protein G agarose (Millipore) for additional 2 hours. Immune complexes were washed 3x with NP-40 lysis buffer, 1x with 0.1 M Tris/HCl pH 7.4, 0.5 M LiCl, 0.2% NP-40, 1x again with NP-40 lysis buffer, and eluted by the addition of Laemmli sample buffer.

BMMCs were collected by centrifugation and lysed in NP-40 lysis buffer supplemented with protease inhibitors, phosphatase inhibitors [40 mM NaF, 10 mM β-glycerophosphate, 5 mM sodium pyrophosphate], 2 mM EDTA and 2 mM EGTA for 15 min on ice. Cell debris were removed by centrifugation, and endogenous or transfected PI3Kγ was immunoprecipitated from the cleared lysate with anti-PI3Kγ (ascites fluid, clone 641) antibodies (1-2 hours) and protein A or G-agarose beads (2-5 hours). Immune complexes were washed as describe above before resuspension in 1x Laemmli sample buffer.

For co-immunoprecipitations from BMMCs, cells were suspended in hypotonic lysis buffer (20 mM Tris/HCl pH 7.4, 20 mM NaCl, 2.7mM KCl, 5% glycerol, 0.5% CHAPS) supplemented with protease inhibitors [20 μM leupeptin, 18 μM pepstatin, 5 μg/ml aprotinin, 1mM phenylmethylsulfonylfluorid (PMSF), 0.5mM diisopropyl fluorophosphate], phosphatase inhibitors [40 mM NaF, 10 mM β-glycerophosphate, 5 mM sodium pyrophosphate], 2 mM EDTA and 2 mM EGTA. PI3Kγ complex was immunoprecipitated from cleared cell lysates with either anti-p110γ (ascites fluid, clone 641) or anti-p84 (goat antisera, for epitopes see [12]) antibodies for 1 h, before protein G-agarose beads were added for another hour. Beads were washed three times with lysis buffer and resuspended in 1x Laemmli sample buffer. Lysates and immunoprecipitations were analysed by Western blotting.

Western Blotting

Protein samples were heated to 95°C for 5 min, centrifuged for 2 min at 16'000g, separated by SDS-polyacrylamide gel electrophoresis (PAGE) and transferred to polyvinylidene fluorid (PVDF)-membranes (Millipore) by semi-dry transfer. Membranes were blocked with 5% (w/v) milk powder (Migros, Schweiz) in TBS-T buffer [20 mM Tris/HCl, pH 7.6, 137 mM NaCl, 0.1% (v/v) Tween 20 (Fluka)]. Blots were incubated overnight at 4°C with the primary antibody, followed by incubation with horseradish peroxidase (HRP)-coupled secondary goat anti-mouse or anti-rabbit antibodies. Protein bands were visualized by enhanced chemiluminescence (ECL) (Millipore). Phospho-specific antibodies were kept in TBS-T/1% BSA [pPKB S473, pPKB T308, pCamKII T286, pCREB S133 and pan-phospho PKC (S660 in PKCβII; all from Cell Signaling); pMAPK (Sigma M8159 or Promega V8031); phospho-p110γ S582 antibodies were raised against Cys-conjugated peptides C+KELLWHFRYE-[phosphoSer]-LKHPKAYPKLFSS and C+WHFRYE-[phosphoSer]-LKHPK, and affinity purified]. All other antibodies were diluted in TBS-T/1% (w/v) dry milk powder [PI3Kγ (raised against amino acids 97-335); PKCβ2 (Santa Cruz, sc-210), PKCα (sc-208), PKCγ (sc-211), β-Tubulin (Boehringer Mannheim), α-Tubulin (Sigma, T9026), HA (Covance, MMS-101R), p84 (rabbit antisera, [12]), total PKB (a kind gift from B. Hemmings)]. Quantifications of Western blots have been done with ImageJ software (NIH).

β-Hexosaminidase Release Assay

Mast cell degranulation was assessed by the release of β-hexosaminidase into cell supernatants [13,14]. BMMCs were cultured at 0.8-1 Mio cells/ml in complete growth medium, and were, pre-loaded with 100 ng/ml IgE (for IgE/Ag experiments). Cells were wash once and resuspended in PIPES-buffered solution [25 mM PIPES pH 7.4, 119 mM NaCl, 5 mM KCl, 5.6 mM glucose, 1 mM $CaCl_2$, 0.4 mM $MgCl_2$, 0.1 % fatty-acid free, low endotoxin bovine serum albumin (LE-BSA, Sigma)]. Cells (0.5 M) were stimulated with IgE/DNP-HSA or thapsigargin in a total volume of 500 μl PIPES-buffered solution in 24 well plates. Following incubation at 37°C for 20 min, plates were centrifuged at 4°C at 330 g for 5 min. Then, 100 μl aliquots of supernatant were transferred to 96 well plates. To determine total β-hexosaminidase, unstimulated cells were lysed by the addition of PIPES-buffered solution with 0.1% Triton X-100 for 10 min, and 100 μl aliquots were transferred to 96 well plates. Activity of β-hexosaminidase was assessed by incubation with 100 μl of substrate solution [100 mM p-nitrophenyl-N-acetyl-β-D-glucosaminidine (p-NAG) in 0.1 M sodium acetate pH 4] for 1 h at 37°C. The reaction was stopped with 100 μl of 0.15 M Na_2CO_3/$NaHCO_3$, and the amount of produced p-nitrophenol was assessed by the absorbance at 410 nm. Background values were obtained from lysates of unstimulated cells incubated without p-NAG. The amount of β-hexosamidinase released was calculated by using the formula: Release (R) [%] = $(A_{Stimulated} - A_{Unstimulated})/(A_{Total\ unstimulated} - A_{Total\ background})*100$

Cytosolic Ca^{2+} concentration measurements

BMMCs were suspended in physiologic HEPES buffer (10 mM HEPES/NaOH pH 7.5, 137 mM NaCl, 2.7 mM KCl, 5 mM glucose, 1 mM $CaCl_2$, 1 mM $MgCl_2$, 0.1 % fatty acid free BSA]. Cells were loaded with 4 μM Fura-4F/AM [K_D for Ca^{2+} *in vitro* is 770 nM; intracellular K_D for Ca^{2+} is ca. 1 μM [15,16]) for 10 min, washed twice, and resuspended in HEPES buffer containing different Ca^{2+} concentrations ($[Ca^{2+}]_{e\ (extracellular)}$ = 0 - 1 mM). Cells were subsequently stimulated in final volume of 3 ml (0.5 M cells/ml) in a continuously stirred cuvette at 37° in a

fluorescence spectrometer (Perkin Elmer LS50B). The excitation wavelength was alternated between 340 and 380 nm and fluorescence emission was measured at 510 nm every 200 ms. After recording a base line cells were stimulated (e.g. with 0.5 µM thapsigargin). To calculate $[Ca^{2+}]_i$ maximal Fura fluorescence (F_{max}) was determined after cell permeabilisation with 0.1% Triton X-100 after addition of 2 mM Ca^{2+}. Minimal fluorescence (F_{min}) values were obtained after the addition of 4 mM EGTA. Autofluorescence was subtracted before $[Ca^{2+}]_i$ was calculated using the equation of [17]:

$$[Ca^{2+}]_i = K_d[(R - R_{min})/(R_{max} - R)](F_{380\ EGTA}/F_{380\ Triton}),\ R = F_{340}/F_{380}$$

To correlate intracellular Ca^{2+} concentrations with PKB phosphorylation, $[Ca^{2+}]_i$ levels were plotted against relative levels of phosphorylated PKB (S473). Phospho-PKB levels were obtained from cells (1.5 ml) taken out of the measurement cuvette 2 min after stimulation. Lysed cells were analyzed by Western blotting and PKB phosphorylation was quantified by intensity measurements with ImageJ software.

Production of recombinant PI3Kγ

Recombinant human PI3Kγ was expressed as N-terminal GST- or C-terminal His_6-tagged-fusion protein in Sf9 cells by infection with recombinant baculovirus. Plasmid (pAcG2T-PI3Kγ, codons 38-1102) and baculovirus for GST-PI3Kγ have been described [9]. Full-length PI3Kγ-His_6 and S582 point mutants were expressed in pVL1393 (BD Biosciences) after co-transfection of Sf9 cells with BaculoGold DNA (BD Biosciences). Proteins were harvested as described in [18]. Baculovirus-infected Sf9 cells were harvested 2-2.5 days postinfection, were washed with PBS und lysed with either GST- or His-lysis buffer [GST: 50 mM Tris/HCl pH 7.5, 150 mM NaCl, 5 mM EDTA, 1 mM NaF, 1 mM DTT, 1% Triton-X100; His: 50 mM $NaH_2PO_4 \cdot 2H_2O$/NaOH, 300 mM NaCl, 20 mM imidazol, 5% glycerol, 1% NP-40] containing protease inhibitors. GST-PI3Kγ was purified on glutathione sepharose 4B (Amersham Biosciences) and eluted with 50 mM Tris/HCl pH 7.5, 150 mM NaCl, 5 mM EDTA, 1 mM DTT, 5% glycerol, 20 mM glutathione after extensive washing. PI3Kγ-His_6 was purified over Ni^{2+}-NTA agarose (Qiagen) and eluted with 50 mM $NaH_2PO_4 \cdot 2H_2O$/NaOH pH 8, 300 mM NaCl, 250 mM imidazol. Proteins were mixed 1:1 with 2x storage buffer [80 mM HEPES/NaOH, 4 mM EDTA, 2 mM DTT, 20 mM benzamidine, ~90% ethylenglycol] and kept at -20°C. Protein concentrations were quantified by Coomassie-staining in SDS-PAGE gels using the Odyssey infrared imaging system (LI-COR Biosciences). Bovine serum albumin served as standard.

In vitro kinase assay

Recombinant GST-PI3Kγ wild type (wt) or kinase inactive mutant (KR, Lys833 mutated to Arg) was incubated at an equal molar ratio (if not stated differently) with recombinant PKCβ2 (40 ng, Invitrogen) in 1x PKC kinase buffer (50 mM HEPES pH 7.4, 10 mM $MgCl_2$, 1 mM $CaCl_2$, 1 mM DTT, 0.03% Triton X-100) in the presence of 10 µM adenosine 5'-triphosphate (ATP) and 5 µCi of [γ^{32}P]-ATP [Perkin Elmer, 6000 Ci/mmol] per sample in a final volume of 40 µl. Ca^{2+}/calmodulin-dependent protein kinase II (CamKII, Life Technologies)-mediated phosphorylation was performed in 1x CamKII kinase buffer (10 mM HEPES, 10 mM $MgCl_2$, 1 mM Na_3VO_4, 10 ug/ml calmodulin, 0.5 mM $CaCl_2$, 5 mM DTT). Kinase reactions were pre-warmed for 2 min at 30°C, started by the addition of 4 µl of ATP-mix (in H_2O), and incubated at 30°C for 30 min. Reactions were terminated by the addition of 5x sample buffer and the proteins were resolved by SDS-PAGE. Gels were stained with Coomassie brilliant blue (Serva blue G); ^{32}P-incorporation was visualized by autoradiography or quantified on a phosphoimager (Typhoon 9400). Band intensities were quantified with ImageQuant TL Software (Amersham Biosciences). A dilution series of the ATP/[γ^{32}P]-γ-ATP-mix served as a standard to calculate absolute $^{32}P_i$-incorporation rates.

Where indicated, phosphatidylserine (PS) lipid vesicles (0.1 mg/ml) containing 1-oleoyl-2-acetyl-sn-glycerol (OAG, 0.01 mg/ml, Cayman Chemical) were added. PS in $CHCl_3$/MeOH 2:1 was mixed with OAG in acetonitril in an Eppendorf tube, dried by a stream of nitrogen gas and resuspended in kinase buffer by sonication.

In vitro lipid kinase assay

Assays were performed in a final volume of 50 µl in 1.5 ml Eppendorf tubes in lipid kinase buffer [40 mM HEPES, pH 7.4, 150 mM NaCl, 4 mM $MgCl_2$, 1 mM DTT, 0.1 mg/ml fatty-acid free BSA] in the presence of PtdIns(4.5)P_2-containing lipid vesicles, 10 µM adenosine 5'-triphosphate (ATP) and 4 µCi of [γ^{32}P]-ATP [Perkin Elmer, 6000 Ci/mmol] per sample. Phospholipid composition of the lipid vesicles has been chosen to mimic relative mole ratios found in the inner leaflet of the plasma membrane (PE/PS/PC/SM/PIP_2 = 30/20/10/4.5/1.2-4.6). Lipids dissolved in $CHCl_3$/MeOH (2:1) were combined in a glass tube [f. c. in assay: 130 µM PE, 87 µM PS, 43 µM PC, 20 µM SM, 5-20 µM PIP_2], dried under a stream of nitrogen gas and resuspended in lipid kinase buffer without BSA by

sonication (3x 15 seconds at an amplitude of 30%) on ice with a tip sonicator (U200S, IKA Labortechnik). Recombinant wild type or mutant PI3Kγ-His6 (200 ng/reaction) were diluted in lipid kinase buffer and added (8 µl) to 4 µl of mastermix [lipid kinase buffer, but with 1.05 mg/ml BSA] followed by the addition of 30 µl of lipid mix. Samples were mixed and kept on ice for additional 20 min, were then warmed up to 30°C for 2 min on a heat block before starting the reaction by the addition of 8 µl of ATP-mix in lipid kinase buffer without BSA. Samples were incubated for 10 min at 30°C with shaking (1200 min^{-1}) on a heat block. The reaction was stopped by the addition of 100 µl 1 N HCl and the lipids were extracted by the addition of 200 µl $CHCl_3$/MeOH 1:1 and vortexing. Phases were separated by centrifugation for 2 min at 9300 g, the lower organic phase was transferred to a new tube and the lipids dried under a low heat vacuum in a Speed-Vac (Univapo 150H). Lipids were re-dissolved in $CHCl_3$/MeOH 4:1 and loaded onto a potassium oxalate-pretreated silica gel 60 W F254S TLC plates (Merck) for separation by thin layer chromatography (TLC) in a horizontal tank using $CHCl_3$/acetone/MeOH/acetic acid/H_2O (80/30/26/24/14 v/v) as mobile phase. Dried plates were exposed to Fuij Super RX x-ray films or Kodak Storage Phosphor Screens to quantified by phospho-imaging.

L-α-phosphatidylcholine from chicken egg (PC), sphingomyelin from porcine brain (SM) and L-α-phosphatidylinositol(4,5)bisphosphate from porcine brain, triammonium salt (PIP_2) were purchased from Avanti Polar Lipids, while L-α-phosphatidylserine (PS) from bovine brain and L-α-phosphatidylethanolamine from egg yolk, type III (PE) was obtained from Sigma-Aldrich.

Mass spectrometry

The PI3Kγ protein band was excised from the gel, reduced with 10 mM DTT, alkylated with 55 mM iodoacetamide and cleaved with porcine trypsin (Promega, Madison, USA) in 50 mM ammonium bicarbonate (pH 8.0) at 37°C overnight [19]. The extracted peptides were analyzed by capillary liquid chromatography tandem mass spectrometry (LC-MSMS) using a Magic C18 100 µm x 10 cm HPLC column (SwissBioanalytics, Switzerland) connected on line to a 4000 Q Trap (MDS Sciex, Concord, Ontario, Canada) as described earlier [20]. Data analysis was done with Mascot [21] searching the protein sequence database UNIPROT_15.6. from Feb 2010 (9421896 sequences; 1248797668 residues). Relative quantification of the peptides was done with multiple reaction monitoring (MRM) using the same instruments and identical chromatographic conditions. The approach was described earlier [22]. The Ser582 site in YE**S^P**[**582**]LKHPK corresponds well to consensus substrate motifs for PKCβ as determined by peptide library screens [23].

Protein expression and purification for deuterium exchange studies

The PI3Kγ alone and PI3Kγ/p84 complex were expressed in Sf9 cells using the pFastBac system (Invitrogen). Cells were resuspended in sonication buffer (50 mM Tris/HCl pH 8, 100 mM NaCl, 1 mM PEFA, 25 mM imidazole) and lysed by sonication on ice for 10 minutes. The lysates were ultracentrifuged at 35'000 rpm for 45 minutes at 4 °C in a Ti45 rotor. The soluble cell lysate was filtered through a 0.45 µM filter. Subsequently, the lysate was passed over a Ni-NTA 5 ml Fast Flow column (GE Healthcare) and eluted with an imidazole concentration gradient from 25 to 200 mM. The protein was further purified by ion-exchange HiTrap Q (5ml), Heparin agarose (5ml) and Superdex 200 (16/60) gel-filtration chromatography. The protein was eluted from the gel filtration column in 20 mM Tris pH 7.5, 100 mM NaCl, 5 mM DTT and 1 mM $(NH_4)_2SO_4$.

Deuterium exchange sample preparation

5 µl of stock protein solutions (Hs_PI3Kγ-His_6: 30 µM; Hs_PI3Kγ-His_6/Mm_p84-His_6: 35µM) were prepared in 20 mM Tris pH 7.5, 100 mM NaCl, 5 mM DTT and 1 mM ammonium sulfate. Exchange reactions were initiated by addition of 25 µl of a 98% D_2O solution containing 10 mM HEPES pH 7.2, 50 mM NaCl, and 2 mM DTT, giving a final concentration of 82% D_2O. Deuterium exchange reactions were allowed to carry on for seven time periods, 3, 10, 30, 100, 300, 1000 and 3000 seconds at 23 ºC. On-exchange was stopped by the addition of 40 µl of quench buffer containing 1.2% formic acid and 0.833 M guanidine-HCl, which lowered the pH to 2.6. Samples were then immediately frozen in liquid nitrogen until mass analysis.

Protein digestion and peptide identification for DXMS analysis

Different digestion conditions were employed to optimize the peptide digestion map. These optimizations included changing denaturant concentration, flow rate over pepsin, and denaturation time. Peptide identification was performed by running tandem MS/MS experiments using a Sciex QStar Pulsar hybrid QqTOF (Applied Biosystems). Data was analyzed using Mascot software v. 2.2 (Matrix Science) to identify all peptides based on fragmentation and

peptide mass, and these identifications were then manually validated using DXMS software (Sierra Analytics) to test for correct m/z state, and the presence of overlapping peptides.

Measurement of deuterium incorporation

Samples were thawed rapidly on ice and then injected onto an online HPLC system that was immersed in ice. The protein was run over an immobilized pepsin column (Applied Biosystems, Poroszyme®, 2-3131-00) at 50 µl/min, and collected over a 1.7 µm particle C18 peptide trap (2.1 mm x 8 mm, Waters Van-guard) for five minutes. The trap was then switched in line with a 1.7 µm particle, 1 mm x100 mm C18 column (Waters Acquity UPLC) with a vanguard pre-column and peptides were eluted by a 5-45% gradient of buffer A (0.1% formic acid) and buffer B (80% acetonitrile, 20% H_2O, 0.02% formic acid) over 22 minutes and injected onto a Sciex QStar Pulsar hybrid QqTOF (Applied Biosystems) which collected mass spectra from a range of 350 to 1300 m/z.

Mass analysis of the peptide centroids was performed as described previously using the software DXMS (Sierra Analytics) [24,25]. Briefly, all selected peptides passed the quality control threshold of the software, and were then manually examined for accurate identification and deuterium incorporation. Results are shown as relative levels of deuteration with no correction for back exchange as described previously [26]. The real level of deuteration will be ~25-35% higher than what is shown, based on tests performed with fully deuterated standard peptides. All experiments were repeated in duplicate, and we found that the average error was less than 0.2 Da, and for this reason we consider all changes between conditions greater than 0.5 Da that occur at more than one time point as significant. The resulting deuterium incorporation was graphed versus the on-exchange time. All deuterium exchange data for all peptides analyzed (~202 peptides) is shown in tabular form (Table S1).

SUPPLEMENTAL REFERENCES

1. Hirsch E, Katanaev VL, Garlanda C, Azzolino O, Pirola L et al. (2000) Central role for G protein-coupled phosphoinositide 3-kinase gamma in inflammation. Science 287: 1049-1053.
2. Leitges M, Plomann M, Standaert ML, Bandyopadhyay G, Sajan MP et al. (2002) Knockout of PKC alpha enhances insulin signaling through PI3K. Mol Endocrinol 16: 847-858.
3. Braz JC, Gregory K, Pathak A, Zhao W, Sahin B et al. (2004) PKC-alpha regulates cardiac contractility and propensity toward heart failure. Nat Med 10: 248-254.
4. Leitges M, Schmedt C, Guinamard R, Davoust J, Schaal S et al. (1996) Immunodeficiency in protein kinase cbeta-deficient mice. Science 273: 788-791.
5. Abeliovich A, Paylor R, Chen C, Kim JJ, Wehner JM et al. (1993) PKC gamma mutant mice exhibit mild deficits in spatial and contextual learning. Cell 75: 1263-1271.
6. Laffargue M, Calvez R, Finan P, Trifilieff A, Barbier M et al. (2002) Phosphoinositide 3-kinase gamma is an essential amplifier of mast cell function. Immunity 16: 441-451.
7. Bondeva T, Pirola L, Bulgarelli-Leva G, Rubio I, Wetzker R et al. (1998) Bifurcation of lipid and protein kinase signals of PI3Kgamma to the protein kinases PKB and MAPK. Science 282: 293-296.
8. Ho SN, Hunt HD, Horton RM, Pullen JK, Pease LR (1989) Site-directed mutagenesis by overlap extension using the polymerase chain reaction. Gene 77: 51-59.
9. Stoyanov B, Volinia S, Hanck T, Rubio I, Loubtchenkov M et al. (1995) Cloning and characterization of a G protein-activated human phosphoinositide-3 kinase. Science 269: 690-693.
10. Pacold ME, Suire S, Perisic O, Lara-Gonzalez S, Davis CT et al. (2000) Crystal structure and functional analysis of Ras binding to its effector phosphoinositide 3-kinase gamma. Cell 103: 931-943.
11. Soltoff SP (2007) Rottlerin: an inappropriate and ineffective inhibitor of PKCdelta. Trends Pharmacol Sci 28: 453-458.
12. Bohnacker T, Marone R, Collmann E, Calvez R, Hirsch E et al. (2009) PI3Kgamma adaptor subunits define coupling to degranulation and cell motility by distinct PtdIns(3,4,5)P3 pools in mast cells. Sci Signal 2: ra27.
13. Schwartz LB, Austen KF, Wasserman SI (1979) Immunologic release of beta-hexosaminidase and beta-glucuronidase from purified rat serosal mast cells. J Immunol 123: 1445-1450.
14. Ozawa K, Szallasi Z, Kazanietz MG, Blumberg PM, Mischak H et al. (1993) Ca(2+)-dependent and Ca(2+)-independent isozymes of protein kinase C mediate exocytosis in antigen-stimulated rat basophilic RBL-2H3 cells. Reconstitution of secretory responses with Ca2+ and purified isozymes in washed permeabilized cells. J Biol Chem 268: 1749-1756.
15. Felmy F, Neher E, Schneggenburger R (2003) Probing the intracellular calcium sensitivity of transmitter release during synaptic facilitation. Neuron 37: 801-811.

16. Ismailov I, Kalikulov D, Inoue T, Friedlander MJ (2004) The kinetic profile of intracellular calcium predicts long-term potentiation and long-term depression. J Neurosci 24: 9847-9861.
17. Grynkiewicz G, Poenie M, Tsien RY (1985) A New Generation of Ca-2+ Indicators with Greatly Improved Fluorescence Properties. J Biol Chem 260: 3440-3450.
18. Wymann MP, Bulgarelli-Leva G, Zvelebil MJ, Pirola L, Vanhaesebroeck B et al. (1996) Wortmannin inactivates phosphoinositide 3-kinase by covalent modification of Lys-802, a residue involved in the phosphate transfer reaction. Mol Cell Biol 16: 1722-1733.
19. Shevchenko A, Wilm M, Vorm O, Mann M (1996) Mass spectrometric sequencing of proteins silver-stained polyacrylamide gels. Anal Chem 68: 850-858.
20. Vichalkovski A, Gresko E, Hess D, Restuccia DF, Hemmings BA (2010) PKB/AKT phosphorylation of the transcription factor Twist-1 at Ser42 inhibits p53 activity in response to DNA damage. Oncogene 29: 3554-3565.
21. Perkins DN, Pappin DJ, Creasy DM, Cottrell JS (1999) Probability-based protein identification by searching sequence databases using mass spectrometry data. Electrophoresis 20: 3551-3567.
22. Hess D, Keusch JJ, Oberstein SA, Hennekam RC, Hofsteenge J (2008) Peters Plus syndrome is a new congenital disorder of glycosylation and involves defective Omicron-glycosylation of thrombospondin type 1 repeats. J Biol Chem 283: 7354-7360.
23. Nishikawa K, Toker A, Johannes FJ, Songyang Z, Cantley LC (1997) Determination of the specific substrate sequence motifs of protein kinase C isozymes. J Biol Chem 272: 952-960.
24. Burke JE, Karbarz MJ, Deems RA, Li S, Woods VLJ et al. (2008) Interaction of group IA phospholipase A2 with metal ions and phospholipid vesicles probed with deuterium exchange mass spectrometry. Biochemistry 47: 6451-6459.
25. Burke JE, Vadas O, Berndt A, Finegan T, Perisic O et al. (2011) Dynamics of the phosphoinositide 3-kinase p110delta interaction with p85alpha and membranes reveals aspects of regulation distinct from p110alpha. Structure 19: 1127-1137.
26. Iacob RE, Pene-Dumitrescu T, Zhang J, Gray NS, Smithgall TE et al. (2009) Conformational disturbance in Abl kinase upon mutation and deregulation. Proc Natl Acad Sci U S A 106: 1386-1391.

10. Acknowledgements

I thank Matthias Wymann for giving me the opportunity to get into the exciting PI3-kinase research field. I also like to thank him for providing good lab equipment and offering me the possibility to train and expand my scientific skills and experiences.

Special thanks go to Daniel Hess for the determination of the PI3Kγ phosphorylation sites and for his advice and any support. Without his outstanding expertise and knowledge this work would not have been possible.

Sincere thanks go to Roger Williams and John Burke for the DXMS analysis and for the careful revision of the DXMS-pertinent paper text sections. I'm very thankful for their excellent inputs and improvements.

I very much like to thank Bernd Nürnberg for joining my thesis committee and for evaluating my dissertation.

Further, I like to thank all lab members for every kind of discussions and help, funny moments, and coffee breaks. Especially, I want to thank Markus and Elena for the friendly atmoshere, cooperative activities, and the lots of enjoyable lunch and coffee breaks.

I very much like to thank Alessia for our interesting collaborative activities and her stay here in Basel, which I enjoyed very much. Kind thanks also go to Xuxiao for helpful tips for protein expression and collaborative efforts. Further, I want to thank Kevin for the intensive, half-year lasting e-mail exchanges and the microscopic analyses, which we however had to stop due to practical hurdles and conceptual reasons.

I also like to thank all the institute members that shared their knowledge, borrowed equipment, and participated in friendly chats.

I'm very grateful to all my friends, relatives, and the unisport for relaxing activities beyond work.

Last but not least, I want to warmly thank my parents for all their emotional support and financial help.

11. Curriculum Vitae

Personal details

Name	Romy Walser
Nationality	Swiss
Date of birth	17.03.1980

Academic education

PhD in biochemistry, University of Basel, Switzerland 03/2005-01/2012
Department of biomedicine (DBM), Institute of biochemistry and genetics, Lab of Prof. Dr. Matthias P. Wymann
Title: Non-canonical activation of PI3Kγ by Ca^{2+}/PKCβ2 in mast cells

Diploma (M. Sc.) in biochemistry, University of Bern, Switzerland 10/2002-10/2004
Diploma exams 10/2004
Diploma (Master's) thesis, Department of chemistry and biochemistry, 07/2003-07/2004
Lab of PD Dr. M. Lienhard Schmitz
Title: Staurosporine-induced degradation of mixed lineage kinase 3

Prediploma in biochemistry, University of Fribourg, Switzerland 10/2000-10/2002
2. Prediploma (B. Sc.) 10/2002
1. Prediploma 10/2001

Scholar education

High school (Gymnasium), Chur, Switzerland 08/1995-06/2000
Matura type C (mathematic-scientific direction)
Secondary school, Bonaduz, Switzerland 08/1993-06/1995
Primary school, Bonaduz, Switzerland 08/1987-06/1993

Prizes

Poster award, category gold, Biovalley Science Day 2009, Basel, Switzerland 10/2009
Selected short talk speaker, Tri-Society Annual Conference 2009, Cellular and Cytokine Interactions in Health and Disease, Lisbon, Portugal 10/2009

Courses

Practical and theoretical laboratory animal course, LTK Modul 1, 5 days, Basel, Switzerland (and continuing education) 03/2006
Patenting in life sciences – challenges and questions, 2 days, Weggis, Switzerland 06/2010

Languages

German	Native speaker
English	Fluent, written and spoken
French	Intermediate, written and spoken
Italian	Basic knowledge

Oral communications and poster presentations

- USGEB (Union of the Swiss Societies for Experimental Biology) Annual Meeting, Zürich, Switzerland, Poster presentation — 2011, January 27-28
- Tri-Society Annual Conference, Cellular and Cytokine Interactions in Health and Disease, Lisbon, Portugal, Oral/poster presentation **(abstract chosen as talk)** — 2009, October 18-21
- BioValley Science Day, Basel, Switzerland, Poster presentation — 2009, October 13
- BioValley Science Day, Basel, Switzerland, Poster presentation — 2007, October 23
- MAIN Students' meeting, Villars-sur-Ollon, Switzerland, Oral/poster presentation **(abstract chosen as talk)** — 2007, May 19-22
- Monthly in-house meeting, Centre for Biomedicine, Basel, Switzerland, Oral presentation — 2007, May 15
- Targeting the kinome, Basel, Switzerland, Poster presentation — 2006, December 4-6
- 3rd Focused Meeting on PI3K signalling and disease, Bath, UK, Poster presentation — 2006, November 6-8
- MAIN Annual meeting, Castelnuovo del Garda, Italy, Poster presentation — 2006, October6-8
- Bioscience06, Glasgow, UK, Oral/poster presentation — 2006, July 23-27
- MAIN Students' meeting, Gwatt, Switzerland, Poster presentation — 2006, May 13-16
- Monthly in-house meeting, Centre for Biomedicine, Basel, Switzerland, Oral presentation — 2005, October 4